

# Biokinetics and inhalation toxicity of cerium dioxide and barium sulfate nanoparticles after 1, 4, 13 and 52 weeks of exposure

INAUGURAL – DISSERTATION

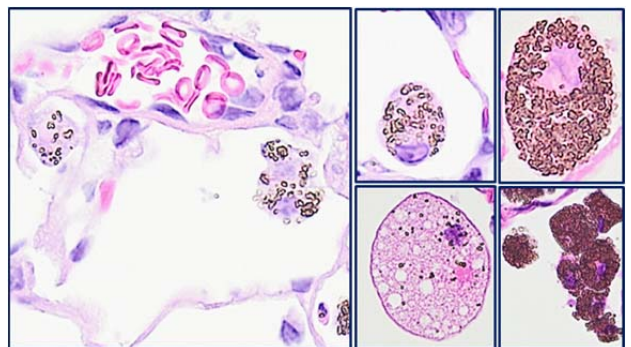
zur Erlangung des Grades eines

**Dr. med. vet.**

beim Fachbereich Veterinärmedizin

der Justus-Liebig-Universität Gießen

**Jana Keller**



Aus dem Institut für Veterinär-Pathologie, Fachbereich Veterinärmedizin,  
Justus-Liebig-Universität, Gießen

Betreuerin: Prof. Dr. med. vet. Christiane Herden

und

Aus der School of Medicine and Dentistry,  
University of Rochester Medical Center, New York, USA

Betreuer: Prof. Dr. med. vet. Günter Oberdörster

# **Biokinetics and inhalation toxicity of cerium dioxide and barium sulfate nanoparticles after 1, 4, 13 and 52 weeks of exposure**

**INAUGURAL-DISSERTATION**

zur Erlangung des Grades eines

**Dr. med. vet.**

beim Fachbereich Veterinärmedizin  
der Justus-Liebig-Universität, Gießen

Eingereicht von

**Jana Keller**

Tierärztin aus Karlsruhe

Gießen, 2015

**Mit Genehmigung des Fachbereiches Veterinärmedizin der  
Justus-Liebig-Universität Gießen**

**Dekan: Prof. Dr. Dr. h. c. med. vet. M. Kramer**

**Gutachter:**

**Prof. Dr. med. vet. Christiane Herden**

**Prof. Dr. med. vet. Günter Oberdörster**

**Tag der Disputation: 13. Juli 2015**

This dissertation work was performed at the laboratories of the  
Experimental Toxicology and Ecology of BASF SE in Ludwigshafen, Germany.

Part of this work was already published in peer-reviewed journals as follows:

Keller, J., Wohleben, W., Ma-Hock, L., Strauss, V., Groeters, S., Küttler, K., Wiench, K., Herden, C., Oberdörster, G., van Ravenzwaay, B., Landsiedel, R.: **Time course of lung retention and toxicity of inhaled particles: short-term exposure to nano-Ceria**, *Archives of Toxicology*, 2014, 88:2033-2059

Konduru, N., Keller, J., Ma-Hock, L., Gröters, S., Landsiedel, R., Donaghey, T. C., Brain, J. D., Wohleben, W. and Molina, R. M: **Biokinetics and effects of barium sulfate nanoparticles**, *Part Fibre Toxicol*, 2014, 11:55

The papers have been accepted for inclusion in this dissertation work by BASF SE.

## Contents

<b>1. Foreword</b>	<b>1</b>
<b>2. Summary</b>	<b>2</b>
<b>3. Zusammenfassung</b>	<b>4</b>
<b>4. Introduction</b>	<b>6</b>
4.1. Engineered nanomaterials and their potential health concerns	6
4.2. Poorly soluble, low toxicity particles (PSLT)	12
4.2.1. Particle deposition, clearance and overload	13
4.2.2. Pulmonary cellular response to inhaled particles	15
4.2.3. Pulmonary effects of inhaled nano-PSLT	20
4.2.4. Systemic Effects of inhaled nano-PSLT	21
4.2.5. Mechanism of action of inhaled PSLT	22
4.2.6. Relevance of rat model to humans	24
4.3. Inhalation toxicology of cerium dioxide (CeO <sub>2</sub> ) and barium sulfate (BaSO <sub>4</sub> ) nanoparticles	25
4.4. Nanotechnology in veterinary medicine	28
<b>5. Aim of this work</b>	<b>29</b>
5.1. Description of work	32
<b>6. Paper 1: Time course of lung retention and toxicity of inhaled particles: short-term exposure to nano-Ceria</b>	<b>34</b>
<b>7. Paper 2: Biokinetics and effects of barium sulfate nanoparticles</b>	<b>62</b>
<b>8. Inhalation exposure to cerium dioxide and barium sulfate nanoparticles for 1, 4, 13 and 52 weeks: Additional examinations</b>	<b>78</b>
8.1. One and 4 weeks of inhalation exposure to nano-CeO <sub>2</sub> and –BaSO <sub>4</sub>	78
8.1.1. Pathology	78
8.1.2. Immunohistology (cell proliferation, BrdU)	89
8.1.3. Statistical analysis	92
8.2. Thirteen and 52 weeks of exposure within the long-term inhalation study	93
8.2.1. Aerosol characterization	93
8.2.2. Results: Lung and lymph node burdens	94
8.2.3. Results: Bronchoalveolar lavage	96

8.2.4. Results: Hematology and acute phase proteins in blood	100
8.3. Summary of relevant results after 1, 4, 13 and 52 weeks of exposure to nano-CeO <sub>2</sub> (NM-212)	103
<b>9. Discussion</b>	<b>105</b>
9.1. Biokinetics and effects of CeO <sub>2</sub> in the lung	105
9.2. Biokinetics and effects of BaSO <sub>4</sub> in the lung	108
9.3. Systemic effects	112
<b>10. Conclusion</b>	<b>114</b>
<b>11. References</b>	<b>116</b>
<b>12. Annex</b>	<b>127</b>
12.1. Abbreviations	127
12.2. Erklärung/Declaration	128
12.3. Acknowledgment	129

## 1. Foreword

Nanomaterials are used in various applications, within consumer products (cosmetics, textiles, food) and for medical (tumor therapy, drug delivery) and technical (catalyst, batteries) purposes (Blasco & Pico 2011; Lewicka *et al.* 2011; Stark *et al.* 2015). Production and applications of engineered nanomaterials have increased during the last two decades.

During production, handling and use of nanomaterials, a release into the air may occur. For airborne nanoparticles, inhalation exposure is the major route of concern. There has been raised the issue that nanomaterials yield new risks for human health. Therefore, possible toxic effects and underlying mechanisms after inhalation of engineered nanoparticles have to be studied in detail. So far, no “nano-specific toxicity”, the toxicity found with nanomaterials, but not seen with other materials, has been observed; there are rather different toxic effects of different nanoparticles. Nevertheless, nanoparticles can be grouped according to certain similarities (Arts *et al.* 2014). Several industrial nanomaterials of high production volume belong to the group of granular, poorly soluble low toxicity particles (PSLT); another group has been classified as biopersistent fibrous materials.

Only little is known about long-term effects after inhalation of nanoparticles (Becker *et al.*, 2011). From studies with micron-scale, non-nano PSLT, it is known, that high lung burdens can lead to impairment of macrophage mediated clearance (ECETOC 2013). Under these lung overload conditions, inhaled PSLT can cause chronic inflammation, increase in lung weights, epithelial cell proliferation, fibrosis, and possibly lung cancer in rats (Cullen *et al.* 1999; Cullen *et al.* 2000; Lee *et al.* 1986). So far, only two nanoparticles, nano-TiO<sub>2</sub> and Carbon black, have been tested in long-term inhalation studies (Heinrich *et al.* 1995, Mauderly *et al.* 1994, Nikula *et al.* 1995). However, these studies were not conducted according to OECD test guidelines and only one single high aerosol concentration was tested. Therefore, a chronic and carcinogenicity inhalation study with two different nanoparticles was initiated in 2013. As a preparation work for the long-term study, two short-term studies with 1 and 4 weeks of exposure were performed to select the aerosol concentrations. The tested materials were nano-CeO<sub>2</sub> (NM-212) and -BaSO<sub>4</sub> both assumed to be PSLT – based on their morphology, chemical water-solubility and previous short-term studies. The long-term study was performed according to OECD test guideline no. 453 (OECD 2009), under GLP (Good Laboratory Practice) and with aerosol concentrations range set according to the outcome of the short-term studies. The results of this long-term study will be used to set (occupational) exposure limit values for humans. Furthermore, these results will help to classify the carcinogenic potential of certain nanomaterials.

This dissertation work contains the results of the short-term studies with 1 and 4 weeks of exposure as well as the interim results of the long-term study after 13 and 52 weeks of inhalation exposure to nano-CeO<sub>2</sub> (NM-212) and BaSO<sub>4</sub>. This work aims to investigate the lung deposition and clearance of inhaled nanomaterials and the resulting effects on the organism at different time points. The results will be the basis to understand and assess the results of the long-term study after two years of exposure.

## 2. Summary

The aim of this work was to compare lung clearance and retention kinetics as well as biological effects of two poorly soluble, low toxicity nanoparticles (nano-PSLT) after 1, 4, 13 and 52 weeks of inhalation exposure. The two tested nano-PSLT may represent a range of biological responses within the group.

Cerium dioxide ( $\text{CeO}_2$ ; NM-212) and barium sulfate ( $\text{BaSO}_4$ ) nanoparticles were tested for toxic effects and organ burden after inhalation exposure. Female Wistar rats inhaled nano- $\text{CeO}_2$  or -  $\text{BaSO}_4$  by whole-body exposure, 6 hours per day, 5 days per week for a total of two years. Interim results after 13 and 52 weeks of exposure including bronchoalveolar lavage fluid (BALF) analysis and determination of lung- and lymph node burdens are presented in this dissertation work. The tested aerosol concentrations were 0.1, 0.3, 1 and 3  $\text{mg/m}^3$   $\text{CeO}_2$  and 50  $\text{mg/m}^3$   $\text{BaSO}_4$ . The aerosol concentrations were selected based on the results of short-term inhalation studies with 1 and 4 weeks of exposure to 0.5, 5 and 25  $\text{mg/m}^3$   $\text{CeO}_2$  and 50  $\text{mg/m}^3$   $\text{BaSO}_4$ . Lung, lymph node and liver burdens (by inductively coupled plasma optical emission spectrometry), histopathology of lung and extrapulmonary organs and examination of BALF and blood were assessed after short-term exposure and post-exposure periods up to 129 days.

In the short-term studies with 1 and 4 weeks of exposure, inhaled nano- $\text{CeO}_2$  at low aerosol concentrations of 0.5  $\text{mg/m}^3$  were cleared from the lung at physiological rates whereas higher aerosol concentrations above 5  $\text{mg/m}^3$  retarded the lung clearance of the deposited particles and caused pulmonary inflammation already after one week of exposure. This pulmonary inflammation was still apparent by increased BALF neutrophils after long-term exposure.

After inhalation of nano- $\text{CeO}_2$ , the first sign of a pulmonary inflammation was the increase of neutrophils in BALF. Neutrophils in the initial inflammation phase were later supplemented by macrophages, and the inflammation progressed towards a granulomatous type after 4 weeks plus 4 weeks post-exposure. This effect was only observable by histopathology. Comparing inflammation upon sustained exposure and after post-exposure periods, it seems that the dose-rate drove the initial inflammation phase whereas the continuous presence of deposited particles in the lungs was driving the granulomatous inflammation. Nano- $\text{CeO}_2$  seems to be a nano-PSLT with an inherent toxicity in the lung; lung inflammation and retarded particle clearance in the lung concurred. Its toxicity mechanism needs further investigations.

In the short-term studies, inhaled nano- $\text{BaSO}_4$  showed an unusually fast clearance. This may be explained by higher *in vivo* dissolution compared to cell-free *in vitro* solubility studies. The observed fast lung clearance and high systemic bioavailability of inhaled  $\text{BaSO}_4$  *in vivo* cannot be achieved by any known physiological process but dissolution of the particles. High  $\text{BaSO}_4$  aerosol concentrations of 50  $\text{mg/m}^3$  achieved a lung burden of 0.8  $\text{mg/lung}$  after 4 weeks of exposure. At these burdens,  $\text{BaSO}_4$  caused, however, no pulmonary inflammation and no morphological changes in the lung while similar lung burdens of nano- $\text{CeO}_2$  (achieved, however, by lower aerosol concentrations) caused already significant lung effects. After 52 weeks, lung burdens of  $\text{BaSO}_4$  were, however, strongly

## Summary

increased indicating a change in the clearance rate and eventually, pulmonary inflammation indicated by increased BALF parameters occurred. There were no indications of barium-ion toxicity and the effects are regarded as being particle effects in the lung. The mechanisms of the fast lung clearance of BaSO<sub>4</sub> and the basis of its low toxicity need further investigations.

Cell proliferation rates in the lung examined by immunohistochemistry (BrdU stain of epithelial cells) were moderately increased after short-term exposure to nano-CeO<sub>2</sub>, but not after exposure to BaSO<sub>4</sub>. Cell proliferation rates in young, growing animals are, however, rather variable and the biological relevance of this moderate increase remains questionable.

Systemic effects were evaluated by analysis of blood including hematology, clinical chemistry and acute phase proteins. Inhalation exposure to nano-CeO<sub>2</sub> and -BaSO<sub>4</sub> elicited no or only minimal systemic effects after short-term and long-term exposure, respectively.

In summary, the two nanoparticles examined in this body of work differed in their particle kinetics and effects in the lung already after one week and up to 52 weeks of exposure. Within the group of nano-PSLT, nano-CeO<sub>2</sub> represents the biopersistent and higher toxicity end. Nano-BaSO<sub>4</sub> could be regarded as not being a classical PSLT, but rather soluble *in vivo* albeit indicated to be insoluble by its chemical properties and behavior *in vitro*. The remarkably low toxicity of inhaled nano-BaSO<sub>4</sub> could only partly be assigned to its fast lung clearance, but may also be the result of its low inherent toxicity.

Whether the lung burdens and biological effects observed within the first 52 weeks of exposure will lead to lung tumour formation will be revealed by histopathology after 2 years of exposure in the current long-term inhalation study.

### 3. Zusammenfassung

Das Ziel dieser Arbeit war der Vergleich zweier gering löslicher und gering toxischer Nanopartikel (Nano-PSLT) bezüglich ihrer Clearance- und Retentionskinetik in der Lunge und ihrer biologischen Effekte nach 1, 4, 13 und 52 Wochen Inhalationsexposition. Hiermit sollte die Bandbreite der Biopersistenz und Toxizität in der Gruppe der inhalierten PSLT-Nanopartikel untersucht werden.

Die Inhalationstoxizität und die Organbelastung (Gehalt der Testmaterialien in verschiedenen Organen) von Ceriumdioxid- ( $\text{CeO}_2$ ) und Bariumsulfat- ( $\text{BaSO}_4$ ) Nanopartikeln wurden nach Langzeitexposition getestet. Weibliche Wistar-Ratten wurden in Ganzkörperinhalationskammern für 6 Stunden pro Tag an fünf Tage pro Woche für insgesamt zwei Jahre exponiert. Die in dieser Arbeit präsentierten Zwischenergebnisse nach 13 und 52 Wochen Exposition beinhalten die Analyse der bronchoalveolären Lavageflüssigkeit (BALF) und die Untersuchung der Partikelbelastungen der Lunge und der assoziierten Lymphknoten. In der Langzeitstudie waren die getesteten Aerosolkonzentrationen 0,1, 0,3, 1 und 3  $\text{mg}/\text{m}^3$  für  $\text{CeO}_2$  und 50  $\text{mg}/\text{m}^3$  für  $\text{BaSO}_4$ . Diese Konzentrationen wurden anhand der Ergebnisse der vorherigen Kurzzeitstudien mit 1 und 4 Wochen Exposition festgelegt. Die Aerosolkonzentrationen dieser Kurzzeitstudien waren 0,5, 5 und 25  $\text{mg}/\text{m}^3$  für  $\text{CeO}_2$  und 50  $\text{mg}/\text{m}^3$  für  $\text{BaSO}_4$ . In den Kurzzeitstudien wurden die Tiere direkt nach der Exposition und nach einer Nachbeobachtungszeit von bis zu 129 Tagen untersucht. Die Partikelbelastungen der Lunge, Lymphknoten und Leber wurden mit Massenspektrometrie mit induktiv gekoppeltem Plasma gemessen. Die Histopathologie der Lunge und extrapulmonalen Organe sowie die bronchoalveoläre Lavageflüssigkeit und das Blut wurden weiterhin untersucht.

Die Inhalation von niedrigen Aerosolkonzentrationen von 0,5  $\text{mg}/\text{m}^3$  Nano- $\text{CeO}_2$  in den Kurzzeitstudien führte zu Partikelbelastungen, die mit einer physiologischen Rate aus der Lunge gereinigt wurde. Aerosolkonzentrationen von 5  $\text{mg}/\text{m}^3$  und höher verlangsamten die Partikelreinigung und verursachten bereits nach einwöchiger Exposition eine Entzündung in der Lunge. Dies war auch nach der Langzeitexposition anhand von erhöhten BALF-Neutrophilenzahlen erkennbar. Nano- $\text{CeO}_2$  repräsentiert innerhalb der Gruppe der Nano-PSLT Nanopartikel mit einer gewissen inhärenten Toxizität in der Lunge, die noch detaillierter untersucht werden muss. Nach der Inhalation der untersuchten  $\text{CeO}_2$ -Nanopartikel war die Erhöhung der neutrophilen Granulozyten in der BALF das erste Anzeichen einer Entzündung in der Lunge. Dieser Entzündungsprozess wurde später durch Makrophagen ergänzt und entwickelte einen granulomatösen Charakter nach vierwöchiger Exposition und vierwöchiger Nachbeobachtungszeit ohne Exposition. Die spätere granulomatöse Entzündung war nur in der Histopathologie erkennbar. Wenn man den Verlauf der Entzündungen bei anhaltender Exposition und nach dem Ende der Exposition vergleicht, ergaben sich Unterschiede. Die Dosisrate (der Partikeleintrag in die Lunge pro Zeiteinheit) schien die initiale Entzündung zu bestimmen; dieser Prozess klang nach dem Ende der Exposition ab. Die Entwicklung der Entzündung zur granulomatösen Entzündung dagegen schien durch die andauernde Präsenz der Partikel in der Lunge verursacht zu sein; hohe Partikelbelastungen in der Lunge trugen auch nach dem Ende der Exposition zu diesem Prozess bei.

In der Kurzzeitstudie wurden die BaSO<sub>4</sub>-Nanopartikel ungewöhnlich schnell aus der Lunge entfernt. Dies kann möglicherweise durch eine höhere Löslichkeitsrate der BaSO<sub>4</sub>-Nanopartikel begründet werden, da die schnelle Clearance aus der Lunge und hohe systemische Bioverfügbarkeit nicht durch einen bekannten physiologischen Reinigungsprozess erklärt werden kann. Nach vierwöchiger Inhalation hoher Aerosolkonzentrationen von 50 mg/m<sup>3</sup> BaSO<sub>4</sub> wurden Lungengehalte von 0.8 mg pro Lunge gemessen, die keine Entzündung oder morphologische Veränderungen in der Lunge zur Folge hatten. Hingegen verursachten vergleichbare Lungengehalte von Nano-CeO<sub>2</sub> bereits deutliche Effekte in der Lunge. Nach 52-wöchiger Exposition von Nano-BaSO<sub>4</sub> stiegen die Lungengehalte jedoch deutlich an. Mit dieser verringerten Partikelreinigungskapazität der Lunge ging ein Entzündungsgeschehen in der Lunge einher, das durch eine Erhöhung der BALF-Parameter gekennzeichnet war. Dies sprach eher für Partikeleffekte in der Lunge. Zudem gab es keinen Hinweis auf toxische Effekte durch Barium-Ionen. Die schnelle Clearance und der ihr zugrundeliegende Mechanismus sowie die geringe Toxizität der BaSO<sub>4</sub>-Nanopartikel benötigen weitere und detailliertere Untersuchungen.

Die Zellproliferationsraten in der Lunge wurden mittels einer immunhistochemischen Färbung von BrdU-markierten Epithelzellen erfasst. Sie zeigten einen moderaten Anstieg nach der Kurzzeitexposition mit Nano-CeO<sub>2</sub>, jedoch keinen Anstieg mit Nano-BaSO<sub>4</sub>. Jedoch können Zellproliferationsraten in jungen und wachsenden Tieren variieren. Die biologische Relevanz dieses Anstiegs ist daher fraglich.

Neben lokalen Effekten in der Lunge wurden auch systemische Effekte anhand der Hämatologie und klinisch-chemischer Untersuchungen des Blutes, einschließlich der Messung von Akute-Phase-Proteinen, untersucht. Nach Kurzzeit- und Langzeitinhalationsexpositionen zeigten Nano-CeO<sub>2</sub> und – BaSO<sub>4</sub> keine oder nur geringgradige systemische Effekte.

Die beiden hier untersuchten Nanopartikel unterschieden sich sowohl in ihrer Partikelkinetik als auch in ihren biologischen Effekten in der Lunge. Dies war bereits nach einer Woche und dann über die Expositionszeit von 52 Wochen zu beobachten. Innerhalb der Nano-PSLT repräsentiert CeO<sub>2</sub> Nanopartikel mit hoher Biopersistenz und inhärenter Toxizität. Nano-BaSO<sub>4</sub> kann nicht als klassischer PSLT-Nanopartikel angesehen werden, obwohl es in abiotischen Systemen wasserunlöslich ist. Die bemerkenswert geringe Toxizität inhalierter BaSO<sub>4</sub>-Nanopartikel kann nur teilweise auf dessen schnellere Clearance zurückgeführt werden; Nano-BaSO<sub>4</sub> hat daneben auch eine geringe inhärente Toxizität.

Ob die Partikelbeladungen der Lunge und die biologischen Effekte, die innerhalb der ersten 52 Wochen der Exposition beobachtet wurden, sich zu Lungentumoren weiterentwickeln, kann erst durch die histopathologischen Untersuchungen nach zweijähriger (Lebenszeit-)Exposition geklärt werden.

## 4. Introduction

### 4.1. Engineered nanomaterials and their potential health concerns

Nanomaterials are used in various applications, within consumer products (cosmetics, textiles, food) and for medical (tumor therapy, drug delivery) and technical (catalyst, batteries) purposes (Blasco & Pico 2011; Lewicka *et al.* 2011). Production and applications of engineered nanomaterials have accelerated in the last decades. By 2015, the European Commission predicts a global volume of € 2 trillion for “nanotechnology involved products” (European Commission 2013b).

An overview of major definitions of the term “nanomaterial” in Europe is presented in table 1. Common to all of these definitions is “nanoscale” but they differ in regard of mass or number size distribution, focusing on natural, engineered or intentionally manufactured nanoparticles, and unique nanospecific properties. Especially European Regulators ask for a harmonized definition to be used in the regulatory environment (Joint Research Centre of the European Commission 2010). The proposed definition of the European Commission (EC) includes number size distribution of 1 to 50 %, size of internal structural elements and surface area (European Commission 2011a; Liden 2011). However, these requirements also cover other materials which may otherwise not be considered to be nanomaterials. Conventional particulate materials (pigments, catalysts) of micron and submicron size have size distributions with a tail of primary particles below 100 nm; this nanoparticle fraction represents a small mass fraction but may account for a large number fraction (Brown *et al.* 2013). The European Commission aims to create a consistent definition and nomenclature of nanomaterials being the prerequisite for their regulation (Bleeker *et al.* 2013).

The European chemical regulation REACH (Registration, Evaluation, Authorisation and Restriction of Chemicals) and CLP (Classification, Labelling and Packaging) addresses substances, on their own, in preparations or in articles, in whatever size, shape or physical state (European Commission 2013a). It further states: “The term ‘nanomaterial’ can be used as a synonym for a substance at the nanoscale/nanoform, on its own, in a preparation or in an article.” However, to date, there are no specific requirements for nanomaterials. Therefore, the European Commission plans to modify the REACH Annexes. A “Study for Impact Assessment of relevant regulatory options for nanomaterials” within REACH contains an assessment of future options to address nanomaterials under REACH with the aim “to ensure further clarity on how nanomaterials are addressed and safety demonstrated in registration dossiers” (Matrix Insign Ltd 2014). Specific regulations (for food and cosmetics) demand nanomaterial ingredients to be labelled (European Commission 2011c). The information that products contain nanomaterials may, however, give no information on their human health hazards (Gebel *et al.* 2014).

Material properties of nanomaterials can be different from properties of the corresponding larger microscale materials. This difference is exploited in many technical applications of nanomaterials, and has raised the concern that they may have novel toxicological properties compared to larger materials (Nel *et al.* 2006; Oberdörster *et al.* 2005). Due to their small size, larger surface area per mass or

volumes and increased surface reactivity, particulate nanomaterials (nanoparticles) may have a higher biological activity on a mass basis and affect other compartments of the body compared to larger size particles with identical composition (Oberdörster *et al.* 2005). One option of this feature can be utilized to develop more effective and efficient formulations of therapeutic drugs (as discussed in chapter 4).

With regard to toxicology, no “nano-specific-effect” could be detected. Effects observed with nanoparticles were also seen with other particles of the same or a different composition and size (Donaldson & Poland 2013; Gebel *et al.* 2013; Oomen *et al.* 2014). Hence, there is no general “nanotoxicity” exhibited by all nanoparticles, but rather different toxic effects of different nanoparticles. Not unlike the toxicity of different microscale particles, the same toxicological concerns are raised for nanoparticles and the type of effect in primary target organs seems to be similar to microscale particles.

During production, handling and use of nanomaterials at the workplace, a release into the air may occur. For airborne nanoparticles, inhalation exposure is the major route of concern. Toxicological data for airborne particles can be derived from human studies (epidemiological studies, volunteers inhaling particles), animal studies and *in vitro* studies (Valberg *et al.* 2009). For broad application and prospective information, *in vivo* inhalation studies are the method of choice. *In vivo* instillation studies in rodents use bolus exposure conditions which are not reflecting the actual human exposure and are not applicable for long-term, repeated exposure studies. Likewise, *in vitro* systems most often do not adequately reflect the real-life concentration and form of nanoparticles and their read-out often interferes with the nanoparticles (Landsiedel *et al.* 2012b). Instillation and *in vitro* studies may be valuable tools to guide testing strategies and provide data to support grouping of nanomaterials (Arora *et al.* 2012; Arts *et al.* 2014; Kroll *et al.* 2012; Oomen *et al.* 2014; Stone *et al.* 2009).

Extensive safety research within the last decade on nanomaterials improved the data base and knowledge on their effects after inhalation. But still, for many nanomaterials, the experimental toxicological database is not complete. Especially information on long-term effects, including carcinogenicity, is missing (Becker *et al.* 2011). Long-term inhalation studies are only available for titanium dioxide and carbon black nanoparticles (and diesel exhaust) (Heinrich *et al.* 1995, Mauderly *et al.* 1994, Nikula *et al.* 1995). Carbon black, however, is used since the early 20<sup>th</sup> century and an increased cancer risk from human exposure to these nanoparticles has not yet been observed (Anderson 2010). In terms of common particle toxicity, exposure to carbon-containing dusts (coal miners) can induce pneumoconiosis which is characterized by particle accumulation in the lungs, inflammation and macrophage involvement leading to granuloma formation (De Capitani *et al.* 2007; Wang & Christiani 2000; Szozda 1996). Silicosis and lung cancer induced by crystalline silica particles in the lungs occurred in humans working in coal- and metal-mining and building industries (IARC 1997). The mechanism involved impaired particle lung clearance together with macrophage activation and persistent pulmonary inflammation leading to inflammation-driven secondary genotoxicity (Borm *et al.* 2011; IARC 1997). Respirable crystalline silica (quartz) particles are considered to be high-toxicity particles and, inhaled from occupational sources, they are classified by the International Agency for Research on Cancer (IARC) as Group 1 human carcinogens (IARC 1997). These

mentioned dust materials have been studied in detail and are known to be able to cause lung tumors in both humans and animals. Transferring conventional particle toxicology to the nanoscale feature, inhaled nanoparticles may cause adverse health effects in the lung as well as in extra-pulmonary organs. The lung is the main portal of entry and primary target site for inhaled particles. However, inhaled nanoparticles have also shown to translocate via the blood system to extrapulmonary organs, such as spleen and liver, and to provoke systemic effects (Elder & Oberdörster 2006; Kreyling *et al.* 2002). Neuronal translocation via the olfactory nerve to the brain and inflammatory changes in the olfactory bulb have also been reported following inhalation exposure to nanosized carbon and manganese oxide (Elder *et al.* 2006; Oberdörster *et al.* 2004). On the other hand, high concentrations of intravenously injected TiO<sub>2</sub> nanoparticles did not cause toxicity in rats (Fabian *et al.* 2008).

Nanomaterials differ in composition (core and shell chemistry and crystal structure) and geometry (shape and size). Moreover, exposure to nanoparticles usually involves the primary particles as well as aggregates and agglomerates of these particles. Their physico-chemical characteristics can influence their uptake and distribution in the body and the subsequent biological effects. Data on modes of action of nanoparticles, mechanisms leading to toxicity and related aspects of biokinetics are still required (European Commission 2004). To avoid extensive toxicological testing of each single nanomaterial, grouping or categorization strategies are needed (Arts *et al.* 2014). This will allow an efficient safety assessment of different nanomaterials and help to reduce animal testing according to the 3R-concept (Reduce, Refine, and Replace) (Russel & Burch 1959). Material properties are linked to biological effects and can be used for grouping (e.g. in classical QSAR approaches) (Burello & Worth 2011a; Burello & Worth 2011b). The biological pathway leading from material properties to the apical toxic effect may be complex and is often not yet fully understood. Rather than correlating material properties to adverse outcome, additional grouping criteria along the biological pathway can be applied.

Arts *et al.* (2014) reviewed the available grouping strategies and recommended a “source-to-adverse-outcome pathway” in which relevant physico-chemical properties, exposure, biokinetics and hazard endpoints are covered (Arts *et al.* 2014; Oomen *et al.* 2014). Grouping should include all aspects of the whole life-cycle of a nanomaterial. This comprehensive “multiple perspective framework” considered nanomaterial properties and biophysical interactions, their use, exposure and disposal, their uptake and kinetics, possible early and apical biological effects. These approaches aid to simplify a future hazard assessment because it is difficult to correlate nanomaterial induced effects to one special material property. Further proposals and concepts for grouping of nanomaterials are currently emerging.

Many industrial relevant nanomaterials belong to the group of respirable granular biodurable particles without known significant specific toxicity (GBS) (as mentioned in chapter 4.2) (Gebel 2012; Roller & Pott 2006). For those dusts, a general threshold value at workplaces has been assigned by the Commission for the Investigation of Health Hazards of Chemical Compounds in the Work Area (DFG, German Research foundation) (DFG Deutsche Forschungsgemeinschaft 2013a). However, the recommendations apply to bulk-, not specifically to nano-dusts (also called “ultrafine”).

The German Maximum Workplace Concentration (MAK; "Maximale Arbeitsplatzkonzentration") value is a threshold limit value (TVL) to which workers can be exposed daily for working-life time (8 hours/day, average of 40 hours/week) without known adverse health effects. The MAK value is often derived from a no observed adverse effect level (NOAEL) of a 90-day inhalation study with animals (Deutsche Forschungsgesellschaft (DFG) 2014). In 2011, the Commission lowered the general threshold value for dust for the respirable fraction (dust particles reaches the alveoli, formerly called "fine dust" until 1996) from 1.5 mg/m<sup>3</sup> to a new MAK value of 0.3 mg/m<sup>3</sup> (respirable (R)-fraction) for a density of 1 g/cm<sup>3</sup>. The R-fraction of biopersistent granular dusts is categorized in Carcinogen Category 4 which includes substances with typically non-genotoxic mechanisms. At the international level, however, occupational exposure limits (OEL) of specific nanomaterials already exist. Recommended exposure limit values of titanium dioxide are 2.4 mg/m<sup>3</sup> (fine (> 0.1 µm)) and 0.3 mg/m<sup>3</sup> (ultrafine, including "engineered nanoscale") recommended by the US National Institute for Occupational Safety and Health (NIOSH) (National Institute for Occupational Safety and Health (NIOSH) 2011). The value covers up to 10 working hours per day during a 40-hour work week.

However, generic OELs of nanomaterials are not yet available in Germany (DFG Deutsche Forschungsgemeinschaft 2013b; Packroff & Baron 2013). OELs for bulk materials applied to nanomaterials may provide no adequate protection for workers (Dankovic *et al.* 2007; Schulte *et al.* 2010). Schulte *et al.* (2010) recommended that OELs should be developed for specific groups of nanomaterials rather than for individual nanomaterials (Schulte *et al.* 2010). For this, grouping approaches using mode of action and material properties can be applied together with concentration-response data from animal studies.

Table 1 Overview of definitions of “nanomaterial” or “nano” related terms

Term	Definition	Source
Nanomaterial	<i>“Material with any external dimension in the nanoscale or having internal structure or surface structure in the nanoscale.”</i>	International Organisation for Standardisation (ISO), Technical Specifications (TS) ISO/TS 80004-1:2010 <a href="http://www.iso.org/iso/home/store/catalogue_tc/catalogue_detail.htm?csnumber=51240">http://www.iso.org/iso/home/store/catalogue_tc/catalogue_detail.htm?csnumber=51240</a> , 09.03.15
Nanoscale	<i>“Size range from approximately 1 nm to 100 nm.”</i>	ISO/TS 27687:2008 <a href="http://www.iso.org/iso/home/store/catalogue_tc/catalogue_detail.htm?csnumber=44278">http://www.iso.org/iso/home/store/catalogue_tc/catalogue_detail.htm?csnumber=44278</a> , 09.03.15
Manufactured nano-object	<i>“Nano-object intentionally produced for commercial purposes to have specific properties or composition”</i>	ISO/TS 12805:2011 <a href="http://www.iso.org/iso/home/store/catalogue_tc/catalogue_detail.htm?csnumber=51766">http://www.iso.org/iso/home/store/catalogue_tc/catalogue_detail.htm?csnumber=51766</a> , 09.03.15
Nanomaterial	<i>“A natural, incidental or manufactured material containing particles, in an unbound state or as an aggregate or as an agglomerate and where, for 50 % or more of the particles in the number size distribution, one or more external dimensions is in the size range 1 nm - 100 nm. In specific cases and where warranted by concerns for the environment, health, safety or competitiveness the number size distribution threshold of 50 % may be replaced by a threshold between 1 and 50 %.”</i>	European Commission (European Commission 2011a) COMMISSION RECOMMENDATION of 18 October 2011 on the definition of nanomaterial, 2011/696/EU, 2011

Continuation of Table 1 Overview of definitions of “nanomaterial” or “nano” related terms

Term	Definition	Source
Nanomaterial	<i>“An insoluble or biopersistent and intentionally manufactured material with one or more external dimensions, or an internal structure, on the scale from 1 to 100 nm.”</i>	European Union Cosmetic Products Regulation Regulation (EC) No 1223/2009 on cosmetic products. – OJ L342, 22.12.2009, p. 59
Engineered nanomaterial	<i>“Any intentionally produced material that has one or more dimensions of the order of 100 nm or less or is composed of discrete functional parts, either internally or at the surface, many of which have one or more dimensions of the order of 100 nm or less, including structures, agglomerates or aggregates, which may have a size above the order of 100 nm but retain properties that are characteristic to the nanoscale.”</i>	European Union Novel Foods, Commission proposal for a Regulation on novel foods and amending Regulation (EC) No 258/97. – 14.1.2008, COM(2007) 872 final, 2008/0002 (COD)

## 4.2. Poorly soluble, low toxicity particles (PSLT)

Respirable granular biodurable particles (GBS) (Gebel 2012; Roller & Pott 2006) (as mentioned in chapter 4.1) are also known as poorly soluble, low toxicity particles (PSLT) (Dankovic *et al.* 2007; Maynard & Kuempel 2005), poorly soluble particles (PSP) (Oberdörster 2002a) or low-solubility low-toxicity particles (LSLTP) (Monteiller *et al.* 2007). They are further termed as low toxicity (LT) dusts (Cherrie *et al.* 2013). PSLT include nano- and larger particles.

Within the group of PSLT, there are high production volume and industrial relevant materials such as titanium dioxide, carbon black, coal dust, barium sulfate (BaSO<sub>4</sub>), zirconium oxide (ZrO<sub>2</sub>) and cerium dioxide (CeO<sub>2</sub>).

PSLT are solid, granular, non-fibrous particles which are poorly soluble ("PS") or insoluble in biological fluids and therefore biopersistent. Chemical dissolution is observed for biosoluble nanoparticles such as Zinc oxide with rapid clearance and release of toxic ions (Zn<sup>2+</sup>) (Xia *et al.* 2008).

Due to their surface energy, dispersed nanoparticles tend to agglomerate. This was also shown for nano-PSLT. Aerosolized and inhaled TiO<sub>2</sub> particles at the workplace comprise of a 20% fraction of particles <100 nm and 80 % larger agglomerates (Ma-Hock *et al.* 2007; Morfeld *et al.* 2012). However, only agglomerates >100 nm were found in the lungs and lymph nodes after 1 week (5 days) of inhalation. Therefore, deposition of inhaled nanoscaled particles in the lung seems to play a minor role and associated potential effects may be rather caused by agglomerated than by nanoscaled particles. On the other hand, disintegration of larger agglomerates to nanosized structures in the lung appears to be unlikely since agglomerated nanostructured TiO<sub>2</sub> particles do not seem to disintegrate into smaller structures after exposure to biological fluids similar to lung surfactant (Maier *et al.* 2006; Morfeld *et al.* 2012). However, there are also other studies available which indicate a certain deagglomeration in the lung, e.g. with multi-walled carbon nanotubes (Mercer *et al.* 2013a, Mercer *et al.* 2013b; Oberdörster *et al.* 1992).

In general, inhaled PSLT exhibit no or low cytotoxicity and no or low acute toxicity ("LT"). Compared to insoluble particles with known specific toxicity, such as the chemically active, cytotoxic crystalline silica (quartz), PSLT are rather non-reactive, without a known, specific toxicity. They exhibit no specific functional chemical surface groups and their toxicity is not based on specific substances present in the particles (Gebel *et al.* 2014). Furthermore, PSLT exhibit no primary genotoxicity which is defined as "genetic damage elicited by particles in the absence of pulmonary inflammation" (ILSI Risk Science Institute Workshop Participants 2000; Schins & Knaapen 2007).

Prolonged exposure and high lung burdens of PSLT can lead to impairment of macrophage mediated clearance (as mentioned in chapter 4.2.1.) (ECETOC 2013). This overload condition is accompanied by increased particle transfer to the lymph nodes and accumulation of particles in the lung. Under overload conditions, inhaled PSLT can cause chronic inflammation, increases in lung weights,

epithelial cell proliferation, fibrosis, and possibly lung cancer in rats (Cullen *et al.* 1999; Cullen *et al.* 2000; Lee *et al.* 1986).

#### 4.2.1. Particle deposition, clearance and overload

Deposition of inhaled particles in the respiratory tract is determined by particle characteristics (size, shape, density, aerodynamic diameter and aggregation), the geometry of the airways and breathing pattern. Mechanisms of deposition are diffusion (Brownian motion), sedimentation, impaction and interception. The latter three are more relevant for larger particles while deposition of nanoparticles is mostly driven by diffusion (Oberdörster *et al.* 2005).

Inhaled particle deposition in the lung is not uniformly distributed. In human and rats, more particles are deposited near the bifurcation and the entry of the alveolar ducts (Brain *et al.* 1976; Brody & Roe 1983; Holma 1969; Snipes 1989). The mass median aerodynamic diameter (MMAD) of particles affects aerosol deposition in the lung. In humans, about 50% of the particles with an aerodynamic diameter of > 20 µm (inhalable fraction) can enter the respiratory system by the nose or mouth. With a 50% probability, particles < 4 µm aerodynamic diameter can reach the alveoli (respirable fraction) (ISO 2008; Maynard & Kuempel 2005). In the alveolar region, particles with a 20 nm size have the highest deposition rate whereas 1 nm particles have nearly no deposition (Oberdörster *et al.* 2005).

Clearance of particles depends on the region where they are deposited (nasopharyngeal, tracheobronchial or pulmonary) (Snipes 1989). Particle removal can include dissolution-absorption processes or physical transport (e.g. uptake by phagocytic cells like alveolar macrophages). The latter is the most prevalent for PSLT in the lower respiratory tract.

In the upper respiratory tract, coughing, sneezing and the mucociliary system are the first line of defense. The mucociliary escalator rapidly clears particles deposited in the tracheobronchial region with retention half-times from 24 to 48 hours (fast clearance) (IARC 1996). In the alveolar region, alveolar macrophages (AM) (and neutrophils) are attracted by chemotactic stimuli and migrate into the alveolar space with the aim to phagocytize, degrade or transport deposited particles. Via migration to terminal bronchioles, particles are transported to the mucociliary escalator and further to the larynx (Oberdörster 1988). These particles are swallowed and then excreted after passage through the gastro-intestinal tract. A smaller particle fraction may also be translocated to the lung-associated lymph nodes either by transepithelial migration of particle-containing alveolar macrophages or by translocation of free particles to the interstitium (IARC 2010; Ma-Hock *et al.* 2009; Ravenzwaay *et al.* 2009). Furthermore, certain conditions, e.g. pulmonary inflammation, can influence mucociliary clearance, phagocytosis, uptake and transport of particles to or through the epithelium (Oberdörster *et al.* 1994a).

Phagocytosis of deposited particles by macrophages in the alveolar space starts within the first 6-12 hours. After phagocytosis of the particles, the macrophages slowly move toward the mucociliary escalator. The subsequent migration of the laden macrophages is, however, rather slow. Retention half-times for rats and humans are around 70 and 700 days, respectively (Bailey *et al.* 1989; Landsiedel *et al.* 2012a ; Oberdörster *et al.* 2005).

Retention is a “time-dependent distribution pattern” of deposited but not yet cleared particles, and is associated with potential lung effects (Morrow 1988; Snipes 1989). The particle content of the lung achieved by inhalation at given time is called lung burden. If the deposition rate is less or equal to the clearance rate at low inhaled concentrations, a steady-state lung burden develops (Oberdörster *et al.* 1992). The steady state of lung burdens can be reached after approximately 5 retention half-times have passed (Oberdörster 1995). High aerosol concentrations and/or prolonged, chronic exposure of PSLT can result in high lung burdens which overwhelm the mechanical macrophage-mediated clearance as observed by the decreased migration of macrophages to the mucociliary escalator. Clearance retardation with a constant exposure results in increasing retention half-times and consequently increasing lung burdens. This general condition was called dust overload and assigned to animals (e.g. rats, dogs) and possibly humans (Morrow 1988).

Morrow (1988) estimated that volumetric overload starts when 6% of the average macrophage volume is filled with particles indicating a threshold above which macrophage clearance may decrease (Morrow 1988; Morrow *et al.* 1996). The 6% volume load of a macrophage can be expressed as a volumetric lung burden of 1  $\mu\text{L}$  particles/ g lung of rats (Oberdörster 1995). Retardation of macrophage-mediated clearance and prolonged particle retention can lead to macrophage aggregates, higher access of particles to the interstitium and increased translocation rate to the lung associated lymph nodes (Tran *et al.* 2000). Overall, overload conditions have been related to pulmonary responses such as increased lung weights, pulmonary inflammation and increased cell proliferation with subsequent fibrosis and tumor formation in rats (ECETOC 2013; ILSI Risk Science Institute Workshop Participants 2000; Muhle *et al.* 1991).

This concept was established in reference to larger PSLT; however, the overload concept may also be applicable to inhaled nano-PSLT. Twelve weeks of inhalation of a 23.5 mg/m<sup>3</sup> TiO<sub>2</sub> aerosol (Degussa, anatase, 25 nm) and a burden of 5.22 mg/lung resulted in a retention half-time of 501 days, increased accumulation of nano-TiO<sub>2</sub> in the regional lymph nodes and lung inflammation (based on analysis of bronchoalveolar lavage) (Oberdörster *et al.* 1994). Pulmonary inflammation was correlated with a large surface area and high interstitialization of nano-TiO<sub>2</sub>. In the same 12-week inhalation study, micron-TiO<sub>2</sub> (Degussa, 250 nm) with a similar concentration of 22.3 mg/m<sup>3</sup> (burden of 6.62 mg/lung) was tested as a separate dose group and showed a lower potential for clearance retardation, particle translocation and inflammation.

Volumetric macrophage loads of micron- and nano-TiO<sub>2</sub> were 9% and 2.6%, respectively, with a clearance of the latter prolonged by a factor of 4 and no correlation to volumetric overload. The authors stated that observed effects and retardation of clearance cannot only be explained by volume

overload of macrophages but that particle surface correlated better with the prolongation of clearance. There may be additional factors which elicited responses similar to those observed with overload conditions (IARC 2010). Macrophages may also be affected by increased oxidative stress due to the large surface area of the nanoparticles or generation of ROS on the surface. In cases of inhaled nano-PSLT, the retained concentration in the alveolar macrophages expressed as particle surface area may be more predictive for retarded clearance than the volume load formerly proposed by Morrow (Oberdörster *et al.* 1994, Tran *et al.*, 2000) (as mentioned in chapter 4.2.5.).

Furthermore, some nano-PSLT may escape macrophage clearance mechanisms and get access to the interstitium (Ferin *et al.* 1992). Twelve week inhalation of two TiO<sub>2</sub> particles (around 21 nm and 250 nm diameters) showed that, at equal masses, more nano-TiO<sub>2</sub> than micron-TiO<sub>2</sub> translocated to the interstitium resulting in prolonged lung retention of these nanoparticles. A neutrophil based inflammation was observed directly after exposure but decreased to control values after a post-exposure period; however, the lung burdens were still elevated.

#### **4.2.2. Pulmonary cellular response to inhaled particles**

Inhaled particles are deposited on the alveolar epithelial surface which consists of type I and II alveolar cells. In close contact with alveolar epithelial cells, alveolar macrophages (and also other phagocytes) have the task to remove particles by phagocytosis, their degradation via released mediators and transport to the mucociliary escalator. Particle transport to the blood or lymph nodes by macrophages may also play a role, depending on size and concentration.

Macrophages belong to the mononuclear phagocytic system (MPS). They originate from short-lived blood monocytes or have an embryonic origin without involving blood monocytes (Scott *et al.* 2014). Four different types of pulmonary macrophages are described: pleural, intravascular, interstitial and alveolar (Geiser 2010). Growth and differentiation from stem cells in the bone marrow to monocytes and later macrophages depends on cytokines like macrophage colony-stimulation factor (M-CSF) and granulocyte-macrophage colony-stimulation factor (GM-CSF) (Gordon 2003). Alveolar macrophages are long-lived, resident tissue cells scattered in the (healthy) lung with a turnover rate of 40% in one year (Janssen *et al.* 2011; Maus *et al.* 2006). Macrophages can be rapidly recruited from circulating monocytes and migrate along a chemoattractant gradient (chemotaxis) into the alveolar space. However, distinction between originally resident macrophages from recently recruited macrophages may be difficult since they adapt to their pulmonary environment (Gordon 2003).

With their surface receptors (toll-like, G-protein coupled receptors, receptors for opsonins and cytokines), macrophages recognize endogenous and exogenous agents such as inhaled particles (Arredouani *et al.* 2004; Conner & Schmid 2003). Regulation, inhibition and activation of blood born macrophages include a cascade of events involving interactions between alveolar macrophages, epithelial cells and soluble mediators (table 2). To maintain homeostasis, type II alveolar epithelial

cells with their CD200 receptor, their  $\alpha\text{v}\beta\text{6}$  Integrin for transforming-growth factor  $\beta$  (TGF- $\beta$ ) attachment and secreted Interleukin-10 (IL-10) balance macrophage activation with inhibitory signals (Hussell & Bell 2014). Activation consists of the classical M1 and the alternative M2 macrophage pathways (Gordon 2003). The M1 is activated by microbes, toll-like receptor ligands or Interferon- $\gamma$  (IFN- $\gamma$ ) which is produced by natural killer cells and activated T-lymphocytes.

The synthesis and release of chemokines, cytokines (such as IL-1, IL-12, IL-23, tumor necrosis factor TNF), growth factors, and proteases by macrophages and other (epithelial) cells prolong inflammation (table 2). This results in an influx of other inflammatory cells, proliferation of fibroblasts and collagen deposition. TNF $\alpha$  as chemoattractant is mainly involved in inflammatory cell recruitment and activation after particle exposure (Driscoll 2000). Monocyte chemoattractant protein-1 (MCP-1) has shown to be chemoattractant for mononuclear phagocytes (e.g. macrophages), lead to their recruitment and stimulate their oxidant production (Driscoll *et al.* 1996; Rollins *et al.* 1991). Therefore, this pathway is responsible for triggering inflammation. The alternative modulators of macrophage activation (M2, alternative way) are IL-4 and IL-13. This way limits inflammation by release of IL-10 and Transforming Growth Factor (TGF- $\beta$ ). However, the M2 macrophage also contributes to repair and fibrosis by TGF- $\beta$ , the inflammatory resistin-like secreted protein FIZZ1 and chitinase-like secretory lectin YM1 (Hussell & Bell 2014). In general, activated macrophages possess a higher phagocytic capacity, oxidative burst and proinflammatory cytokine production than inactivated (Lohmannmatthes *et al.* 1994; Steinmuller *et al.* 2000). During chronic inflammation, macrophages may persist due to local proliferation and sustained recruitment from the blood (Gentek *et al.* 2014).

Depending on the concentration, inhaled (nano)particles cause inflammation. They may directly interact with and affect alveolar macrophages. Particulate nano-TiO<sub>2</sub> (size of 20 nm) was taken up by alveolar macrophages and stored as aggregates in lysosome-like vesicles (Liu *et al.* 2010b). After instillation of 5 and 50 mg/kg nano-TiO<sub>2</sub> in rats, alveolar macrophages showed membrane damage, decreased phagocytic and chemotactic ability and an increase in nitric oxide (NO)- and TNF $\alpha$ -levels. These effects could be explained by the high exposure concentration of 50 mg/kg, surface area and crystal structure of nano-TiO<sub>2</sub> (Liu *et al.* 2010a). Other nanoparticles, such as nano-SiO<sub>2</sub>, were shown to be M1-polarising proinflammatory stimuli by increasing the production of IL-1 $\beta$  and TNF- $\alpha$ , both major cytokines for acute inflammation (Lucarelli *et al.* 2004).

The optimum size of particles which are effectively phagocytized is 1.5 - 3  $\mu\text{m}$ . After particle engulfment, the alveolar macrophages exert to kill microorganisms or degrade particles in the phagolysosome by release of reactive oxygen species (ROS), NO and lysosomal enzymes. ROS can have intracellular impact on macrophages and other phagocytes, but they can also affect epithelial cells resulting in DNA damage, influencing signal transduction pathways and altering gene expression (Deutsche Forschungsgesellschaft (DFG) 2014; Driscoll *et al.* 1995a; Driscoll *et al.* 1995b; Driscoll *et al.* 1995c; Driscoll 2000).

For example, ROS increase the synthesis and release of IL-1, IL-6 and TNF- $\alpha$  in alveolar macrophages and epithelial cells (Driscoll *et al.* 1995a). TNF- $\alpha$ , in turn, increases the synthesis of

prostaglandin E2 and prostacyclin and the synthesis of ROS and NO radicals in leukocytes (Deutsche Forschungsgesellschaft (DFG) 2014). ROS also activate transcription factor NF- $\kappa$ B which stimulates inflammatory and proliferative gene expression. For instance, the gene promoter of neutrophil chemoattractant macrophage inflammatory protein-2 (MIP-2 $\alpha$ ) has a NF- $\kappa$ B-binding site and activation of them by ROS leads to formation of MIP-2 $\alpha$ . Increased lung mRNA expression of MIP-2 and increased neutrophil numbers in BAL were observed after 13 weeks of inhalation exposure to 7.1 and 52.8 mg/m<sup>3</sup> carbon black (Monarch 880, particle diameter of 0.016  $\mu$ m) (Driscoll *et al.* 1996). MIP-2 and also interleukin 8 (IL-8)/ cytokine-induced-neutrophil-chemoattractant (CINC-1; rat homologue of IL-8) further appeared to be proliferative and mitogenic stimuli for epithelial cells since IL-8 can increase mRNA synthesis in airway epithelial cells (Donaldson *et al.* 2008; Driscoll *et al.* 1995b; Standiford *et al.* 1990). The chemokine CINC-1 which is released by activated macrophages is also responsible for activation and chemotaxis of neutrophils (Driscoll *et al.* 1997; Grommes & Soehnlein 2011) (table 2).

Further recruitment of inflammatory cells includes the lymphocytes and polymorph nuclear neutrophils involved in acute and subchronic inflammatory processes. Since neutrophils respond faster to chemotaxis and inflammatory signals evoked by deposited particles in the lung, they appear earlier than recruited macrophages. Peak numbers of neutrophils are described within 6-48 hours after particle deposition and they are replaced by monocytes and lymphocytes thereafter (Alber *et al.* 2012). TNF- $\alpha$  from surveillance macrophages increases expression of E-selectin and vascular cell adhesion molecule (VCAM-1) on capillary endothelial cells which enable trapping of neutrophils and monocytes at the blood wall and migration through the endothelial pores (Hussell & Bell 2014). Depending on the degree of neutrophil activation, neutrophil recruitment into the interstitium and alveolar airspace of the lung can result in tissue injury (Grommes & Soehnlein 2011).

However, mechanistic details of nanoparticle macrophage interaction leading to inflammation and secondary development of oxidative stress have not been sufficiently studied (Deutsche Forschungsgesellschaft (DFG) 2014). In cases of macrophage damage and death, the formerly phagocytized particles are re-released into the alveolar space. Free (non-phagocytized), persistent and small sized particles on the alveolar surface can be re-uptaken by other alveolar macrophages which can lead to particle redistribution among the alveolar macrophages of the lungs (Lehnert 1992). However, particles can also get in contact with epithelial cells and be taken up by alveolar epithelial cells, especially by type I cells (Ferin *et al.* 1992). Uptake by alveolar type II cells is not or rarely observed. Particle-epithelial contact can also result in the release of cytokines and chemokines (e.g. MCP-1, CINC-1) stimulating inflammatory cell infiltration. In case of damage (necrosis or apoptosis) of epithelial cells, type II cells divide and differentiate to replace type I cells. However, the process is not instantaneous and the epithelial surface can be left bare. Hyperplasia and compensatory cell proliferation of type II alveolar and bronchial epithelial cells follow (Barlow *et al.* 2005). Furthermore, epithelial cells (type II) are considered to be cell of origin for tumours related to PSLT exposure (IARC 2010; Nikula *et al.* 1995).

Under overload conditions (as mentioned in chapter 4.2.1.), the phagocytosis efficiency of macrophages, including their mobility and function, is decreased or even fails with increasing particle burdens (Morrow 1988). Increased numbers of particles reaching the interstitium (interstitialization) remain there and stimulate interstitial cells or transfer to the lymph nodes (Morrow 1988). Beyond the epithelium, interstitial macrophages (IM) represent around 40% of the total macrophages in total tissue and are able to phagocytize particles (below 1  $\mu\text{m}$  diameter) (Crowell *et al.* 1992; Geiser 2002). They are close to matrix and connective-tissue cells (e.g. fibroblasts) which is important for effects elicited by their released mediators (Laskin *et al.* 2001). Their activation may result in a change of the chemotactic gradient from the alveoli towards the interstitium after which inflammatory cell infiltration follow (Oberdörster *et al.* 1992). Since interstitial macrophages may possess a higher proliferative capacity than alveolar macrophages, these particle-macrophage cell interaction can lead to release of fibrotic mediators (fibroblast growth factors, FGF; TNF- $\alpha$ ) and initiation of fibrosis (Bowden *et al.* 1989; Laskin *et al.* 2001). Phagocytosis of deposited silica particles by interstitial macrophages was associated with increased fibroblastic proliferation and collagen deposition resulting in fibrosis and granuloma formation (Adamson *et al.* 1989).

Dendritic cells (DC) in the lungs also have nanoparticle phagocytizing capabilities but their function here is rather unknown (Geiser 2002). Interstitial macrophages may be able to regulate and inhibit maturation and migration of pulmonary DCs (Bedoret *et al.* 2009). Monocyte-derived alveolar macrophages may re-enter the blood circulation and differentiate into DCs (Randolph 2001). DCs can further enter efferent lymphatics or the thoracic duct which may be important for particle clearance mechanisms (Gordon 2003). At increasing lung burdens, nanoparticles can be drained to a higher extent into the lung associated lymph nodes or in the blood circulation reaching extra-pulmonary organs (Semmler *et al.* 2004).

Overall, inhaled PSLT may lead to activation and accumulation of particle loaded alveolar macrophages, infiltration of inflammatory cells such as neutrophils and lymphocytes, release of pro-inflammatory mediators, oxidant generation, alveolar hypertrophy and cell proliferation of the epithelium.

Biomarkers for initial inflammation (neutrophils, macrophages, cytokines and chemokines; see chapter 8.2.3.) in the lungs can partly be assessed by bronchoalveolar lavage fluid (BALF) analysis, even after only 1 week of exposure (5-days, short-term inhalation test), depending on the inhaled concentration (Landsiedel *et al.* 2014). These markers indicate early morphological changes in the lung (Henderson *et al.* 1987). Morphological changes appear rather late after exposure to low toxicity nanoparticles. Sustained inflammation can be characterized by persistent elevation of the number of neutrophils (in BALF) and by an increased number of inflammatory cells (e.g. macrophages) in lung (detected by histopathology). Therefore, a combination of different methods (histopathology, BAL) enables an early detection as well as progression and regression of effects over time.

**Table 2 Selected mediators relevant for macrophage function and inflammation**

**Macrophage colony-stimulation factor (M-CSF)/granulocyte-macrophage colony-stimulation factor (GM-CSF):**

Differentiation from stem cells in the bone marrow to monocytes and later macrophages (Gordon 2003)

**Monocyte chemoattractant protein-1 (MCP-1):**

Chemoattractant; macrophage recruitment and stimulation of their oxidant production

(Driscoll *et al.* 1996; Rollins *et al.* 1991).

**Tumor necrosis factor  $\alpha$  (TNF $\alpha$ ):**

Inflammatory cell recruitment and macrophage activation after particle exposure (Driscoll 2000)

Increased expression of E-selectin and vascular cell adhesion molecules on capillary endothelial cells (relevant for monocyte migration into tissue) (Hussel & Bell 2014)

**Cytokine-induced-neutrophil-chemoattractant (CINC-1)/Interleukin IL-8 (rat homologue)**

Chemokine, released by activated macrophages, responsible for activation and chemotaxis of neutrophils (Grommes & Soehnlein 2011; Driscoll *et al.* 1997)

Proliferative and mitogenic to epithelial cells (Standiford *et al.* 1990, Donaldson *et al.* 2008)

**Neutrophil chemoattractant macrophage inflammatory protein (MIP-2 $\alpha$ ):**

Proliferative and mitogenic to epithelial cells (Standiford *et al.* 1990, Donaldson *et al.* 2008)

**Fibroblast growth factor (FGF):**

Fibrotic mediator released by macrophages; initiation of fibrosis (Browden *et al.* 1989, Laskin *et al.* 2001)

### 4.2.3. Pulmonary effects of inhaled nano-PSLT

Effects of inhaled PSLT in rats seem not to be fundamentally different from those observed for crystalline silica (quartz) besides the much higher potency of the latter (Roller & Pott 2006). Furthermore, the type of pulmonary effects of nano- and larger PSLT seem to be comparable. Therefore, this section will focus mainly on inhalation studies with nano-PSLT and their induced pulmonary effects.

Multiple short-term rat inhalation studies of nano-PSLT are available. Nano-TiO<sub>2</sub> and -carbon black were studied in short-term as well as subchronic studies (Driscoll *et al.* 1996; Johnston *et al.* 2000; Klein *et al.* 2012; Landsiedel *et al.* 2014; Ma-Hock *et al.* 2009; Noel *et al.* 2012). One week (5 days) of inhalation exposure of 10 mg/m<sup>3</sup> nano-TiO<sub>2</sub> (P25, Degussa, 25 nm, around 80% anatase, 20 % rutile) resulted in a lung burden of 1.6 mg/lung and caused an increase of inflammatory cells and mediators in BALF (e.g. elevated neutrophils, LDH) and alveolar infiltration with histiocytes (alveolar macrophages) (Landsiedel *et al.* 2014; Ma-Hock *et al.* 2009). Nano-ZrO<sub>2</sub> (BASF, pyrolytic research product of *NanoCare*, 25-60 nm), on the other hand, caused no adverse effects at 0.5, 2.5 and 10 mg/m<sup>3</sup> (Kuhlbusch *et al.* 2009, Landsiedel *et al.* 2014, Wohlleben *et al.* 2013). After 13 weeks inhalation of 10 mg/m<sup>3</sup> (resulting in burdens of about 11 mg/g lung), nano-TiO<sub>2</sub> (P25, Degussa, 21 nm) induced increases in neutrophils, macrophages and lymphocytes in BALF and proliferation of type II alveolar cells, epithelial metaplasia and interstitial fibrosis in histopathology (Bermudez *et al.* 2004). The lung retention half-time was 395 days indicating overload conditions. Rats developed interstitial lung fibrosis after 13 weeks of inhalation exposure to 23 mg/m<sup>3</sup> nano-TiO<sub>2</sub> (P25, Degussa, 20 nm) and a post-exposure period of 6 months (Baggs *et al.* 1997). Thirteen week inhalation of 7 and 50 mg/m<sup>3</sup> carbon black (Printex 90, 16 nm) in rats caused burdens of 0.97 and 4.87 mg/lung, respectively, and an increase in neutrophils in BAL indicating inflammation (Gallagher *et al.* 2003). Exposure to 50 mg/m<sup>3</sup> carbon black induced also an increase in 8-OH-2'-deoxyguanosine (8-oxo-dG) in pulmonary epithelial cells indicating oxidative stress and secondary genotoxicity. Oxidative stress in the lungs can be caused by retained particles provoking the influx of immune cells into the lung (as mentioned in chapter 4.2.2.). Overwhelmed antioxidant capacities and chronic inflammation in the lung can lead to subsequent oxidant-induced DNA damage as a secondary genotoxic effect (Driscoll 1997).

However, the long-term effects of inhaled nano-PSLT are tentative since only two chronic/carcinogenicity inhalation studies on nanomaterials are currently available (Becker *et al.* 2011). Epidemiological studies, e.g. on carbon black, provide no sufficient evidence of a carcinogenic potential in humans (Deutsche Forschungsgesellschaft (DFG) 2014). In the eighties and nineties of last century, inhalation studies were performed to investigate potential adverse effects after long-term exposure to particles. The main focus of these studies was diesel soot particles; nanoparticles were also simultaneously tested at a single high aerosol concentration. Female Wistar rats inhaled average aerosol concentrations of 10 mg/m<sup>3</sup> nano-TiO<sub>2</sub> (P25, Degussa, 80% anatase and 20% rutile, primary particle diameter 15-40 nm) and 11.6 mg/m<sup>3</sup> carbon black (Printex 90, Degussa, primary particle

diameter 14 nm) (Heinrich *et al.* 1995). Lung burdens of nano-TiO<sub>2</sub> and carbon black were around 40 and 44 mg/lung after 24 months, respectively. Squamous cell carcinomas, bronchioalveolar adenomas and adenocarcinomas with tumor rates between 32 - 39% were observed in the rat lungs after 24 months of inhalation exposure and a post-exposure period of 6 months. However, high aerosol concentrations, no dose-response-relationship and non-standardized study design with missing endpoints limit the use of these long-term inhalation studies for regulatory assessment (Becker *et al.* 2011). Dose-response relations and long-term effects at low aerosol concentrations remain unknown.

#### **4.2.4. Systemic Effects of inhaled nano-PSLT**

Pulmonary exposure to ambient particulate matter seems to be associated with effects on cardiovascular function. Intratracheal instillation of 0.1 or 0.25 mg/rat micron-TiO<sub>2</sub> to rats induced a dose-dependent impairment of endothelium-dependent arteriolar dilation in the systemic microcirculation, increased leukocyte rolling and adhesion in paired venules and local oxidative stress (Nurkiewicz *et al.* 2006).

Besides local effects in the lung, systemic effects have also been studied after inhalation exposure to nanoparticles. Translocation of nanoparticles from the lung, across the air-blood barrier, to extra-pulmonary organs has been observed (Elder & Oberdörster 2006, Kreyling *et al.* 2002). Increasing nanoparticle accumulation in extra-pulmonary organs and consequent effects have to be taken into account after long-term inhalation. However, the translocation rate of inhaled nano-PSLT to the blood and extrapulmonary organs is low. This was demonstrated after inhalation of insoluble nano-Iridium (15 nm and 80 nm) in rats (Kreyling *et al.* 2002; Kreyling *et al.* 2009). Biodistribution and uptake of nanoparticles was associated with mononuclear phagocyte system-organs like spleen and liver but also with the skeleton and soft tissues (Kreyling *et al.* 2009). Whole-body inhalation exposure of 180 µg/m<sup>3</sup> aerosolized nano-<sup>13</sup>C (count median diameter 20-29 nm) led to particle accumulation in liver 24 hours post-exposure (5-times higher <sup>13</sup>C liver burdens than lung) but not in any other extra-pulmonary organ (Oberdörster *et al.* 2002). Systemic toxicity seems to be less relevant for inhaled PSLT since they translocate to extrapulmonary organs less (<10 % by mass) and rarely induce toxic effects in those organs (Landsiedel *et al.* 2012a; Molina *et al.* 2014; Moreno-Horn & Gebel 2014).

#### 4.2.5. Mechanism of action of inhaled PSLT

PSLT are assumed to share a common mode of toxic action, but the overall mode of action is still under debate (Greim *et al.* 2001; Greim & Ziegler-Skylakakis 2007). A sequence of events describes the biological procedure starting with particle deposition in the lung and related cells and ending with potential lung tumour formation (IARC 2010). Most of the inhaled PSLT dusts commonly induce pulmonary inflammation which appears to be the main driver for further pathological changes. Activation of alveolar macrophages and neutrophils results in acute inflammation which, with increased particle accumulation, may progress to chronic inflammation and fibrosis (Oberdörster 1995).

ROS exceeding antioxidant defenses (oxidative stress) and secondary DNA damage seem to be also linked to PSLT exposure (Greim & Ziegler-Skylakakis 2007; Li *et al.* 2010). Oxidative stress can be mediated by persistent inflammation; ROS species are generated by alveolar macrophages and epithelial cells. This can lead to secondary genotoxicity and subsequent target-cell mutations (Driscoll 1997; Madl *et al.* 2014). Epithelial cell metaplasia, proliferation and mutations seem to be the latest steps in lung tumour formation (such as adenocarcinomas, squamous cell carcinomas).

For carbon black and crystalline silica particles, cell proliferation as well as inflammation, fibrosis, epithelial hyperplasia and squamous metaplasia may relate to tumor frequencies (Kolling *et al.* 2011; Kreyling *et al.* 2009; Oberdörster *et al.* 1992; Oberdörster *et al.* 1994; Rittinghausen *et al.* 2013). For other PSLT, such as TiO<sub>2</sub>, persistent inflammation, inflammatory cell derived ROS and increased cell proliferation rather than genotoxicity were associated with transformation of pulmonary epithelial and lung tumor formation (Deutsche Forschungsgesellschaft (DFG) 2013b; DFG Deutsche Forschungsgemeinschaft 2014; Driscoll 1997). It was proposed that additional or alternative pathways can be involved in PSLT-induced tumor formation although few data are available (IARC 2010): PSLT may also be able to translocate from the alveolar space to epithelial cells, enter them and interfere with the cytoskeleton during cell division inducing mutagenic effects.

The mode of action of nano- and micron-PSLT is assumed to be the same (Gebel *et al.* 2014). Mechanisms, such as inflammation and oxidative stress, are also commonly known for larger particles (Gebel *et al.* 2013). The biological effects of nano- and larger PSLT, however, may differ in potency (Deutsche Forschungsgesellschaft (DFG) 2014). Correlated to the dose metric mass concentration, nano-PSLT showed a 2 to 3 times higher carcinogenic potency compared to larger PSLT (Gebel 2012), but when adjusted to the dose-metric surface area, the potencies were comparable. This was explained by the higher surface area per mass of nano-PSLT. However, to date, no long-term inhalation study comparing nano- and micron-PSLT is available (Becker *et al.* 2011).

Nano-PSLT are able to induce significantly greater inflammatory effects on a mass basis than their bulk materials with same chemical composition (Oberdörster *et al.* 2005). Differences in alveolar macrophage reaction were also observed: after phagocytosis of nano-PSLT, alveolar macrophages

initiate oxidative stress and inflammation at lower mass concentrations compared to larger PSLT (Donaldson *et al.* 2002; Gebel *et al.* 2014). The higher inflammatory potency of nano-PSLT might be explained by increased proinflammatory cytokine levels; carbon black induced TNF- $\alpha$  release by macrophage via increased intracellular Ca<sup>2+</sup> levels (Donaldson *et al.* 2002). In a 3-month inhalation study, nano-TiO<sub>2</sub> (20 nm) elicited higher fibrotic lung response than its bulk form (250 nm) at similar aerosol concentrations after 6 months of post-exposure (Baggs *et al.* 1997).

Across the group of PSLT, there seem to be also a difference in potency to induce overload since nano-PSLT may impair macrophage clearance at mass doses that are much lower than those associated with micron-PSLT overload (Bellmann *et al.* 1991; ILSI Risk Science Institute Workshop Participants 2000). Here, adjustment of dose metrics is necessary since there seems to be different dose-response relationships between lung burdens and overload (Donaldson 2000). Lung burdens are usually expressed as mass burdens since this is the common dose metrics used for regulatory assessments. Particle surface area seems to be a good marker predicting pulmonary response (e.g. inflammation) (Driscoll *et al.* 1996; Oberdörster 2002a; Tran *et al.* 2000). A correlation was shown for pulmonary inflammation as well for tumor potential and incidences. Tran and others suggested particle surface area as better metric for overload, specifically inflammatory response per unit particle surface area (Oberdörster 2002b; Rushton *et al.*, 2010; Tran *et al.* 2000).

An increase in potency of overload effects was explained by higher “biologically-accessible surface” of these nanoparticles (Donaldson & Poland 2012). Possible cytotoxic effects due to generation of ROS on the large surface area, surface reactivity, coating and crystallinity of nano-PSLT may contribute to these differences since cytotoxic materials can also affect macrophage mediated particle clearance (Oberdörster 1995; Sager *et al.* 2008). Particle volume was the central focus of Morrow’s hypothesis for overload (Morrow 1988) but was also recognized as appropriate dose-metrics by others (Pauluhn 2011a; Roller & Pott 2006). Lower agglomerate densities of nano-PSLT and higher void space of their agglomerates lead to a macrophage response by volumetric overload mediating inflammatory responses (Pauluhn 2011b).

With an appropriate dose-metric representing lung burdens, similar pulmonary responses of PSLT may be expected (Cherrie *et al.* 2013). The relationship of (chronic) inflammation and overload is discussed to be strongly associated with tumour formation (as mentioned in chapter 4.2.1. and 4.2.2.) (ECETOC 2013). In concentrations below the overload range, no lung inflammation and also no tumours should occur (Gebel 2012). However, to date, other inhaled nano-PSLT, such as ZrO<sub>2</sub> and BaSO<sub>4</sub>, showed only low or no inflammation and toxic effects, even at concentrations in the overload range (Cullen *et al.* 2000; Landsiedel *et al.* 2014; Tran *et al.* 2000). This may indicate a range with a lower and upper end across the group of PSLT.

#### 4.2.6. Relevance of rat model to humans

The relevance of a rat model to humans is questionable due differences in particle kinetics and pulmonary responses (Cherrie *et al.* 2013; ILSI Risk Science Institute Workshop Participants 2000). There is no overall agreement whether the rat overload phenomena is applicable to humans (ILSI Risk Science Institute Workshop Participants 2000), although accumulation of particles in lungs of humans comparable to the levels observed in rats can be seen, e.g. in coal miners after inhalation of coal dust (Gregoratto *et al.* 2011). Stöber *et al.* (1965) indicated prolonged lung clearance in coal workers (Stöber *et al.* 1965). In general, responses of humans comprise higher interstitialization of particles (Green 2000, Gregoratto *et al.* 2011).

Human PSLT exposure may be linked to nonmalignant respiratory diseases rather than tumour formation since high particle lung burdens elicited chronic obstructive lung disease (COPD) and pneumoconiosis in exposed coal miners (Kuempel *et al.* 2001). In both, humans and rats, PSLT exposures lead to an alveolar macrophage response, accumulation of particles in the interstitium and mild interstitial fibrosis. Epithelial hyperplasia and fibrosis can be seen in humans, even without impaired macrophage-mediated clearance (Kuempel *et al.* 2014). In general, rats show a higher acute inflammatory and proliferative pulmonary response than humans (Green 2000).

Lung tumours in humans differed from tumours found in rats after chronic dust inhalation (Deutsche Forschungsgesellschaft (DFG) 2014). Rat tumours observed in long-term studies (adenocarcinomas, squamous cell carcinoma) are mainly located in the peripheral (bronchiolo-alveolar) lung with high proliferation rates of type II alveolar cells whereas lung tumours found in humans are most frequently bronchial carcinomas. Thus, a direct comparison between coal-dust-exposed rats and coal miners may not be feasible. It was concluded that rats may be predictive for humans in case of non-neoplastic responses after inhalation to PSLT (Donaldson & Tran 2002; ILSI Risk Science Institute Workshop Participants 2000; ECETOC 2013).

For neoplastic responses at overload conditions, rats seem to show a greater response in developing lung tumours than humans. However, epidemiological studies or sufficient human data are too sparse to rule out the risk in lung tumour formation for all inhaled PSLT appropriately, especially with respect to uncertainties related to nanostructures (Green 2000; Kuempel *et al.* 2014).

### 4.3. Inhalation toxicology of cerium dioxide (CeO<sub>2</sub>) and barium sulfate (BaSO<sub>4</sub>) nanoparticles

The Working Party on Manufactured Nanomaterials (WPMN) of the Organisation for Economic Co-operation and Development (OECD) aims to assess the toxic potential of nanomaterials with a set of commercially relevant reference materials (OECD 2010). The following nanomaterials are on the list of the representative manufactured nanomaterials of the OECD sponsorship programme selected to be tested for human health and environmental safety: fullerenes (C<sub>60</sub>), single-walled carbon nanotubes (SWCNTs), multi-walled carbon nanotubes (MWCNTs), silver nanoparticles, iron nanoparticles, titanium dioxide, aluminium oxide, barium sulfate, cerium oxide, zinc oxide, silicon dioxide, dendrimers, nanoclays and gold nanoparticles (OECD 2010; OECD 2012; Singh *et al.* 2011). Data on measurement, toxicology and risk assessment of these nanomaterials may serve as international benchmarks. In 2011, the Institute for Health and Consumer Protection of the European Commission established a repository with samples of representative nanomaterials (European Commission 2011b). Samples of different nano-CeO<sub>2</sub> and -BaSO<sub>4</sub> are available within the repository (Singh *et al.* 2011). Each nanomaterial got a corresponding nanomaterial (NM) number: two CeO<sub>2</sub> were coded as NM-211 and NM-212 and BaSO<sub>4</sub> as NM-220 in the list of OECD WPMN Sponsorship Programme for the Testing of Manufactured Nanomaterials. In 2014, all nanomaterials in the JRC Repository were re-numbered. Currently, CeO<sub>2</sub> NM-211 and NM-212 are coded as JRCNM02101a and JRCNM02102a, respectively. However, in this body of work, the acronyms NM-211 and NM-212 were still used.

As already mentioned in paper 2, nano-BaSO<sub>4</sub> (NM-220) used in the intratracheal (IT) instillation, gavage and intravenous (IV) injection studies was a reference material for the Nanomaterial Testing Sponsorship Program of the OECD and its characterization of this original batch was described by Wohlleben *et al.* (2013) (Wohlleben *et al.* 2013). The long-term inhalation study required large amounts of the test material. Therefore, nano-BaSO<sub>4</sub> was reproduced at a different production plant using the same synthesis protocol and characterized by the same methods. It was used for the studies with 4, 13 and 52 weeks of exposure.

CeO<sub>2</sub> is used in various commercial and industrial applications, e.g. as a diesel fuel combustion catalyst, as sun protection in UV resistant coatings or as polishing agent for silicon wafers (Antaria 2014; Corma *et al.* 2004; Murray *et al.* 1999; Wakefield *et al.* 2008). Furthermore, CeO<sub>2</sub> is also considered to be a versatile biocompatible material with promising use in therapeutics capturing ROS *in vitro* (Hirst *et al.* 2013). Nano-CeO<sub>2</sub> has anti-oxidative and oxidative effects with the coexistence of tri- (Ce<sup>3+</sup>) and tetravalent (Ce<sup>4+</sup>) states resulting in both protective and toxic impacts (Xia *et al.* 2008; Kilbourn 2003). Representative test materials of commercially manufactured nano-CeO<sub>2</sub> (NM-211 and NM-212; NM-213 is the bulk reference) were completely characterized by the European Commission's Joint Research Centre (JRC) (European Commission 2014).

Associated with its industrial and commercial use, exposure of airborne nano-CeO<sub>2</sub> has been identified since it was detected in diesel exhaust emissions (Cassee *et al.* 2011; PROSPeCT 2010). A male

patient with a history of 35 years in optical lens grinding (with exposure to CeO<sub>2</sub> and other metal dusts) suffered from rare earth pneumoconiosis and pulmonary fibrosis (McDonald *et al.* 1995). SEM and EDX analysis of a lung biopsy showed mainly cerium particles (diameter range from <1 µm to 5 - 10 µm) deposited in the lung associated with pulmonary interstitial fibrosis in this patient.

Nano-CeO<sub>2</sub> has been further studied *in vitro* and *in vivo* including animal studies with inhalation, instillation, oral and intravenous exposure (Aalapati *et al.* 2014; Babin *et al.* 2013; Environmental Protection Agency (EPA) 2009; Gosens *et al.* 2013; Kumari *et al.* 2014; Ma *et al.* 2014; Molina *et al.* 2014; Yokel *et al.* 2008; Yokel *et al.* 2012). *In vitro*, human aortic endothelial cells exposed to 50 µg/ml nano-CeO<sub>2</sub> (spray flame synthesized, median diameter 40 nm) did not exhibit significant inflammation measured as mRNA levels of inflammatory markers (IL-8, MCP-1, ICAM-1) (Gojova *et al.* 2009). Hepatotoxicity due to systemic bioavailability was observed after intratracheal instillation of 1.0, 3.5, or 7.0 mg/kg b.w. of nano-CeO<sub>2</sub> (Sigma-Aldrich, 10.14 nm) in male Sprague-Dawley rats (Nalabotu *et al.* 2011). Nano-CeO<sub>2</sub> may translocate via blood from lungs to liver and induced increase liver levels associated with decreases in liver weight and alterations in blood chemistry. Nano-CeO<sub>2</sub> (Sigma-Aldrich, 20 nm in water) caused significant lung inflammation (increase in AM, PMN, LDH) after instillation of 0.15, 0.5, 1.3, 5 and 7 mg/kg b.w. in male Sprague Dawley rats (Ma *et al.* 2011). It also increased IL-12 production and apoptosis of alveolar macrophages via caspase-3 and -9 activation. Male Sprague–Dawley rats were exposed to 0.15, 0.5, 1, 3.5 or 7 mg/kg b.w. nano-CeO<sub>2</sub> (6.4 - 14.8 nm) by a single intratracheal instillation (Ma *et al.* 2014). Nano-CeO<sub>2</sub> exposure induced a sustained inflammatory response, macrophage secretion of proinflammatory cytokine IL-12 and phospholipidosis and fibrosis in histopathology 4 weeks post-exposure. The authors concluded that nano-CeO<sub>2</sub> might be able to shift a proinflammatory to a fibrotic environment, ending up in pulmonary fibrosis (Ma *et al.* 2012).

In an acute inhalation study with rats, 4 hours of nose-only exposure to 641 mg/m<sup>3</sup> nano-CeO<sub>2</sub> (primary particle size of 55 nm) resulted in pulmonary inflammation and formation of multifocal lung microgranulomas explained by impaired lung clearance (Srinivas *et al.* 2011). In short-term studies with one week (5 days) of inhalation to 2.5 and 10 mg/m<sup>3</sup> of nano-CeO<sub>2</sub> (BASF, laboratory batch for experimental uses, primary particle sizes of 10-200 nm, burdens of 166 and 417 µg/lung, respectively) caused increased levels of neutrophils, CINC-1, IFN-γ, IL-1α, MCP-1 and M-CSF in BAL and lung tissue as well as a mild histiocytosis in histopathology (Kuhlbusch *et al.* 2009; Landsiedel *et al.* 2014). Observed effects were not fully reversible after 3 weeks of post-exposure. Four weeks of inhalation exposure to dose-equivalent concentrations of 1.2 mg/m<sup>3</sup> NM-211 and 2.5 mg/m<sup>3</sup> NM-212 nano-CeO<sub>2</sub> (European Nanomaterial Repository, 5-10 and 40 nm, respectively) induced increases in either neutrophils and/ or lymphocytes in BAL and only mild morphological changes, such as particles within alveoli and macrophages, increased septal cellularity (Geraets *et al.* 2012; Gosens *et al.* 2013).

Along with nano-TiO<sub>2</sub>, nano-CeO<sub>2</sub> was ranked within substances causing lung effects in the STIS at aerosol concentrations of 0.5 mg/m<sup>3</sup>, and may be among the materials with higher biological activity (Landsiedel *et al.* 2014).

BaSO<sub>4</sub> is a water-insoluble salt of barium. Hence, it is used for radiographic contrast media (Romero-Ibarra *et al.* 2010; Zhang *et al.* 2011). Nano-BaSO<sub>4</sub> particles are used as fillers in coatings (e.g. in motor vehicles) due to their mechanical, optical and chemical properties. Recently, nano-BaSO<sub>4</sub> has been used in orthopedic medicine, diagnostic imaging and other applications, such as bone cement additive (Gillani *et al.* 2010). Incorporation of nano-BaSO<sub>4</sub> into pellethane improved its antimicrobial activity and decreased biofilm formation and hospital-acquired infections (Aninwene *et al.* 2013).

Human aspiration of radiographic contrast containing BaSO<sub>4</sub> elicited thickened interlobular septa, subpleural cysts, and centrilobular micronodules along with barium particles in a subpleural distribution indicating clinical fibrosis (Voloudaki *et al.* 2003). Nine cases of baritosis (benign pneumoconiosis) in factory workers exposed to barium dusts were reported (Doig 1976). Two patients developed acute dyspnea after aspiration of the contrast agent BaSO<sub>4</sub> into the lung (Tamm & Kortsik 1999). In a simulated physiological saline, BaSO<sub>4</sub> showed negligible dissolution (Cullen *et al.* 2000; Tran *et al.* 2000).

Nano-BaSO<sub>4</sub> was found to have no or very low toxicity in short-term inhalation studies, in any case less toxic than nano-TiO<sub>2</sub> and -CeO<sub>2</sub> (Klein *et al.* 2012; Landsiedel *et al.* 2014). One week of exposure (5-days, STIS) to 50 mg/m<sup>3</sup> nano-BaSO<sub>4</sub> (Solvay, primary particle size of 25 nm, burden of 1.1 mg/lung) elicited no effects in BAL and histopathology (besides a negligible, transient increase in IL-1 $\alpha$  in tissue homogenates of the lavaged lungs). No other inhalation study with nano-BaSO<sub>4</sub> has been performed until now. However, a subchronic rat inhalation study with 75 mg/m<sup>3</sup> micron-BaSO<sub>4</sub> (Aldrich, burden of 10 mg/lung) did not cause neutrophil response in BAL and showed no retarded clearance (Cullen *et al.* 2000; Tran *et al.* 2000). These studies showed that compared to other PSLT, nano-BaSO<sub>4</sub> is remarkable un toxic, even at high concentrations (Landsiedel *et al.* 2014). The effects observed with nano-BaSO<sub>4</sub> and -CeO<sub>2</sub> nanoparticles illustrate that the inhalation toxicity within the group of PSLT spans a range of biological effects.

#### 4.4. Nanotechnology in veterinary medicine

Higher biological activity of nanomaterials can be desirable and intended, as for therapeutics, but can also be undesirable when humans are unintentionally exposed to airborne nanoparticles released from industrial products (see previous chapters). Nanoparticles can also be used as delivery systems, e.g. for pharmaceuticals or bioactive food ingredients (Oberdörster 2010). The delivered compound and the *in vivo* internal concentration determine the potential benefit or risk for this type of application.

Nanotechnology will be a promising field in human and veterinary medicine and animal health (Etheridge *et al.* 2013). Nanomaterials used in human pharmaceutical applications can also be applied to veterinary medicine. Pharmaceutical applications are under development for drug delivery, disease diagnosis and treatment (Chakravarthi & Balaji 2010, Lobatto *et al.* 2011).

For instance, synthetic polymers, e.g. dendrimers, can be used as pharmacological agents. Due to their small size, they are able to enter cells easily and deliver drugs directly to the target site, e.g. direct delivery into tumour microvasculature for tumour treatment and therapy. Polymeric nanoparticles are also used in pulmonary applications, mostly as drug delivery systems with all the benefits of modified surface properties, high drug encapsulation and degradation protection of the drug and prolonged drug delivery (Paranjpe & Muller-Goymann 2014). Loaded with an anti-cancer compound, polymeric micelles as pulmonary drug carriers were administered to animals via intratracheal instillation resulting in no toxicity and sustaining high target concentrations in lung over time (Gill *et al.* 2014).

Barium sulfate has been widely used as contrast agent for the visualization of abnormalities of the gastrointestinal tract. Mouse studies showed that it can also be used in angiography producing high-contrast images using basic X-ray imaging (Givvimani *et al.* 2011). Here, various structural abnormalities in the vascular system of small animals, such as atherosclerotic coronary arteries, can be visualized.

The advantages of nanomaterials in the field of diagnosis and treatment are many but at the same time the toxic potential of nanomaterials have to be studied to prevent harm to humans and animals (Lynch *et al.* 2014).

## 5. Aim of this work

Long-term effects of inhaled engineered nanomaterials have been identified as a research priority (Becker *et al.*, 2011). So far, for the group of PSLT, only nano-TiO<sub>2</sub> and carbon black have been tested in long-term inhalation studies (Heinrich *et al.* 1995, Mauderly *et al.* 1994, Nikula *et al.* 1995). However, these studies were either not conducted according to OECD test guidelines or only one single high aerosol concentration was tested. There are no data on pulmonary or extrapulmonary effects after long-term exposure to low aerosol concentrations of nanomaterials.

Nano-CeO<sub>2</sub> and -BaSO<sub>4</sub> are industrial relevant nanomaterials. They were further pointed out as high priority nanomaterials for toxicological testing by the Organisation for Economic Co-operation and Development (OECD) (OECD 2010; OECD 2012; Singh *et al.* 2011). Nano-CeO<sub>2</sub> is known to possess a certain toxic potential since short-term inhalation studies showed high particle retention and slow pulmonary clearance (nearly no elimination from the lung within 48-72 hours), as well as corresponding biological effects in the lungs, such as pulmonary inflammation and granuloma formation (Geraets *et al.* 2012; Srinivas *et al.* 2011; see chapter 4.3). In the few published data available, nano-BaSO<sub>4</sub> was found to have no or low toxicity with a remarkably fast pulmonary clearance in short-term inhalation studies, even at high aerosol concentrations (Klein *et al.* 2012; Landsiedel *et al.* 2014). Within this work, inhalation studies were carried out regarding the short-term (paper 1 and 2) and (sub)chronic effects of nano-CeO<sub>2</sub> and BaSO<sub>4</sub>.

The work addressed the following hypotheses:

1. Inhaled nano-PLSTs are able to cause pulmonary inflammation and further biological effects after short-term exposure. Nano-CeO<sub>2</sub> and -BaSO<sub>4</sub> are both assumed to be PSLT – based on their morphology and chemical water-solubility – and may represent a range of biological responses.
2. Repeated inhalation of nano-CeO<sub>2</sub> and -BaSO<sub>4</sub> exerts long-term effects by progression of these short-term effects.
3. The long-term effects are driven by the particle (bio)kinetics and cellular effects in the lung, such as lung clearance and retention and inflammation.
4. These effects are not observable below a certain aerosol concentration (no observed adverse effect concentration; NOAEC) depending on the kinetics and biological potency of the particles
5. Translocation of inhaled nano-CeO<sub>2</sub> and -BaSO<sub>4</sub> to extra-pulmonary organs and systemic effects are less relevant at concentrations used in this work.

The experimental approaches consisted of two main phases (table 3).

**Phase 1** included two short-term inhalation studies with 1 and 4 weeks of exposure (paper 1 and 2). The specific objective was:

1. To determine the lung and lymph node burdens as well as pulmonary and extrapulmonary effects after 1 week of exposure to two concentrations of CeO<sub>2</sub> NM-211 and three concentrations of CeO<sub>2</sub> NM-212;
2. To examine the course of lung retention and clearance kinetics of CeO<sub>2</sub> NM-212 and BaSO<sub>4</sub> after 4 weeks of exposure and a post-exposure period up to 129 days
3. To examine particle burdens of extra-pulmonary organs (in this work based on liver)
4. To assess the inflammatory response and morphological changes in the lung based on bronchoalveolar lavage and histopathology;
5. To examine cell proliferation in the lung using a bromodeoxyuridine (BrdU) stain of pulmonary epithelial cells
6. To assess systemic effects by hematology, clinical chemistry and acute phase proteins in serum, systemic genotoxicity (micronucleus test) in blood and histopathology in extrapulmonary organs

For the short-term studies, 25 mg/m<sup>3</sup> CeO<sub>2</sub> were selected as highest test concentration, calculated to be in the overload range. In contrast, 5 mg/m<sup>3</sup> were chosen as mid and 0.5 mg/m<sup>3</sup> as low concentrations, expected not to be in the overload range and without significant biological effects. Aerosol concentrations of 50 mg/m<sup>3</sup> were selected for BaSO<sub>4</sub> based on the earlier published 1 week inhalation study and were expected to be in the overload range (Klein *et al.* 2012; Landsiedel *et al.* 2014). The study with 4 weeks of exposure made reference to OECD Guidelines for Testing of Chemicals, Section 4: Health Effects, No. 412, with additional modifications to the study design (Organization for Economic Cooperation and Development (OECD) 2009). The two short-term studies were performed under GLP (Organisation for Economic Cooperation and Development (OECD) 1998). Part of the 1-week study contributed to the European project “NanoMILE” (“Engineered nanomaterial mechanisms of interactions with living systems and the environment”).

## **Phase 2**

Based on the lung burdens and toxicological findings after short-term exposure, aerosol concentrations of 0.1, 0.3, 1 and 3 mg/m<sup>3</sup> nano-CeO<sub>2</sub> and 50 mg/m<sup>3</sup> nano-BaSO<sub>4</sub> were selected for a long-term inhalation study with up to two years of exposure. Results of the subchronic study on nano-BaSO<sub>4</sub> are presented in paper 2. The reported subchronic and chronic studies with 13 and 52 weeks of exposure were interim results of this long-term study which included

1. Lung retention and clearance kinetics based on lung and associated lymph node burdens
2. Pulmonary effects based on bronchoalveolar lavage fluid analysis
3. Systemic effects by hematology, clinical chemistry and acute phase proteins

The long-term inhalation study with nano-CeO<sub>2</sub> (NM-212) and -BaSO<sub>4</sub> was initiated in 2013 and performed within the framework of the EU project “NanoREG” (Teunenbroek *et al.* 2013). The study was performed according to OECD test guideline No. 453, under GLP and with a relevant aerosol concentration range (OECD 2009). The results of this long-term study will be used to set exposure limit values for humans. The obtained NOAEC will be used as basis of future threshold limit values. Furthermore, these results will help to classify the carcinogenic potential of nanomaterials which will be based on mechanisms of tumour formation and incidences. Thus, the interim results after 13 and 52 weeks of exposure have enabled early insights into lung retention, clearance and pulmonary effects within the course of the long-term study.

Results of the short-term studies with exposure to nano-CeO<sub>2</sub> and –BaSO<sub>4</sub> are presented in the paper 1 and 2 (chapter 6 and 7). Additional results of the short-term and (sub)chronic studies are presented in chapter 8, followed by a general discussion (chapter 9) and conclusion (chapter 10).

### 5.1. Description of work

All endpoints and examinations of this body of work are summarized in table 3. Available data and their location in the manuscript are highlighted in the italic brackets.

**Table 3 Study design of 1, 4, 13 and 52 weeks of exposure**

	1 week	4 weeks	13 weeks	52 weeks
Days of exposure	5	20	67	253
Post-exposure period [days]	24	129	-	-
Test substance	CeO <sub>2</sub> NM-211	CeO <sub>2</sub> NM-212	CeO <sub>2</sub> NM-212	CeO <sub>2</sub> NM-212
Test Concentrations [mg/m <sup>3</sup> ]	0.5 / 25	0.5 / 5 / 25	0.1 / 0.3 / 1 / 3	0.1 / 0.3 / 1 / 3
Endpoints				
<b>Organ burden<sup>2</sup></b> [examined time-points]	2 (paper 1)	7 (paper 1)	1 (chapter 8.2)	1 (chapter 8.2)
<b>BALF</b> cytology, cell mediators, protein and enzyme activities <sup>1</sup>	x (paper 1)	x (paper 1)	x (chapter 8.2)	x (chapter 8.2)
<b>Necropsy</b> , organ weights and <b>histopathology</b> <sup>1</sup>	x (paper 1 and chapter 8.1)	x (paper 1 and chapter 8.1)	ND (chapter 8.1)	ND (chapter 8.2)
Immunohistochemistry lung <b>(cell proliferation)</b> <sup>1</sup>	x (chapter 8.1)	x (chapter 8.1)	ND (chapter 8.1)	ND (chapter 8.1)
			BaSO <sub>4</sub>	BaSO <sub>4</sub>
			67	253
			-	-
			35	-
			50	50
			50	50
			50	50

<sup>1</sup> n= 5 animals per concentration and time point; <sup>2</sup> n= 3 or 5; x=performed endpoint; brackets highlight the location of the available data in the dissertation; ND: not determined

Continuation of Table 3 Study design of 1, 4, 13 and 52 weeks of exposure

Days of exposure	1 week		4 weeks		13 weeks		52 weeks			
	5	24	20	129	20	35	67	253	253	
Post-exposure period [days]										
Test substance	CeO <sub>2</sub> NM-211	CeO <sub>2</sub> NM-212	CeO <sub>2</sub> NM-212	CeO <sub>2</sub> NM-212	BaSO <sub>4</sub>	BaSO <sub>4</sub>	CeO <sub>2</sub> NM-212	BaSO <sub>4</sub>	CeO <sub>2</sub> NM-212	BaSO <sub>4</sub>
Test Concentrations [mg/m <sup>3</sup> ]	0.5 / 25	0.5 / 5 / 25	0.5 / 5 / 25	0.5 / 5 / 25	50	50	0.1 / 0.3 / 1 / 3	50	0.1 / 0.3 / 1 / 3	50
Endpoints										
<b>Hematology</b> according to OECD TG 412; acute phase proteins <sup>1</sup>	x (paper 1)		x (paper 1 and table 12)		x (paper 2 and table 12)		x (chapter 8.2)	x (paper 2 and chapter 8.2)	x (chapter 8.2)	x (chapter 8.2)
<b>Systemic genotoxicity</b> (MNT) peripheral blood <sup>1</sup>	x (paper 1)		x (paper 1)		x (paper 2)		ND	ND	ND	ND

<sup>1</sup> n= 5 animals per concentration and time point; x=performed endpoint; brackets highlight the location of the available data in the dissertation; ND: not determined.

**6. Paper 1: Time course of lung retention and toxicity of inhaled particles:  
short-term exposure to nano-Ceria**

## Time course of lung retention and toxicity of inhaled particles: short-term exposure to nano-Ceria

Jana Keller · Wendel Wohlleben · Lan Ma-Hock · Volker Strauss · Sibylle Gröters ·  
Karin Küttler · Karin Wiench · Christiane Herden · Günter Oberdörster ·  
Bennard van Ravenzwaay · Robert Landsiedel

Received: 27 June 2014 / Accepted: 25 August 2014  
© The Author(s) 2014. This article is published with open access at Springerlink.com

**Abstract** Two Ceria nanomaterials (NM-211 and NM-212) were tested for inhalation toxicity and organ burdens in order to design a chronic and carcinogenicity inhalation study (OECD TG No. 453). Rats inhaled aerosol concentrations of 0.5, 5, and 25 mg/m<sup>3</sup> by whole-body exposure for 6 h/day on 5 consecutive days for 1 or 4 weeks with a post-exposure period of 24 or 129 days, respectively. Lungs were examined by bronchoalveolar lavage and histopathology. Inhaled Ceria is deposited in the lung and cleared with a half-time of 40 days; at aerosol concentrations higher than 0.5 mg/m<sup>3</sup>, this clearance was impaired resulting in a half-time above 200 days (25 mg/m<sup>3</sup>). After 5 days, Ceria (>0.5 mg/m<sup>3</sup>) induced an early inflammatory reaction by increases of neutrophils in the lung which decreased with time, with sustained exposure, and also after

the exposure was terminated (during the post-exposure period). The neutrophil number observed in bronchoalveolar lavage fluid (BALF) was decreasing and supplemented by mononuclear cells, especially macrophages which were visible in histopathology but not in BALF. Further progression to granulomatous inflammation was observed 4 weeks post-exposure. The surface area of the particles provided a dose metrics with the best correlation of the two Ceria's inflammatory responses; hence, the inflammation appears to be directed by the particle surface rather than mass or volume in the lung. Observing the time course of lung burden and inflammation, it appears that the dose rate of particle deposition drove an initial inflammatory reaction by neutrophils. The later phase (after 4 weeks) was dominated by mononuclear cells, especially macrophages. The progression toward the subsequent granulomatous reaction was driven by the duration and amount of the particles in the lung. The further progression of the biological response will be determined in the ongoing long-term study.

**Electronic supplementary material** The online version of this article (doi:10.1007/s00204-014-1349-9) contains supplementary material, which is available to authorized users.

J. Keller · W. Wohlleben · L. Ma-Hock · V. Strauss · S. Gröters ·  
K. Küttler · B. van Ravenzwaay · R. Landsiedel (✉)  
Experimental Toxicology and Ecology, BASF SE,  
67056 Ludwigshafen am Rhein, Germany  
e-mail: robert.landsiedel@basf.com

W. Wohlleben  
Material Physics, BASF SE, Ludwigshafen am Rhein, Germany

K. Wiench  
Product Safety, BASF SE, Ludwigshafen am Rhein, Germany

C. Herden  
Institute of Veterinary Pathology, Justus-Liebig-University,  
Giessen, Germany

G. Oberdörster  
Department of Environmental Medicine, University of Rochester,  
Rochester, NY, USA

**Keywords** Nanomaterial (NM) · Inhalation · Ceria ·  
Respiratory tract · Bronchoalveolar lavage

### Abbreviations

AAALAC	Association for Assessment and Accreditation of Laboratory Animal Care International
AAN	Average agglomeration numbers
ALP	Alkaline phosphatase
AUC	Area under the curve
BALF	Bronchoalveolar lavage fluid
BALT	Bronchus-associated lymphoid tissue
BET	Brunauer–Emmet–Teller
Ceria	Cerium dioxide
CINC	Cytokine-induced neutrophil chemoattractant
FaSSIF	Fasted state simulated intestinal fluid

GGT	$\gamma$ -Glutamyltransferase
GSD	Geometric standard deviation
ICP-AES	Inductively coupled plasma atomic emission spectrometry
ICP-MS	Inductively coupled plasma optical emission spectrometry
IL	Interleukin
LDH	Lactate dehydrogenase
M-CSF	Macrophage colony-stimulating factor
MCP	Monocyte chemoattractant protein
MMAD	Mass median aerodynamic diameter
MPPD	Multiple-path particle dosimetry model
NAG	<i>N</i> -acetyl- $\beta$ -glucosaminidase
NOAEC	No observed adverse effect concentration
OPN	Osteopontin
PMN	Polymorphnuclear neutrophil
PSF	Phagolysosomal simulant fluid
PSP	Poorly soluble particles with low toxicity
SAD	Selected area electron diffraction
SEM	Scanning electron microscopy
SIMS	Secondary ion mass spectrometry
SMPS	Scanning mobility particle sizer
STIS	Short-term inhalation study protocol
TEM	Transmission electron microscopy
TGA	Thermogravimetric analysis
TiO <sub>2</sub>	Titanium dioxide
XPS	X-ray photoelectron spectroscopy

## Introduction

During the production and processing of nanomaterials in the workplace, releases into the air may occur (Kuhlbusch et al. 2011). Therefore, inhalation is considered to be the major route of concern. Furthermore, pulmonary inflammation, fibrosis, and lung cancer are most important adverse effects after chronic inhalation exposure of rats to poorly soluble, non-fibrous (nano)particles of low toxicity (PSP) (Oberdorster 2002). Tumor formation in rat lungs after long-term PSP exposure is thought to be caused by altered particle clearance kinetics involving chronic inflammation associated with oxidative stress, secondary genotoxicity, and cell proliferation (Greim and Ziegler-Skylakakis 2007; ILSI Risk Science Institute Workshop Participants 2000). A previous study observed that excessive amounts of the microscale Titania induced lung tumors in rats after 2-year inhalation exposure to a high concentration of 250 mg/m<sup>3</sup> (Lee et al. 1985). Also, nanoscale materials, Titania (P25) and carbon black (Printex 90), caused lung tumors in rats after 2 years of inhalation to 10 and 11.7 mg/m<sup>3</sup>, respectively (Heinrich et al. 1995; Nikula et al. 1995). The tumor incidence observed in these studies was high (32–29 %). Only high concentrations were tested in these studies, and

no information about detailed deposition, clearance, and retention was provided. Thus, the existing studies contribute little to the understanding of the mechanisms of nanoparticle-induced tumor formation by long-term inhalation (Becker et al. 2011). Standardized long-term studies according to the test guidelines with a distinct study design and concentration selection focusing on exposure dose–response relationships are crucial for risk assessment and derivation of occupational safety values, as well as for classification and labeling under REACH (Becker et al. 2011; European Commission 2013).

Therefore, an appropriate long-term inhalation study has been initiated as a collaboration of the German government with BASF within the OECD sponsorship programme and the EU-project NanoREG (Teunenbroek et al. 2013; Federal Ministry for the Environment 2012). This study is performed according to OECD test guideline No. 453 (OECD 2009a). Nano-Ceria was selected as a test material representing a poorly soluble particle because of its importance for industrial applications. Nano-Ceria is used as an UV-absorbent, a polishing agent for silicon wafers, and a fuel additive to decrease diesel particle emission (Cargnello et al. 2013). The OECD has added Ceria to the list of representative manufactured nanomaterials for toxicological evaluations (NM-211, NM-212, NM-213) (Demokritou et al. 2012; OECD 2010). The short-term studies with 5 days and 4 weeks of exposure presented in this manuscript provide information on biokinetics and effects of nano-Ceria required for the design of a long-term inhalation study.

Till now, the available knowledge concerning inhalation toxicity of Ceria is limited. In an acute study, 4-h nose-only exposure to 641 mg/m<sup>3</sup> nano-Ceria in rats resulted in pulmonary inflammation and the formation of multifocal microgranulomas in lung after 14 days of post-exposure. This was explained by the impaired clearance of the particles from the lung (Srinivas et al. 2011). In a whole-body 4-day inhalation study, exposing rats to 2.7 mg/m<sup>3</sup> nano-Ceria 2 h/day, lung injury, and inflammation were observed after 1 day post-exposure (Demokritou et al. 2012). In a 28-day inhalation study of micro- and nano-Ceria (10.79 mg/m<sup>3</sup> NM-211, 19.95 mg/m<sup>3</sup> NM-212, 55.0 mg/m<sup>3</sup> NM-213) in rats, high lung burdens, distribution of inhaled Ceria to various extrapulmonary organs, and slow tissue clearance from the lung were observed (Geraets et al. 2012). Furthermore, 28-day nose-only inhalation of 2 mg/m<sup>3</sup> nano-Ceria in mice induced severe and chronic inflammation including necrosis; proteinosis; fibrosis and granulomas in the lungs; and severe changes in kidney, liver, and heart (Aalapati et al. 2014). These strong effects were associated with significant accumulation of the nanoparticles in the (extra)pulmonary tissues and indicated that inhalation of Ceria can lead to pulmonary and extrapulmonary toxicity. There were also a few instillation studies assessing

toxicity of nano-Ceria (He et al. 2010; Nalabotu et al. 2011; Ma et al. 2011, 2014; Molina et al. 2014). After single intratracheal instillation of 0.15, 0.5, 1.3, 5, and 7 mg/kg in male Sprague–Dawley rats, Ceria caused concentration-dependent alveolar macrophage functional change, significant lung inflammation, and cytotoxicity, indicating a potential shift from a proinflammatory environment to final pulmonary fibrosis (Ma et al. 2011). However, instillation studies usually have a bolus of high dose and high dose rate in the lung and are therefore less suitable to determine the exposure concentrations, biokinetics, and biological effects toward the design of a long-term inhalation study (Baisch et al. 2014). The majority of the published studies indicate an inflammatory potential of Ceria but lack appropriate dose metrics and biokinetic information (Casseo et al. 2011; Becker et al. 2011).

The short-term studies with 5 days and 4 weeks of exposure described in this manuscript provide data on biokinetics as well as pulmonary and potential extrapulmonary effects of two nano-Ceria (NM-211 and NM-212) using established and standardized study protocols. Whole-body exposure is the only option for exposure routes in long-term studies for animal welfare reasons because the animals are not restrained during the exposure. Furthermore, oral and dermal uptake of different micro- and nano-sized test materials has been proven to be negligible (Landsiedel et al. 2012; Gamer et al. 2006; Pflucker et al. 2001; Molina et al. 2014).

Physicochemical properties of nanoparticles can have a significant influence on their fate and biological effects (Oberdorster et al. 1994a; Anjilvel and Asgharian 1995). Therefore, the two nanoparticles were characterized in accordance with the nano-specific guidance in REACH, as validated earlier with other materials from the OECD sponsorship programme (Wohlleben et al. 2013). Persistence and solubility in different media were investigated to study the bioavailability of the tested Ceria. Comprehensive characterizations of the test atmospheres were performed according to the respective guidelines and OECD guidance documents (ECHA 2012; Hussain et al. 2009).

## Materials and methods

### General

Two short-term studies (5 days and 4 weeks of exposure) were designed using two different nano-Ceria. In the short-term study with 5 days of exposure, we compared two Ceria (NM-212 and NM-211) with regard to their inhalation toxicity, deposition, and clearance kinetics. Ceria (NM-212) was tested further after 4 weeks of exposure. In order to compare the effects after different exposure

durations, same target concentrations were selected for the two studies. Biological effects of Ceria were studied by the analysis of bronchoalveolar lavage fluid (BALF) and blood and histopathology of the respiratory tract. Biokinetics were assessed by the determination of lung and lung-associated lymph node burdens at different time points. The short-term inhalation studies were performed according to the OECD Principles of Good Laboratory Practice (GLP) [Organization for Economic Cooperation and Development (OECD) 1998]. The study design of the study with 4 weeks of exposure was carried out according to the OECD guidelines for testing of chemicals, Section 4: Health Effects, No. 412, with additional modifications [Organization for Economic Cooperation and Development (OECD) 2009b]. To increase the comparability, the short-term studies were performed in the same inhalation laboratory under the same test conditions, determining same end points for assessing biological effects and deposition and clearance kinetics. This facilitated a direct comparison between the measured parameters.

### Test materials and characterization

The two Ceria test materials in this work are NM-211 and NM-212 received from the OECD sponsorship programme for safety testing of manufactured nanomaterials (Hussain et al. 2009). Very recently, the European Chemicals Agency (ECHA) drafted a nano-specific guidance document, designated as Appendix R7-1 (Hermans 1963). The following end points for the characterization of the aerosol materials were considered as follows: agglomeration/aggregation, particle size distribution, water solubility/dispersability, crystalline phase and size, representative electron microscopy (TEM) for morphology, specific surface area, zeta-potential (surface charge), surface chemistry, photocatalytic activity, purity and impurities, and porosity. The methods to characterize these properties are described in detail in a previous work (Wohlleben et al. 2013). The agglomerate density of Ceria NM-212 was derived from mercury porosimetry (see Fig. S1). By integrating all void volumes up to the agglomerate outer dimensions of 1.1  $\mu\text{m}$ , the agglomerate density of NM-212 would be 2.0  $\text{g}/\text{m}^3$  based on the mercury porosimetry measurement. The density of NM-211 was determined consistently. The agglomerate density was used in the calculation of expected lung burden by multiple-path particle dosimetry (MPPD) model (Anjilvel and Asgharian 1995).

### Animals

This study was approved by the local authorizing agency for animal experiments (Landesuntersuchungsamt Koblenz, Germany) as referenced by the approval number G

12-3-028. Animals were housed in an AAALAC-accredited facility in accordance with the German Animal Welfare Act and the effective European Council Directive. Female Wistar rats [strain: CrI:WI(Han)] were obtained at an age of 7 weeks from Charles River Laboratories (Sulzfeld, Germany). The animals were maintained in groups up to five animals in a polysulfone cage [H-Temp (PSU)], TECNIPLAST, Germany) with a floor area of about 2,065 cm<sup>2</sup> (610 × 435 × 215 mm) with access to wooden gnawing blocks, GLP-certified feed (Kliba laboratory diet, Provimi Kliba SA, Kaiseraugst, Basel Switzerland), and water ad libitum. Animal room was kept at 20–24 °C and relative humidity 30–70 % with 15 air changes/h. A light/dark cycle of 12 h each was kept throughout the study periods. To adapt to the exposure conditions, the animals were acclimatized to fresh air under the study flow conditions in whole-body inhalation chambers for 2 days before the start of the exposure period. Up to 2 animals/cage were exposed in wire cages, type DKIII (BECKER & Co., Castrop-Rauxel, Germany) in a whole-body chamber. During the exposure, feed and drinking water were withdrawn from the animals.

#### Inhalation system

The animals were exposed in wire cages that were located in a stainless steel whole-body inhalation chamber ( $V = 2.8 \text{ m}^3$  or  $V = 1.4 \text{ m}^3$ ). The inhalation atmospheres were passed into the inhalation chambers with the supply air and were removed by an exhaust air system with 20 air changes/h. For the control animals, the exhaust air system was adjusted in such a way that the amount of exhaust air was lower than the filtered clean, supply air (positive pressure) to ensure that no laboratory room air reaches the control animals. For the treated animals, the amount of exhaust air was higher than the supply air (negative pressure) to prevent the contamination of the laboratory as a result of potential leakages from the inhalation chambers.

#### Aerosol generation and monitoring

Ceria aerosols were produced by dry dispersion of powder pellets with a brush dust generator (developed by the Technical University of Karlsruhe in cooperation with BASF, Germany) using compressed air (1.5 m<sup>3</sup>/h). The so generated dust aerosol was diluted by conditioned air (54.5 m<sup>3</sup>/h) passed into whole-body inhalation chambers. The control group was exposed to conditioned, clean air. The desired concentrations were achieved by varying the feeding speed of the substance pellet and by varying the rotating speed of the brush. Based on the data of a comprehensive technical trial, the aerosol concentrations within the chambers were considered to be homogenous (data not shown). Nevertheless, the positions of the exposure cages were rotated within

each chamber. Generated aerosols were continuously monitored by scattered light photometers (VisGuard, Sigrist). Particle concentrations in the inhalation atmospheres were analyzed by gravimetric measurement of air filter samples. Particle size distribution was determined gravimetrically by cascade impactor analysis using eight stages Marple personal cascade impactor (Sierra Anderson, USA). In addition, light-scattering aerosol spectrometer (WELAS<sup>®</sup> 2000, Palas, Karlsruhe, Germany) was used to measure particles from 0.24 to 10 μm. To measure particles in the submicrometer range, scanning mobility particle sizer (SMPS 5.400, Grimm Aerosoltechnik, Ainring, Germany) was used. The sampling procedures and measurements to characterize the generated aerosols were described in detail in a previous work (Ma-Hock et al. 2007).

#### Study design of short-term studies (5 days and 4 weeks of exposure)

In general, the animals were whole-body exposed to dust aerosols for 6 h/day on 5 consecutive days/week with a respective post-exposure period (see Fig. 1). The highest aerosol concentration was 25 mg/m<sup>3</sup>, which was expected to cause biological effects and should lead to lung overload at least for 20 exposures. The mid and low aerosol concentrations were 5 and 0.5 mg/m<sup>3</sup>. The low aerosol concentration with an expected lung burden far below the overload condition should not lead to any adverse effects. The mid aerosol concentration, which was spaced tenfold higher than the low concentration, was expected to cause some biological effects. The post-exposure period and the examination time points were scheduled to address the progression or regression of the biological effects, with their correlation to lung burden and lung clearance kinetics.

#### Clinical examinations

Clinical observations of the animals were recorded for each animal at least three times per day on exposure days and once a day during the pre-exposure and post-exposure periods. Signs and findings were recorded for each animal. During exposure, examination was possible only on a group basis. The animals were weighed prior to the pre-exposure period, at the start of the exposure period (day 0), and twice weekly until killing or twice within the 5 exposure days.

#### Hematology and clinical chemistry

Blood sampling of five fasted rats per test group was performed in the morning by retro-orbital venous plexus puncture under isoflurane anesthesia (Isoba<sup>®</sup>, Essex GmbH

**Fig. 1** Study design of short-term studies with 5 days and 4 weeks of exposure

**5 days of exposure with 24 days of post-exposure**

Study day	1-4	5	6-7	8	9-25	26	27-28	29
Study phase	x	x	R	R	R	R	R	R
Examination		OB H		L		OB H		L

**4 weeks of exposure with 129 days of post-exposure**

Study day	1-28	29	30	31	32-36	37	38-61	62	63	64-92	93	94-156	157
Study phase	x	R	R	R	R	R	R	R	R	R	R	R	R
Examination		OB L	OB H	OB		OB		H	OB L		OB		OB

X: Whole-body exposure to aerosol for 6h/d, 5 d  
R: Post-exposure period (24 or 129 days)  
OB: Organ burden  
L: Examination of bronchoalveolar lavage fluid  
H: Histology of selected organs

Munich, Germany). The extent of the examination was according to the data requirements of OECD test guideline 412. The parameters such as red blood cell counts, hemoglobin, hematocrit, mean corpuscular volume (MCV), mean corpuscular hemoglobin content (MCH), mean corpuscular hemoglobin concentration (MCHC), platelet counts, total white blood cell as well as differential blood cell counts were determined in the EDTA-stabilized blood with a hematology analyzer (ADVIA<sup>®</sup> 120, Siemens Diagnostics, Fernwald, Germany). Additionally, acute-phase proteins were determined in serum: rat haptoglobin and rat  $\gamma$ 2-macroglobulin (ELISA by Immunology Consultants Laboratory Inc., Newberg, OR, USA) were measured with a Sunrise MTP Reader (Tecan AG, Switzerland) by using the Magellan Software provided by the instrument producer. The enzyme levels [alanine aminotransferase (ALT), aspartate aminotransferase (AST), alkaline phosphatase (ALP),  $\gamma$ -glutamyltransferase (GGT)] and different blood parameters of clinical chemistry were evaluated by using an automatic analyzer (Hitachi 917; Roche, Mannheim, Germany).

**Systemic genotoxicity (micronucleus test)**

Systemic genotoxicity (micronucleus test) was performed in the short-term studies with 5 days and 4 weeks of exposure (3 and 2 days after the end of exposure, respectively). Micronucleus analysis in erythrocytes of rat peripheral blood was performed with the MicroFlow<sup>®</sup> plus (Rat Blood) kit from Litron Laboratories, Rochester, NY, USA. The flow cytometric differentiation of reticulocytes as well as normochromic erythrocytes with and without micronuclei was done on the FacsCalibur instrument (Becton Dickinson, Heidelberg, Germany) after staining of the cells with CD71 and propidium iodide.

**Bronchoalveolar lavage**

Five animals per test group were killed by exsanguination from the aorta abdominals and vena cava under

pentobarbital (Narcoren<sup>®</sup>) anesthesia. The lungs of the animals were lavaged in situ twice with 6 mL (22 mL/kg body weight) of 9 % (w/v) saline solution. A total of 11 mL BALF was obtained per animal for analysis. Aliquots of the BALF were used for the determinations of total protein concentration, total cell count, differential cell count, and activity of the enzymes. In the short-term study with 5 days of exposure, BALF was analyzed 3 and 24 days after the end of exposure. After 4 weeks of exposure, lavaged lungs and aliquots of the BALF (1 mL) were stored at  $-80^{\circ}\text{C}$  and used for the determination of the Cer content in the lung (lung burden) 1 and 35 days after the end of exposure. Total BALF cell counts were determined with an ADVIA<sup>®</sup> 120 (Siemens Diagnostics, Fernwald, Germany) hematology analyzer. Counts of macrophages, polymorphonuclear neutrophils (PMN), lymphocytes, eosinophils, monocytes, and atypical cells were performed on Wright-stained cytocentrifuge slide preparations (Warheit and Hartsky 1993). The differential cell count was evaluated manually by counting at least 400 BALF cells per sample. Using a Hitachi 917 (Roche Diagnostics, Mannheim, Germany) reaction rate analyzer, levels of BALF total protein and activities of lactate dehydrogenase (LDH), alkaline phosphatase (ALP),  $\gamma$ -glutamyltransferase (GGT), and N-acetyl- $\beta$ -glucosaminidase (NAG) were measured.

**Cytokines and chemokines (in BALF and serum)**

Cytokines and chemokines in BALF and serum were measured at Rules-based Medicine Inc., Austin, TX, USA, with xMAP technology (Luminex Corp., Austin, TX, USA). The measured parameters comprised various cytokines, chemokines, adhesion molecules, matrix metalloproteinases, acute-phase proteins, signal proteins of apoptosis, or cell proliferation. Briefly, a list of parameters was described previously (Ma-Hock et al. 2009). After evaluation of the most sensitive parameters or reaction patterns in previous studies, the following standard parameters were chosen for characterizing the lung inflammation in BALF:

- Rat monocyte chemoattractant protein-1 level (*rat MCP-1*; Instant ELISA, Bender MedSystems, Vienna, Austria (cat. no. BMS631INST);
- Rat cytokine-induced polymorphonuclear neutrophil chemoattractant-1 level (*rat CINC-1/IL-8*; ELISA, R&D Systems Inc., Minneapolis, USA (Quantikine rat CINC-1, cat. no. RCN100);
- Macrophage colony-stimulating factor (*M-CSF*; Quantikine Mouse M-CSF ELISA, R&D Systems Inc., Minneapolis, USA (cat. no. MMC00);
- *Rodent osteopontin*; ELISA, R&D Systems, Inc., Minneapolis, US (Quantikine mouse osteopontin, cat. no. MOST00).
- The cell mediators were measured at a sunrise MTP reader (Tecan AG, Switzerland) by using the Magellan Software provided by the instrument producer. Four chemokines and cytokines were measured using ELISA test kits: MCP-1, IL-8/CINC-1, M-CSF, and osteopontin. The detailed procedure was described previously (Ma-Hock et al. 2009).

#### Pathology

In the short-term studies, necropsy and histopathology were performed after 5 days of exposure and 21 days after the end of exposure (5 days of exposure) and 2 and 34 days after the end of exposure (4 weeks of exposure). In general, five animals per test group were investigated for pathological examination in both short-term studies. For the short-term study with 4 weeks of exposure, however, ten animals were examined for pathological examination of the respiratory tract and all gross lesions. At necropsy, animals were exsanguinated by opening of the abdominal great vessels under deep pentobarbital anesthesia. All organs were preserved according to OECD TG No. 412. Following organs were weighed: adrenal glands, brain, heart, ovaries, uterus with cervix, kidney, liver, lungs, spleen, thymus, and thyroid glands. The lungs were instilled (30 cm water column) with and fixed in 10 % neutral-buffered formalin (NBF). After 24- to 48-h fixation in 10 % NBF, the lungs were transferred to 70 % ethanol. All other organs were fixed in 10 % NBF. All the organs and tissues described in the OECD TG No. 412 were trimmed according to the RITA trimming guides for inhalation studies (Kittel et al. 2004; Ruehl-Fehlert et al. 2003). After paraplast-embedding, the blocks were cut at 2- to 3- $\mu$ m thickness, mounted on glass slides and stained with hematoxylin and eosin. Extrapulmonary organs and the respiratory tract compromising nasal cavity (four levels), larynx (three levels), trachea (transverse and longitudinal with carina), lung (five lobes), and mediastinal and tracheobronchial lymph nodes were assessed by light microscopy. For the lungs, whole histopathological examination was performed in animals of all

test groups. For all other tissues, only the animals of the control and high concentration group of Ceria were initially examined. When changes were observed in the high concentration group, respective organs and tissues of the animals exposed to low and intermediate aerosol concentrations were also examined by light microscopy. All histopathological examinations were performed by a well-experienced board-certified veterinarian toxicopathologist followed by an internal pathology peer review.

#### Organ burden analysis

Lung burden of the two different Ceria was evaluated twice, immediately after 5 days of exposure and after 21 days after the exposure end. In the short-term study with 4 weeks of exposure, Cerium content was determined at seven time points over 129 days of post-exposure period. Cerium content in the lungs, lung-associated lymph nodes, and liver of either three or five animals per test group were examined. 1 and 35 days after the end of exposure (4 weeks of exposure), the lavaged lungs and aliquots of BALF of five animals per group were used for the determination of lung burden. This examination method has likely caused a loss of the test material during preparation and handling of the lungs. Furthermore, lung burdens were measured 2 days after the end of exposure using the left half lungs of five animals/test group, only. On the basis of the availability of total lung weights, lung burdens were calculated up from the half lung burden values with the corresponding weight of the half lungs. Lung burden of the remaining time points was determined using the whole (not lavaged) lung. After digestion with mixed acid, samples of each lung or lymph node were dissolved in sulfuric acid and ammonium sulfate.  $^{140}\text{Ce}$  content in the obtained solution was analyzed by inductively coupled plasma mass spectrometry (ICP-MS, Agilent 7500 C) or by inductively coupled plasma optical emission spectrometry (ICP-OES, Varian 720-ES) with a wavelength of 419 nm. With this method, limit of detection for Cer is 0.3  $\mu\text{g}$ . The amounts of Ceria in the respective tissues were calculated by measuring elemental Cerium with ICP-MS.

#### Statistical analysis

For body weight changes, Dunnett's test was used for a comparison of each test group with the control group test (Dunnett 1955; Dudewicz et al. 1975). Clinical pathology parameters (BALF cytology, enzyme data, and BALF and serum cell mediator data) were analyzed by nonparametric one-way analysis using the Kruskal–Wallis test (two-sided). If the resulting  $p$  value was  $\leq 0.05$ , a pair-wise comparison of each test group with the control group was performed using the Wilcoxon test or the Mann–Whitney  $U$

test (both two-sided) ( $p \leq 0.05$  for statistical significance). Comparison of organ weights among test groups was performed by nonparametric one-way analysis using the two-sided Kruskal–Wallis test, followed by a two-sided Wilcoxon test for the hypothesis of equal medians in case of  $p \leq 0.05$ .

## Results

### Characterization of test material

Both Ceria were yellowish white powders that were produced by precipitation and were nominally uncoated. We completely re-characterized the Ceria NM-211 and NM-212 based on the nano-specific guidance on physical–chemical properties (Wohlleben et al. 2013). Table 1 indicates the techniques chosen for each end point (see “Materials and methods” section) and summarizes the results. The Ceria NM-212 material had an average primary particle diameter of 40 nm, in excellent accordance of electron microscopy with the crystallite size derived from the diffraction peak width and with the sphere-equivalent diameter derived from the BET-specific surface area of  $27 \text{ m}^2/\text{g}$  (see Fig. 2). The Ceria NM-211 material consisted of considerably smaller primary particles with number-based median diameter of 8.2 nm (from TEM) and correspondingly larger specific surface ( $53 \text{ m}^2/\text{g}$ , from BET). Primary particles of both materials were crystalline with cubic lattice as it is the characteristic for cerianite and had irregular, but roughly globular shapes. In the as-produced powder, porosimetry by Hg intrusion indicated that these particles were aggregated and agglomerated to sizes that range from a few hundred nm to tens of  $\mu\text{m}$ .

The surface of Ceria NM-212 beared organic contaminations. An assessment by thermogravimetry (TGA) confirmed that the total organic content remained below 0.7 %, but the photoelectron signal of XPS, which had an information depth between 3 and 10 nm, indicated 80 % carbon atoms on the surface. The contamination was hence a very thin and homogeneous layer around the purely inorganic particles. According to the fit of photoelectron energies from C(1s) level and from O(1s) level, the contamination could be an ester with a long alkyl chain. In contrast, the Ceria NM-211 had only 14 % carbon atoms on the surface (by XPS), and the even more sensitive SIMS techniques confirmed that Ceria dominated the surface, with vanishing amounts of nitrates and alkyls. The Cerium atoms at crystalline edges were known to be redox-active, which was confirmed by the detection of 14 % of the Cerium as Ce(III) (within the XPS-accessible surface layer) in Ceria NM-212, respectively, 22 % for the Ceria NM-211 with its decreased radius of curvature.

If dispersed in clean water, the Ceria NM-212 surface was positively charged across the entire physiological pH range, with a zeta-potential of +42 mV at pH 7. The surface of Ceria NM-212 was rather reactive in a photocatalytic assay with a photon efficiency of  $1.3 \times 10^{-2}$ , which was 5 times higher than the well-known Titania P25 (NM-105) and an order of magnitude higher than for the Ceria NM-211, leaving the possibility of the organic contaminations being responsible for that catalytic activity, observed only under UV irradiation (Wohlleben et al. 2013; Molina et al. 2014). After dispersion in water by stirring only, the dispersability was limited with average agglomeration numbers (AAN = the ratio of agglomerate diameter to primary particle diameter) above 10, based on the measurement of the resulting agglomerates that were just below the micron range (by analytical ultracentrifugation), and tended to be larger for the Ceria NM-211 than for NM-212, confirming earlier findings of the PROSPECT consortium and the European Commission’s JRC report (Hermans 1963; PROSPECT: Ecotoxicology Test Protocols for Representative Nanomaterials in Support of the OECD Sponsorship Programme 10 A.D.; European Commission 2014).

The solubility in physiological media was investigated by 28-day abiotic incubation in different fluids and detection of both the remaining particulate fraction (by SEM, centrifugation, LD, zeta-potential) and of the released metal ions (by ICP-MS). Both Ceria were insoluble except for marginal solubility in 0.1 N HCl (simulate oral ingestion), whereas a nanoscale precipitated Silica as positive control dissolved readily and Titania (NM-105) showed marginal solubility in phagolysosomal simulant fluid (PSF, simulate uptake and digestion in macrophages) (Wohlleben et al. 2013). In buffers with organic constituents (PSF, fasted state simulated intestinal fluid = FaSSIF), the surface charge reversed to negative zeta-potentials, which was identified earlier as indicator for the adsorption of constituents of the buffer for a range of the nano-Ceria (Wohlleben et al. 2013). Under all conditions, primary particles remained recognizable in TEM scans, but both Ceria NM-211 and NM-212 formed large structures after 28-day incubation in the acidic PSF medium that simulates the lysosome of macrophages (see Fig. 3). We found by selected area electron diffraction (SAD) that these aged structures retained the same cubic cerianite crystalline phase of the as-produced powder for both Ceria NM-211 and NM-212. Under identical conditions, also other nanomaterials, e.g., the Titania (NM-105), aged into similar structures, and we added the respective TEM and SAD for comparison (Wohlleben et al. 2013).

To summarize the comparative physical–chemical characterization, Ceria NM-211 and NM-212 had identical composition, agglomeration state, crystallinity, and insolubility. Compared to NM-212, the Ceria NM-211

**Table 1** Physical–chemical characterization of Ceria NM-212 and NM-211

OECD end points	Ceria NM-212	Ceria NM-211
Particle size distribution (TEM: primary particle diameter)/ state of agglomeration (SEM: agglomerate diameter)	40 nm SEM: 3,000–150,000 nm Hg pore sizes: 35 nm, around 7 µm	4–15 nm D50: 8.2 nm Hg pore sizes: 5, 70 nm, around 10 µm
Crystallite size (XRD)	40.0 nm	12.5 nm
Crystallite phase (XRD)	Cerianite, Ceria-cubic	Cerianite, Ceria-cubic
Specific surface area (Hg, BET)	30 m <sup>2</sup> /g (Hg), 27 m <sup>2</sup> /g (BET)	33 m <sup>2</sup> /g (Hg), 53 m <sup>2</sup> /g (BET)
Surface chemistry (XPS)	C 79.9 (C–C 62.6; C–O 7.0; C=O 3.5; COOH 6.9)	Ce 28.7 O 57.2 C 14.1
Atom percent	O 17.7 Ce 2.4 With oxidation state Ce(III) 14 %, Ce(IV) 86 %	With oxidation state Ce(III) 22 %, Ce(IV) 78 %
Surface charge	IEP: >pH 10 (always cationic) +42 mV	IEP = pH 8.3 +16 mV
Isoelectric point = IEP		
ζ-Pot at pH 7 from electrophoretic mobility		
Photocatalytic activity		
Photon efficiency (methylene blue)	0.01 ± 0.005	0.0005 ± 0.0002
Dispersability		
D50 and average agglom. number (centrifugation)	D50 = 432 nm/AAN = 11(in water)	D50 = 2,839 nm/AAN = 346 (in water)
Solubility (ICP-MS)		
In water	0.002 wt%	<0.001 wt%
In DMEM/FCS	<0.001 wt%	<0.001 wt% (recrystallizes)
In PSF	<0.001 wt% (recrystallizes)	<0.001 wt%
In PBS	<0.001 wt%	
In FassiF	<0.001 wt%	
In 0.1 N HCl	0.02 wt% (ripening)	
Impurities (TGA, XPS)	Total content of 0.7 % organic contaminations, identified as ester + alkyl groups, found mostly on the particle surface	Total content of 1.6 % contaminations, thereof small amounts of alkyls found on the particle surface

**Fig. 2** Structure of Ceria. Electron microscopy images of a representative ensemble of particles of Ceria NM-211 (a) and NM-212 (b) (see Table 1 for size characterization by complementary methods)

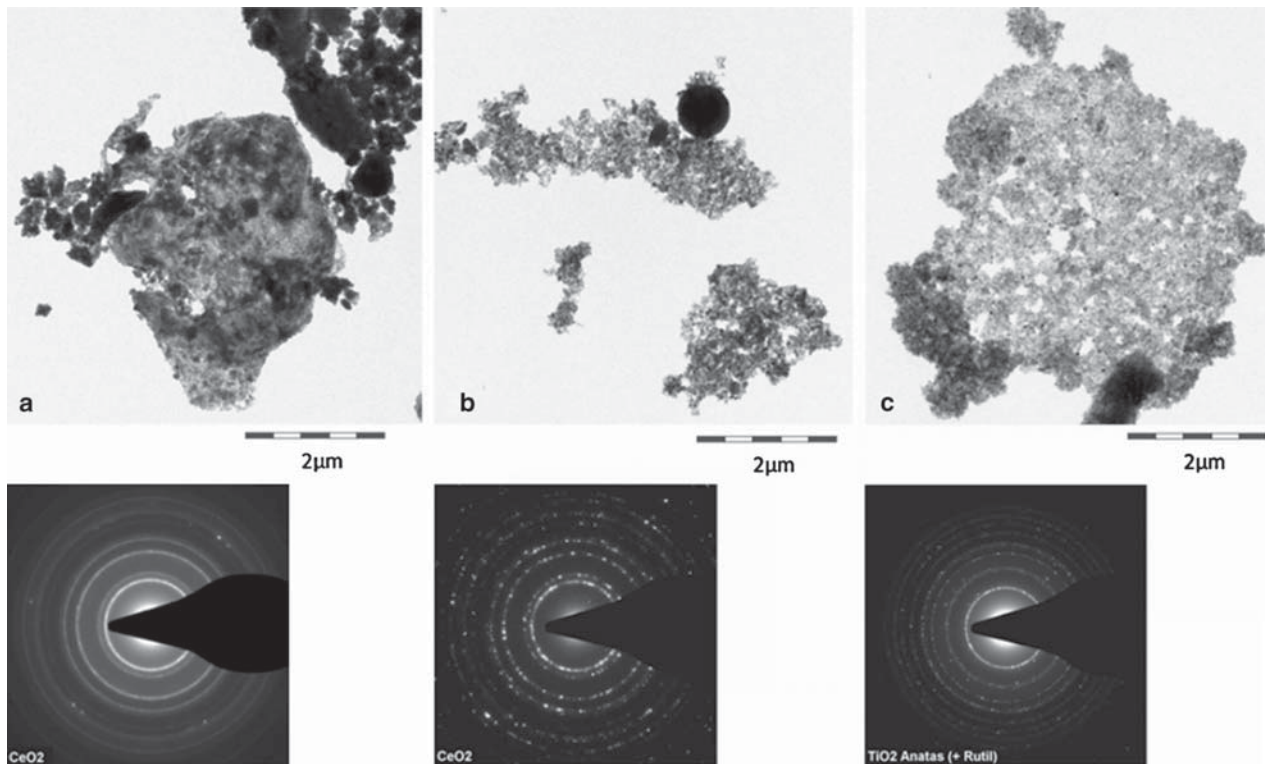
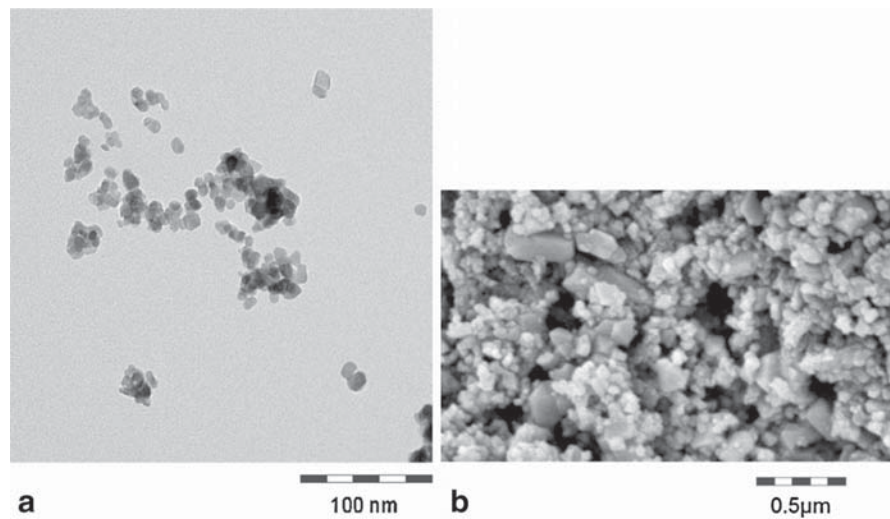


**Fig. 3** Persistence of Ceria NM-211 (a), NM-212 (b), and Titania NM-105 (c) as benchmark. Transmission electron microscopy (TEM) and selected area diffraction (SAD) after 28-day incubation in phagolysosomal simulant fluid (PSF) [see Table 1 for dissolution detected

by ions in the supernatant (ICP-MS)]. The large almost spherical structures are no contaminations, but are confirmed as Ceria in the same crystalline phase

had considerably smaller primary particles, larger specific surface, significantly fewer organic contaminations on the surface, and much reduced photocatalytic activity. Despite these differences, Ceria NM-211 and NM-212 shared the same tendency to recrystallize in PSF.

#### Characterization of test atmosphere

The target concentrations were 0.5, 5, and 25 mg/m<sup>3</sup> in the short-term studies (5 days and 4 weeks of exposure) with nano-Ceria NM-212. In the study with 5 days of exposure,

**Table 2** Measured concentrations and particle size distributions of Ceria

Study	Test substance	Targeted concentrations (mg/m <sup>3</sup> )	Measured concentrations mean ± SD (mg/m <sup>3</sup> )	MMAD (μm)/GSD mean	Particle count concentration measured by SMPS (particle/cm <sup>3</sup> )	Particle count median (nm)
5 days of exposure	Ceria NM-212	0.5	0.5 ± 0.2	1.4/2.3	2,583	283
		5	5.3 ± 0.9	1.2/2.1	137,096	206
		25	25.9 ± 6.0	1.0/2.5	537,548	171
	Ceria NM-211	0.5	0.48 ± 0.0	1.6/2.1	5,689	256
		25	5.2 ± 1.1	1.3/2.1	84,655	167
4 weeks of exposure	Ceria NM-212	0.5	25.6 ± 6.0	0.9/2.5	514,193	203
		5	0.45 ± 0.1	1.9/2.9	1,503	242
		25	25.8 ± 1.7	2.2/2.4	160,162	188

0.5 and 25 mg/m<sup>3</sup> were selected for nano-Ceria NM-211. Analyzed concentrations and particle size distributions are summarized in Table 2. The target concentrations were met and maintained well throughout the studies. Particle size distribution demonstrated that Ceria particles were in the respirable range for rats.

#### Clinical examination

Five days and 4 weeks of inhalation exposure to Ceria NM-212 and NM-211 did not affect the body weight development of the animals (data not shown). The animals exposed to Ceria NM-211 and NM-212 showed no clinical signs or findings compared to the control animals (data not shown).

Hematology, clinical chemistry, cytokines, and chemokines in serum

#### Five days of exposure

Absolute and relative neutrophil counts in blood were increased 3 days after the end of exposure to 25 mg/m<sup>3</sup> Ceria NM-212 and NM-211, whereas relative lymphocyte counts were decreased (see Table S2). The changes were in a concentration-related manner. 24 days after the end of exposure, all parameters had returned to near control values. No other blood parameters were affected.

#### Four weeks of exposure

Hematological, clinical chemistry parameters, and acute-phase protein levels were not affected in rats exposed to Ceria NM-212 (see Table S2; the other data are not shown).

#### Systemic genotoxicity (micronucleus test)

Micronuclei in the erythrocytes of peripheral blood cells were counted to assess chromosomal aberrations of

hematopoietic cells in the bone marrow. Peripheral blood cells were examined in the short-term studies with 5 days and 4 weeks of exposure (3 and 2 days after the end of exposure, respectively). All examined parameters were in the range of control values (see Table S3).

#### Bronchoalveolar lavage (BAL)

In the short-term studies with 5 days and 4 weeks of exposure, BALF analysis of five animals per test group was obtained 3 days or 1 day after the end of exposure and 24 or 35 days after the end of exposure, respectively (see Fig. 1). The resulting BALF parameters are presented in Table 3.

#### Five days of exposure

In animals exposed to Ceria NM-212, the majority of BALF parameters were increased at aerosol concentrations of 5 mg/m<sup>3</sup>. At 0.5 mg/m<sup>3</sup>, the neutrophil counts and cytokine-induced neutrophil chemoattractant-1 (CINC-1) were both statistically increased and were slightly above the historical control range (see Table S4). With Ceria NM-211, but not NM-212, monocyte chemoattractant protein-1 (MCP-1) and macrophage colony-stimulating factor (M-CSF) were increased at aerosol concentrations of 0.5 mg/m<sup>3</sup> and above. 24 days after the end of exposure, a full recovery was observed at aerosol concentrations of 0.5 mg/m<sup>3</sup> and a partial recovery at aerosol concentrations of 5 and 25 mg/m<sup>3</sup>. The recovery of animals exposed to 25 mg/m<sup>3</sup> Ceria NM-211 seems to be slower than those exposed to NM-212.

#### 4 weeks of exposure

Four weeks of inhalation exposure to 5 and 25 mg/m<sup>3</sup> Ceria NM-212 resulted in an increase in total cells in BALF due to increases in polymorph nuclear neutrophils, lymphocytes, and monocytes in BALF (see Table 3). Consistent

**Table 3** Clinical pathology parameters in BALF of short-term studies with 5 days and 4 weeks of exposure

Target conc. (mg/m <sup>3</sup> )	5 days of exposure						4 weeks of exposure					
	Control			Ceria NM-211			Control			Ceria NM-212		
	0	5	25	0.5	5	25	0	5	25	0.5	5	25
Measured conc. (mg/m <sup>3</sup> ) ± SD	0	0.48 ± 0.0	5.2 ± 1.1	25.6 ± 6.0	0.45 ± 0.1	25.8 ± 1.70	0	0.5 ± 0.2	5.3 ± 0.9	0.5 ± 0.2	5.3 ± 0.9	25.9 ± 6.0
BALF cell counts (cv/μL)												
Total cells												
Time point 1 <sup>a</sup>	63.73 ± 11.03	98.24** ± 16.38	337.35** ± 125.24	46.71 ± 8.16	71.32 ± 22.69	374.98** ± 77.84	76.42 ± 23.97	75.10 ± 21.51	133.44* ± 48.40	296.90** ± 124.92	133.44* ± 48.40	296.90** ± 124.92
Time point 2 <sup>b</sup>	53.09 ± 13.33	43.98 ± 17.70	49.19** ± 17.68	4.63** ± 3.83	47.01 ± 11.34	81.20 ± 38.87	75.29 ± 14.10	62.23 ± 11.59	97.44 ± 34.23	220.50** ± 105.27	97.44 ± 34.23	220.50** ± 105.27
Neutrophils (PMN)												
Time point 1 <sup>a</sup>	0.82 ± 0.80	3.70** ± 2.53	49.19** ± 17.68	4.63** ± 3.83	4.41* ± 3.38	297.21** ± 59.23	0.85 ± 0.35	1.75 ± 1.13	65.66** ± 50.23	222.29** ± 99.25	65.66** ± 50.23	222.29** ± 99.25
Time point 2 <sup>b</sup>	0.69 ± 0.38	1.34 ± 2.01	5.15 ± 9.91	4.63** ± 3.83	2.27** ± 0.56	25.57** ± 33.95	2.44 ± 1.01	2.52 ± 1.37	41.70** ± 22.0	161.69** ± 87.82	41.70** ± 22.0	161.69** ± 87.82
Lymphocytes												
Time point 1 <sup>a</sup>	0.22 ± 0.32	0.17 ± 0.22	1.57* ± 0.97	9.20** ± 4.51	0.39 ± 0.34	19.14** ± 15.13	0.55 ± 0.50	0.63 ± 0.74	5.41** ± 3.21	8.93** ± 6.04	5.41** ± 3.21	8.93** ± 6.04
Time point 2 <sup>b</sup>	0.32 ± 0.33	0.11 ± 0.10	0.43 ± 0.31	1.03 ± 0.95	0.51 ± 0.25	2.74** ± 2.17	1.65 ± 1.13	0.77 ± 0.49	7.43* ± 9.02	10.89** ± 3.48	7.43* ± 9.02	10.89** ± 3.48
Macrophages												
Time point 1 <sup>a</sup>	62.65 ± 11.56	75.72 ± 15.10	46.83 ± 23.88	51.21 ± 24.76	66.47 ± 22.13	52.99 ± 42.89	74.94 ± 23.79	72.71 ± 21.16	60.25 ± 20.82	59.32 ± 26.28	60.25 ± 20.82	59.32 ± 26.28
Time point 2 <sup>b</sup>	52.05 ± 13.00	42.32 ± 3.66	38.34 ± 11.92	40.93 ± 6.31	44.23 ± 11.53	52.61 ± 15.51	71.14 ± 13.31	58.78 ± 11.04	47.58 ± 16.48	45.17 ± 25.33	47.58 ± 16.48	45.17 ± 25.33
Monoocytes												
Time point 1 <sup>a</sup>	0.04 ± 0.08	0.00 ± 0.00	0.52* ± 0.37	3.50 ± 1.86**	0.05 ± 0.11	4.40** ± 2.68	0.00 ± 0.00	0.00 ± 0.00	1.65* ± 1.90	3.95* ± 4.65	1.65* ± 1.90	3.95* ± 4.65
Time point 2 <sup>b</sup>	0.00 ± 0.00	0.00 ± 0.00	0.03 ± 0.07	0.07 ± 0.11	0.00 ± 0.00	0.28 ± 0.34	0.06 ± 0.09	0.04 ± 0.08	0.68* ± 0.43	2.46* ± 3.03	0.68* ± 0.43	2.46* ± 3.03
Eosinophils												
Time point 1 <sup>a</sup>	0.00 ± 0.00	0.00 ± 0.00	0.00 ± 0.00	0.39 ± 0.54	0.00 ± 0.00	0.00 ± 0.00	0.09 ± 0.12	0.00 ± 0.00	0.00 ± 0.00	0.34 ± 0.49	0.00 ± 0.00	0.34 ± 0.49
Time point 2 <sup>b</sup>	0.03 ± 0.06	0.00 ± 0.00	0.03 ± 0.06	0.00 ± 0.00	0.00 ± 0.00	0.00 ± 0.00	0.00 ± 0.00	0.12 ± 0.11	0.05 ± 0.11	0.00 ± 0.00	0.05 ± 0.11	0.00 ± 0.00
Atypical cells												
Time point 1 <sup>a</sup>	0.00 ± 0.00	0.00 ± 0.00	0.12 ± 0.17	0.76 ± 0.73	0.00 ± 0.00	1.25* ± 0.85	0.00 ± 0.00	0.00 ± 0.00	0.48 ± 0.72	2.07* ± 1.71	0.48 ± 0.72	2.07* ± 1.71
Time point 2 <sup>b</sup>	0.00 ± 0.00	0.00 ± 0.00	0.00 ± 0.00	0.05 ± 0.07	0.00 ± 0.00	0.00 ± 0.00	0.00 ± 0.00	0.00 ± 0.00	0.00 ± 0.00	0.29 ± 0.40	0.00 ± 0.00	0.29 ± 0.40
Total protein/enzymes												
Total protein (mg/L)												
Time point 1 <sup>a</sup>	39 ± 15	47 ± 16	75* ± 23	198** ± 52	44 ± 7	207** ± 54	60 ± 4	83** ± 5	94** ± 21	245** ± 77	83** ± 5	245** ± 77
Time point 2 <sup>b</sup>	97 ± 122	59 ± 28	51 ± 16	60* ± 9	92 ± 91	82 ± 14	81 ± 23	60 ± 22	98 ± 49	175** ± 98	60 ± 22	175** ± 98
GGT (nkat/L)												
Time point 1 <sup>a</sup>	20 ± 15	36 ± 20	106** ± 26	125** ± 15	37 ± 26	128** ± 16	37 ± 17	51 ± 11	111** ± 21	149** ± 31	51 ± 11	149** ± 31
Time point 2 <sup>b</sup>	30 ± 7	28 ± 17	33 ± 14	61** ± 16	25 ± 10	87** ± 20	42 ± 12	44 ± 20	83** ± 30	123** ± 30	44 ± 20	123** ± 30
LDH (μkat/L)												
Time point 1 <sup>a</sup>	0.46 ± 0.09	0.58 ± 0.17	0.89** ± 0.25	2.17** ± 0.21 0.67	0.58 ± 0.40	2.60** ± 0.31	0.51 ± 0.18	0.55 ± 0.15	1.08** ± 0.37	2.28** ± 0.52	0.55 ± 0.15	2.28** ± 0.52
Time point 2 <sup>b</sup>	0.36 ± 0.14	0.47 ± 0.25	0.42 ± 0.04	0.72** ± 0.20	0.58 ± 0.40	1.08** ± 0.32	0.58 ± 0.08	0.50 ± 0.20	0.84* ± 0.22	1.88** ± 1.20	0.50 ± 0.20	1.88** ± 1.20

**Table 3** continued

Target conc. (mg/m <sup>3</sup> )	5 days of exposure					4 weeks of exposure				
	Control		Ceria NM-212		Ceria NM-211		Control		Ceria NM-212	
	0	5	25	0.5	5	25	0	0.5	5	25
ALP (µkat/L)										
Time point 1 <sup>a</sup>	0.43 ± 0.10	<b>1.31**</b> ± 0.53	<b>1.56**</b> ± 0.15	<b>0.55*</b> ± 0.09	<b>1.56**</b> ± 0.35	<b>0.83</b> ± 0.16	<b>1.16**</b> ± 0.10	<b>1.05**</b> ± 0.16	<b>1.16**</b> ± 0.10	<b>1.53**</b> ± 0.21
Time point 2 <sup>b</sup>	1.0	<b>1.5*</b>	<b>1.9**</b>	0.51 ± 0.20	<b>0.87**</b> ± 0.12	0.70 ± 0.09	<b>1.05**</b> ± 0.16	<b>1.05**</b> ± 0.16	<b>1.05**</b> ± 0.16	<b>1.09**</b> ± 0.25
NAG (nkat/L)										
Time point 1 <sup>a</sup>	46 ± 9	47 ± 11	<b>74**</b> ± 7	51 ± 19	<b>94**</b> ± 16	45 ± 5	<b>53*</b> ± 8	<b>53*</b> ± 8	<b>53*</b> ± 8	<b>86*</b> ± 26
Time point 2 <sup>b</sup>	41 ± 10	37 ± 12	46 ± 7	46 ± 7	<b>59*</b> ± 10	47 ± 8	47 ± 7	47 ± 7	47 ± 7	71 ± 35
Cell mediators (pg/mL)										
MCP-1										
Time point 1 <sup>a</sup>	14.7 ± 0.6	<b>101.1**</b> ± 31.3	<b>1,342.9**</b> ± 530.0	<b>17.5*</b> ± 1.6	<b>1,581.0**</b> ± 771.3	14.0 ± 0.0	<b>559.4**</b> ± 444.4	<b>3,587.2**</b> ± 281.0	<b>559.4**</b> ± 444.4	<b>3,587.2**</b> ± 281.0
Time point 2 <sup>b</sup>	48.2 ± 59.1	22.8 ± 12.5	<b>144.1*</b> ± 82.8	30.6 ± 26.0	<b>329.2**</b> ± 290.5	17.3 ± 2.6	<b>492.5**</b> ± 553.1	<b>1,854.2**</b> ± 1,184.0	<b>492.5**</b> ± 553.1	<b>1,854.2**</b> ± 1,184.0
CINC-1/IL-8										
Time point 1 <sup>a</sup>	59.8 ± 17.7	<b>83.4*</b> ± 24.6	<b>322.4**</b> ± 93.9	<b>88.3*</b> ± 21.1	<b>436.0**</b> ± 228.3	104.2 ± 26.7	<b>506.7**</b> ± 195.9	<b>1,190.9**</b> ± 294.9	<b>506.7**</b> ± 195.9	<b>1,190.9**</b> ± 294.9
Time point 2 <sup>b</sup>	88.3 ± 25.7	87.5 ± 24.7	<b>155.1**</b> ± 13.5	99.7 ± 39.4	<b>254.3**</b> ± 70.4	158.8 ± 38.1	<b>449.4**</b> ± 226.7	<b>831.0**</b> ± 497.1	<b>449.4**</b> ± 226.7	<b>831.0**</b> ± 497.1
M-CSF										
Time point 1 <sup>a</sup>	41 ± 17	52 ± 23	<b>91**</b> ± 28	<b>61*</b> ± 16	<b>114**</b> ± 48	26 ± 17	27 ± 18	48 ± 29	27 ± 18	48 ± 29
Time point 2 <sup>b</sup>	45 ± 19	48 ± 5	49 ± 3	51 ± 12	60 ± 24	46 ± 26	41 ± 14	53 ± 12	41 ± 14	53 ± 12
Osteopontin										
Time point 1 <sup>a</sup>	172.28 ± 48.04	194.81 ± 131.24	<b>849.04**</b> ± 386.44	134.32 ± 82.72	<b>1,116.02**</b> ± 653.35	391.44 ± 187.39	<b>755.44*</b> ± 206.21	592.14 ± 336.47	<b>755.44*</b> ± 206.21	592.14 ± 336.47
Time point 2 <sup>b</sup>	320.38 ± 177.64	191.47 ± 116.09	247.44 ± 189.46	111.92 ± 80.28	398.72 ± 140.88	337.36 ± 282.91	<b>1,003.18*</b> ± 434.20	838.48 ± 529.45	<b>1,003.18*</b> ± 434.20	838.48 ± 529.45

\* Statistically significant,  $p < 0.05$

\*\* Statistically significant,  $p < 0.01$ ;  $n = 5$ ; SD standard deviation

<sup>a</sup> Time point 1: 3 days after the end of exposure (5 days of exposure) and 1 day after the end of exposure (4 weeks of exposure)

<sup>b</sup> Time point 2: 24 days after the end of exposure (5 days of exposure) and 35 days after the end of exposure (4 weeks of exposure)

with these findings, several other parameters including the examined cell mediators were increased. 35 days after the end of exposure, some of the BALF parameters returned to control levels, whereas several of them were still significantly increased at 5 and 25 mg/m<sup>3</sup> (e.g., total cells, lymphocytes, neutrophils; GGT, LDH, ALP; MCP-1, CINC-1).

Five days of exposure caused slightly higher neutrophil and lymphocyte counts at aerosol concentrations of 25 mg/m<sup>3</sup> Ceria NM-212 compared to 4 weeks of exposure (see Fig. 4). CINC-1 was already increased at 0.5 mg/m<sup>3</sup> after 5 days but not after 4 weeks of exposure. The regression of the BALF parameters was faster after 5 days than after 4 weeks of inhalation exposure. Cell mediators, especially MCP-1, were higher elevated at concentrations of 5 and 25 mg/m<sup>3</sup> after 4 weeks than after 5 days of exposure.

## Pathology

### *Organ weights and macroscopic findings*

*Five days of exposure* After 5 days of exposure, no increase in lung weights was observed after exposure to Ceria NM-212 (see Table S5). An aerosol concentration of 25 mg/m<sup>3</sup> Ceria NM-211, however, resulted in significant increases in absolute and relative lung weights (+20 and 24 %, respectively,  $p < 0.01$ ). The increase in lung weight was no longer present 21 days after the end of exposure. After 5 days of exposure, the macroscopic finding enlarged mediastinal lymph nodes were found in individual animals of all test groups (see Table S5). 21 days after the end of the exposure, enlarged mediastinal lymph nodes were observed in almost all animals exposed to Ceria NM-211 or NM-212. The tracheobronchial lymph nodes and all other examined organs did not show any macroscopic findings.

*Four weeks of exposure* Absolute and relative lung weights were significantly increased at aerosol concentrations of 25 mg/m<sup>3</sup> Ceria NM-212 (+30 and 29 %, respectively) 2 days after the end of the exposure and were still significantly elevated (+16 and 20 %) 34 days after the end of the exposure (see SI, S5). 2 days after the end of the exposure, absolute and relative lung weights of animals exposed to 5 mg/m<sup>3</sup> were increased significantly by +13 and 10 %, respectively. They returned to control levels within the following 34 days. No effects on organ weights were observed after inhalation of 0.5 mg/m<sup>3</sup>. 2 days after the end of exposure, mediastinal lymph nodes of two animals (out of ten) were enlarged at aerosol concentrations of 25 mg/m<sup>3</sup> Ceria NM-212. 34 days after the end of exposure, the incidence of animals with enlarged, yellow white-colored mediastinal lymph nodes increased considerably from two to eight (out of ten) per group at aerosol concentrations of 25 mg/m<sup>3</sup> Ceria NM-212, respectively.

Mediastinal lymph nodes of animals exposed to 5 mg/m<sup>3</sup> were firstly enlarged 34 days after the end of exposure.

All other extrapulmonary organs including the tracheo-bronchial lymph nodes revealed no macroscopical findings after inhalation exposure to Ceria.

## Histopathology

Overall, histopathological evaluations were consistent in the short-term studies with 5 days and 4 weeks of exposure. The findings assessed in the short-term study with 5 days showed lower severities (see Table 4; Fig. 5a–c).

## Lungs

### *Five days of exposure*

After 5 days of exposure, single or accumulated macrophages were located in the lumen of the alveoli and a few macrophages occurred also in the alveolar wall and ducts. They were distributed multifocally in all lobes over the whole lung. Most of them were loaded with amber-like colored particles of different sizes (below 1 µm diameter). These particles were considered to represent agglomerated or aggregated Ceria particles (“alveolar histiocytosis with particles”). Alveolar histiocytosis and free eosinophilic granular material with particles, interpreted as remnants of destroyed macrophages, were found in the lung of almost all animals exposed to 25 mg/m<sup>3</sup> Ceria NM-211 and NM-212. At aerosol concentrations of 0.5 mg/m<sup>3</sup> Ceria NM-211, 0.5 and 5 mg/m<sup>3</sup> Ceria NM-212, amber-colored particles were noted within single histiocyte in the alveoli. In the bronchus-associated lymphoid tissue (BALT), particles were detected free or in single macrophages, mostly at 5 mg/m<sup>3</sup> Ceria and above. Findings regressed but were still present 21 days after the end of exposure. The finding “eosinophilic granular material with particles” was no longer visible after the post-exposure period. Particles were detected free or in single macrophages in BALT, even at the lowest concentration of 0.5 mg/m<sup>3</sup> Ceria NM-211. Only one animal exposed to 25 mg/m<sup>3</sup> Ceria NM-211 showed macrophage aggregates in BALT 21 days after the end of exposure.

### *Four weeks of exposure*

Two days after the end of the exposure, a concentration-related increase in alveolar macrophages was observed in the lungs in all Ceria NM-212-exposed animals (Table 4; Fig. 5a). Eosinophilic granular material and small particles were distributed in the alveoli of animals exposed to 5 and 25 mg/m<sup>3</sup> Ceria NM-212. The occurrence of alveolar histiocytosis and of eosinophilic granular material was

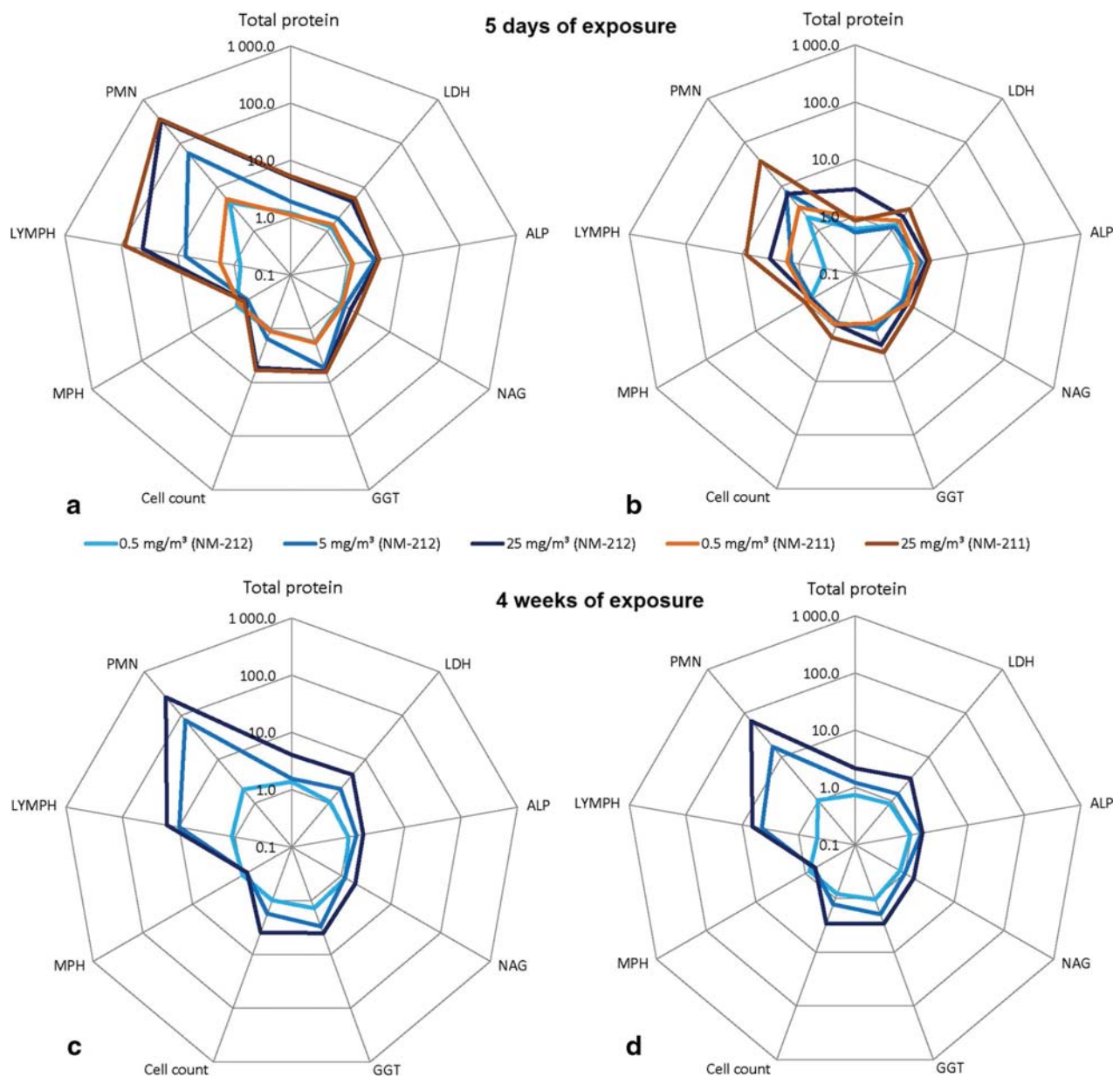


**Fig. 4** Comparison of changes in BALF parameters after 5 days (**a**, **b**) and 4 weeks (**c**, **d**) of exposure to Ceria NM-211 and NM-212: short-term study with 5 days of exposure: **a** 3 days after the end of exposure, **b** 24 days after the end of exposure; short-term study with

4 weeks of exposure, **c** 1 day after the end of exposure, **d** 35 days after the end of exposure. Changes are shown as  $x$ -fold differences compared to controls using a logarithmic scaling

correlated with increased lung weights in animals exposed to 5 and 25 mg/m<sup>3</sup> Ceria NM-212. In BALT, single, small macrophage aggregates with particles occurred in animals exposed to 25 mg/m<sup>3</sup> (see Fig. 5b). In addition, single or a few amber-like colored particles occurred extracellularly in BALT without any macrophage activation at aerosol concentrations of 5 and 25 mg/m<sup>3</sup>. 34 days after the end of exposure, alveolar histiocytosis and eosinophilic granular material with particles were still observed

at concentrations of 5 and 25 mg/m<sup>3</sup> Ceria NM-212. At 0.5 mg/m<sup>3</sup>, in contrast, amber-like colored particles could only be noted within single histiocyte. In one animal of 5 mg/m<sup>3</sup> and in five out of ten animals exposed to 25 mg/m<sup>3</sup> Ceria NM-212, a multifocal granulomatous inflammation appeared first. In BALT, single or few amber-colored particles at 0.5, 5, and 25 mg/m<sup>3</sup> Ceria NM-212 as well as an increasing number of animals with macrophage aggregates with particles at 5 and 25 mg/m<sup>3</sup> were still observed

**Table 4** Histopathology of short-term studies with 5 days and 4 weeks of exposure

Target conc. (mg/m <sup>3</sup> )	5 days of exposure to Ceria NM-212						5 days of exposure to Ceria NM-211				4 weeks of exposure to Ceria NM-212					
	Time point 1 <sup>a</sup>			Time point 2 <sup>b</sup>			Time point 1 <sup>a</sup>		Time point 2 <sup>b</sup>		Time point 1 <sup>a</sup>			Time point 2 <sup>b</sup>		
	0.5	5	25	0.5	5	25	0.5	25	0.5	25	0.5	5	25	0.5	5	25
<b>Histopathology</b>																
<b>Lungs</b>																
Alveolar histiocytosis with particles	-	-	<b>5</b>	-	<b>3</b>	<b>5</b>	-	<b>5</b>	-	<b>4</b>	<b>10</b>	<b>10</b>	<b>10</b>	-	<b>10</b>	<b>10</b>
Grade 1			1		3	5		3		4	10	4			3	
Grade 2			4					2				6	5		7	
Grade 3													5			10
Eosinophilic granular material/particles	-	-	<b>5</b>	-	-	-	-	<b>5</b>	-	-	-	<b>10</b>	<b>10</b>	-	<b>2</b>	<b>10</b>
Grade 1			2					5				10			2	5
Grade 2			3										6			4
Grade 3													4			1
BALT: macrophage aggregates particles	-	-	-	-	-	-	-	-	-	<b>1</b>	-	-	<b>5</b>	-	<b>1</b>	<b>8</b>
Grade 1										1			5			3
Grade 2															1	2
Grade 3																3
BALT: occurrence of particles	-	<b>2</b>	<b>5</b>	-	<b>3</b>	<b>5</b>	-	<b>5</b>	<b>2</b>	<b>4</b>	-	<b>8</b>	<b>5</b>	<b>3</b>	<b>8</b>	<b>2</b>
Inflammation, granulomatous	-	-	-	-	-	-	-	-	-	-	-	-	-	-	<b>1</b>	<b>5</b>
Grade 1															1	
Grade 2																5
Particles within histiocytes	<b>5</b>	<b>5</b>	-	<b>5</b>	<b>2</b>	-	<b>5</b>	-	<b>5</b>	-	-	-	-	<b>10</b>	-	-
<b>Mediastinal lymph nodes</b>																
Macrophage aggregates particle.	-	-	-	-	-	<b>4</b>	-	-	-	<b>2</b>	-	-	<b>4</b>	-	<b>9</b>	<b>9</b>
Grade 1						2				1			2			
Grade 2						1									2	
Grade 3										1			2		6	2
Grade 4						1									1	7
Occurrence of particles	-	-	<b>2</b>	-	<b>1</b>	<b>1</b>	-	<b>3</b>	-	<b>2</b>	-	<b>6</b>	<b>6</b>	<b>1</b>	-	<b>1</b>
Hyperplasia, lympho-reticulocellular	<b>1</b>	-	<b>3</b>	-	-	<b>3</b>	<b>3</b>	<b>3</b>	-	<b>1</b>	<b>1</b>	<b>1</b>	<b>4</b>	-	<b>2</b>	<b>7</b>
Grade 1	1		3			2	3	1					1			
Grade 2						1		1		1	1	1	3		2	6
Grade 3								1								1
<b>Tracheobronchial lymph nodes</b>																
Macrophage aggregates particle.	-	-	-	-	-	<b>4</b>	-	-	-	<b>3</b>	-	<b>1</b>	<b>8</b>	-	<b>10</b>	<b>10</b>
Grade 1										1		1	3		1	1
Grade 2						2				1			5		1	1
Grade 3						2									5	2
Grade 4										1					3	6
Occurrence of particles	-	-	<b>5</b>	-	<b>3</b>	<b>1</b>	-	<b>4</b>	-	<b>2</b>	-	<b>7</b>	<b>2</b>	<b>1</b>	-	-

**Table 4** continued

Target conc. (mg/m <sup>3</sup> )	5 days of exposure to Ceria NM-212						5 days of exposure to Ceria NM-211				4 weeks of exposure to Ceria NM-212					
	Time point 1 <sup>a</sup>			Time point 2 <sup>b</sup>			Time point 1 <sup>a</sup>		Time point 2 <sup>b</sup>		Time point 1 <sup>a</sup>			Time point 2 <sup>b</sup>		
	0.5	5	25	0.5	5	25	0.5	25	0.5	25	0.5	5	25	0.5	5	25
Hyperplasia, lympho-reticulocellular	–	–	<b>4</b>	<b>1</b>	<b>1</b>	<b>2</b>	–	<b>1</b>	<b>1</b>	<b>1</b>	–	<b>1</b>	<b>7</b>	–	<b>1</b>	<b>6</b>
Grade 1			4				1				1	2		1	1	
Grade 2				1	1	2			1	1		3				4
Grade 3												2				1

Number of examined organs per test group:  $n = 10$  (4 weeks of exposure);  $n = 5$  (5 days of exposure)

Grade 1: minimal, grade 2: slight, grade 3: moderate, grade 4: severe, grade 5: extreme; whenever a grading was not used, the microscopic finding was indicated to be present

<sup>a</sup> Time point 1: after the end of exposure (5 days of exposure) and 2 days after the end of exposure (4 weeks of exposure)

<sup>b</sup> Time point 2: 21 days after the end of exposure (5 days of exposure) and 34 days after the end of exposure (4 weeks of exposure)

(see Fig. 5b). All compound-related findings after exposure of 5 and 25 mg/m<sup>3</sup> Ceria NM-212 were correlated with increased lung weights in these test groups.

Lung-associated lymph nodes (mediastinal and tracheobronchial lymph nodes)

#### Five days of exposure

After 5 days of exposure to 25 mg/m<sup>3</sup> Ceria NM-211 and NM-212, comparable to the finding of particles in BALT of the lung, amber-like colored particles were seen partly within macrophages or extracellularly in the lymphoid tissue, without any macrophage activation or aggregation. 21 days after the end of exposure to 25 mg/m<sup>3</sup> Ceria NM-211, findings in both lymph nodes progressed. In the mediastinal and the tracheobronchial lymph nodes, multifocal macrophage aggregates with amber-like colored particles were noted in animals exposed to Ceria NM-211 and NM-212 (see Table 4). In both lymph nodes, lympho-reticulocellular hyperplasia was observed after 5 days of exposure and 21 days after the end of exposure to Ceria NM-211 and NM-212.

#### Four weeks of exposure

Two days after the end of exposure to 5 and 25 mg/m<sup>3</sup> Ceria NM-212, multifocal macrophage aggregates with particles were observed in the mediastinal as well as in the tracheobronchial lymph nodes (see Fig. 5c). A lympho-reticulocellular hyperplasia was present in both lymph nodes, mostly seen in animals in the group of 25 mg/m<sup>3</sup>. The hyperplasia of the mediastinal lymph nodes was correlated with their corresponding macroscopic enlargement after exposure to

25 mg/m<sup>3</sup> Ceria NM-212. 34 days after the end of exposure, the number of animals with macrophage aggregates (incidence and grading) and with hyperplasia in both lymph nodes was higher compared to the animals examined 2 days after the end of the exposure. Nearly all other findings were still present 34 days after the end of the exposure.

#### Upper respiratory tract

##### Five days of exposure

After 5 days of exposure to 25 mg/m<sup>3</sup> Ceria NM-211 and NM-212, extracellular, amber-like colored particles with diameters up to 1.5 μm were found in the lamina propria mucosae of the dorsal area of the larynx (level III). At aerosol concentrations of 25 mg/m<sup>3</sup> Ceria NM-211 and NM-212, resembling amber-like colored particles were detected within the subepithelial tissue in the carina of the trachea. 21 days after the end of exposure, findings in the larynx were only observed for animals exposed to Ceria NM-212, whereas particles in the carina (trachea) were still present in animals exposed to Ceria NM-211 and NM-212.

##### Four weeks of exposure

Two days after the end of the exposure to 5 and 25 mg/m<sup>3</sup> Ceria NM-212, amber-like colored particles occurred similarly in the dorsal area of the larynx (level III). Animals exposed to 25 mg/m<sup>3</sup> showed particles in the carina of the trachea. At aerosol concentrations of 25 mg/m<sup>3</sup> Ceria NM-212, single amber-like colored particles were firstly found in the nasal-associated lymphoid tissue (NALT), inside single macrophages or extracellularly. These findings were still present 34 days after the end of exposure.

## Extrapulmonary organs

### *Five days of exposure*

Extrapulmonary organs of animals exposed for 5 days to Ceria NM-211 and NM-212 were not examined.

### *Four weeks of exposure*

Histological examination of extrapulmonary organs, e.g., liver, spleen, and kidneys, did not show any substance-related morphological changes in animals exposed to 0.5, 5, and 25 mg/m<sup>3</sup> Ceria NM-212 in the short-term study with 4 weeks of exposure (data not shown).

## Organ burden analysis

In the short-term studies with 5 days and 4 weeks of exposure, Ceria burden of lung, lymph nodes, and partly liver is summarized in Tables S6–S8. The time course of lung and lymph node burdens is presented in Fig. 6.

### *Five days of exposure*

Exposure to 0.5 mg/m<sup>3</sup> Ceria NM-212 resulted in a lung burden of 0.011 mg/lung, directly after 5 days of exposure and decreased to 0.006 mg/lung 21 days after the end of the exposure, whereas exposure to 5 and 25 mg/m<sup>3</sup> yielded higher lung burdens (0.1 and 0.53 mg/lungs, respectively) with only little decrease (0.088 and 0.4 mg/lung, respectively) within 21 days after the end of the exposure.

Lung burdens of Ceria NM-211 were around twofold lower compared to those of Ceria NM-212 (see Table S6). Cerium content in the lung-associated lymph nodes at aerosol concentrations of 25 mg/m<sup>3</sup> increased from 1.7 to 5 µg for Ceria NM-212 and from 1.4 µg to 3 µg for Ceria NM-211 in the short-term study with 5 days of exposure (see Table S7).

### *Four weeks of exposure*

The time course of the lung burdens is presented in Fig. 6 (for detailed values, see Table S6). Inhalation exposure of 0.5, 5, or 25 mg/m<sup>3</sup> Ceria NM-212 resulted in mean lung burdens of 0.04, 0.52, or 2.62 mg 1 day after the end of exposure. 2 days after the end of exposure, higher lung burdens of the left lungs were measured and these data were disregarded for half-time calculations. Applying the following equation, retention half-times of Ceria in the lungs were calculated as

$$N(t) = N_0 \times e^{-\lambda t}$$

where  $N(t)$  was the lung burden at time point  $t$ ,  $N_0$  was the lung burden shortly after last exposure,  $t$  as days after last exposure.

At aerosol concentrations of 0.5 mg/m<sup>3</sup> Ceria NM-212, a retention half-time of 40 days was determined. Higher aerosol concentrations of 25 mg/m<sup>3</sup> Ceria NM-212 resulted, however, in a much longer half-time above 200 days.

The Cerium burden in the lung-associated lymph nodes (tracheobronchial and mediastinal lymph nodes) was 10 µg 3 days after the end of the exposure to 25 mg/m<sup>3</sup> Ceria NM-212 and increased to 350 µg 129 days after the end of exposure (see Table S7).

After the exposure to 25 mg/m<sup>3</sup> Ceria NM-212, Cerium was also detected in the liver (1.56 and 1.93 µg) 3 and 65 days after the end of the exposure, respectively (see Table S8).

## Discussion

Objectives of this body of work were to determine lung deposition and clearance kinetics as well as the inhalation toxicity of two nano-Ceria (NM-211 and NM-212) in short-term studies with 5 days and 4 weeks of inhalation exposure. The results should serve as basis for selecting appropriate exposure concentrations for a subsequent long-term inhalation study. The following sections focus on a discussion of (1) deposition and clearance, (2) local and systemic effects, (3) comparison of the two Ceria NM-211 and NM-212, and (4) comparison of 5 days and 4 weeks of exposure.

### Deposition and clearance

Four weeks of exposure to 0.5 mg/m<sup>3</sup> Ceria NM-212 resulted in a lung burden of 41 µg/lung; the post-exposure retention half-time was 40 days. This is in the range of physiological retention half-times of poorly soluble particles between 60 and 70 days (Oberdorster 2002). A higher aerosol concentration of 25 mg/m<sup>3</sup> elicited a lung burden of 2,620 µg/lung resulting in a retarded retention half-time above 200 days. At the mid concentration of 5 mg/m<sup>3</sup>, the lung burdens at three time points indicated a retarded retention half-time as the lung burden (500 µg/lung) stayed at a constant level during 4 weeks of post-exposure. A prolonged lung clearance of the same Ceria NM-212 was also observed in a rat instillation study with neutron-activated <sup>141</sup>Ceria NM-212 at an instilled dose of 1 mg/kg body weight, corresponding to 200–300 µg/lung (Molina et al. 2014). During 28 days post-exposure, only 12 % of the <sup>141</sup>Cerium in the lung has been cleared.

Pulmonary inflammation was only observed at concentrations of 5 and 25 mg/m<sup>3</sup>, which also caused significant

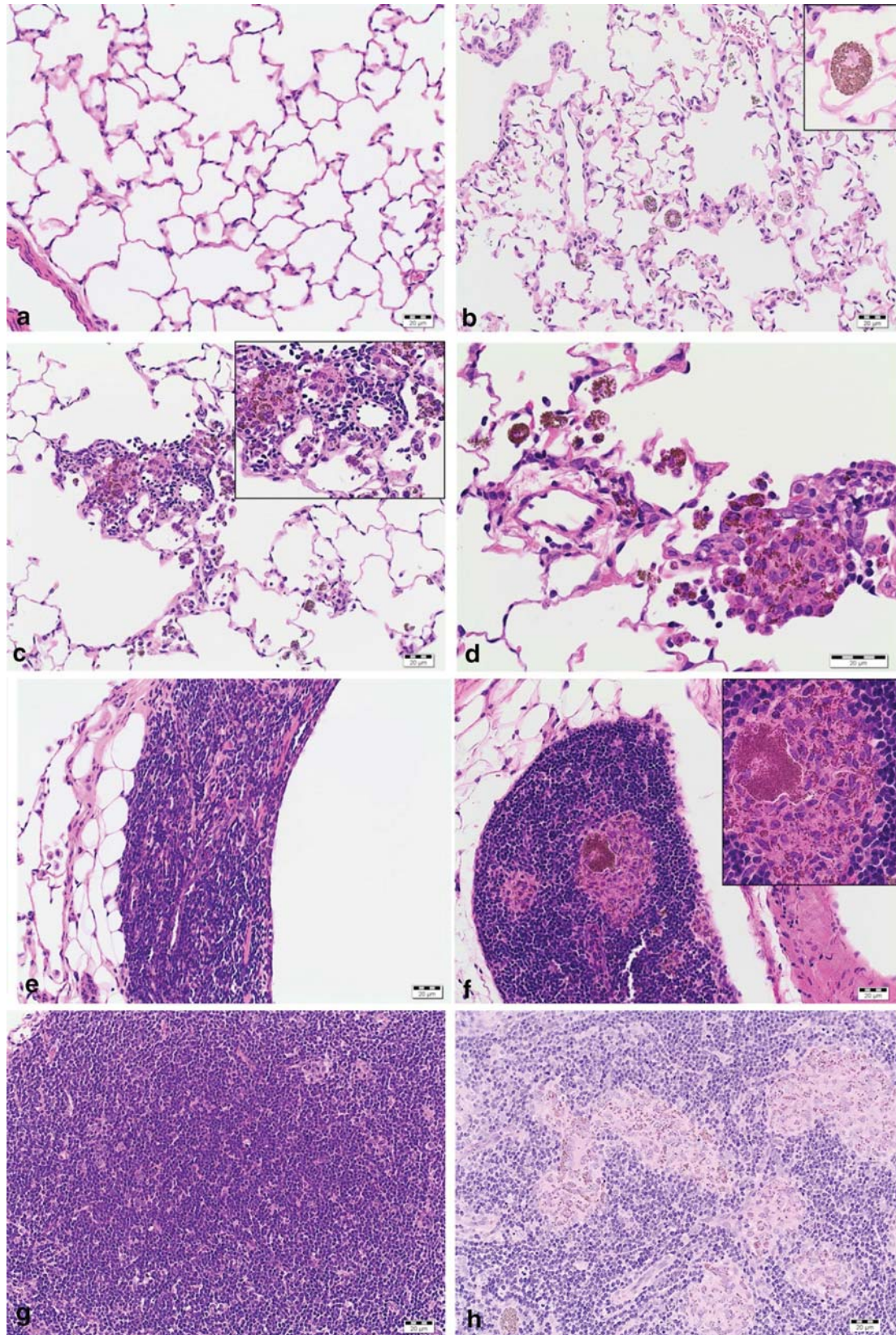


**Fig. 5** **a** Microscopic appearance of lungs (**a–d**) in the short-term study with 4 weeks of exposure. **a** Control, lung; **b** 2 days after the end of exposure to 25 mg/m<sup>3</sup> Ceria NM-212: lung, alveolar histiocytosis with particles; **c, d** 34 days after the end of exposure to 25 mg/m<sup>3</sup> Ceria NM-212: lung, granulomatous inflammation. **b** Microscopic appearance of lungs (**e, f**) in the short-term study with 4 weeks of exposure; **e** control, BALT; **f** 34 days after the end of exposure to 25 mg/m<sup>3</sup> Ceria NM-212: BALT macrophage aggregates with particles. **c** Microscopic appearance of lung-associated lymph nodes (**g, h**) in the short-term study with 4 weeks of exposure; **g** control, lymph node; **h** 34 days after the end of exposure to 25 mg/m<sup>3</sup> Ceria NM-212: tracheobronchial lymph node, macrophage aggregation with particles

retardation of pulmonary clearance. Concerning the threshold for overload conditions, mass lung burden of 41 µg, achieved at 0.5 mg/m<sup>3</sup>, was well below the overload threshold proposed by Morrow, while the lung burden of 2,620 µg, achieved at 25 mg/m<sup>3</sup>, was above it (Morrow 1988). At 25 mg/m<sup>3</sup>; a strong pulmonary inflammation was apparent. The mid concentration of 5 mg/m<sup>3</sup> Ceria NM-212 elicited pulmonary inflammation at a constant lung burden of around 520 µg, which is slightly below or at the border of the overload threshold.

Morrow assumed overload conditions when particle volume exceeds 60 µm<sup>3</sup>/alveolar macrophage (Morrow 1988). Oberdoerster et al. (1994a) suggested retained surface area as appropriate metrics for correlating overload with retarded clearance, particularly if nanoparticles are involved. Tran et al. (2000) proposed overload threshold values of 0.02–0.03 m<sup>2</sup>/g lung. In the current study, 4 weeks of exposure to an aerosol concentration of 25 mg/m<sup>3</sup> caused a particle surface burden of 0.07 m<sup>2</sup>/lung and 5 mg/m<sup>3</sup> resulted in 0.014 m<sup>2</sup> surface burden per lung (see Fig. 7; Table S9). This is slightly below the surface burden threshold proposed by Tran et al. and caused already inflammation and retarded clearance in the lung. Therefore, it can be assumed that a threshold, however, is highly material-dependent and may not be based on one or two particle types alone. The thresholds published previously may need adaptations for the specific type of nanomaterial in order to address its toxicological properties.

Lung burdens after 5 days of exposure were about one-fourth of those after 4 weeks of exposure reflecting a linear kinetics. This is the consequence of a linear deposition and a slow clearance. In the long term, however, the kinetics will not be linear due to clearance.

In the lung-associated lymph nodes, 350 µg Ceria was found 129 days after the exposure to 25 mg/m<sup>3</sup> for 4 weeks. The lung burden decreases from 2,620 to 1,800 µg in the same time period. The lymphatic clearance of Ceria was around 13 % of the initial retained burden after the end of the exposure. Lymphatic clearances of 1–5 % were previously reported for microscale particles but were also shown to be higher for nanoscale particles (Kreyling and Scheuch

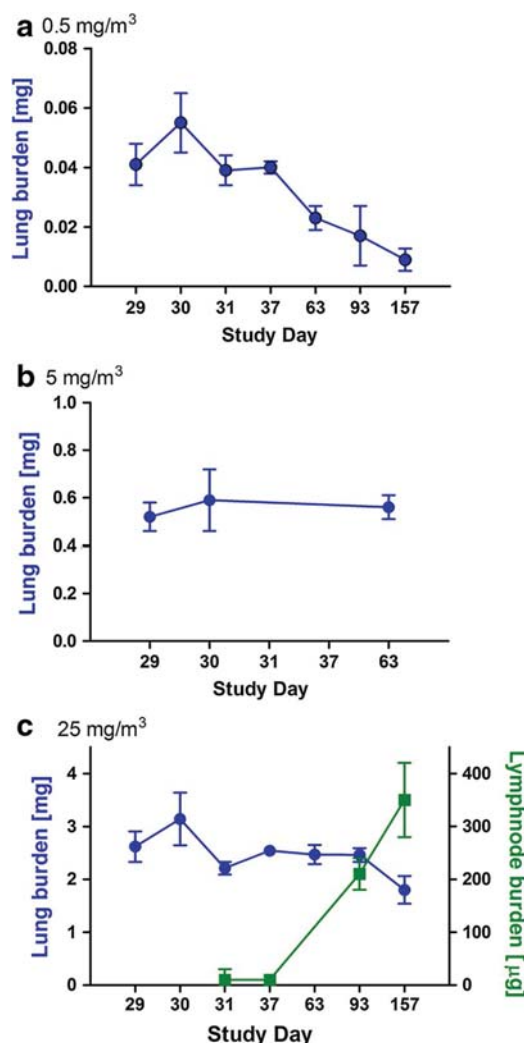


**Fig. 6** Biokinetics of lung (**a–c**) and lymph node burdens (**c**) in the short-term study with 4 weeks of exposure. Lung burden after exposure to 0.5 mg/m<sup>3</sup> (**a**), 5 mg/m<sup>3</sup> (**b**), and 25 mg/m<sup>3</sup> (**c**) Ceria NM-212 and burden of lung-associated lymph nodes after exposure to 25 mg/m<sup>3</sup> Ceria NM-212 (**c**, green) after 4 weeks of exposure and during 129 days post-exposure

2000; Kreyling et al. 1986; Oberdorster et al. 1994b). Most of the Ceria nanoparticles were presumably cleared by mucociliary clearance and subsequent fecal excretion, which was not evaluated in this work.

A very low content of Ceria was detected in the liver in the presented inhalation study with 4 weeks of exposure to 25 mg/m<sup>3</sup> Ceria NM-212. Consistent with our findings, accumulation of Ceria NM-212 in extrapulmonary tissue and associated toxicity appeared to be low as reported in a rat study using intravenous injection of neutron-activated <sup>141</sup>Cer NM-212 (Molina et al. 2014). Moreover, dissolution of Ceria within alveolar macrophages or other extracellular fluids, and subsequent absorption/bioavailability

of ionic Cerium into the blood and transport to extrapulmonary organs, may occur (Oberdörster et al. 2005). The exploration in simulant fluids indicated structural changes mediated by marginal solubility in (acidic) PSF, but not in (neutral) PBS (see Table 1). Hence, there is only a minor, if any, contribution of ionic Cerium.

#### Local effects

Local pulmonary effects after inhalation of nano-Ceria were consistent after 5 days and 4 weeks of exposure. The reported pulmonary inflammation was assessed by the changes in BALF parameters (e.g., neutrophils) and histopathological findings (alveolar histiocytosis and granulomatous inflammation).

In BALF, proinflammatory cytokines are also indicators of an inflammatory process in the lung (Henderson 1984). Increased activities of the enzymes ALP and NAG indicated the proliferation of pneumocyte type II cells and activation of macrophages, respectively (Henderson 2005; Capelli 1997). Consistently, the chemokine MCP-1 released by macrophages was concentration-related increased indicating a recruitment of blood monocytes into the alveolar compartment. The pro-inflammatory and neutrophil-attractant chemokine CINC-1 were increased in parallel but did not exceed MCP-1. Both parameters were assessed as predictive markers for early pulmonary inflammation and macrophage recruitment into the lungs in previous inhalation studies testing 14 different nanomaterials (Landsiedel et al. 2014). However, MCP-1 was the only cell mediator, which could be correlated with the progression of alveolar histiocytosis in histopathology. Consistently to ascending gradings and incidences in histopathology after 4 weeks exposure, MCP-1 levels were higher increased after 4 weeks than 5 days of exposure. The other cell mediators were not able to predict or indicate any of the observed morphological changes. The cytokine M-CSF is a marker for the differentiation of monocytes into histiocytes. Produced by macrophages, it may be responsible for increases in macrophage numbers (Landsiedel et al. 2014), but was not increased overall. Osteopontin is known to be involved in pulmonary granuloma development in rodents (Chiba et al. 2000), but was not increased in our studies, although a granulomatous inflammation was observed.

In BALF, macrophages counts were not elevated significantly. However, increase in alveolar macrophage number, different stages of (recruited, activated, highly particle loaded, destroyed) macrophages, and granulomatous inflammation was apparent in histopathology. This discrepancy between macrophage numbers in BALF and histopathology during an inflammatory state in the lungs was already recognized in different other inhalation studies (Porter et al. 2002, 2007). Most probably, the lung

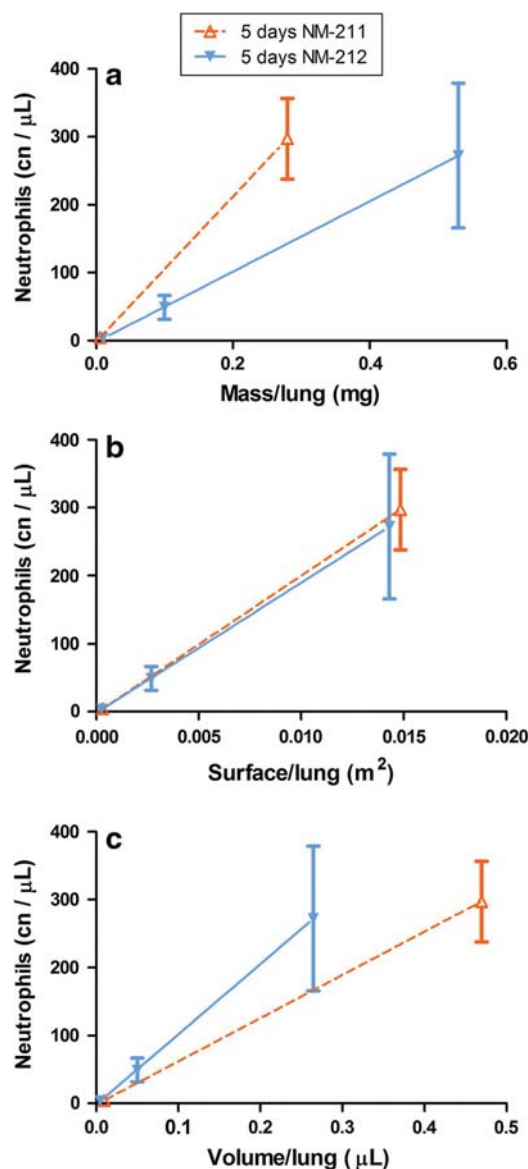


**Fig. 7** Dose–response curves using different dose metrics after 5 days of exposure to 0.5 and 25 mg/m<sup>3</sup> Ceria NM-211 and 0.5, 5, and 25 mg/m<sup>3</sup> Ceria NM-212; **a** mass, **b** surface, **c** volume

macrophages were not detached and washed out using the lavage technique with only two washes in our studies (Henderson 2005). Other studies with Ceria reported higher macrophage counts in BALF using the same or a higher number of washes (Gosens et al. 2013; Ma et al. 2011). The BAL method used in the here-presented studies is highly standardized and yields highly reproducible results compared to more rigorous lavage techniques but is obviously not capable of detaching more sessile macrophages of the lung. Hence, neutrophil counts in BALF were used as sensitive parameter to indicate an inflammatory response (Henderson 2005; Henderson et al. 1979a, b).

In pathology, lung weights were increased in the studies with 5 days (25 mg/m<sup>3</sup> Ceria NM-211) and 4 weeks (5 and 25 mg/m<sup>3</sup> Ceria NM-212) of exposure. By light microscopy, Ceria particles were primarily seen extracellularly and intra-alveolar or engulfed by alveolar macrophages. Different to observations after inhalation to other nanoparticles such as Titania, Ceria was not detected within alveolar epithelial cells in the current study (Warheit and Hartsky 1993). This supports the hypothesis that macrophage activation and immobilization together with cytokine and fibrogenic effects may be the mode of action for micro-scale Ceria inhalation toxicity [Environmental Protection Agency (EPA) 2009]. Furthermore, apoptosis of alveolar macrophages, their stimulation (pro-inflammatory cytokine and ROS release), and switch from the inflammatory M1 to a fibrotic M2 type was shown by the interaction of nano-Ceria with these cells after an intratracheal instillation study with rats (Ma et al. 2011).

At the lowest concentration of 0.5 mg/m<sup>3</sup> in the present studies, the histopathological findings alveolar histiocytosis and particles, either free or within macrophages, reflect an expected physiological response (Brain et al. 1976). However, after 4 weeks of exposure, the alveolar histiocytosis had progressed to a multifocal granulomatous inflammation at 5 mg/m<sup>3</sup> and at 25 mg/m<sup>3</sup> within 4 weeks after the end of exposure. The combination of moderate alveolar histiocytosis with particles and the presence of eosinophilic material, potentially precursors of granulomatous inflammation, are thus considered to be adverse. Granulomatous inflammation, multifocal microgranulomas, or granulomas due to inhalation of nano-Ceria have previously been reported in a number of animal studies (Srinivas et al. 2011; Cho et al. 2010; Snipes 1989; Aalapati et al. 2014). Granulomatous inflammation represents one type of chronic inflammation which is characterized by inflammatory lesions with large numbers of macrophages forming interlacing palisades, lymphocytes, and plasma cells (Renne et al. 2009). Other cells of the mononuclear phagocyte system (epithelioid and multinucleated cells) also contribute to maintain the inflammatory process. However, in the present studies, later stages of granuloma formation, transformation of macrophages to epithelioid, or giant cells were not observed. However, granulomatous inflammation can lead to tissue damage and fibrosis at later stages as observed by Ma et al. 4 weeks after a single intratracheal instillation of 7 mg/kg nano-Ceria in rats (Ma et al. 2014).

Concerning the two different methods (BAL and histopathology) in the study with 4 weeks of exposure, BALF parameters showed a regression during the post-exposure period. Histopathological findings, in contrast, progressed after the end of the exposure at concentrations of 5 mg/m<sup>3</sup> Ceria and above. A regression of the BALF parameter (e.g., neutrophils) and a certain progression of histopathological

findings during the post-exposure were already recognized in previous works with Ceria (Gosens et al. 2013; Srinivas et al. 2011). It was concluded that during a sustained inflammation in the lungs, parameters in BALF do not represent the current inflammatory state and damage in the lungs.

Lymphatic clearance of inhaled Ceria via the lymphatic vessels from the pulmonary region to the lung-associated lymph nodes was demonstrated by histological evaluations and confirmed by measured Cerium lymph node burdens. Accumulation of free particles or particles within macrophage aggregates was detected in the BALF or mediastinal and tracheobronchial lymph nodes. Increasing Cerium clearance into the lung-associated lymph nodes was correlated with an increase in grading and severity of macrophage aggregates during the post-exposure period (see pathological score, Table 4). Moderate macrophage aggregates with particles in the lung-associated lymph nodes, combined with lympho-reticulocellular hyperplasia, were considered to be adverse. It is more likely that the particles reached the associated lymph nodes by phagocytizing macrophages than by entering the interstitium.

Aerosol concentrations of 5 and 25 mg/m<sup>3</sup> caused inflammatory effects in the lung, which can be considered adverse. At 0.5 mg/m<sup>3</sup>, slight effects were still detected by BALF after 5 days of exposure but not by histopathology or after 4 weeks of exposure. BALF parameters proved to be more sensitive to short-term effects but less predictive for the progression of these effects.

The observations of the current study resemble the findings of previously published inhalation (and instillation) studies with different Ceria (Gosens et al. 2013; Ma et al. 2011; Demokritou et al. 2012; Aalapati et al. 2014). In an 28-day inhalation study with the Ceria NM-212, Gosens et al. (2013) observed pulmonary effects at an aerosol concentration equivalent to 2.5 mg/m<sup>3</sup>. These effects were less pronounced compared to the current study. The dose-equivalent concentration of 2.5 mg/m<sup>3</sup> was achieved by the exposure of the animals to 50 mg/m<sup>3</sup> for different daily exposure durations, whereas the studies reported here exposed animals to actual 0.5, 5, and 25 mg/m<sup>3</sup> for 6 h/day. The difference in daily exposure times and dose rate may account for the differences in the severity of the effects. Aalapati et al. (2014) observed pulmonary inflammation, necrosis, fibrosis, and granulomas in the lung of mice exposed to 2 mg/m<sup>3</sup> nano-Ceria for 14 and 28 days resulting in a burden of 1,200 µg/g lung after exposure for 28 days. Rats exposed for 4 weeks in the study reported here inhaled 12.5-fold higher aerosol concentrations, which yielded a lung burden of around 3,000 µg/lung (equivalent to 2,730 µg/g lung) and resulted in less morphological changes. The results of the 2 mg/m<sup>3</sup> Ceria inhalation study to mice leave open questions which need to be discussed.

## Systemic effects

Substance-related adverse effects after inhalation exposure to two Ceria in the short-term studies were limited to the lung. Potential systemic genotoxicity was assessed by micronuclei test (MNT). The MNT is a frequently used genotoxicity test on nanomaterials (Oesch and Landsiedel 2012). This *in vivo* assay is able to demonstrate the potential interaction of nanomaterials with chromosomes or mitotic apparatus of replicating erythroblasts as well as their influence on erythropoiesis in the bone marrow (LeBaron et al. 2013). No genotoxic potential after inhalation of Ceria NM-211 or NM-212 was observed in both short-term studies. Cerium bone marrow content was not determined in our inhalation studies, but a tissue concentration of 6.61 ng/g bone marrow was reported 7 days after intratracheal instillation of 1 mg/kg of neutron-activated Ceria NM-212 (Molina et al. 2014). Ceria inhalation exposure has been reported to result in a wide range of systemic responses ranging from no effects to severe effects in blood or extrapulmonary organs, such as liver or kidneys (Aalapati et al. 2014; Gosens et al. 2013; Srinivas et al. 2011). In the study reported here, 5 days of exposure to 25 mg/m<sup>3</sup> (retained lung burden of 0.53 mg) resulted in higher absolute and relative neutrophil cell counts in the blood, without an increase in total cell counts. This slight neutrophilia was detected directly after the end of exposure and was no longer present after 3 weeks of post-exposure. Considering the pronounced inflammation in the lung at 25 mg/m<sup>3</sup>, the neutrophilia in blood was considered to be secondary to the local effects (systemic acute-phase response). The inflammatory response in the lung based on the increase in neutrophil counts in BALF was also lower after 4 weeks compared to 5 days of exposure. And no altered blood parameters could be detected after 4 weeks of inhalation exposure. Furthermore, a whole panel of extrapulmonary organs and tissues was examined histologically as required by OECD test guideline 412. Very low Cerium contents were detected in the liver at two time points after 4 weeks of inhalation exposure to 25 mg/m<sup>3</sup> Ceria NM-212 (which is a general finding for inhaled nanoparticles) without any related morphological abnormalities. None of the other extrapulmonary organs showed any morphological abnormalities. The absence of systemic effects is consistent with the very low extrapulmonary tissue Ceria concentrations in this and other studies (Gosens et al. 2013; Geraets et al. 2012; Molina et al. 2014). After instillation of 1 mg/kg body weight neutron-activated <sup>141</sup>Cer NM-212, only 0.3 % of the administered dose was found in the liver after 28 days post-instillation (Molina et al. 2014). However, after a single intravenous (i.v.) administration of 30 nm nano-Ceria (87 mg/kg body weight) into rats, oxidative stress was seen

in liver and spleen and granulomas were observed in the liver (Yokel et al. 2012). The Ceria-induced adverse effects were explained by mechanical irritation or its chemical (catalytic) activity (Yokel et al. 2012). The high Cerium concentrations in the liver after i.v. administration were far beyond the concentrations achievable by oral, dermal, or inhalation exposure. In contrast, severe systemic findings were reported in mice after 28-day inhalation exposure to 2 mg/m<sup>3</sup> nano-Ceria plus 28 days of post-exposure (lung burden of 500 mg/g tissue). The findings comprised necrosis in kidneys, hepatocytomegaly, and cytoplasmic vacuolization in the heart (Aalapati et al. 2014), which was claimed to be associated with moderate accumulation of Cerium in extrapulmonary organs. However, even i.v. injection of high doses of Ceria did not lead to similar changes in rat kidney and heart (Yokel et al. 2012).

## Comparison of NM-211 with NM-212

The effects of two different Ceria (NM-211 and NM-212) were compared after 5 days of inhalation exposure. Ceria NM-211 and NM-212 have identical composition, agglomeration state, crystallinity, and insolubility. Compared to Ceria NM-212, NM-211 has considerably smaller primary particles, larger specific surface, significantly fewer organic contaminations on the surface, and reduced photocatalytic activity. Despite these differences, Ceria NM-211 and NM-212 share the same tendency to recrystallize in acidic PSF, which simulates the lysosome of macrophages. These properties are comparable to each other, but significantly different from other metal oxide nanomaterials and seem to be primarily substance-related themselves. Compared to Ceria NM-212, Ceria NM-211 elicited higher increases in lymphocytes, cell mediators (e.g., MCP-1), and neutrophils in BALF at 25 mg/m<sup>3</sup> with a slower recovery during the post-exposure period. Moreover, significant increase in lung weights was noted in animals exposed to 25 mg/m<sup>3</sup> Ceria NM-211, but not NM-212. When biological effects (e.g., inflammation) of two particles are compared, the lung burden may be more appropriately expressed as particle volume, particle surface area (Oberdorster et al. 1994b). Morrow first introduced volume as dose metric for overload (Morrow 1988). Pauluhn modified the overload hypothesis by introducing agglomerate density (instead of physical density) into the calculation of volumetric loading (Pauluhn 2011). The effective particle density is needed to calculate the particle volume. In a guidance document published by Webb (2001), various definitions of the powder volumes are given (e.g., apparent density and tapping density). In the current study, an agglomerate density of 2 g/cm<sup>3</sup> for NM-212 and 0.6 g/cm<sup>3</sup> for NM-211 was selected. The densities were extracted by integrating the porosity

below 1  $\mu\text{m}$  (from Hg intrusion porosimetry) and then derived empirically by approaching MPPD model calculations together with measured mass lung burden. According to our calculation, volumetric lung overload can only be assumed after 4 weeks exposure to 25  $\text{mg}/\text{m}^3$ . Impaired lung clearance—which is one of the consequences of lung overload conditions—was, however, already observed after inhalation of 5  $\text{mg}/\text{m}^3$  Ceria.

It is not fully understood which characteristics of nano-Ceria lead to the effects observed in previous and current studies [Environmental Protection Agency (EPA) 2009]. Assessing the immune toxicity of another member of the group of poorly soluble particle namely Titania after instillation in rats, lower phagocytic ability and disruption of pulmonary alveolar macrophage function were correlated with surface reactivity and size of surface area (Liu et al. 2010). A number of studies over the past 15 years suggested that the smaller the particle size (the greater the surface area dose), the greater the induced inflammatory response (Oberdorster et al. 1994a; Cullen et al. 2000; Sager and Castranova 2009; Sager et al. 2008). Furthermore, surface area of retained particles seems to correlate with acute inflammatory reactions after inhalation. The correlation of lung burden, expressed as mass, volume, and surface area, and neutrophil (PMN) counts in BALF as parameter for biological effects is presented in Fig. 7 (Table S9).

In the present study with 5 days of exposure, the larger specific surface area of Ceria NM-211 seems to contribute to the higher biological activity as compared to Ceria NM-212. Surface area normalized the dose response of the two Ceria materials. This result is consistent with other studies, which used surface area as dose metric to quantify the toxicity of the PSPs Titania and barium sulfate (Tran et al. 2000; Oberdorster et al. 1994a, b).

#### Comparison of 5 days and 4 weeks of exposure

Rats were exposed to Ceria NM-212 for 5 days and 4 weeks. Exposure to 25  $\text{mg}/\text{m}^3$  for 5 days resulted in the same lung burden as 4 weeks of exposure to 5  $\text{mg}/\text{m}^3$ . In consideration of the same lung burdens, the dose rates are 106  $\mu\text{g}$  (5 days of exposure to 25  $\text{mg}/\text{m}^3$ ) and 26  $\mu\text{g}/\text{day}$  (4 weeks of exposure to 5  $\text{mg}/\text{m}^3$ ) (see Table 5). One

should note that the calculated dose rates still include the clearance and, therefore, reflect rather the retained than the deposited Ceria concentration in the lung.

The dose rate of particles seems to influence the acute inflammatory reaction in the lung (Baisch et al. 2014). Despite the same lung burdens but different dose rates, a stronger neutrophil response in BALF was observed after the shorter exposure time (Figs. 8, 9). The decay in neutrophil numbers after 4 weeks was by far slower than after 5 days, suggesting that inflammation developing at lower dose rate is longer lasting and more persistent. Moreover, BALF effects almost completely regressed after the end of the 5 days exposure to 5  $\text{mg}/\text{m}^3$  even though the lung burden was only cleared by about 10 % (Fig. 9).

Hence, the dose rate rather than the lung burden seems to drive the neutrophil count in BALF (Fig. 9; Table 5).

Neutrophils are one of the first cell types recruited by inflammatory signals evoked by deposited particles in the lung, with peak numbers within 48 h (Alber et al. 2012). Neutrophils in BALF are a sensitive measure of this initial phase. With sustained inflammatory conditions, neutrophil recruitment undergoes a certain physiological adaptation in the body. The number of neutrophils observed in BALF was decreasing and supplemented by mononuclear cells, especially macrophages that were visible in histopathology but not in BALF. The sustained presence of particles in the lung can drive macrophages to form granulomatous lesions. Although a small dose rate over a long exposure time achieved the same lung burden as a high dose rate over a short time period, the effects observed may be more severe due to consistent irritation of the tissue by small dose rates of fresh materials. Apparently, the initial neutrophil reaction is directed by the dose rate while the progression of the inflammation in the lung is also driven by the continuing presence of particles in the lung.

#### Conclusion

Inhaled nano-Ceria was deposited in the lung. The particles were cleared from the lung with a retention half-time of 40 days at a concentration of 0.5  $\text{mg}/\text{m}^3$ ; higher aerosol concentrations impaired this clearance. A smaller

**Table 5** Dose rate of Ceria NM-212

Study	Test substance	Concentration ( $\text{mg}/\text{m}^3$ )	Lung burden <sup>a</sup> ( $\mu\text{g}$ )	Dose rate ( $\mu\text{g}/\text{day}$ )
5 days (5 exposures)	Ceria NM-212	0.5	11	2.2
		5	100	20
		25	530	106
4 weeks (20 exposures)	Ceria NM-212	0.5	41	2.05
		5	520	26
		25	2,620	131

<sup>a</sup> Lung burden values after 5 days of exposure (5 days exposure) and 2 days after the end of exposure (4 weeks exposure)

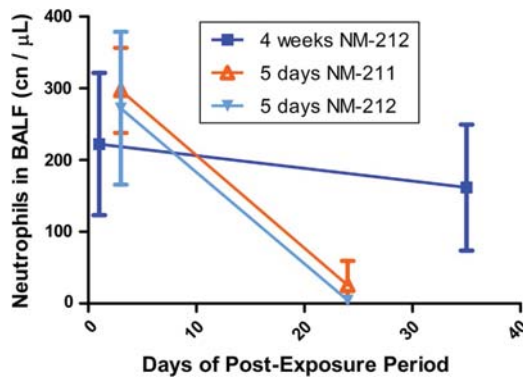


**Fig. 8** Inflammatory potency of the short-term studies with 5 days and 4 weeks of exposure over post-exposure period: absolute neutrophil counts in BALF in the short-term studies: 3 and 24 days after end of exposure to 25 mg/m<sup>3</sup> Ceria NM-211 (orange 5-day exposure) and NM-212 (light blue 5-day exposure) or one and 35 days after the end of exposure to 25 mg/m<sup>3</sup> NM-212 (dark blue 4-week exposure)

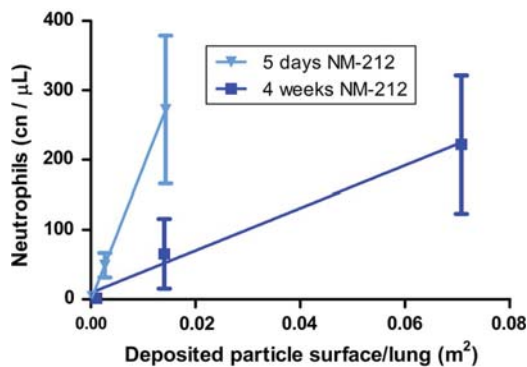
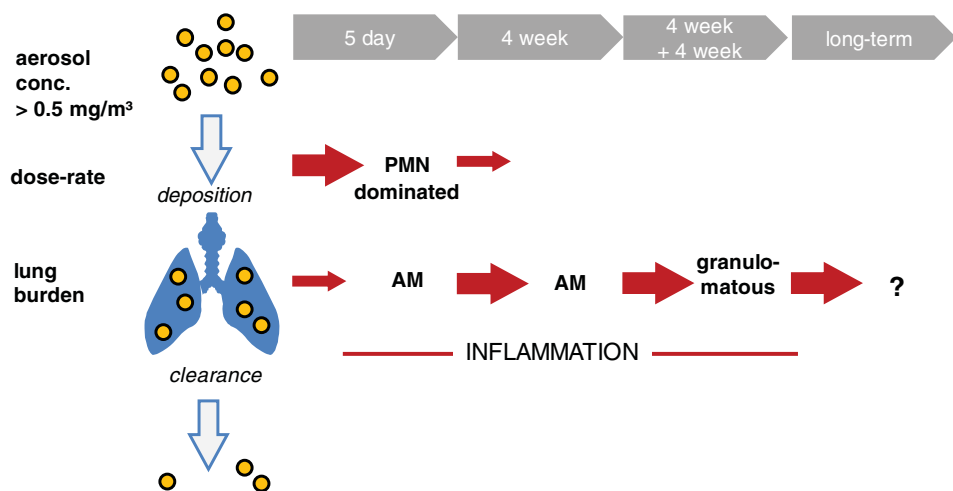


**Fig. 9** Neutrophil counts in BALF correlated with deposited particle per surface lung after 5-day and 4-week exposure using the aerosol concentrations of 0.5, 5, and 25 mg/m<sup>3</sup> CeO<sub>2</sub> NM-212 for each point

fraction of the particles was transferred to the lung-associated lymph nodes. The initial inflammatory reaction was observed by an increase in neutrophils which correlated with dose rate rather than absolute lung burden. With time, the neutrophil number decreased. The decrease was observed after the exposure ended but also with sustained exposure (longer than 5 days in the current studies). In the later phase (after 4 weeks of exposure), the inflammatory reaction was dominated by mononuclear cells, especially macrophages. The inflammatory response was driven by the surface of the particles presented to the lung, as this was the dose metrics with the best correlation of the two Ceria materials. An aerosol concentration of 0.5 mg/m<sup>3</sup> did not cause inflammatory responses in the lung. 5 mg/m<sup>3</sup> was the lowest aerosol concentration at which the early as well as the later inflammatory response was observed, even though lung burdens were different at the onset of the two phases. The progression of the later inflammatory reaction toward a granulomatous type depended on the duration and amount of the particle (surface) burden in the lung (Fig. 10). Thus, the potency of an inhaled particle to induce inflammatory responses in the lung could be assessed by the aerosol concentration causing the initial neutrophil response, whereas the later granulomatous phase could only be detected by histopathology. The further progression of the biological response was determined by the continuing presence of the particles in the lung. Ultimately, the further progression of the biological responses needs to be studied by the long-term inhalation study assessing the effects as well as the time course of the lung burdens. The results of the short-term studies presented here were used to set the aerosol concentrations of the long-term study with Ceria which is currently being performed. Four aerosol concentrations are being tested, 0.1, 0.3, 1, and 3 mg/m<sup>3</sup>, expected to result in no inflammation and no overload (two concentrations),

**Fig. 10** Summary of results after 5 days and 4 weeks of exposure to Ceria



inflammation without overload, and inflammation and overload, respectively.

**Acknowledgments** The authors wish to thank the inhalation team and pathology team of BASF for their excellent technical assistance in performing the inhalation study, the clinical, and histopathological examinations. The study with 5 days of exposure (NM-212) was funded via the European Commission's 7th Framework Programme project NanoMILE (Contract No. NMP4-LA-2013-310451). The rest of the work was sponsored by BASF SE.

**Conflict of interest** BASF SE is a company producing and marketing nanomaterials.

**Open Access** This article is distributed under the terms of the Creative Commons Attribution License which permits any use, distribution, and reproduction in any medium, provided the original author(s) and the source are credited.

## References

- Aalapati S, Ganapathy S, Manapuram S, Anumolu G, Prakya BM (2014) Toxicity and bio-accumulation of inhaled cerium oxide nanoparticles in CD1 mice. *Nanotoxicology* 8:786–798
- Alber A, Howie SEM, Wallace WAH, Hirani N (2012) The role of macrophages in healing the wounded lung. *Int J Exp Pathol* 93:243–251
- Anjilvel S, Asgharian B (1995) A multiple-path model of particle deposition in the rat lung. *Fundam Appl Toxicol* 28:41–50
- Baisch BL, Corson NM, Wade-Mercer P, Gelein R, Kennell AJ, Oberdorster G, Elder A (2014) Equivalent titanium dioxide nanoparticle deposition by intratracheal instillation and whole body inhalation: the effect of dose rate on acute respiratory tract inflammation. *Part Fibre Toxicol* 11:5
- Becker H, Herzberg F, Schulte A, Kolossa-Gehring M (2011) The carcinogenic potential of nanomaterials, their release from products and options for regulating them. *Int J Hyg Environ Health* 214:231–238
- Brain JD, Knudson DE, Sorokin SP, Davis MA (1976) Pulmonary distribution of particles given by intratracheal instillation or by aerosol inhalation. *Environ Res* 11:13–33
- Capelli A (1997) Lung alkaline phosphatase as a marker of fibrosis in chronic interstitial disorders. *Am J Respir Crit Care Med* 155(1):249–253
- Cargnello M, Doan-Nguyen V, Gordon T, Diaz R, Stach E, Gorte R, Fornasiero P, Murray C (2013) Control of metal nanocrystal size reveals metal-support interface role for ceria catalysts. *Science* 341(6147):771–773
- Cassee FR, van Balen EC, Singh C, Green D, Muijser H, Weinstein J, Dreher K (2011) Exposure, health and ecological effects review of engineered nanoscale cerium and cerium oxide associated with its use as a fuel additive. *Crit Rev Toxicol* 41:213–229
- Chiba S, Rashid MM, Okamoto H, Shiraiwa H, Kon S, Maeda M, Murakami M, Inobe M, Kitabatake A, Chambers AF, Uede T (2000) The role of osteopontin in the development of granulomatous lesions in lung. *Microbiol Immunol* 44:319–332
- Cho WS, Duffin R, Poland CA, Howie SEM, MacNee W, Bradley M, Megson IL, Donaldson K (2010) Metal oxide nanoparticles induce unique inflammatory footprints in the lung: important implications for nanoparticle testing. *Environ Health Perspect* 118:1699–1706
- Cullen RT, Tran CL, Buchanan D, Davis JMC, Searl A, Jones AD, Donaldson K (2000) Inhalation of poorly soluble particles. I. Differences in inflammatory response and clearance during exposure. *Inhal Toxicol* 12:1089–1111
- Demokritou P, Gass S, Pyrgiotakis G, Cohen JM, Goldsmith W, McKinney W, Frazer D, Ma J, Schwegler-Berry D, Brain J, Casanova V (2012) An in vivo and in vitro toxicological characterization of realistic nanoscale CeO<sub>2</sub> inhalation exposures. *Nanotoxicology* 7:1338–1350
- Dudewicz EJ, Ramberg JS, Chen HJ (1975) New tables for multiple comparisons with a control (unknown variances). *Biometrische Zeitschrift* 17:13–26
- Dunnett CW (1955) A Multiple comparison procedure for comparing several treatments with a control. *J Am Stat Assoc* 50:1096–1121
- ECHA (2012) Guidance on information requirements and chemical safety assessment: appendix R7-1 recommendations for nanomaterials applicable to chapter R7a—endpoint specific guidance. European Chemical Agency. [http://echa.europa.eu/documents/10162/13632/appendix\\_r7a\\_nanomaterials\\_en.pdf](http://echa.europa.eu/documents/10162/13632/appendix_r7a_nanomaterials_en.pdf)
- Environmental Protection Agency (EPA) (2009) Toxicological review of cerium oxide and cerium compounds, Report, EPA/635/R-08/002F. Environmental Protection Agency, Washington, DC. <http://www.epa.gov/iris/toxreviews/1018tr.pdf>, EPA/635/R-08/002F
- European Commission (2013) Classification, labeling and packaging of nanomaterials in REACH and CLP (Doc. CA/90/2009 Rev2). European Commission, Brussels, Report. [http://ec.europa.eu/enterprise/sectors/chemicals/files/reach/nanos\\_in\\_reach\\_and\\_clp\\_en.pdf](http://ec.europa.eu/enterprise/sectors/chemicals/files/reach/nanos_in_reach_and_clp_en.pdf)
- European Commission (2014) Science and policy report by the joint research centre, the European Commission, JRC89825, EUR 26649 EN. Publications office of the European union, Luxembourg. doi:10.2788/80203
- Federal Ministry for the Environment (2012) NCBaNS Langzeitforschungsprojekt zur Sicherheit von Nanomaterialien gestartet, press release no. 066/12. Federal Ministry for the Environment, Berlin. <http://www.bmub.bund.de/presse/pressemitteilungen/pm/artikel/langzeitforschungsprojekt-zur-sicherheit-von-nanomaterialien-gestartet-1/>
- Gamer AO, Leibold E, van Ravenzwaay B (2006) The in vitro absorption of microfine zinc oxide and titanium dioxide through porcine skin. *Toxicol In Vitro* 20:301–307
- Geraets L, Oomen AG, Schroeter JD, Coleman VA, Cassee FR (2012) Tissue distribution of inhaled micro- and nano-sized cerium oxide particles in rats: results from a 28-day exposure study. *Toxicol Sci* 127:463–473
- Gogens I, Mathijssen L, Bokkers B, Muijser H, Cassee FR (2013) Comparative hazard identification of nano- and micro-sized cerium oxide particles based on 28-day inhalation studies in rats. *Nanotoxicology* 8(6):643–653
- Greim H, Ziegler-Skylakakis K (2007) Risk assessment for biopersistent granular particles. *Inhal Toxicol* 19(Suppl 1):199–204
- He X, Zhang H, Ma Y, Bai W, Zhang Z, Lu K, Ding YY, Zhao YL, Chai Z (2010) Lung deposition and extrapulmonary translocation of nano-ceria after intratracheal instillation. *Nanotechnology* 21(28):285103
- Heinrich U, Fuhst R, Rittinghausen S, Creutzenberg O, Bellmann B, Koch M, Levsen K (1995) Chronic inhalation exposure of Wistar rats and two different strains of mice to diesel engine exhaust, carbon black, and titanium dioxide. *Inhal Toxicol* 7:533–556
- Henderson R (1984) Use of bronchoalveolar lavage to detect lung damage. *Environ Health Perspect* 56:115–129
- Henderson R (2005) Use of bronchoalveolar lavage to detect respiratory tract toxicity of inhaled material. *Exp Toxicol Pathol* 57:155–159
- Henderson R, Rebar A, Pickrell JA, Newton GJ (1979a) Early damage indicators in the lung. 3. Biochemical and cytological response of the lung to inhaled metal-salts. *Toxicol Appl Pharmacol* 50:123–136
- Henderson R, Rebar AH, Denicola DB (1979b) Early damage indicators in the lungs. 4. Biochemical and cytological response of

- the lung to lavage with metal-salts. *Toxicol Appl Pharmacol* 51:129–135
- Hermans JJ (1963) Density gradient centrifugation of a mixture of polymers differing in molecular weight and specific volume. *J Polym Sci Part C 1*:179–86. ISSN: 0022-3832
- Hussain SM, Braydich-Stolle L, Schrand AM, Murdock RC, Yu KO, Mattie DM, Schlager JJ, Terrones M (2009) Toxicity evaluation for safe use of nanomaterials: recent achievements and technical challenges. *Adv Mater* 21:1–11
- ILSI Risk Science Institute Workshop Participants (2000) The relevance of the rat lung response to particle overload for human risk assessment: a workshop consensus report. *Inhal Toxicol* 12:1–17
- Kittel B, Ruehl-Fehlert C, Morawietz G, Klapwijk J, Elwell MR, Lenz B, O'Sullivan MG, Roth DR, Wadsworth PF (2004) Revised guides for organ sampling and trimming in rats and mice—part 2—a joint publication of the RITA and NACAD groups. *Exp Toxicol Pathol* 55:413–431
- Kreyling W, Scheuch G (2000) Clearance of particles deposited in the lungs. In: Gehr P, Heyder J (eds) *Particle lung interactions*, chap 7. CRC Press, pp 323–376
- Kreyling WG, Ferron GA, Haider B (1986) Metabolic-fate of inhaled co aerosols in beagle dogs. *Health Phys* 51:773–795
- Kuhlbusch TA, Asbach C, Fissan H, Göhler D, Stintz M (2011) Nanoparticle exposure at nanotechnology workplaces: a review. *Part Fibre Toxicol* 8(1):22
- Landsiedel R, Fabian E, Ma-Hock L, Wohlleben W, Wiench K, Oesch F, van Ravenzwaay B (2012) Toxicology/biokinetics of nanomaterials. *Arch Toxicol* 86:1021–1060
- Landsiedel R, Ma-Hock L, Hofmann T, Wiemann M, Strauss V, Treumann S, Wohlleben W, Groeters S, Wiench K, van Ravenzwaay B (2014) Application of short-term inhalation studies to assess the inhalation toxicity of nanomaterials. *Part Fibre Toxicol* 11:16
- LeBaron MJ, Schisler MR, Torous DK, Dertinger SD, Gollapudi BB (2013) Influence of counting methodology on erythrocyte ratios in the mouse micronucleus test. *Environ Mol Mutagen* 54:222–228
- Lee KP, Trochimowicz HJ, Reinhardt CF (1985) Pulmonary response of rats exposed to titanium dioxide (TiO<sub>2</sub>) by inhalation for two years. *Toxicol Appl Pharmacol* 79:179–192
- Liu R, Zhang XY, Pu YP, Yin LH, Li YH, Zhang XQ, Liang GY, Li XB, Zhang J (2010) Small-sized titanium dioxide nanoparticles mediate immune toxicity in rat pulmonary alveolar macrophages in vivo. *J Nanosci Nanotechnol* 10:5161–5169
- Ma JY, Zhao H, Mercer RR, Barger M, Rao M, Meighan T, Schwegler-Berry D, Castranova V, Ma JK (2011) Cerium oxide nanoparticle-induced pulmonary inflammation and alveolar macrophage functional change in rats. *Nanotoxicology* 5(3):312–325
- Ma J, Young S, Mercer R, Barger M, Schwegler-Berry D, Ma JK, Castranova V (2014) Interactive effects of cerium oxide and diesel exhaust nanoparticles in inducing pulmonary fibrosis. *Toxicol Appl Pharmacol*
- Ma-Hock L, Gamer AO, Landsiedel R, Leibold E, Frechen T, Sens B, Linsenbuehler M, van Ravenzwaay B (2007) Generation and characterization of test atmospheres with nanomaterials. *Inhal Toxicol* 19:833–848
- Ma-Hock L, Burkhard S, Strauss V, Gamer AO, Wiench K, van Ravenzwaay B, Landsiedel R (2009) Development of a short-term inhalation test in the rat using nano-titanium dioxide as a model substance. *Inhal Toxicol* 21:102–118
- Molina RM, Konduru N, Jimenez R, Wohlleben W, Brain JD (2014) Bioavailability, distribution and clearance of tracheally instilled, gaged or injected cerium dioxide nanoparticles and ionic cerium. *Nano Environ Sci* (submitted)
- Morrow PE (1988) Possible mechanisms to explain dust overloading of the lungs. *Fundam Appl Toxicol* 10:369–384
- Nalabotu SK, Kolli MB, Triest WE, Ma JY, Manne NDPK, Katta A, Addagarla HS, Rice KM, Blough ER (2011) Intratracheal instillation of cerium oxide nanoparticles induces hepatic toxicity in male Sprague–Dawley rats. *Int J Nanomed* 6:2327–2335
- Nikula KJ, Snipes MB, Barr EB, Griffith WC, Henderson RF, Mauderly JL (1995) Comparative pulmonary toxicities and carcinogenicities of chronically inhaled diesel exhaust and carbon black in F344 rats. *Fundam Appl Toxicol* 25:80–94
- Oberdorster G (2002) Toxicokinetics and effects of fibrous and nonfibrous particles. *Inhal Toxicol* 14:29–56
- Oberdorster G, Ferin J, Lehnert BE (1994a) Correlation between particle size, in vivo particle persistence, and lung injury. *Environ Health Perspect* 102(Suppl. 5):173–179
- Oberdorster G, Ferin J, Soderholm SC, Gelein R, Cox C, Baggs R, Morrow PE (1994b) Increased pulmonary toxicity of inhaled ultrafine particles: due to lung overload alone? *Ann Occup Hyg* 38:295–302
- Oberdorster G, Oberdorster E, Oberdorster J (2005) Nanotoxicology: an emerging discipline evolving from studies of ultrafine particles. *Environ Health Perspect* 113:823–839
- Oesch F, Landsiedel R (2012) Genotoxicity investigations on nanomaterials. *Arch Toxicol* 86:985–994
- Organisation for Economic Cooperation and Development (OECD) (1998) OECD principles on good laboratory practice (as revised in 1997). ENV/MC/CHEM(98)17. Organisation for Economic Cooperation and Development, Paris
- OECD (2009a) Test no. 453: combined chronic toxicity/carcinogenicity studies, OECD guidelines for the testing of chemicals, sect 4. OECD Publishing. doi:10.1787/9789264071223-en
- Organization for Economic Cooperation and Development (OECD) (2009b) Test No. 412: Subacute inhalation toxicity: 28-day study, OECD Guidelines for the testing of chemicals, sect 4, OECD Publishing. doi:10.1787/9789264070783-en
- OECD (2010) List of manufactured nanomaterials and list of endpoints for phase one of the OECD testing programme. Series on the safety of manufactured nanomaterials, environment directorate OECD, Paris, Report ENV/JM/MONO(2010)46. [http://www.oecd.org/officialdocuments/publicdisplaydocumentpdf/?cote=en/jm/mono\(2010\)46&doclanguage=en](http://www.oecd.org/officialdocuments/publicdisplaydocumentpdf/?cote=en/jm/mono(2010)46&doclanguage=en)
- Pauluhn J (2011) Poorly soluble particulates: searching for a unifying denominator of nanoparticles and fine particles for DNEL estimation. *Toxicology* 279:176–188
- Pflucker F, Wendel V, Hohenberg H, Gartner E, Will T, Pfeiffer S, Wepf R, Gers-Barlag H (2001) The human stratum corneum layer: an effective barrier against dermal uptake of different forms of topically applied micronised titanium dioxide. *Skin Pharmacol Appl Skin Physiol* 14:92–97
- Porter DW, Ye J, Ma J, Barger M, Robinson VA, Ramsey D, McLaurin J, Khan A, Landsittel D, Teass A, Castranova V (2002) Time course of pulmonary response of rats to inhalation of crystalline silica: NF-kappa B activation, inflammation, cytokine production, and damage. *Inhal Toxicol* 14:349–367
- PROSPECT: Ecotoxicology Test Protocols for Representative Nanomaterials in Support of the OECD Sponsorship Programme (2010) Toxicological review of nano cerium oxide. [http://www.nanotechia.org/sites/default/files/files/PROSPECT\\_Nano-CeO2\\_Literature\\_Review.pdf](http://www.nanotechia.org/sites/default/files/files/PROSPECT_Nano-CeO2_Literature_Review.pdf)
- Porter DW, Hubbs AF, Baron PA, Millecchia LL, Wolfarth MG, Battelli LA, Schwegler-Berry DE, Beighley CM, Andrew ME, Castranova V (2007) Pulmonary toxicity of Expancel microspheres in the rat. *Toxicol Pathol* 35:702–714
- Renne R, Brix A, Harkema J, Herbert R, Kittel B, Lewis D, March T, Nagano K, Pino M, Rittinghausen S, Rosenbruch M, Tellier P, Wahrman T (2009) Proliferative and nonproliferative lesions of the rat and mouse respiratory tract. *Toxicol Pathol* 37:5S–73S

- Ruehl-Fehlert C, Kittel B, Morawietz G, Deslex P, Keenan C, Mahrt CR, Nolte T, Robinson M, Stuart BP, Deschl U (2003) Revised guides for organ sampling and trimming in rats and mice—part 1—a joint publication of the RITA and NACAD groups. *Exp Toxicol Pathol* 55:91–106
- Sager TM, Castranova V (2009) Surface area of particle administered versus mass in determining the pulmonary toxicity of ultrafine and fine carbon black: comparison to ultrafine titanium dioxide. *Part Fibre Toxicol* 6:15
- Sager TM, Kommineni C, Castranova V (2008) Pulmonary response to intratracheal instillation of ultrafine versus fine titanium dioxide: role of particle surface area. *Part Fibre Toxicol* 5:17
- Snipes MB (1989) Long-term retention and clearance of particles inhaled by mammalian-species. *Crit Rev Toxicol* 20:175–211
- Srinivas A, Rao PJ, Selvam G, Murthy PB, Reddy PN (2011) Acute inhalation toxicity of cerium oxide nanoparticles in rats. *Toxicol Lett* 205:105–115
- Teunenbroek T, Dijkzeul A, Hoehener K (2013) NANoREG-A common European approach to the regulatory testing of nanomaterials, Press release, NANoREG. [http://www.nanoreg.eu/images/NANOREG\\_PressRelease\\_final.pdf](http://www.nanoreg.eu/images/NANOREG_PressRelease_final.pdf)
- Tran CL, Buchanan D, Cullen RT, Searl A, Jones AD, Donaldson K (2000) Inhalation of poorly soluble particles. II. Influence of particle surface area on inflammation and clearance. *Inhal Toxicol* 12:1113–1126
- Warheit DB, Hartsky MA (1993) Role of alveolar macrophage chemotaxis and phagocytosis in pulmonary clearance responses to inhaled particles: comparisons among rodent species. *Microsc Res Tech* 26:412–422
- Webb PA (2001) Volume and density determinations for particle technologists. *Micromeritics Instrument Corp* 2(16):01. [http://www.particletesting.com/Repository/Files/density\\_determinations.pdf](http://www.particletesting.com/Repository/Files/density_determinations.pdf)
- Wohlleben W, Ma-Hock L, Boyko V, Cox G, Egenolf H, Freiburger H, Hinrichsen B, Hirth S, Landsiedel R (2013) Nanospecific Guidance IN REACH: a comparative physical–chemical characterization of 15 materials with methodical correlations. *J Ceram Sci Technol* 4:93–104
- Yokel RA, Au TC, MacPhail R, Hardas SS, Butterfield DA, Sultana R, Goodman M, Tseng MT, Dan M, Haghaziar H, Unrine JM, Graham UM, Wu P, Grulke EA (2012) Distribution, elimination, and biopersistence to 90 days of a systemically introduced 30 nm ceria-engineered nanomaterial in rats. *Toxicol Sci* 127:256–268

## **7. Paper 2: Biokinetics and effects of barium sulfate nanoparticles**

## RESEARCH

## Open Access

# Biokinetics and effects of barium sulfate nanoparticles

Nagarjun Konduru<sup>1†</sup>, Jana Keller<sup>2†</sup>, Lan Ma-Hock<sup>2</sup>, Sibylle Gröters<sup>2</sup>, Robert Landsiedel<sup>2\*</sup>, Thomas C Donaghey<sup>1</sup>, Joseph D Brain<sup>1</sup>, Wendel Wohlleben<sup>2</sup> and Ramon M Molina<sup>1\*</sup>

## Abstract

**Background:** Nanoparticulate barium sulfate has potential novel applications and wide use in the polymer and paint industries. A short-term inhalation study on barium sulfate nanoparticles (BaSO<sub>4</sub> NPs) was previously published [*Part Fibre Toxicol* 11:16, 2014]. We performed comprehensive biokinetic studies of <sup>131</sup>BaSO<sub>4</sub> NPs administered via different routes and of acute and subchronic pulmonary responses to instilled or inhaled BaSO<sub>4</sub> in rats.

**Methods:** We compared the tissue distribution of <sup>131</sup>Ba over 28 days after intratracheal (IT) instillation, and over 7 days after gavage and intravenous (IV) injection of <sup>131</sup>BaSO<sub>4</sub>. Rats were exposed to 50 mg/m<sup>3</sup> BaSO<sub>4</sub> aerosol for 4 or 13 weeks (6 h/day, 5 consecutive days/week), and then gross and histopathologic, blood and bronchoalveolar lavage (BAL) fluid analyses were performed. BAL fluid from instilled rats was also analyzed.

**Results:** Inhaled BaSO<sub>4</sub> NPs showed no toxicity after 4-week exposure, but a slight neutrophil increase in BAL after 13-week exposure was observed. Lung burden of inhaled BaSO<sub>4</sub> NPs after 4-week exposure (0.84 ± 0.18 mg/lung) decreased by 95% over 34 days. Instilled BaSO<sub>4</sub> NPs caused dose-dependent inflammatory responses in the lungs. Instilled BaSO<sub>4</sub> NPs (0.28 mg/lung) was cleared with a half-life of ≈ 9.6 days. Translocated <sup>131</sup>Ba from the lungs was predominantly found in the bone (29%). Only 0.15% of gavaged dose was detected in all organs at 7 days. IV-injected <sup>131</sup>BaSO<sub>4</sub> NPs were predominantly localized in the liver, spleen, lungs and bone at 2 hours, but redistributed from the liver to bone over time. Fecal excretion was the dominant elimination pathway for all three routes of exposure.

**Conclusions:** Pulmonary exposure to instilled BaSO<sub>4</sub> NPs caused dose-dependent lung injury and inflammation. Four-week and 13-week inhalation exposures to a high concentration (50 mg/m<sup>3</sup>) of BaSO<sub>4</sub> NPs elicited minimal pulmonary response and no systemic effects. Instilled and inhaled BaSO<sub>4</sub> NPs were cleared quickly yet resulted in higher tissue retention than when ingested. Particle dissolution is a likely mechanism. Injected BaSO<sub>4</sub> NPs localized in the reticuloendothelial organs and redistributed to the bone over time. BaSO<sub>4</sub> NP exhibited lower toxicity and biopersistence in the lungs compared to other poorly soluble NPs such as CeO<sub>2</sub> and TiO<sub>2</sub>.

**Keywords:** Lung absorption, Bioavailability, Particokinetics, Particle dissolution, Translocation, Inhalation

## Background

Barium sulfate nanoparticles (BaSO<sub>4</sub> NPs) are used as fillers in coatings (e.g. in motor vehicles) due to their mechanical, optical and chemical properties. Recently, BaSO<sub>4</sub> NPs have also been used in orthopedic medicine, diagnostic imaging and other applications [1-5]. It has

been reported that pellethane, a polyurethane elastomer, when incorporated with BaSO<sub>4</sub> NPs exhibited antimicrobial properties *in vitro* [6]. Exposure to aerosolized BaSO<sub>4</sub> NPs may occur during their production, shipping, handling, incorporation into final products, and the use and disposal of those products. Chronic exposure to high levels of micron-scale BaSO<sub>4</sub> sulfate may induce pneumoconiosis (baritosis) in miners [7-9].

Barium sulfate is considered a member of the poorly soluble particles (PSP) or poorly soluble low toxicity (PSLT) particle groups, as are cerium dioxide (CeO<sub>2</sub>) and titanium dioxide (TiO<sub>2</sub>) [10-12]. These biodurable

\* Correspondence: robert.landsiedel@basf.com; rmolina@hsph.harvard.edu

†Equal contributors

<sup>2</sup>Experimental Toxicology and Ecology, BASF SE, GV/TB - Z470, Carl-Bosch-Straße 38, Ludwigshafen 67056, Germany

<sup>1</sup>Department of Environmental Health, Molecular and Integrative Physiological Sciences Program, Harvard School of Public Health, 665 Huntington Avenue, Boston, MA 02115, USA



nanomaterials are usually poorly absorbed after oral and inhalation exposure [13-15]. Particokinetics of nanoparticles are influenced by particle size and route of exposure [16]. Poorly soluble particles may also differ in clearance and biological effects compared to soluble particles [12,17-19]. It is not established whether the biokinetics of inhaled BaSO<sub>4</sub> NPs are similar to other PSLT NPs. Therefore, it is of interest whether the biokinetics of inhaled BaSO<sub>4</sub> NPs are different from other PSLT NPs. Previous studies have described the lung clearance of intratracheally instilled micron-sized radioactive BaSO<sub>4</sub> and showed that the particle size influences lung clearance of Ba [20,21]. A subchronic inhalation study in rats showed a neutrophil increase in bronchoalveolar lavage (BAL) with micron-scale TiO<sub>2</sub> but not with BaSO<sub>4</sub> at comparable overload lung burdens (~10 mg Ba) [12,17]. The difference was attributed to the lower surface area of BaSO<sub>4</sub> than TiO<sub>2</sub>. Toxicity of nanoparticles is influenced by particle physicochemical properties [16,22-24]. The biological responses to small particles differ from bigger particles of the same composition [25,26]. Furthermore, a short-term inhalation study on BaSO<sub>4</sub> NPs has been reported recently [27,28]. Rats were exposed (nose-only) to 50 mg/m<sup>3</sup> BaSO<sub>4</sub> (NM-220) for 6 hours/day for 5 days. It was found that the lung burden of BaSO<sub>4</sub> at the end of exposure was 1.1 mg/lung which decreased to 0.24 mg/lung within 21 days. This short-term exposure to BaSO<sub>4</sub> did not elicit significant pulmonary or systemic responses consistent with previous reports in various *in vitro* and *in vivo* test systems [26]. The mechanisms underlying the lower toxicity and rapid lung clearance of BaSO<sub>4</sub> NPs are not fully understood. For example, more research is needed to quantify the components of clearance attributable to intact particles versus particle dissolution and clearance of barium ions. Thus, there is continuing interest in the biokinetics and effects of BaSO<sub>4</sub> NPs, especially after pulmonary exposure. A two-year inhalation study of BaSO<sub>4</sub> and CeO<sub>2</sub> has been initiated in collaboration between the German Federal Ministry for the Environment German government and BASF (Ludwigshafen, Germany). The project is within the Organization for Economic Cooperation and Development (OECD) sponsorship program and the European Union Project NANoREG (a European approach to the regulatory testing of manufactured nanomaterials).

The data presented here were used in designing this long-term inhalation study. Our objective was to characterize the pulmonary and systemic effects of inhaled BaSO<sub>4</sub> NPs after short-term and subchronic exposure. In addition, we report here a comprehensive study on the biokinetics of <sup>131</sup>Ba after intratracheal instillation (IT), intravenous injection (IV) and gavage administration of radiolabeled <sup>131</sup>BaSO<sub>4</sub> NPs. These studies are important in assessment of risks from exposure to BaSO<sub>4</sub> NPs.

## Results

### Physicochemical characterization of NM-220 and the reproduced batch of BaSO<sub>4</sub> nanoparticles

Barium sulfate NPs (NM-220) used in all IT instillation, gavage and IV injection studies were obtained from BASF SE (Ludwigshafen, Germany). This sample was a reference material for the Nanomaterial Testing Sponsorship Program of the OECD. The characterization of this original batch was published recently [29]. Since the chronic inhalation study requires large amounts (>100 kg), BaSO<sub>4</sub> NPs were reproduced at a different production plant using the same synthesis protocol. This reproduced batch was characterized by the same methods and was used for the 4-week and 13-week inhalation studies. All physicochemical endpoints are summarized in Additional file 1: Table S1 (online Supporting Information), which includes the previously published characterization of NM-220 for comparison [29]. Transmission and scanning electron micrographs show that BaSO<sub>4</sub> NPs in both batches were nonspherical globular with no fiber, rod or platelet impurities. The primary particle size was 25 nm for both batches (Figure 1A and 1B). The NPs form larger spherical agglomerates (2–15 μm diameter) in the as-produced powder (Additional file 1: Table S1). This agglomerate structure was confirmed by porosimetry which showed dominant pore sizes of 30 nm and 5 μm for both batches (Additional file 1: Figure S1A). X-ray diffraction (XRD) analysis showed that the particle mineralogy was orthorhombic barite (Additional file 1: Figure S1B) for both batches. Photocatalytic activity of both batches was extremely low as shown by the absence of methylene blue degradation (Additional file 1: Figure S2).

The shape, particle size distribution, primary particle diameter, state of agglomeration (powder), crystalline phase, specific surface area, surface charge, photocatalytic activity, and dispersability in water and in Dulbecco's modified Eagle/fetal calf serum (DMEM/FCS) media were similar in both batches. Analyses by several methods (EM, minimal pore size, specific surface area) indicate that the two batches have similar primary particle sizes. The properties that were determined by surface chemistry such as dispersability, charge/zeta potential and photocatalytic reactivity were also similar (Additional file 1: Figure S2). However, significant differences were observed in crystallite size (36 nm for NM-220 vs. 23 nm for reproduced batch). The reproduced material also had an intermediate pore size of 200 nm (agglomerate structure) which was absent in the original NM-220 material. XPS analyses showed significantly less carbon atoms exposed on the surface of the reproduced material (2 vs. 17%). Additionally, elemental analysis by neutron activation showed that the NM-220 batch had 599 μg Ba/mg material (59.9 wt%), as expected for relatively pure BaSO<sub>4</sub> (Table 1).

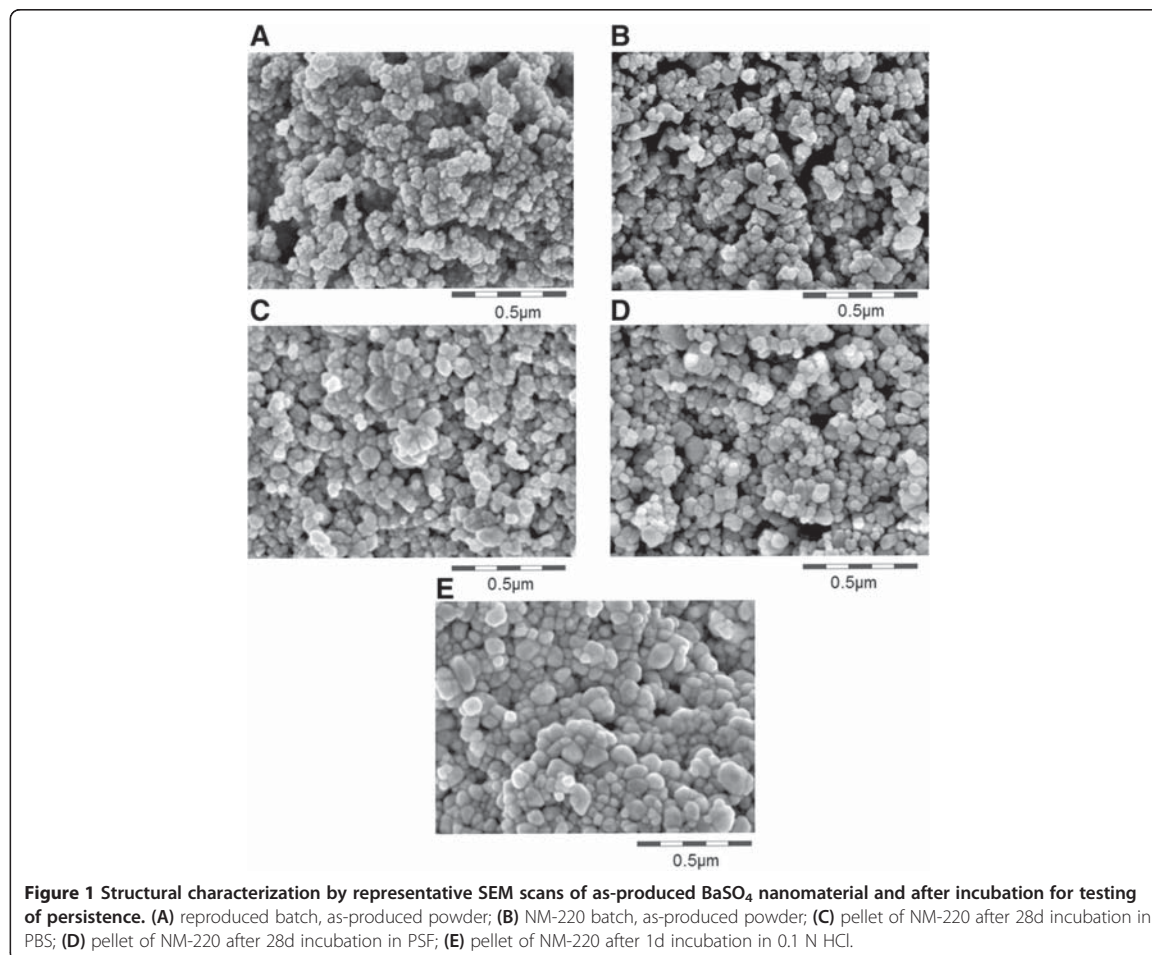


**Figure 1** Structural characterization by representative SEM scans of as-produced BaSO<sub>4</sub> nanomaterial and after incubation for testing of persistence. (A) reproduced batch, as-produced powder; (B) NM-220 batch, as-produced powder; (C) pellet of NM-220 after 28d incubation in PBS; (D) pellet of NM-220 after 28d incubation in PSF; (E) pellet of NM-220 after 1d incubation in 0.1 N HCl.

In physiological simulant fluids, BaSO<sub>4</sub> NPs (NM-220) dissolved only slightly at pH 1 (1% dissolution in 0.1 N HCl) although its particle shapes changed (Additional file 1: Table S1, Figure 1E) [29]. Very low (0.1%) dissolution was observed in phosphate buffered saline (PBS) or phagolysosomal simulant fluid (PSF, pH 4.5) after

**Table 1** Neutron activation analysis of BaSO<sub>4</sub> NM-220

Element	Concentration (μg/g)
Ba	599,000 ± 33,000
Sr	9,820 ± 570
Na	3,022 ± 69
Zn	31.1 ± 2
Mn	0.41 ± 0.21
Co	0.164 ± 0.038
Au	0.04 ± 0.003
Sc	0.0206 ± 0.0055

Data are mean ± standard deviation.

28 days incubation (Additional file 1: Table S1). No morphologic changes were seen in PBS (Figure 1C). However, the non-spherical BaSO<sub>4</sub> NPs lost their structural features with lowest radius of curvature and recrystallized to spherical structures in PSF (Figure 1D) [30]. It was confirmed by selected area electron diffraction that the crystallinity was retained (data not shown). BaSO<sub>4</sub> NPs remained in a low agglomeration state and retained a significant dispersed fraction (80%) of ≤1 μm diameter in all simulant buffer conditions. The zeta potential ranged from -20 mV to -32 mV.

The agglomerate size of BaSO<sub>4</sub> NPs in deionized water suspension employed in IT instillation (0.67 mg/ml), gavage (10 mg/ml) and IV injection (1 mg/ml) was assessed using dynamic light scattering (DLS). We found that BaSO<sub>4</sub> NP agglomerate size was influenced by particle concentration (Table 2): the higher the concentration, the larger the hydrodynamic diameter. For the inhalation studies, the particle concentrations and size

**Table 2 Dynamic light scattering analysis of BaSO<sub>4</sub> NM-220 suspensions**

Concentration (mg/ml dH <sub>2</sub> O)	d <sub>H</sub> (nm)	Pdl	ζ (mV)
0.66	144 ± 4	0.20 ± 0.03	-18.5
1	154 ± 21	0.24 ± 0.07	-18.7
10	354 ± 3	0.46 ± 0.03	-16.5

Data are mean ± standard deviation, n = 3.  
d<sub>H</sub>, hydrodynamic diameter, Pdl, polydispersity index, ζ, zeta potential.

distributions are summarized in Table 3. The target concentration of 50 mg/m<sup>3</sup> was achieved and maintained throughout the inhalation exposures. Particle size distribution of aerosolized BaSO<sub>4</sub> NPs was in the respirable range for rats.

#### **Pulmonary responses to instilled or inhaled BaSO<sub>4</sub> nanoparticles**

To determine whether BaSO<sub>4</sub> NPs elicit toxic or inflammatory response in rats and to identify a suitable dose for the IT biokinetic studies, groups of six rats were IT-instilled with BaSO<sub>4</sub> NP suspension (NM-220) at 0, 1, 2, and 5 mg/kg body weight. We found that BaSO<sub>4</sub> NPs caused an acute dose-dependent inflammatory response evidenced by significant increases in BAL parameters (Table 4). Neutrophils, myeloperoxidase (MPO) and lactate dehydrogenase (LDH) levels in bronchoalveolar lavage (BAL) were elevated 24 hours post-instillation. We also found that 2 and 5 mg/kg doses caused pulmonary hemorrhage and edema as indicated by increased BAL haemoglobin and albumin levels. Based on these data, we concluded that 1 mg/kg was the maximum safe dose for the IT biokinetic study, since injury and inflammation were minimal, yet it was sufficient for gamma detection of <sup>131</sup>Ba in the lungs and other tissues over a period of 28 days.

To assess pulmonary responses of rats after short-term and subchronic inhalation of BaSO<sub>4</sub> NPs, BAL analysis was performed one day (4- and 13-week groups) and 35 days (4-week group) after the end of each exposure protocol. Results for all BAL parameters are presented in Table 5. After 4 weeks of exposure, neutrophils were significantly increased compared to concurrent controls (filtered air-exposed) one day after the end of exposure. However, these values were within the historical control range in our previous studies. Rats exposed for 13 weeks showed significant increases in BAL total cells and neutrophils compared to control. These neutrophil counts were

significantly lower than those seen in instilled rats (Table 4, Additional file 1: Figure S3). Cytokine levels of monocyte chemoattractant protein-1 (MCP-1) and cytokine-induced neutrophil chemoattractant-1 (CINC-1) were elevated in both exposure groups (Table 5). The longer 13-week exposure to BaSO<sub>4</sub> NPs induced higher levels of the cytokine MCP-1 compared to the 4-week exposure. All BAL parameters elevated at 1 day post-exposure returned to control levels in the 4-week exposure group at 35 days. No morphological changes were detected by histopathology in the lungs (Additional file 1: Figure S4) and extrapulmonary organs. Other parameters such as body weights, micronucleus test of erythrocytes in peripheral blood, showed no significant change. Rats exposed for 13 weeks showed significantly higher gamma glutamyl transferase (GGT) and alkaline phosphatase (ALP) levels than their corresponding controls (Table 5).

#### **In vivo clearance and translocation of <sup>131</sup>BaSO<sub>4</sub> nanoparticles after IT instillation in rats**

The clearance of <sup>131</sup>BaSO<sub>4</sub> NPs from the lungs post-instillation is shown in Figure 2A. Approximately 47% of the total dose was cleared from the lungs by day 7 and 84% by day 28. A linear regression on the natural logarithm of the lung <sup>131</sup>BaSO<sub>4</sub> levels (% dose) over time was performed ( $y = e^{-0.003011x}$ ,  $R^2 = 0.96$ ,  $p < 0.0001$ ). The estimated clearance half-life was 9.6 days. Extrapulmonary translocation of <sup>131</sup>Ba is shown in Figure 2B. A significant fraction of <sup>131</sup>Ba radioactivity was found in the bones (29% of dose) and lower fractions in all other tissues combined (7%). The rest of the <sup>131</sup>Ba was excreted mostly in the feces (30%) and to a lesser extent in the urine (3.9%) (Figure 3). The complete distribution data of <sup>131</sup>Ba after instillation of <sup>131</sup>BaSO<sub>4</sub> are summarized in Additional file 1: Table S2.

#### **Fate of <sup>131</sup>BaSO<sub>4</sub> nanoparticles after oral administration in rats**

The tissue distribution of <sup>131</sup>Ba activity following oral administration is summarized in Figure 4 and listed in Additional file 1: Table S3. Nearly 100% of the administered dose was measured in the stomach at 5 minutes post-gavage (Figure 4A). At 7 days, very low percentages of the total dose were detected in blood, bone and bone marrow (<0.1%) (Figure 4B). Gavaged <sup>131</sup>BaSO<sub>4</sub> NPs were mostly cleared from the GI tract and eliminated in the

**Table 3 Aerosol concentrations and particle size distributions of BaSO<sub>4</sub> NM-220**

Duration of exposure	Targeted concentrations (mg/m <sup>3</sup> )	Measured concentrations (mg/m <sup>3</sup> )	MMAD (μm)/GSD mean	Particle count concentration (particle/cm <sup>3</sup> )	Particle count median diameter (nm)
4 weeks	50	46.2 ± 5.9	2.3/2.0	92752	326
13 weeks	50	50.1 ± 5.6	1.9/2.1	77992	304

**Table 4 Bronchoalveolar lavage analysis at 1 day after intratracheal instillation of BaSO<sub>4</sub> NPs**

Dose	Control	1 mg/kg	2 mg/kg	5 mg/kg
BaSO <sub>4</sub> lung burden (mg)	0	0.28 ± 0.004	0.56 ± 0.004	1.4 ± 0.004
Total Cells (million)	8.31 ± 1.01	12.59 ± 1.71	14.26 ± 0.74*	16.76 ± 1.15*
Macrophage (million)	8.31 ± 1.01	12.28 ± 1.62	11.41 ± 0.67	10.31 ± 1.40
Neutrophils (million)	0.001 ± 0.00	0.29 ± 0.10	2.85 ± 0.29*	6.45 ± 1.09*
LDH (mU/ml)	38.10 ± 0.30	57.23 ± 4.98	171.52 ± 33.05	167.68 ± 18.53*
MPO (mU/ml)	0.94 ± 0.07	0.80 ± 0.21	26.48 ± 8.50	34.95 ± 8.82
Albumin (µg/ml)	3.28 ± 1.39	6.12 ± 0.38*	11.88 ± 1.20*	14.53 ± 1.12*
Hemoglobin (µg)	9.44 ± 1.39	16.56 ± 0.89*	24.79 ± 2.78*	37.24 ± 2.64*

Data are mean ± SE, n = 4-5/group.

\*p < 0.05, BaSO<sub>4</sub> versus 0 mg/kg (Control, equivalent volume of distilled water).

feces (Figure 5A). Only 0.02% was excreted in the urine (Figure 5B).

#### Tissue distribution of <sup>131</sup>BaSO<sub>4</sub> nanoparticles after intravenous injection in rats

At 2 hours after intravenous injection of <sup>131</sup>BaSO<sub>4</sub> NPs, the blood levels of <sup>131</sup>Ba were less than 0.5% of the

administered dose (Figure 6). The complete distribution data at various time point post-injection are summarized in Additional file 1: Table S4. The tissue distribution was typical of circulating particles that are taken up in organs comprising the mononuclear phagocyte system with access to the circulation [31]. Notably, <sup>131</sup>BaSO<sub>4</sub> NPs were predominantly localized in the liver, spleen, bone and

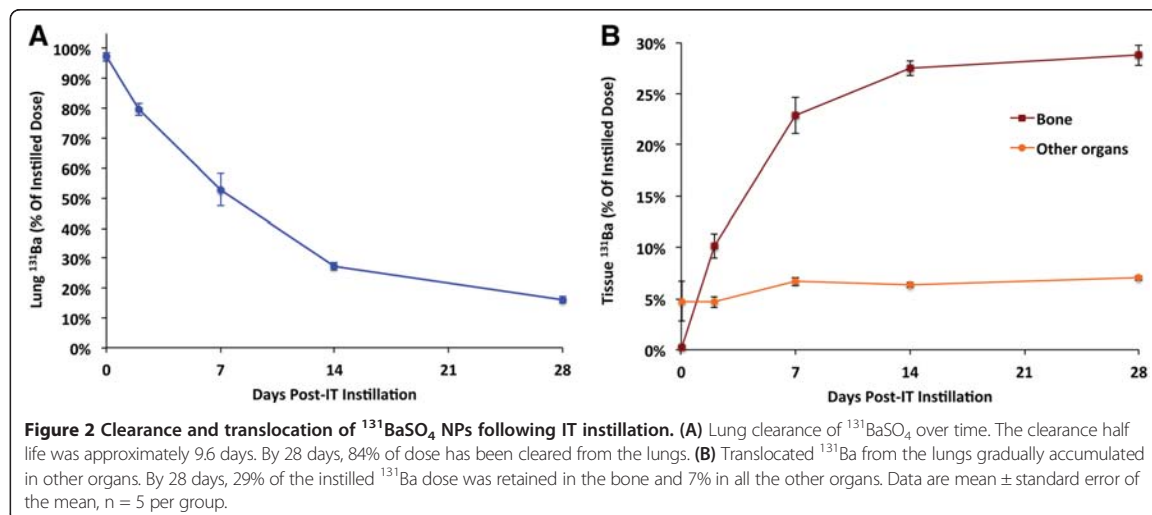
**Table 5 Bronchoalveolar lavage analysis at 1 or 35 days after inhalation exposure to BaSO<sub>4</sub> NPs**

	4-week exposure		13-week exposure	
	Control	BaSO <sub>4</sub>	Control	BaSO <sub>4</sub>
BaSO <sub>4</sub> lung burden (mg)		0.84 ± 0.18		1.73 ± 0.85
Total cells (million)				
1 day	0.649 ± 0.20	0.562 ± 0.12	0.610 ± 0.20	0.836 ± 0.15*
35 days	0.580 ± 0.11	0.454 ± 0.12	ND	ND
Neutrophils (million)				
1 day	0.007 ± 0.003	0.021 ± 0.010*	0.016 ± 0.006	0.204 ± 0.175*
35 days	0.019 ± 0.008	0.032 ± 0.024	ND	ND
Total protein (mg/L)				
1 day	60 ± 4	77 ± 13*	52 ± 10	64 ± 13
35 days	81 ± 23	59 ± 13	ND	ND
GGT (nkat/L)				
1 day	37 ± 17	40 ± 10	41 ± 7	64 ± 13*
35 days	42 ± 12	37 ± 12	ND	ND
ALP (µkat/L)				
1 day	0.83 ± 0.16	0.83 ± 0.20	0.51 ± 0.10	0.87 ± 0.21*
35 days	0.70 ± 0.09	0.70 ± 0.12	ND	ND
MCP-1 (pg/ml)				
1 day	14.0 ± 0.0	54.7 ± 14.3*	24.2 ± 8.4	176.7 ± 126.1*#
35 days	17.3 ± 2.6	14.7 ± 1.7	ND	ND
CINC-1/IL-8 (pg/ml)				
1 day	104.2 ± 26.7	158.7 ± 22.4*	93.7 ± 18.7	223.8 ± 125.7*
35 days	158.8 ± 38.1	167.6 ± 41.1	ND	ND

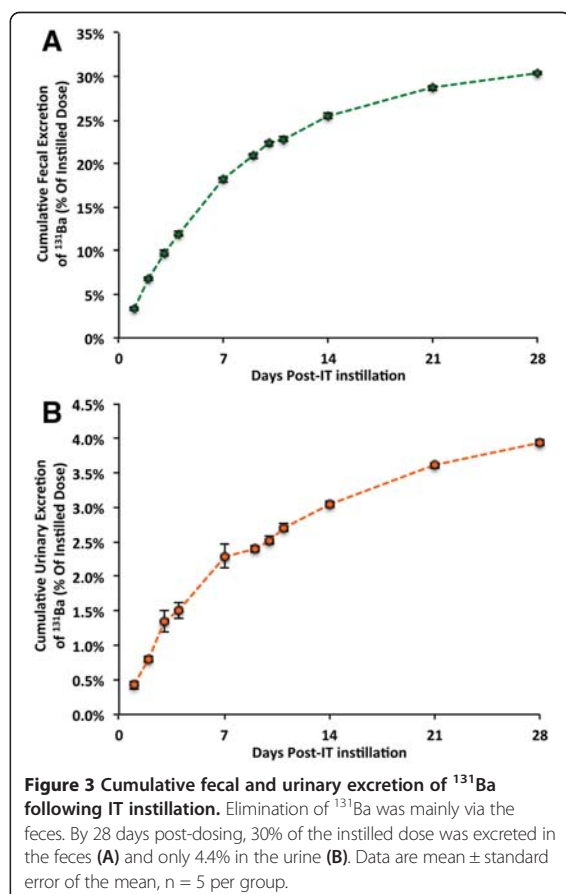
Data are mean ± SD, n = 5/group. Control rats were exposed to filtered air.

ND, not determined.

\*p < 0.05, BaSO<sub>4</sub>-exposed vs. control; #p < 0.05, 13-week vs. 4-week exposure.Neutrophils counts were significantly much lower compared to data from rats instilled with 1.4 mg BaSO<sub>4</sub> (5 mg/kg BaSO<sub>4</sub>) (Table 4).



bone marrow. Interestingly, a significant fraction was also measured in the lungs. This may represent the larger agglomerates that may be lodged within pulmonary capillaries. Over the period of 7 days after IV administration,  $^{131}\text{Ba}$  in the liver significantly decreased and redistributed into lungs, bone, and bone marrow (Figure 6).  $^{131}\text{Ba}$  activity in the lungs also significantly decreased over time (Figure 6). By day 7, a significant fraction of  $^{131}\text{Ba}$  radioactivity was found in the bones (46%). The cumulative fecal and urinary excretions of  $^{131}\text{Ba}$  are shown in Additional file 1: Figure S5. The cumulative fecal excretion was 17% while only 4% of the total injected dose was excreted in the urine over a period of 7 days (Additional file 1: Figure S5B).

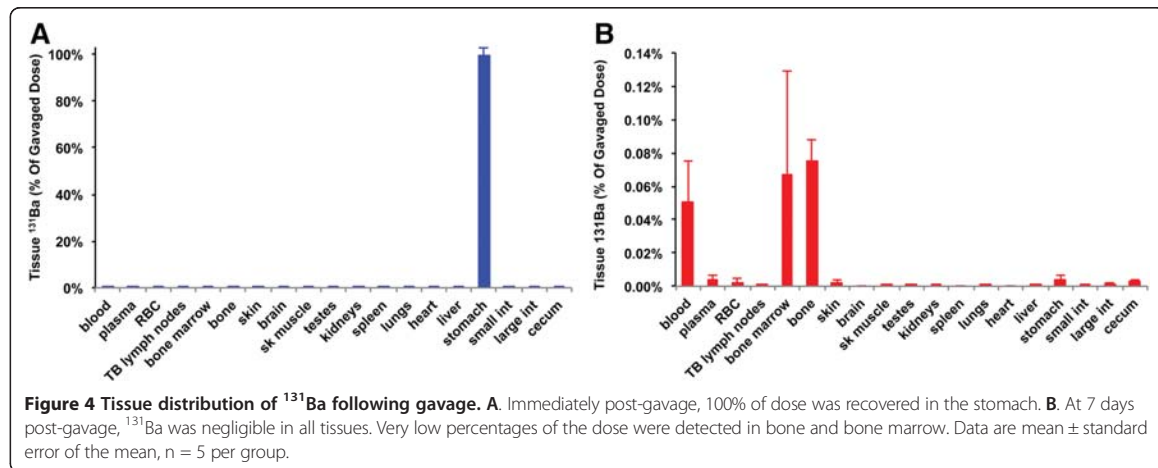


#### Barium tissue concentration - influence of route of exposure

We examined how the route of exposure affects tissue barium concentrations after dosing with  $^{131}\text{BaSO}_4$  NPs. Using the measured specific activity of  $^{131}\text{BaSO}_4$  NPs and each tissue  $^{131}\text{Ba}$  concentration, we estimated Ba concentration in ng Ba/g tissue. The Ba concentrations at 7 days post-dosing are shown in Table 6. These data demonstrate that IT instillation resulted in significantly higher tissue concentrations than gavage, especially in the bone. Barium tissue levels ranged from very low to not detectable post-gavage despite dosing the animals with a higher mass dose (1 v. 5 mg/kg). As expected, IV injection resulted in higher Ba concentrations in most tissues compared to IT and gavage administration.

#### Lung and lymph node barium analysis after inhalation exposure to $\text{BaSO}_4$ nanoparticles

The amounts of  $\text{BaSO}_4$  in the lungs and lymph nodes were estimated by measuring Ba with ICP-MS. Inhalation

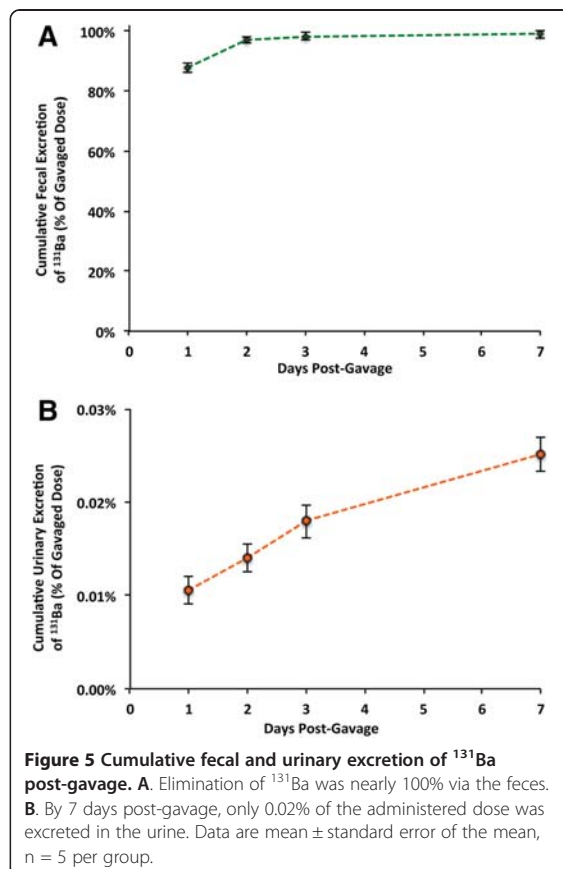


exposure to 50 mg/m<sup>3</sup> resulted in an equivalent BaSO<sub>4</sub> lung burden of 0.84 ± 0.18 mg at 1 day after the end of a 4-week exposure. Lung BaSO<sub>4</sub> burden decreased by 95% (0.84 ± 0.18 to 0.04 mg) on day 1 versus day 35 after exposure. After 13 weeks of exposure, the lung,

tracheobronchial and mediastinal lymph node burdens were 1.73 ± 0.85 mg, 5.92 ± 6.52 µg, 2.72 ± 3.38 µg BaSO<sub>4</sub>, respectively.

### Discussion

Our studies examined the effects of short-term (4-week) and subchronic (13-week) inhalation exposure and a single IT instillation of BaSO<sub>4</sub> NPs in rats. We also performed comprehensive biokinetic studies of <sup>141</sup>Ba when <sup>141</sup>BaSO<sub>4</sub> NPs were administered in rats via different routes. Four weeks of inhalation of 50 mg/m<sup>3</sup> BaSO<sub>4</sub> resulted in no pulmonary toxicity by 35 days post-exposure. BAL parameters were comparable to control values after the post-exposure period. Delayed onset of adverse effects beyond this post-exposure period is unknown. Histopathologic examination performed in 4-week exposed animals showed no morphological changes in lungs and extrapulmonary organs (e.g. brain, heart, liver, spleen, kidneys). These results are consistent with our previous short-term inhalation study that tested a variety of nano-materials including BaSO<sub>4</sub> NPs [27]. A 13-week exposure elicited a slight inflammatory response in rat lungs. The long-term effects of inhalation exposure to BaSO<sub>4</sub> NPs are being evaluated in an ongoing two-year study. Our instillation data showed a moderate dose-dependent inflammatory response to BaSO<sub>4</sub> NPs at 24 hours. Lung burdens at 1 day after 4 or 13 weeks of inhalation exposure were 0.84 ± 0.18 and 1.73 ± 0.85 mg BaSO<sub>4</sub>/lung, respectively. At the 5 mg/kg instilled dose (1.4 mg BaSO<sub>4</sub> lung burden) the neutrophil response was significantly higher than at 24 hours after the last inhalation exposure. The difference in neutrophil response may be due to the differences in dose rate, particle distribution, particle clearance, agglomerate surface properties and gender between the two studies. That the two exposure methods yield different responses is also consistent with previous reports [32,33]. A



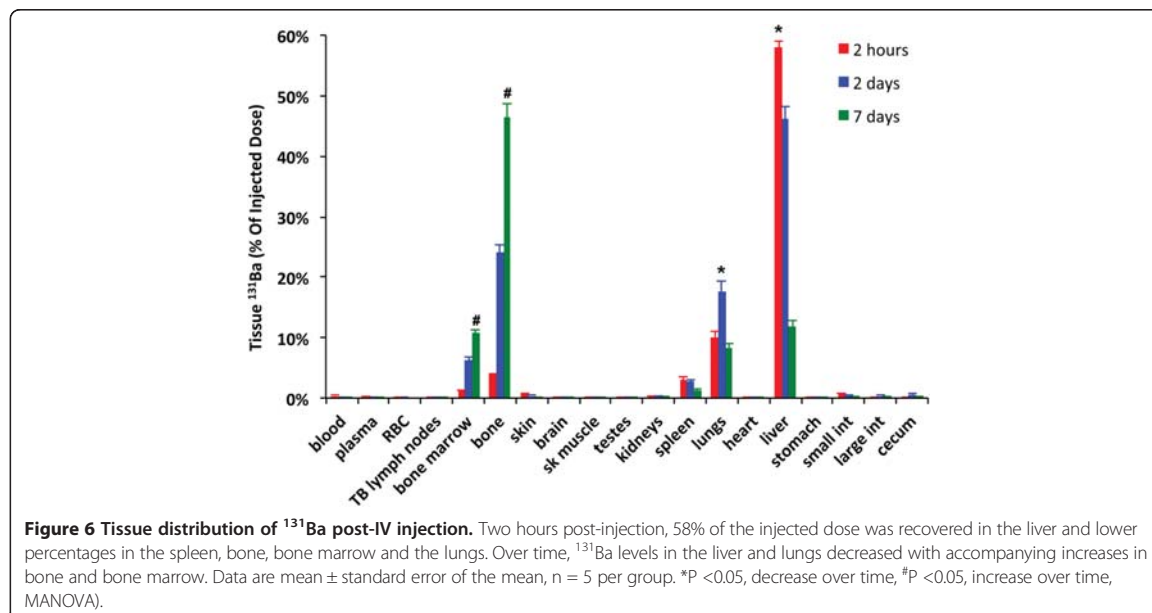


**Table 6 Comparison of tissue barium concentrations at 7 days after dosing**

Route (dose)	IT Instillation (1 mg/kg) ng/g ± SE	Gavage (5 mg/kg) ng/g ± SE	IV Injection (1 mg/kg) ng/g ± SE
Lungs	69074.5 ± 4993.8	< 0.01	9847.5 ± 983.8
Bone	2271.9 ± 124.6*	0.079 ± 0.014	3788.5 ± 156.6 <sup>#</sup>
Bone marrow	1018.3 ± 71.4*	0.13 ± 0.12	1641.3 ± 62.2 <sup>#</sup>
Cecum	119.3 ± 23.8	< 0.01	61.2 ± 4.2 <sup>#</sup>
TB LN	113.1 ± 16.3	< 0.01	64.8 ± 14.1
Large Intestine	106.6 ± 31.2	< 0.01	72.8 ± 6.1 <sup>#</sup>
Small Intestine	43.2 ± 6.7	< 0.01	28.5 ± 2.3
Spleen	37.5 ± 1.5	< 0.01	3256.4 ± 391.2 <sup>#</sup>
Stomach	30.3 ± 18.6*	0.016 ± 0.016	46.3 ± 10.1
Kidneys	7.8 ± 2.7	< 0.01	140.8 ± 12.9 <sup>#</sup>
Plasma	3.6 ± 1.2	< 0.01	0.1 ± 0.1
Heart	3.6 ± 1.2	< 0.01	77.5 ± 10.8 <sup>#</sup>
Brain	3.5 ± 0.8	< 0.01	18.6 ± 4.5 <sup>#</sup>
RBC	3.1 ± 0.5	< 0.01	< 0.01
Skeletal Muscle	3.0 ± 0.8	< 0.01	8.3 ± 0.5 <sup>#</sup>
Liver	2.5 ± 0.5	< 0.01	1760.0 ± 221.9 <sup>#</sup>
Skin	2.5 ± 1.0	< 0.01	2.5 ± 0.8
Testes	0.7 ± 0.7	< 0.01	3.3 ± 3.3

Data are mean ± SE, n = 5/group.

\*P <0.05, IT instillation higher than gavage. All other tissues post-gavage were lower than detection limit ~0.01 ng/g Barium.

<sup>#</sup>P <0.05, IV injection higher than IT instillation.

TB LN, tracheobronchial lymph nodes.

study by Baisch et al. reported a higher inflammatory response to a similar deposited dose of TiO<sub>2</sub> NPs when delivered via IT instillation rather than whole body inhalation [32]. It is clear that although IT instillation is a reliable method for administering a precise dose to the lungs, it does not model inhalation exposure. Particle distribution and dose rate are different between these two exposure methods. However, IT instillation is useful in biokinetic studies that require precise dosing and timing especially for radioactive materials such as <sup>131</sup>BaSO<sub>4</sub> NPs. Our use of radiolabelled NPs provided a very sensitive method that measured only <sup>131</sup>Ba from the nanoparticles and excluded background Ba from other sources, such as food and water. The sensitivity of <sup>131</sup>Ba detection also avoided the use of high BaSO<sub>4</sub> doses while allowing us to measure very low levels in tissues.

Pulmonary clearance kinetics post-inhalation was similar to the previous 5-day inhalation study [28]. We observed a 95% clearance of Ba from the lungs in 34 days. This is consistent with the previously observed 77% clearance over 21 days [28]. The lung burden of BaSO<sub>4</sub> after 13-week exposure to a high concentration of BaSO<sub>4</sub> was also similar to those of rats exposed to lower concentrations of TiO<sub>2</sub> and CeO<sub>2</sub> [28,34]. This shows that clearance of BaSO<sub>4</sub> is much faster than these other two nanomaterials. But the similar lung burdens from exposure to TiO<sub>2</sub> and CeO<sub>2</sub> resulted in greater inflammatory responses [10,28]. Our data suggest that the low toxicity of inhaled BaSO<sub>4</sub> is inherent to the nanomaterial as well as its relatively faster clearance.

The biokinetic data based on radioactive <sup>131</sup>BaSO<sub>4</sub> showed a fast clearance of <sup>131</sup>Ba from the lungs. We observed that 50% of the initial dose was cleared from the lungs after 9.6 days. By 28 days only 16% of the initial dose was retained in the lungs. This clearance rate also roughly correlated with that obtained from our inhalation experiment. Based on a linear regression on the natural logarithm of lung <sup>131</sup>Ba levels (% of instilled dose) over time, the extrapolated clearance of instilled <sup>131</sup>BaSO<sub>4</sub> dose at 35 days is 92%. The lung burden post-instillation was 0.28 ± 0.004 which was lower than lung burden after 4-week inhalation (0.84 ± 0.18 mg BaSO<sub>4</sub>). Despite this difference in initial lung burden, the clearance rate of BaSO<sub>4</sub> NPs was not different between the two exposure methods.

The lung clearance of BaSO<sub>4</sub> NPs was similar to that shown for micron-sized radiolabeled BaSO<sub>4</sub> where 17% of radiolabeled barium remained at 22 days post-instillation in rat lungs [20,21]. The fate of the 16% of <sup>131</sup>Ba remaining in the lungs at the end of our observation needs longer-term studies. Since lung epithelial injury may alter the fate of instilled NPs, we chose a dose that would not cause significant injury that might affect the outcome of our IT biokinetic study. Our data

suggest that <sup>131</sup>Ba from instilled <sup>131</sup>BaSO<sub>4</sub> NPs was cleared from the entire animal mainly via the gastrointestinal route. The excreted fraction in the feces might include contributions from both the mucociliary and biliary clearance pathways. Although lung clearance of <sup>131</sup>BaSO<sub>4</sub> NPs is relatively fast and only 16% of the administered dose remained 4 weeks post-instillation, a substantial fraction (37%) was retained elsewhere in the body. The tissue distribution of <sup>131</sup>Ba following IT instillation showed a significant translocation to bone, consistent with other heavy earth alkaline metals like calcium and strontium [35] as well as to the thoracic lymph nodes. Whether the <sup>131</sup>Ba measured in these extrapulmonary organs was <sup>131</sup>BaSO<sub>4</sub> NPs or ionic <sup>131</sup>Ba could not be ascertained in this study. A previous study showed that IT-instilled ionic barium cleared much more rapidly than BaSO<sub>4</sub> particles [36]. We have also demonstrated that ionic cerium was more toxic and was cleared more rapidly than CeO<sub>2</sub> NPs [37].

The clearance of inhaled BaSO<sub>4</sub> NPs was fast as evidenced by the decrease in BaSO<sub>4</sub> lung burden over time. Only 5% of retained BaSO<sub>4</sub> in the lungs (4-week-exposure) remained 35 days after the end of exposure. The relatively high bioavailability of inhaled or instilled BaSO<sub>4</sub> does not correlate with its very low dissolution rate in phagolysosomal simulant fluid, a proposed model of macrophage dissolution/clearance of particles [30]. This strongly suggests that PSF does not fully simulate the complex kinetic processes of lung transport and clearance, especially the mechanism of particle dissolution within macrophage phagolysosomes. Our cell-free *in vitro* dissolution studies showed very low dissolution in PSF even after 28 days. However, we observed that the non-spherical BaSO<sub>4</sub> NPs lost their feature of lowest radius of curvature and later recrystallized over this period. Interestingly, it has been shown that the NP surface charge and interactive properties may vary with the local radius of curvature [38]. The regions of the particle surface with different curvature become charged at differing pH values of the surrounding solution [38]. Previous studies showed that non-spherical nanomaterial may exhibit different toxicity from that of spherically shaped nanomaterial of the same composition due to the varying local charge density [39]. Likewise, quartz and vitreous silica NPs, with irregular surfaces and sharp edges were more toxic than spherical silica [40]. The significance of the noted structural changes of BaSO<sub>4</sub> NPs *in vitro* remains to be studied in the phagolysosomal compartment of lung macrophages. How these structural changes relate to cytotoxicity is likewise yet to be determined.

Whole-body exposure of rats to NP aerosols results in not only pulmonary deposition but also in ingestion of NPs due to the grooming behavior of rats. This ingestion can complicate the pattern of bioavailability from whole-

body inhalation exposures. However, for animal welfare considerations, whole-body is more convenient than nose-only exposure for long-term inhalation studies. For some applications of BaSO<sub>4</sub>, the gastrointestinal tract is also a common route for human exposures. Thus, we investigated the fate of orally administered <sup>131</sup>BaSO<sub>4</sub> NPs. Since the GI transit time is generally less than one day, it is less likely for nanoparticles to remain in the GI tract for a prolonged period of time. Even particles adherent to or ingested by columnar epithelial cells are eliminated rapidly since the epithelium sloughs off and regenerates constantly. Our data showed that 88% of the dose was eliminated in the feces within 24 hours, and almost 100% by 7 days post-gavage. Since very low radioactivity was detected in other organs, we conclude that neither <sup>131</sup>BaSO<sub>4</sub> NPs nor <sup>131</sup>Ba ions significantly crossed the intestinal barrier. This low oral bioavailability correlates with our observation of very low dissolution of BaSO<sub>4</sub> NPs in simulated gastric and intestinal fluid (Additional file 1: Table S1). This indicates that there is negligible contribution from fur deposition and ingestion during inhalation exposure. It also means that barium detected in extrapulmonary organs after inhalation translocates from the lungs to the blood.

As we and others have shown, a small fraction of inhaled nanoparticles may translocate into the systemic circulation [41]. Although our study focused on normal lungs, when they are compromised by injury or inflammation increased rates of NP translocation may occur. Therefore, we evaluated the biokinetics and tissue distribution of intravenously injected <sup>131</sup>BaSO<sub>4</sub> NPs to elucidate their fate in the circulation. When we sacrificed animals at 2 hours post-IV injection of <sup>131</sup>BaSO<sub>4</sub> NPs, we found very low radioactivity in the blood. Since the first time point we examined was at 2 hours, we could not determine the vascular clearance rate. Previously, we have shown that clearance half-lives of circulating particles are on the order of minutes even for nanoparticles such as gold colloid [31]. Initially, a significant hepatic accumulation of <sup>131</sup>Ba was observed but liver retention was decreased by 7 days. This likely reflects rapid ingestion of <sup>131</sup>BaSO<sub>4</sub> NPs by the abundant hepatic macrophages (Kupffer cells) and possibly subsequent dissolution followed by release of barium ions into the blood. The decrease was accompanied by increasing accumulation in bone similar to that observed following IT instillation. Despite the significant uptake of Ba in the bone, no evidence of genotoxicity in the bone marrow was noted. We found no micronucleus formation in peripheral blood cells that originate from hematopoiesis in the bone marrow.

## Conclusions

Our data show that inhaled BaSO<sub>4</sub> NPs elicited minimal pulmonary response and no systemic effects. Equivalent

lung burdens of CeO<sub>2</sub> and TiO<sub>2</sub> elicit more pulmonary response than BaSO<sub>4</sub> [28]. This difference might be due to its lower inherent toxicity and also to its faster lung clearance. The mechanism of this faster clearance needs further investigation. There is no direct correlation between abiotic *in vitro* dissolution of BaSO<sub>4</sub> in several cell-free biological simulation fluids and actual *in vivo* biopersistence and bioavailability of barium from BaSO<sub>4</sub> NPs. Our data suggest that cell-free *in vitro* assays either lack crucial constituents or do not adequately simulate the processes that facilitate particle dissolution and increase bioavailability. The Ba in BaSO<sub>4</sub> from the lungs translocates to many tissues, especially the bones. The comparison of pulmonary versus ingestion routes of exposure provides a quantitative measure of relative doses to a variety of non-pulmonary tissues. From our data, it is evident that the bioavailability of Ba from ingestion of BaSO<sub>4</sub> NPs is very low and that no significant contribution from ingestion should occur during whole-body inhalation studies in rats.

Our study underscores the high Ba bioavailability and clearance of BaSO<sub>4</sub> NPs deposited in the lungs. Unlike CeO<sub>2</sub> and TiO<sub>2</sub>, BaSO<sub>4</sub> NPs are retained to a lesser extent in the lungs after inhalation. Even at lung burdens similar to CeO<sub>2</sub> and TiO<sub>2</sub>, BaSO<sub>4</sub> NPs cause lower pulmonary toxicity. Barium sulfate exhibits lower toxicity and biopersistence in the lungs compared to poorly soluble CeO<sub>2</sub> and TiO<sub>2</sub>.

## Methods

### Physicochemical characterization of BaSO<sub>4</sub> nanoparticles

BaSO<sub>4</sub> NPs (NM-220) used for IT instillation studies were obtained from BASF SE (Ludwigshafen, Germany). It was a reference material for the Nanomaterial Testing Sponsorship Program of the Organization for Economic Co-operation and Development (OECD). The characterization of the original batch distributed as "NM-220" was published recently [29]. The reproduced BaSO<sub>4</sub> used in inhalation studies was characterized by the same methods (See Supporting Information).

### Animals for intratracheal instillation, gavage and intravenous injection studies

The protocols used in this study were approved by the Harvard Medical Area Animal Care and Use Committee. Male Wistar rats (8 weeks old) were obtained from Charles River Laboratories (Wilmington, MA) and were housed in standard microisolator cages under controlled conditions of temperature, humidity, and light at the Harvard Center for Comparative Medicine. They were fed commercial chow (PicoLab Rodent Diet 5053, Framingham, MA) and reverse-osmosis purified water was provided *ad libitum*. The animals were acclimatized in the facility for 7 days before the start of experiments.

**Preparation of BaSO<sub>4</sub> suspension for animal dosing**

Suspensions of BaSO<sub>4</sub> NPs were prepared at appropriate concentrations in sterile polyethylene tubes. The critical dispersion sonication energy (DSE<sub>cr</sub>) required to achieve the lowest reported particle agglomeration was used as previously reported [42]. Suspensions in sample tubes were sonicated with a Branson Sonifier S-450A (Branson Ultrasonics, Danbury, CT) fitted with a cup sonicator at 242 J/ml, the critical dispersive energy shown to maximally disperse these particles in water [42] while immersed in running cold water to minimize heating of the particles. The hydrodynamic diameter (d<sub>H</sub>), polydispersity index (Pdl), and zeta potential (ζ) of each suspension were measured by dynamic light scattering using a Zetasizer Nano-ZS (Malvern Instruments, Worcestershire, UK).

**Pulmonary responses to intratracheally instilled BaSO<sub>4</sub> nanoparticles – Bronchoalveolar lavage and analyses**

This experiment was performed to determine a particle dose for pulmonary particle instillation that does not cause significant injury or inflammation. Twenty rats (mean wt ± standard deviation, 280 ± 15 g) were IT-instilled with BaSO<sub>4</sub> suspension at 1, 2 and 5 mg/kg dose (5 rats per dose) to determine the acute pulmonary effects of BaSO<sub>4</sub> particles. The nanoparticle concentrations were 0.67, 1.33, and 3.33 mg/ml for the 1, 2, and 5 mg/kg dose, respectively. Rats instilled with an equivalent volume of sterile distilled water served as controls. The volume dose was 1.5 ml/kg. The particle suspensions were delivered to the lungs through the trachea, as described earlier [43]. Twenty-four hours later, the rats were anesthetized and euthanized via exsanguination. The trachea was exposed and cannulated. The lungs were then lavaged 12 times with 3 mL of Ca- and Mg-free 0.9% sterile PBS. The cells of all washes were separated from the supernatant by centrifugation (350 × g at 4°C for 10 min). Total cell count and hemoglobin measurements were made from the cell pellets. After smearing and staining the cells, a differential cell count was performed. The supernatant of the two first washes was clarified via centrifugation (14,500 × g at 4°C for 30 min), and used for spectrophotometric assays for lactate dehydrogenase (LDH), myeloperoxidase (MPO) and albumin.

**Neutron activation of BaSO<sub>4</sub> nanoparticles for pharmacokinetic studies**

Barium sulfate NM-220 particles were neutron activated at the MIT Nuclear Reactor Laboratory (Cambridge, MA) with a thermal neutron flux of  $5 \times 10^{13}$  n/cm<sup>2</sup>s for 24 hours. The process generated <sup>131</sup>Ba, which decays with a half life of 10.5 days and emits multiple gamma rays with varying energies. The specific activity was 2.6 μCi <sup>131</sup>Ba per mg BaSO<sub>4</sub> NPs.

**Pharmacokinetics of tracheally-instilled, gavaged or intravenously-injected <sup>131</sup>BaSO<sub>4</sub> nanoparticles**

Fifty rats (mean wt ± standard deviation, 270 ± 12 g) were used for this study. Neutron-activated <sup>131</sup>BaSO<sub>4</sub> NPs were suspended in sterile distilled water at 0.67 mg/ml for intratracheal instillation (IT), 10 mg/ml for gavage, and 1 mg/ml for intravenous (IV) injection. The mass and volume doses were 1) IT - 1 mg/kg (1.5 ml/kg), 2) gavage - 5 mg/kg (0.5 ml/kg), and 3) IV - 1 mg/kg (1 ml/kg). The particle suspensions were dispersed as described earlier. Aliquots of each suspension were measured in a WIZARD gamma counter (PerkinElmer, Inc., Waltham, MA) to estimate each rat's <sup>131</sup>Ba dose. Gamma energies at 200–270 KeV were utilized for <sup>131</sup>Ba quantitation. Each rat was anesthetized with isoflurane (Piramal Healthcare, Bethlehem, PA) during particle administration. After dosing, each rat was placed in a metabolic cage with food and water *ad libitum*. Twenty-four-hour samples of urine and feces were collected at 0–1, 2–3, 6–7, 9–10, 13–14, 20–21, and 27–28 days after dosing.

The <sup>131</sup>BaSO<sub>4</sub> NP suspension was delivered to the lungs through the trachea as described earlier. For gavage, <sup>131</sup>BaSO<sub>4</sub> NPs were delivered into the stomach via the esophagus. IV injection was done using the penile vein in similarly anesthetized animals. Five rats from the IT group were humanely killed at each time point: 5 minutes and 2, 7, 14 and 28 days post-dosing. Analysis of rats at 5 minutes post-instillation was performed to get an accurate measure of the initial deposited dose. Equal numbers of rats (5 per timepoint) were analyzed at 5 minutes and 7 days post-gavage, and at 2 hours, 2 days, and 7 days post-IV injection. At each time point, rats were anesthetized and blood collected from the abdominal aorta. Plasma and red blood cells were separated by centrifugation. The lungs, brain, heart, spleen, kidneys, gastrointestinal tract, liver, testes, and samples of skeletal muscle, bone marrow, skin, and femoral bone were collected and placed in pre-weighed tubes. Sample weight was recorded and radioactivity (200–270 KeV) was measured in a WIZARD gamma counter (PerkinElmer, Inc., Waltham, MA). Disintegrations per minute were calculated from the counts per minute and the counter efficiency. The limit of detection for <sup>131</sup>Ba was 0.05 nCi. All radioactivity data were adjusted for physical decay over the entire observation period. Data were expressed as μCi/g and as a percentage of the administered dose retained in each organ. Total radioactivity in organs and tissues not measured in their entirety was computed using the following estimates of tissue percentage of total body weight: skeletal muscle, 40%; bone marrow, 3.2%; peripheral blood, 7%; skin, 19%; and bone, 6% [44,45].

**Animals for inhalation studies**

Protocols for the inhalation studies were approved by the local authorizing agency in Landesuntersuchungsamt

Koblenz, Germany. Animals were housed in an AAALAC-accredited facility in accordance with the German Animal Welfare Act and the effective European Council Directive. Female Wistar Han rats were obtained at 5 or 7 weeks of age from Charles River Laboratories (Sulzfeld, Germany). The animals were maintained in groups of up to 5 animals in a polysulfon cage (H-Temp [PSU], TECNIPLAST, Germany) with a floor area of about 2065 cm<sup>2</sup> with access to wooden gnawing blocks, GLP certified diet (Kliba laboratory diet, Provimi Kliba SA, Kaiseraugst, Basel Switzerland) and water *ad libitum*. Animal rooms were kept under controlled conditions (20 - 24°C temperature, 30-70% relative humidity, 15 air changes per hour, 12-hour light/dark cycle). To adapt to the exposure conditions, the animals were acclimatized to exposure conditions over two days (3 and 6 hours, respectively). Up to two animals per wire cage type DK III (BECKER & Co., Castrop-Rauxel, Germany) were exposed in the whole-body exposure chamber.

#### Study design - inhalation exposure for four and thirteen weeks

Thirty female rats (in groups of five) were whole-body exposed to 50 mg/m<sup>3</sup> BaSO<sub>4</sub> NPs for 6 hours per day on five consecutive days for 4 weeks (15 rats). Another cohort of 15 rats was exposed for 13 weeks. Body weights were recorded before and every week throughout the duration of the experiments. After 4 weeks of exposure, one group was examined and another after a post-exposure period of 35 days. The short-term inhalation study with 4 weeks of exposure was performed according to the OECD Principles of Good Laboratory Practice (GLP) [46], according to OECD Guidelines for Testing of Chemicals, Section 4: Health Effects, No. 412 [47]. This study provides information on biokinetics and effects of BaSO<sub>4</sub> NPs required for the design of the long-term inhalation study. Barium burden in lungs was measured at three time points to determine the retention half-life. BAL analysis and histopathology of the lungs were performed. In addition, systemic effects were investigated with histopathology of extrapulmonary organs, examination of blood and systemic genotoxicity by micronucleus test (MNT). Based on the result of the short-term study with 4 weeks of exposure, the long-term study was started at the same concentration of 50 mg/m<sup>3</sup> BaSO<sub>4</sub>. The long-term inhalation study is performed according to OECD Guidelines for Testing of Chemicals, Section 4: Health Effects, No. 453 [48].

#### Inhalation system

The animals were exposed while in wire cages that were located in a stainless-steel whole-body inhalation chamber ( $V = 2.8 \text{ m}^3$  or  $V = 1.4 \text{ m}^3$ ). The aerosols were passed into the inhalation chambers with the supply air and were removed by an exhaust air system with 20 air changes per

hour. For the control animals, the exhaust air system was adjusted in such a way that the amount of exhaust air was lower than the filtered clean, supply air (positive pressure) to ensure that no laboratory room air reaches the control animals. For the BaSO<sub>4</sub>-exposed rats, the amount of exhaust air was higher than the supply air (negative pressure) to prevent contamination of the laboratory as a result of potential leakages from the inhalation chambers.

#### Aerosol generation and monitoring

BaSO<sub>4</sub> aerosols were produced by dry dispersion of powder pellets with a brush dust generator using compressed air at 1.5 m<sup>3</sup>/h (developed by the Technical University of Karlsruhe in cooperation with BASE, Germany). The dust aerosol was diluted by conditioned air passed into the whole-body inhalation chambers. The control group was exposed to conditioned clean air. The desired concentrations were achieved by varying the feeding speed of the powder pellet or by varying the rotation speed of the brush. Based on a comprehensive technical trial, atmospheric concentrations within the chambers were found to be homogenous (Table 3). Nevertheless, exposure cages were rotated within each chamber daily for the 4-week, and weekly for the 13-week group.

Generated aerosols were continuously monitored by scattered light photometers (VisGuard, Sigrist). Particle concentrations in the inhalation chambers were analyzed by gravimetric measurement of air filter samples. Particle size distribution was determined gravimetrically by cascade impactor analysis using eight stages Marple Personal Cascade Impactor (Sierra-Anderson, USA). In addition, a light-scattering aerosol spectrometer (WELAS 2000, Palas, Karlsruhe, Germany) was used to measure particle sizes from 0.24 to 10 μm. To measure particles in the sub-micrometer range, a scanning mobility particle sizer (SMPS 5.400, Grimm Aerosoltechnik, Ainring, Germany) was used. The sampling procedures and measurements to characterize the generated aerosols were previously described [49].

#### Pulmonary responses to inhaled BaSO<sub>4</sub> nanoparticles - Bronchoalveolar lavage and analysis

Five animals per group were examined. After euthanasia, the lungs were lavaged twice *in situ* with 22 mL/kg body weight (4 to 5 ml) of normal saline. The recovered volume ranged from 8 to 10 ml per animal. Aliquots of BAL were used for determinations of total protein concentration, total cell count, differential cell count and enzyme activities. In the 4 week-exposure group and its control, BAL analysis was performed twice (1 and 35 days after the end of exposure) but only at 1 day post-exposure in the 13-week exposure group. Lavaged lung tissue and aliquots of the BAL fluid (1 ml) were stored at -80°C and used for determination of barium content.

Total BAL cell counts were determined with an Advia 120 (Siemens Diagnostics, Fernwald, Germany) hematology analyzer. Differential cell counts were made on Wright-stained cytocentrifuge slide preparations. Using a Hitachi 917 (Roche Diagnostics, Mannheim, Germany) reaction rate analyzer, levels of BAL total protein and activities of lactate dehydrogenase (LDH), alkaline phosphatase (ALP),  $\gamma$ -glutamyltransferase (GGT) and N-acetyl- $\beta$ -glucosaminidase (NAG) were measured. Inflammatory cytokines (MCP-1, IL-8/CINC-1, M-CSE, osteopontin) in BAL were measured using ELISA test kits as described previously [50].

#### Tissue analysis of barium content

Ba levels were measured in the lungs and lung-associated lymph nodes of exposed animals and controls. The lavaged lungs and aliquots of BAL of five animals per group were used. Barium content in the 4 week-exposure group lungs was measured three times (1, 2 and 35 days after the end of exposure) but only once (1 day post-exposure) in the 13-week exposure group. Each tissue sample was dried and sulfuric acid was added. The sample was then ashed and acid was vaporized at 500°C for 15 min. Sulfuric and nitric acid were added to the residue. Then a mixture of nitric acid, sulfuric acid and perchloric acid (2:1:1 v/v/v) was added and the solution was heated to oxidize organic matter. After evaporation, the residue was dissolved in concentrated sulfuric acid. The resulting solution was analyzed for  $^{137}\text{Ba}$  content by inductively coupled plasma mass spectrometry (ICP-MS) using Agilent 7500C (Agilent, Frankfurt, Germany). The limit of detection for Ba is 0.3  $\mu\text{g}$  per tissue sample.

#### Necropsy and histopathology

After 4 weeks of exposure, necropsy and histopathology were performed on selected rats at 1 day and 34 days after the end of exposure. Gross and histopathological examination of the lungs and extrapulmonary organs were performed on ten rats per group. The animals were euthanized by cutting the abdominal aorta and vena cava under sodium pentobarbital anesthesia. According to OECD no. 412, the following organs were weighed: adrenal glands, brain, heart, ovaries, uterus with cervix, kidney, liver, lungs, spleen, thymus, thyroid glands. The lungs were IT-instilled with neutral buffered 10% formalin at 30 cm water pressure. All other organs were fixed in the same fixative. The organs and tissues were trimmed, paraffin embedded and sectioned according to RITA trimming guides for inhalation studies [51-53]. Paraffin sections were stained with hematoxylin and eosin. Extrapulmonary organs and the respiratory tract, comprised of the nasal cavity (four levels), larynx (three levels), trachea (transverse and longitudinal with carina), lungs (five lobes), and mediastinal and

tracheobronchial lymph nodes, were examined by light microscopy.

#### Statistical analyses

##### Pharmacokinetic and single instillation studies

All BAL parameters and tissue  $^{131}\text{Ba}$  distribution data were analyzed using multivariate analysis of variance (MANOVA) followed by Bonferroni (Dunn) *post hoc* tests using SAS Statistical Analysis software (SAS Institute, Cary, NC). Lung clearance data were analyzed by linear regression of the natural logarithm of the lung  $^{131}\text{BaSO}_4$  levels (% dose) over time using R Program v. 3.1.0 (The R Foundation for Statistical Computing, Vienna, Austria).

##### Inhalation studies

Body weight differences were compared between  $\text{BaSO}_4$ -exposed and control groups using Dunnett's test. Bronchoalveolar lavage cytology, enzyme and cell mediator data were analyzed by non-parametric one-way analysis of variance using the Kruskal-Wallis test (two-sided). If the resulting p value was equal or less than 0.05, a pair-wise comparison of each test group with the control group was performed using the Wilcoxon test or the Mann-Whitney U-test. Comparison of organ weights was performed by nonparametric one-way analysis using the two-sided Kruskal-Wallis test, followed by a two-sided Wilcoxon test for the hypothesis of equal medians.

#### Additional file

##### Additional file 1: Online Supporting Information. Table S1.

Physicochemical characterization of  $\text{BaSO}_4$  nanoparticles. **Table S2.** Distribution of recovered  $^{131}\text{Ba}$  post-intratracheal instillation of  $^{131}\text{BaSO}_4$  nanoparticles. **Table S3.** Distribution of recovered  $^{131}\text{Ba}$  post-gavage of  $^{131}\text{BaSO}_4$  nanoparticles. **Table S4.** Distribution of recovered  $^{131}\text{Ba}$  post-intravenous injection of  $^{131}\text{BaSO}_4$  nanoparticles. **Figure S1.** Structure of  $\text{BaSO}_4$  NM-220. A) Pore size distribution by Hg intrusion. B) Crystallinity by XRD (black line), with assignment of peaks to reference spectrum of bulk  $\text{BaSO}_4$  orthorhombic (red). There were no unexpected peaks. **Figure S2.** Photocatalytic reactivity of A) NM-220 batch, B) reproduced batch: shown are UV-vis absorption spectra at 0, 2, 6 and 22 h incubation of Methylene Blue with  $\text{BaSO}_4$ , irradiated with 1  $\text{mW}/\text{cm}^2$  UV (350 nm) as specified in DIN 52980:2008-10, adapted for dispersed surfaces [1]. The blue curves are spectra of samples kept in the dark, the red-yellow curves are spectra of irradiated samples. The evaluation is compatible with zero degradation of the dye. **Figure S3.** Total lavaged neutrophils at 1 day post-instillation (A) or after the end of 4 and 13 weeks inhalation exposure of  $\text{BaSO}_4$  NPs (B). The x-axis represents the lung burden of barium at the end of 4-week (0.8 mg) or 13-week inhalation exposure (1.7 mg) (B). The neutrophil counts were significantly higher in instilled (A) than aerosol-exposed rats (B). **Figure S4.** Microscopic appearance of lungs after 4 weeks of inhalation exposure. Lung section of control animal (A) and animal exposed to 50  $\text{mg}/\text{m}^3$   $\text{BaSO}_4$  (B). **Figure S5.** Cumulative fecal and urinary excretion of  $^{131}\text{Ba}$  post-IV injection. Elimination of  $^{131}\text{Ba}$  was 17% via the feces (A) and only 4.4% of dose via the urine (B).

#### Abbreviations

ALP: Alkaline phosphatase; BAL: Bronchoalveolar lavage; BALF: Bronchoalveolar lavage fluid; CINC: Cytokine-induced neutrophil chemoattractant; DLS: Dynamic

light scattering; FaSIF: Fasted state simulated intestinal fluid; GGT:  $\gamma$ -Glutamyl-transpeptidase; GSD: Geometric standard deviation; ICP-MS: Inductively coupled plasma mass spectrometry; IL: Interleukin; LDH: Lactate dehydrogenase; M-CSF: Macrophage colony stimulating factor; MCP: Monocyte chemoattractant protein; MMAD: Mass median aerodynamic diameter; MPO: Myeloperoxidase; NAG: N-Acetyl- $\beta$ -glucosaminidase; NM: Nanomaterial; OPN: Osteopontin; PBS: Phosphate buffered saline; PMN: Polymorphonuclear; PSF: Phagolysosomal simulant fluid; PSLT: Poorly soluble low toxicity; SEM: Scanning electron microscopy; SMPs: Scanning mobility particle sizer; TEM: Transmission electron microscopy; TGA: Thermogravimetric analysis.

#### Competing interests

JK, LM, SG, RL and WW are employees of BASF SE, a company that produces and markets nanomaterials. NVK was a BASF fellow for the duration of the study. All other authors declare that they have no competing interests.

#### Authors' contributions

RL, RMM and JDB designed the project and evaluated the experimental results. RMM, NVK, TCD and JDB carried out the biokinetic studies with radioactive barium sulfate and pulmonary toxicity experiments after intratracheal instillation. JK, LM, SG, RL and WW performed the inhalation toxicity studies and physico-chemical characterizations of barium sulfate nanoparticles. NVK and JK drafted the manuscript. All authors read, revised and approved the manuscript.

#### Acknowledgment

This study was funded by BASF SE (Ludwigshafen, Germany) and by the National Institute of Environmental Health Sciences (ES000002). Nagarjun Konduru was supported with a BASF Fellowship. We thank Thomas Bork for technical assistance with neutron activation, the inhalation and pathology team of BASF for their technical support, Christa Watson for technical help with DLS analysis and Melissa Curran for her editorial assistance.

Received: 7 August 2014 Accepted: 4 October 2014

Published online: 21 October 2014

#### References

- Gillani R, Ercan R, Qiao A, Webster TJ: **Nanofunctionalized zirconia and barium sulfate particles as bone cement additives.** *Int J Nanomed* 2010, **5**:1–11.
- Gomoll AH, Fitz W, Scott RD, Thornhill TS, Bellare A: **Nanoparticulate fillers improve the mechanical strength of bone cement.** *Acta Orthop* 2008, **79**:421–427.
- Mohn D, Zehnder M, Imfeld T, Stark WJ: **Radio-opaque nanosized bioactive glass for potential root canal application: evaluation of radiopacity, bioactivity and alkaline capacity.** *Int Endod J* 2010, **43**:210–217.
- Noreen R, Pineau R, Chien CC, Cestelli-Guidi M, Hwu Y, Marcelli A, Moenner M, Petibois C: **Functional histology of glioma vasculature by FTIR imaging.** *Anal Bioanal Chem* 2011, **401**:795–801.
- Villalobos-Hernandez JR, Muller-Goymann CC: **Novel nanoparticulate carrier system based on carnauba wax and decyl oleate for the dispersion of inorganic sunscreens in aqueous media.** *Eur J Pharm Biopharm* 2005, **60**:113–122.
- Aninwene GE 2nd, Stout D, Yang Z, Webster TJ: **Nano-BaSO<sub>4</sub>: a novel antimicrobial additive to pellethane.** *Int J Nanomed* 2013, **8**:1197–1205.
- Doig AT: **Baritosis: a benign pneumoconiosis.** *Thorax* 1976, **31**:30–39.
- Dosios T, Karydas AG: **Baritosis of the mediastinal lymph nodes.** *Ann Thorac Surg* 2003, **76**:297.
- Levi-Valensi P, Drif M, Dat A, Hadjadj G: **Apropos of 57 cases of pulmonary baritosis. (Results of a systematic investigation in a baryta factory).** *J Fr Med Chir Thorac* 1966, **20**:443–455.
- Maynard AD, Kuempel ED: **Airborne nanostructured particles and occupational health.** *J Nanopart Res* 2005, **7**:587–614.
- Oberdorster G: **Toxicokinetics and effects of fibrous and nonfibrous particles.** *Inhal Toxicol* 2002, **14**:29–56.
- Tran CL, Buchanan D, Cullen RT, Searl A, Jones AD, Donaldson K: **Inhalation of poorly soluble particles. II. Influence of particle surface area on inflammation and clearance.** *Inhal Toxicol* 2000, **12**:1113–1126.
- He X, Zhang H, Ma Y, Bai W, Zhang Z, Lu K, Ding Y, Zhao Y, Chai Z: **Lung deposition and extrapulmonary translocation of nano-ceria after intratracheal instillation.** *Nanotechnology* 2010, **21**:285103.
- Park E-J, Park Y-K, Park K: **Acute toxicity and tissue distribution of cerium oxide nanoparticles by a single oral administration in rats.** *Toxicol Res* 2009, **25**:79–84.
- Shi H, Magaye R, Castranova V, Zhao J: **Titanium dioxide nanoparticles: a review of current toxicological data.** *Part Fibre Toxicol* 2013, **10**:15.
- Buzea C, Pacheco II, Robbie K: **Nanomaterials and nanoparticles: sources and toxicity.** *Biointerphases* 2007, **2**:MR17–MR71.
- Cullen RT, Tran CL, Buchanan D, Davis JM, Searl A, Jones AD, Donaldson K: **Inhalation of poorly soluble particles. I. Differences in inflammatory response and clearance during exposure.** *Inhal Toxicol* 2000, **12**:1089–1111.
- Dhawan A, Sharma V, Parmar D: **Nanomaterials: A challenge for toxicologists.** *Nanotoxicology* 2008, **3**:1–9.
- Konduru NV, Murdaugh KM, Sotiriou GA, Donaghey TC, Demokritou P, Brain JD, Molina RM: **Bioavailability, distribution and clearance of tracheally-instilled and gavaged uncoated or silica-coated zinc oxide nanoparticles.** *Part Fibre Toxicol* 2014, **11**:44.
- Cember H, Hatch TF, Watson JA, Gucci T: **Pulmonary effects from radioactive barium sulfate dust.** *AMA Arch Ind Health* 1955, **12**:628–634.
- Cember H, Hatch TF, Watson JA, Gucci T, Bell P: **The elimination of radioactive barium sulfate particles from the lung.** *AMA Arch Ind Health* 1956, **13**:170–176.
- Reijnders L: **The release of TiO<sub>2</sub> and SiO<sub>2</sub> nanoparticles from nanocomposites.** *Polym Degrad Stab* 2009, **94**:873–876.
- Song G, Wang Q, Wang Y, Lv G, Li C, Zou R, Chen Z, Qin Z, Huo K, Hu R, Hu J: **A low-toxic multifunctional nanoplatfrom based on Cu<sub>2</sub>S<sub>2</sub>@mSiO<sub>2</sub> core-shell nanocomposites: combining photothermal- and chemotherapies with infrared thermal imaging for cancer treatment.** *Ad Func Mat* 2013, **23**:4281–4292.
- Stec AA, Hull TR: **Toxic Combustion of Products from Fire Retarded Nanocomposite Polymers.** Edinburgh, UK: Proceedings of the 5th International Seminar on Fire and Explosion Hazards; 2007. 23–27 April 2007, Edinburgh, UK.
- Johnston H, Pojana G, Zuin S, Jacobsen NR, Moller P, Loft S, Semmler-Behnke M, McGuinness C, Balhary D, Marcomini A, Wallin H, Kreyling W, Donaldson K, Tran L, Stone V: **Engineered nanomaterial risk. Lessons learnt from completed nanotoxicology studies: potential solutions to current and future challenges.** *Crit Rev Toxicol* 2013, **43**:1–20.
- Landsiedel R, Ma-Hock L, Kroll A, Hahn D, Schnekenburger J, Wiench K, Wohlleben W: **Testing metal-oxide nanomaterials for human safety.** *Adv Mater* 2010, **22**:2601–2627.
- Klein CL, Wiench K, Wiemann M, Ma-Hock L, Van Ravenzwaay B, Landsiedel R: **Hazard identification of inhaled nanomaterials: making use of short-term inhalation studies.** *Arch Toxicol* 2012, **86**:1137–1151.
- Landsiedel R, Ma-Hock L, Hofmann T, Wiemann M, Strauss V, Treumann S, Wohlleben W, Groters S, Wiench K, van Ravenzwaay B: **Application of short-term inhalation studies to assess the inhalation toxicity of nanomaterials.** *Part Fibre Toxicol* 2014, **11**:16.
- Wohlleben W, Ma-Hock L, Boyko V, Cox G, Egenolf H, Freiberger H, Hinrichsen B, Hirth S, Landsiedel R: **Nanospecific guidance in REACH: a comparative physical-chemical characterization of 15 materials with methodical correlations.** *J Ceram Sci Tech* 2013, **4**:93–104.
- Stefaniak AB, Guilmette RA, Day GA, Hoover MD, Breyse PN, Scripsick RC: **Characterization of phagolysosomal simulant fluid for study of beryllium aerosol particle dissolution.** *Toxicol In Vitro* 2005, **19**:123–134.
- Brain JD, Molina RM, DeCamp MM, Warner AE: **Pulmonary intravascular macrophages: their contribution to the mononuclear phagocyte system in 13 species.** *Am J Physiol* 1999, **276**:L146–L154.
- Baisch BL, Corson NM, Wade-Mercer P, Gelein R, Kennell AJ, Oberdorster G, Elder A: **Equivalent titanium dioxide nanoparticle deposition by intratracheal instillation and whole body inhalation: the effect of dose rate on acute respiratory tract inflammation.** *Part Fibre Toxicol* 2014, **11**:5.
- Osier M, Oberdorster G: **Intratracheal inhalation vs intratracheal instillation: differences in particle effects.** *Fundam Appl Toxicol* 1997, **40**:220–227.
- Keller J, Wohlleben W, Ma-Hock L, Strauss V, Groters S, Kuttler K, Wiench K, Herden C, Oberdorster G, van Ravenzwaay B, Landsiedel R: **Time course of lung retention and toxicity of inhaled particles: short-term exposure to nano-Ceria.** *Arch Toxicol* 2014. doi:10.1007/s00204-014-1349-9.
- Moore W Jr: **Comparative metabolism of barium-133 and calcium-45 by embryonic bone grown in vitro.** *Radiat Res* 1964, **21**:376–382.

36. Cember H, Watson JA, Novak ME: **The influence of radioactivity and lung burden on the pulmonary clearance rate of barium sulfate.** *Am Ind Hyg Assoc J* 1961, **22**:27–32.
37. Molina RM, Konduru NV, Jimenez RJ, Pyrgiotakis G, Demokritou P, Wohlleben W, Brai JD: **Bioavailability, distribution and clearance of tracheally instilled, gavaged or injected cerium dioxide nanoparticles and ionic cerium.** *Part Fibre Toxicol* 2014. doi:10.1039/c4en00034j.
38. Walker DA, Leitsch EK, Nap RJ, Szeifer I, Grzybowski BA: **Geometric curvature controls the chemical patchiness and self-assembly of nanoparticles.** *Nat Nanotechnol* 2013, **8**:676–681.
39. Wani MY, Hashim MA, Nabi F, Malik MA: **Nanotoxicity: dimensional and morphological concerns.** *Adv Phys Chem* 2011, **2011**:1–15.
40. Ghiazza M, Polimeni M, Fenoglio I, Gazzano E, Ghigo D, Fubini B: **Does vitreous silica contradict the toxicity of the crystalline silica paradigm?** *Chem Res Toxicol* 2010, **23**:620–629.
41. Choi HS, Ashitate Y, Lee JH, Kim SH, Matsui A, Insin N, Bawendi MG, Semmler-Behnke M, Frangioni JV, Tsuda A: **Rapid translocation of nanoparticles from the lung airspaces to the body.** *Nat Biotechnol* 2010, **28**:1300–1303.
42. Cohen J, Deloid G, Pyrgiotakis G, Demokritou P: **Interactions of engineered nanomaterials in physiological media and implications for in vitro dosimetry.** *Nanotoxicology* 2013, **7**:417–431.
43. Brain JD, Knudson DE, Sorokin SP, Davis MA: **Pulmonary distribution of particles given by intratracheal instillation or by aerosol inhalation.** *Environ Res* 1976, **11**:13–33.
44. Brown RP, Delp MD, Lindstedt SL, Rhomberg LR, Beliles RP: **Physiological parameter values for physiologically based pharmacokinetic models.** *Toxicol Ind Health* 1997, **13**:407–484.
45. Schoeffner DJ, Warren DA, Muralidara S, Bruckner JV, Simmons JE: **Organ weights and fat volume in rats as a function of strain and age.** *J Toxicol Environ Health A* 1999, **56**:449–462.
46. Organization for Economic Cooperation and Development (OECD): *OECD Principles on Good Laboratory Practice (as revised in 1997)*. ENV/MC/CHEM(98)17, Guidance Manual for the testing of manufactured nanomaterials. Paris: OECD; 1998.
47. Organization for Economic Cooperation and Development (OECD): *OECD Guidelines for Testing of Chemicals, Section 4: Health Effects, No.412, "Repeated Dose Inhalation Toxicity: 28day or 14day Study"*, Guidance Manual for the Testing of Manufactured Nanomaterials: OECD's Sponsorship Programme. Paris: OECD; 2009.
48. Organization for Economic Cooperation and Development (OECD): *OECD Guidelines for the Testing of Chemicals, Section 4, Test No. 453: Combined Chronic Toxicity/Carcinogenicity Studies*. Paris: OECD; 2009.
49. Ma-Hock L, Gamer AO, Landsiedel R, Leibold E, Frechen T, Sens B, Linsenbuehler M, Van Ravenzwaay B: **Generation and characterization of test atmospheres with nanomaterials.** *Inhal Toxicol* 2007, **19**:833–848.
50. Ma-Hock L, Burkhardt S, Strauss V, Gamer AO, Wiench K, Van Ravenzwaay B, Landsiedel R: **Development of a short-term inhalation test in the rat using nano-titanium dioxide as a model substance.** *Inhal Toxicol* 2009, **21**:102–118.
51. Kittel B, Ruehl-Fehlert C, Morawietz G, Klapwijk J, Elwell MR, Lenz B, O'Sullivan MG, Roth DR, Wadsworth PF: **Revised guides for organ sampling and trimming in rats and mice—part 2. A joint publication of the RITA and NACAD groups.** *Exp Toxicol Pathol* 2004, **55**:413–431.
52. Morawietz G, Ruehl-Fehlert C, Kittel B, Bube A, Keane K, Halm S, Heuser A, Hellmann J: **Revised guides for organ sampling and trimming in rats and mice—part 3. A joint publication of the RITA and NACAD groups.** *Exp Toxicol Pathol* 2004, **55**:433–449.
53. Ruehl-Fehlert C, Kittel B, Morawietz G, Deslex P, Keenan C, Mahrt CR, Nolte T, Robinson M, Stuart BP, Deschl U: **Revised guides for organ sampling and trimming in rats and mice—part 1.** *Exp Toxicol Pathol* 2003, **55**:91–106.

doi:10.1186/s12989-014-0055-3

Cite this article as: Konduru et al.: Biokinetics and effects of barium sulfate nanoparticles. *Particle and Fibre Toxicology* 2014 **11**:55.

Submit your next manuscript to BioMed Central and take full advantage of:

- Convenient online submission
- Thorough peer review
- No space constraints or color figure charges
- Immediate publication on acceptance
- Inclusion in PubMed, CAS, Scopus and Google Scholar
- Research which is freely available for redistribution

Submit your manuscript at  
www.biomedcentral.com/submit

## 8. Inhalation exposure to cerium dioxide and barium sulfate nanoparticles for 1, 4, 13 and 52 weeks: Additional examinations

The here presented inhalation studies were approved by the local authorizing agency for animal experiments (Landesuntersuchungsamt Koblenz, Germany) as referenced by the approval number G12-3-028. Animals were housed in an AAALAC-accredited facility in accordance with the German Animal Welfare Act and the effective European Council Directive. Female Wistar rats [strain: Crl:WI(Han)] were obtained from Charles River Laboratories (Sulzfeld, Germany; for further details see paper 1 and 2).

### 8.1 One and 4 weeks of inhalation exposure to nano-CeO<sub>2</sub> and -BaSO<sub>4</sub>

The following chapter 8.1 complements the paper 1 and 2 concerning (histo-)pathology and immunohistochemistry after short-term exposure of 1 and 4 weeks to nano-CeO<sub>2</sub> and -BaSO<sub>4</sub>.

#### 8.1.1. Pathology

**Table 4 Overview of histopathological examinations**

Test substance	1 week		4 weeks	
	CeO <sub>2</sub> NM-211	CeO <sub>2</sub> NM-212	CeO <sub>2</sub> NM-212	BaSO <sub>4</sub>
Test concentrations [mg/m <sup>3</sup> ]	0.5 / 25	0.5 / 5 / 25	0.5 / 5 / 25	50
Days after exposure	Directly after last exposure and 3 weeks after exposure end		2 days and 4 weeks after exposure end	
Number of animals for each group	5		5	

In the studies with 1 and 4 weeks of exposure, necropsy and histopathology were performed after the last exposure and after an exposure free period of 3 or 4 weeks, respectively (table 4). Five animals per test group were investigated for pathological examination of the respiratory tract. Extrapulmonary organs were examined additionally (paper 1).

Materials and methods of the histopathological examination were described in paper 1 and 2. The histotechnical processing, examination by light microscopy and assessment of findings after 1 and 4 weeks of exposure were described in table 5 and 6. All the organs and tissues described in the OECD TG No. 412 were trimmed according to the Registry of Industrial Toxicology Animal-data (RITA) trimming guides for inhalation studies (Kittel *et al.* 2004).

### *Results and summary*

In the upper and lower respiratory tract, amber-like colored particles were observed freely or within macrophages in tissues of the trachea (figure 8-1), nasal cavity (figure 8-2) and larynx (figure 8-3), without any inflammatory response or morphological changes in the corresponding tissues after 1 and 4 weeks of exposure to CeO<sub>2</sub> NM-212 (see also paper 1). These findings have already been reported earlier: particles within the epithelium or in subepithelial tissue of larynx and nasal cavity were seen after a 21 day inhalation study to 9 and 45 mg/m<sup>3</sup> TiO<sub>2</sub> (MMAD 1.1 µm) and after a 1 week inhalation study to 88 mg/m<sup>3</sup> nano-TiO<sub>2</sub>, respectively (Eydner *et al.* 2012; Ma-Hock *et al.* 2009). In contrast to our studies, slight focal alterations of the epithelium at the base of the epiglottis of the larynx were observed together with the particles at aerosol concentrations of 50 mg/m<sup>3</sup> nano-TiO<sub>2</sub> (Ma-Hock *et al.* 2009).

In addition to the histopathology pictures in the papers, further histopathology pictures of nano-CeO<sub>2</sub> and -BaSO<sub>4</sub> exposed animals are presented in figure 8-4 for demonstration of inflammatory changes in lung tissue sections and 8-5, respectively.

Few CeO<sub>2</sub>- and BaSO<sub>4</sub>- particle-laden macrophages were also seen in pulmonary blood vessels, in the neighborhood of the bronchi (figure 8-6 and 8-7).

**Table 5 Scheme of histotechnical processing, examination by light microscopy and assessment of findings (1 week)**

Organs	1 week of exposure													
	Directly after exposure end							3 weeks after exposure end						
	Control	0.5 mg/m <sup>3</sup> CeO <sub>2</sub> NM-212	5 mg/m <sup>3</sup> CeO <sub>2</sub> NM-212	25 mg/m <sup>3</sup> CeO <sub>2</sub> NM-211	0.5 mg/m <sup>3</sup> CeO <sub>2</sub> NM-211	5 mg/m <sup>3</sup> CeO <sub>2</sub> NM-212	25 mg/m <sup>3</sup> CeO <sub>2</sub> NM-211	Control	0.5 mg/m <sup>3</sup> CeO <sub>2</sub> NM-212	5 mg/m <sup>3</sup> CeO <sub>2</sub> NM-212	25 mg/m <sup>3</sup> CeO <sub>2</sub> NM-212	0.5 mg/m <sup>3</sup> CeO <sub>2</sub> NM-211	5 mg/m <sup>3</sup> CeO <sub>2</sub> NM-211	25 mg/m <sup>3</sup> CeO <sub>2</sub> NM-211
1. All gross lesions	A2	A2	A2	A2	A2	A2	A2	A2	A2	A2	A2	A2	A2	A2
2. Larynx (3 levels) <sup>a</sup>	A1		A1				A1					A1		A1
3. Lungs (5 lobes)	A1,I1	A1,I1	A1,I1	A1,I1	A1,I1	A1,I1	A1,I1	A1,I1	A1,I1	A1,I1	A1,I1	A1,I1	A1,I1	A1,I1
4. Mediastinal lymph nodes	A1	A1	A1	A1	A1	A1	A1	A1	A1	A1	A1	A1	A1	A1
5. Nasal cavity (4 levels) <sup>b</sup>	A1		A1				A1					A1		A1
6. Pharynx	A1		A1				A1					A1		A1
7. Trachea <sup>c</sup>	A1		A1				A1					A1		A1
8. Tracheo-bronchial lymph nodes	A1	A1	A1	A1	A1	A1	A1	A1	A1	A1	A1	A1	A1	A1

Methods/Scope of examinations:

A = Hematoxylin-eosin stain

I = Immunohistology (BrdU)

1 = All animals/test group

2 = All animals affected/test group

<sup>a</sup> one level does include the base of the epiglottis, <sup>b</sup> one level will include nasopharyngeal duct; the 4 levels allow adequate examination of the squamous, transitional, respiratory and olfactory epithelium, and the draining lymphatic tissue (NALT), <sup>c</sup> one transverse section and one longitudinal section through the carina of the bifurcation of the extrapulmonary bronchi

**Table 6 Scheme of histotechnical processing, examination by light microscopy and assessment of findings (4 weeks)**

Organs	4 weeks of exposure					
	Control	2 days and 4 weeks after exposure end		25 mg/m <sup>3</sup>		50 mg/m <sup>3</sup>
		0.5 mg/m <sup>3</sup>	5 mg/m <sup>3</sup>	CeO <sub>2</sub>	CeO <sub>2</sub>	CeO <sub>2</sub>
1. All gross lesions	A2	A2	A2	A2	A2	A2
2. Larynx (3 levels) <sup>a</sup>	A1	B1	B1	A1	A1	A1
3. Liver	A1	B1	B1	A1	A1	A1
4. Lungs (5 lobes, right lobe only for I)	A1, I1	A1, I1	A1, I1	A1, I1	A1, I1	A1, I1
5. Lymph nodes (tracheobronchial and mediastinal lymph nodes)	A1	A1	A1	A1	A1	A1
6. Nose (nasal cavity/ 4 levels) <sup>b</sup>	A1	D1	C1	A1	A1	A1
7. Pharynx	A1	B1	B1	A1	A1	A1
8. Trachea (longitudinal, with carina) <sup>c</sup>	A1	B1	B1	A1	A1	A1

Methods/Scope of examinations:

A = Hematoxylin-eosin stain

B = Paraplast embedding

C = Nasal cavity level III and IV

D = Nasal cavity level III, only

I = Immunohistology (BrdU),

1 = All animals/test group

2 = All animals affected/test group

<sup>a</sup> one level does include the base of the epiglottis, <sup>b</sup> one level will include nasopharyngeal duct; the 4 levels allow adequate examination of the squamous, transitional, respiratory and olfactory epithelium, and the draining lymphatic tissue (NALT), <sup>c</sup> one transverse section and one longitudinal section through the carina of the bifurcation of the extrapulmonary bronchi

**Figure 8-1 Histopathological images of bifurcation of trachea after 4 weeks of exposure**  
A Control animal, B Animal exposed to 5 mg/m<sup>3</sup> CeO<sub>2</sub> (NM-212): Occurrence of particles (arrow), small image: higher magnification

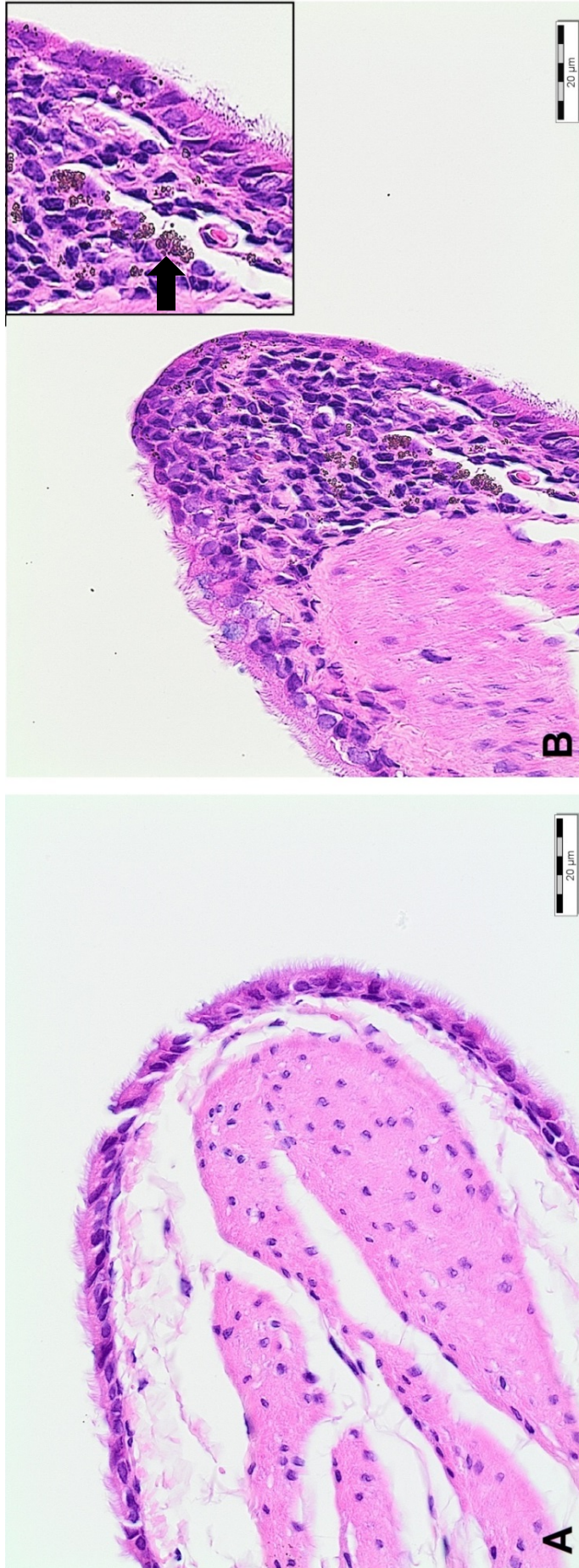


**Figure 8-2 Histopathological images of nasal cavity after 4 weeks of exposure**

**A** Control animal, **B** Animal exposed to 25 mg/m<sup>3</sup> CeO<sub>2</sub> (NM-212): Occurrence of particles (arrow), **C** Higher magnification of image B

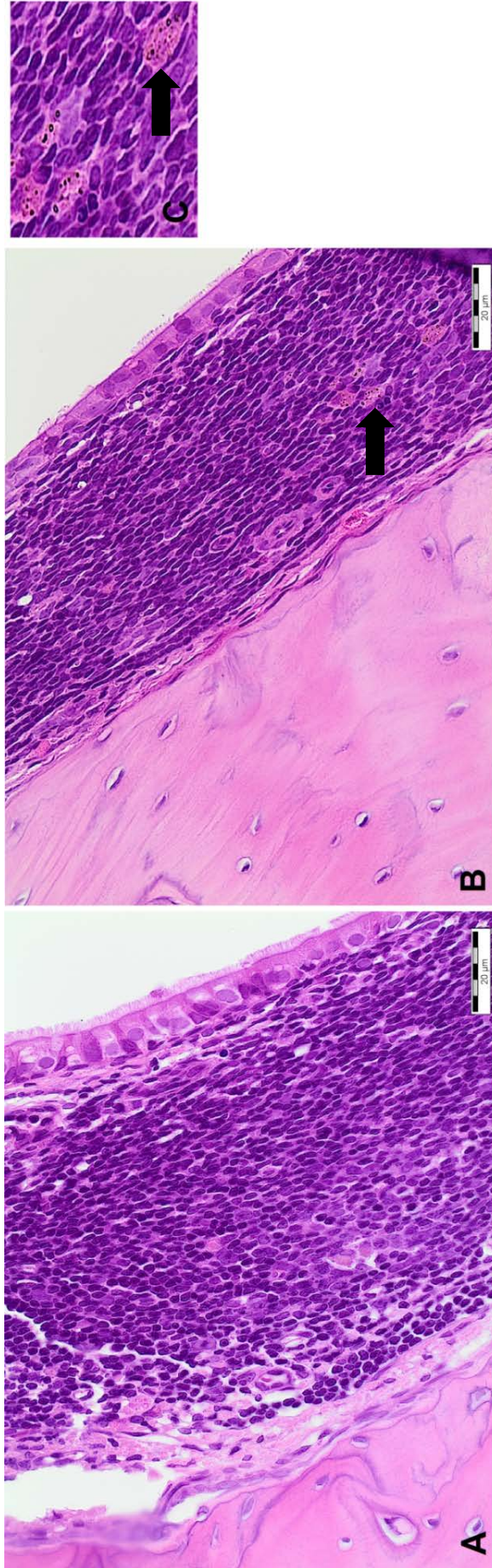


**Figure 8-3 Histopathological images of larynx after 4 weeks of exposure:**  
**A** Control animal, **B** Animal exposed to 25 mg/m<sup>3</sup> CeO<sub>2</sub> (NM-212):  
Occurrence of particles (arrows)

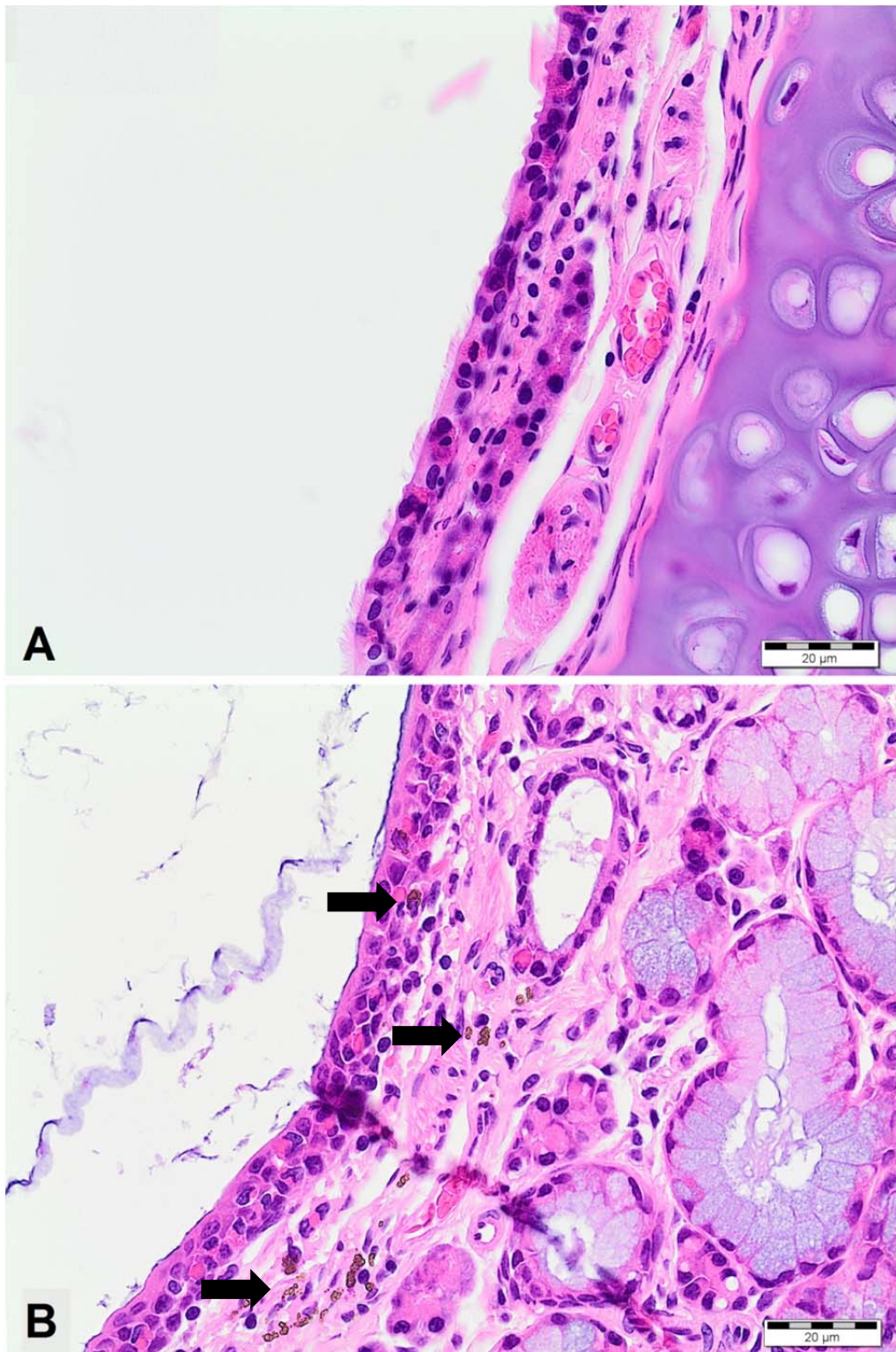


**Figure 8-4 Histopathological images of the lung after 4 weeks inhalation plus 4 weeks post-exposure: A** Control animal, **B-D** Animal exposed to 25 mg/m<sup>3</sup> CeO<sub>2</sub> (NM-212); **B-C** Alveolar histiocytosis with particles, **D** Granulomatous inflammation

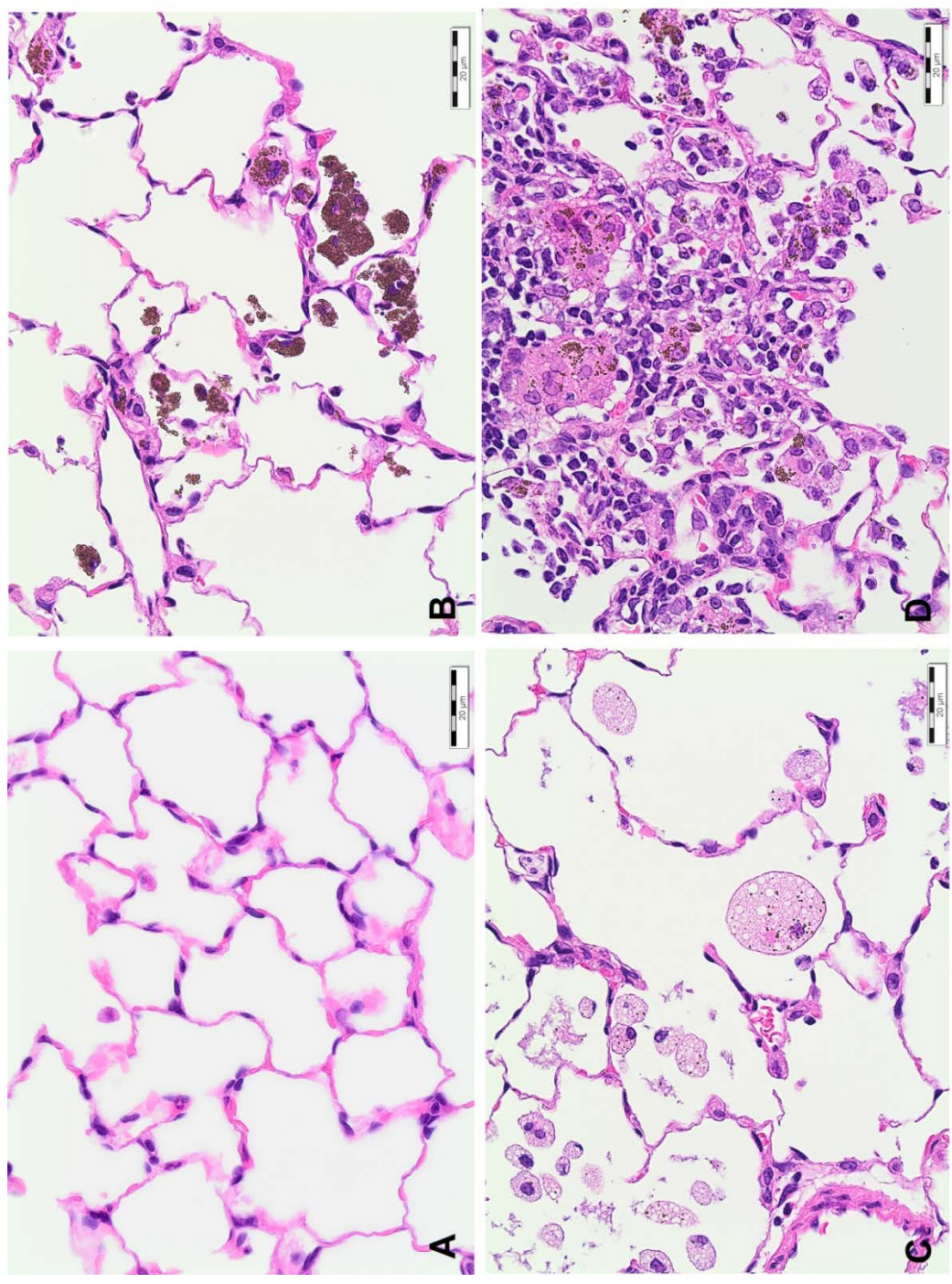


**Figure 8-5 Histopathological images of lungs after 4 weeks of inhalation exposure:**  
**A** Control animal and **B** Animal exposed to 50 mg/m<sup>3</sup> BaSO<sub>4</sub>

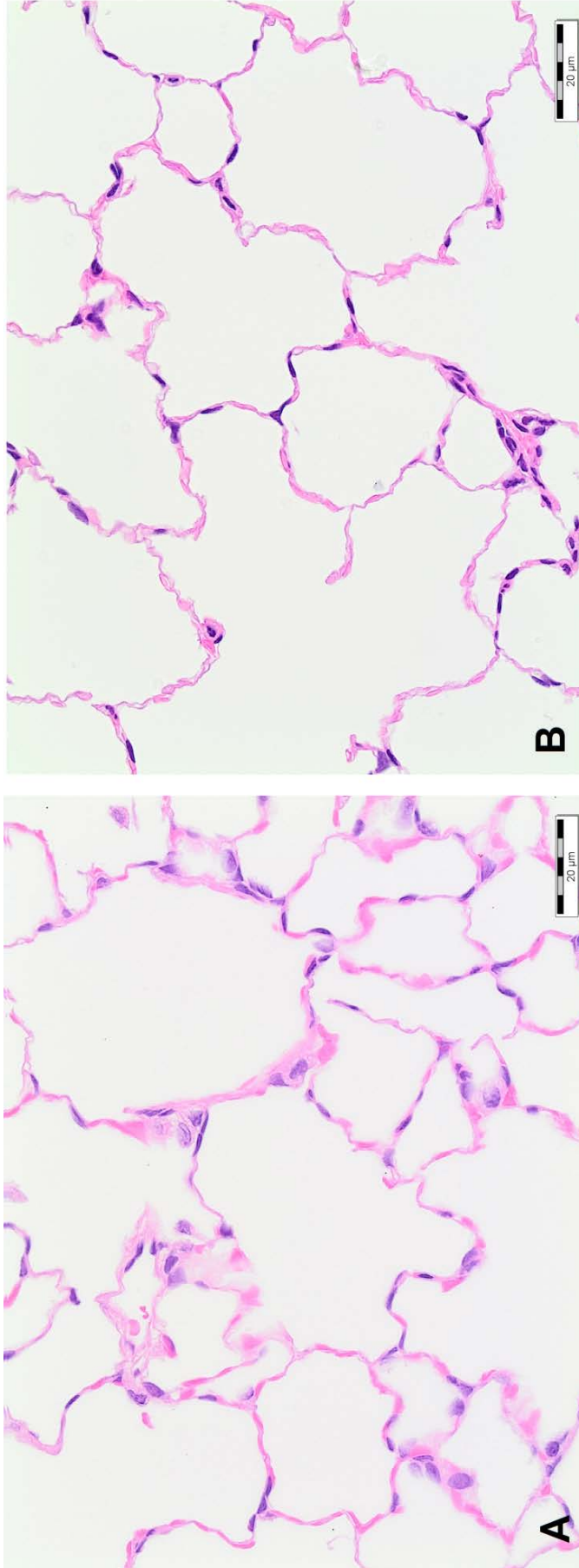


**Figure 8-6 Histopathological images of pulmonary blood vessels after 4 weeks of exposure: A and B** Animal exposed to 5 mg/m<sup>3</sup> CeO<sub>2</sub> (NM-212): Occurrence of macrophages with particles (arrows), small image with higher magnification

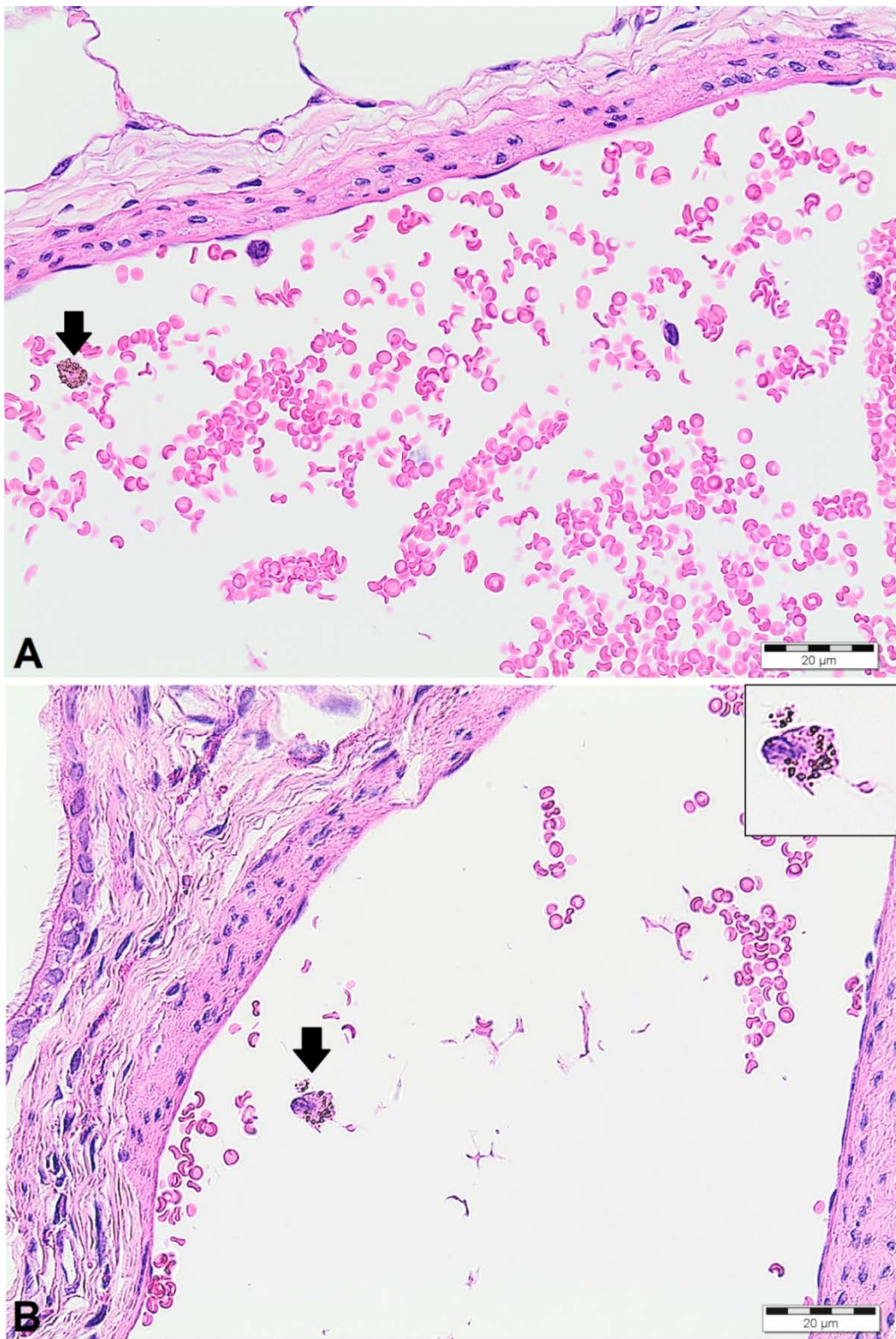
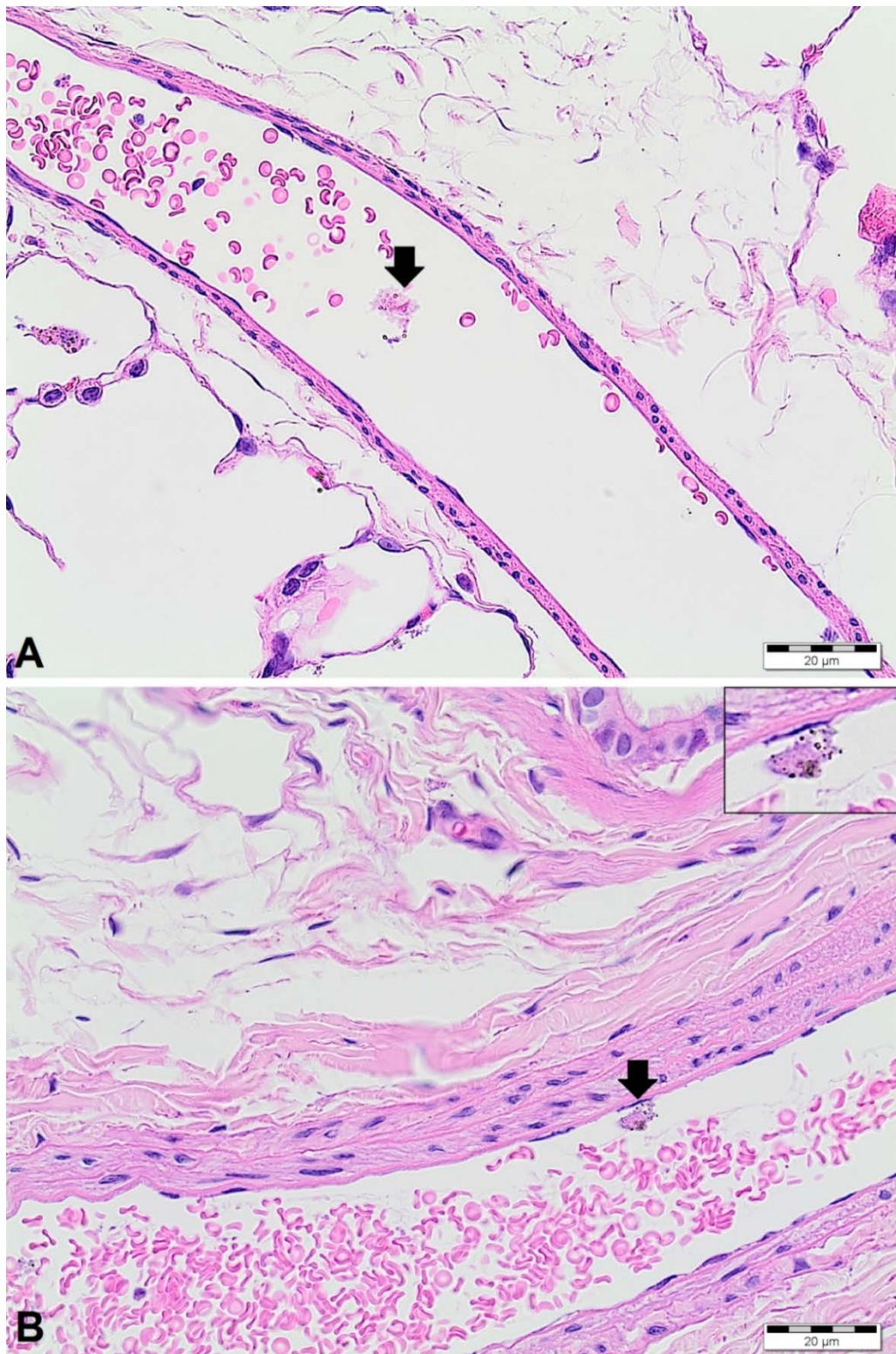


**Figure 8-7 Histopathological images of pulmonary blood vessels after 4 weeks of exposure: A and B** Animal exposed to 25 mg/m<sup>3</sup> CeO<sub>2</sub> (NM-212): Occurrence of macrophages with particles (arrows), smaller image with higher magnification



### **8.1.2. Immunohistology (cell proliferation, BrdU)**

#### *Material and Methods*

Cell proliferation was determined in large/medium bronchi, terminal bronchioli and alveoli (table 7).

For evaluation of cell proliferation in the lung, rats were subcutaneously implanted with Alzet (Alzet Corporation, Palo Alto, CA, USA) osmotic pumps (Model 2ML1) three days prior to necropsy. The pumps contained 20 mg/mL 5-bromo-2-deoxyuridine (BrdU, Sigma Chem.), a thymidine structural analog, which can be incorporated into DNA as a substitute for thymidine. Implantation was subcutaneously to the dorsal region under Isofluran anesthesia (Essex GmbH, Munich, Germany). In order to reduce pain during and after the implantation, the animals received a subcutaneous injection of an appropriate analgetic compound (Buprenorphine, 0.01 mg/kg body weight) 10 to 30 minutes prior to surgery.

Cell proliferation was determined after immunostaining of dewaxed sections and was performed with a mouse anti-BrdU antibody (BioGenex, Hamburg, Germany; see protocol below). The BrdU-staining identified cells passed through the S-phase of the cell cycle during the BrdU-labeling period. This enabled detection of DNA replication in proliferating cells. Dividing cells in a defined time period and area were related to non-dividing cells. At least 1000 cells per compartment and overall 3000 cells per lung were counted (see below). For the microscope, 400x and 100x magnification were used for counting type 1 cells (alveoli) and cells in the bronchioles, respectively. Numbers of dividing cells were expressed as Labeling Index (LI). The percentage of nuclei was counted which underwent replicative DNA synthesis (cells located in the S-phase of the cell cycle).

For the 1 week study, the left and accessory lung lobes of animals were used (one time point only). In the 4 week study, the right half lungs (three lobes) were examined in order to reduce the animal number per examination method. Two slides of each lung were prepared: one serving as test slides and the other as a negative control slide. Jejunum served as positive control for the BrdU stain.

Immunohistological staining:

Sections were dewaxed by Xylol (2x 5 min) and rehydrated with descending 100, 96, 70 % alcohol (2 x 5 min each). Afterwards sections were rinsed in deionized water. For antigen retrieval, samples were predigested with 0.05 % protease (2 min at 37° C) and hydrolysed with HCL (4N) for 20 min. After washing with deionized water, 6 % H<sub>2</sub>O<sub>2</sub> was added for 10 min. Samples were washed again and PBS buffer were added. To reduce the areas which were moistened by the antibody, the tissue were traced with a wax pencil (Pap-pen, BioGenex, USA). Then the primary monoclonal antibody (mouse anti-BrdU; dilution of 1:1200) was added for 2 h. After rinsing twice with PBS buffer, the secondary antibody (BioGenex, USA; link, anti-mouse, biotinilated; dilution of 1:20) were added for 20 min. After rinsing again, the HR-Peroxidase/Streptavidin enzyme complex (BioGenex, Germany) for labelling were added (20 min, 1:20). The secondary antibody system was used to visualize antibody binding.

Staining was developed with diaminobenzidine (DAB; Zytomed Systems GmbH, Germany) and the slides were counterstained with Mayer's hematoxylin (30 sec). For the negative control slides, PBS replaced the primary antibody.

Quantitative assessment:

Performing quantitative assessment, positively stained cells were identified by red/brown pigment over the nuclei. An image analysis system (KS 400, ZEISS, Germany) were used. Type 1 cells (alveoli) and cells in the bronchioles were discriminated from mesenchymal cell on the base of their shape and size. To facilitate comparability of counted cells, comparable lung compartments were selected for all animals. Labeling indices (percentage of nuclei counted undergoing replicative DNA synthesis) were determined for the lung compartments, the large/medium sized bronchi, the terminal bronchiole and the alveoli (pneumocytes type I cells). In each compartment a minimum of 1 000 cells were counted. For the alveoli, a minimum of 15 areas were used to count 1 000 cells. For the large/medium sized bronchi and the terminal bronchiole, cell counts were based on a previously defined line of epithelial cells including 1 000 cells.

The Labeling index (LI) in BrdU immunostained sections were calculated as follows:

$$\text{BrdU LI (\%)} = (\text{labeled cells}) / (\text{unlabeled cells} + \text{labeled cells}) \times 100$$

### *Results*

After 1 week of exposure to CeO<sub>2</sub> NM-212, increased cell proliferation rates were observed in the large/medium bronchi (5 and 25 mg/m<sup>3</sup>), terminal bronchioli (25 mg/m<sup>3</sup>) and alveoli (> 0.5 mg/m<sup>3</sup>) (table 7). After 4 weeks of exposure, increased cell proliferation rates were comparable as after 1 week of exposure, besides a higher increase in the terminal bronchioli at 25 mg/m<sup>3</sup> after 1 week. Two days after 4 weeks of exposure, increased cell proliferation rates were observed in the large/medium bronchi, terminal bronchioli and alveoli at aerosol concentrations of 25 mg/m<sup>3</sup> CeO<sub>2</sub> (NM-212). After 4 weeks plus 4 weeks post-exposure, cell proliferation rates were concentration-dependent increased in all three compartments. Higher proliferation rates of large/medium bronchi and terminal bronchiole were recorded after the post-exposure period than after exposure end whereas the proliferation rates of the alveoli were comparable for both time points.

BaSO<sub>4</sub> did not cause any increased cell proliferation rates (4 weeks of exposure) (table 7).

**Table 7 Effects on cell proliferation rates in the lung after 1 and 4 weeks of inhalation exposure to CeO<sub>2</sub> and BaSO<sub>4</sub>**

Aerosol concentration [mg/m <sup>3</sup> ]	1 week of exposure <sup>+</sup>										4 weeks of exposure <sup>++</sup>									
	Directly after last exposure					2 days after exposure end					4 weeks after the end of exposure									
	Control	0.5	5	25	0.5	25	0.5	5	25	0.5	5	25	0.5	5	25	0.5	5	25	50	
Large/medium bronchi	CeO <sub>2</sub>	1.59	1.95	2.58*	3.70*	1.42	2.05	2.05	0.66	1.64	3.29*	1.36	1.36	0.24	1.80**	2.87**	4.92**	0.65		
	NM-212	±0.76 (100)	±0.54 (123)	±0.60 (162)	±2.31 (181)	±0.55 (89)	±0.74 (129)	±0.74 (129)	±0.46 (46)	±0.74 (113)	±1.27 (228)	±0.64 (94)	±0.64 (94)	±0.20 (100)	±0.70 (750)	±1.09 (1196)	±1.77 (2050)	±0.42 (270)		
Terminal bronchioli	CeO <sub>2</sub>	1.67	1.92	1.96	9.83**	1.34	4.38**	1.69	1.08	1.94	3.30**	1.41	1.41	0.34	1.34*	3.90**	5.24**	0.44		
	NM-212	±0.75 (100)	±0.60 (115)	±0.77 (117)	±1.20 (589)	±0.53 (80)	±0.79 (262)	±0.94 (100)	±0.65 (64)	±0.50 (115)	±0.41 (195)	±0.43 (83)	±0.43 (83)	±0.23 (100)	±0.94 (394)	±1.29 (1147)	±1.95 (15410)	±0.27 (129)		
Alveoli	CeO <sub>2</sub>	2.22	3.80**	5.92**	5.76**	2.50	4.09**	3.02	2.29	4.45	6.84**	2.51	2.51	2.22	3.96**	4.62**	5.45**	2.22		
	NM-212	±0.44 (100)	±0.77 (171)	±0.64 (267)	±0.52 (258)	±0.16 (113)	±0.57 (184)	±1.68 (100)	±0.56 (76)	±0.83 (147)	±1.77 (226)	±0.55 (83)	±0.55 (83)	±0.31 (100)	±0.61 (178)	±0.51 (208)	±0.86 (250)	±0.48 (100)		

Results are presented as mean labelling indices ± standard deviation. Figures in parentheses show relative increases or decreases to the corresponding control levels; n=5. One sided Wilcoxon test was used: \*p < 0.05, \*\*p < 0.01;

<sup>+</sup>In the 1 week study, the left and accessory lung lobes were used (one time point), <sup>++</sup>In the 4 week study, the right half lungs (three lobes) were examined.

### 8.1.3. Statistical analysis

Clinical pathology parameters (BALF cytology, enzyme data and BALF and serum cell mediator data) were analyzed by non-parametric one-way analysis using the Kruskal-Wallis test (two-sided). If the resulting p value was equal or less than 0.05, a pair-wise comparison of each test group with the control group was performed using the Wilcoxon test or the Mann-Whitney U-test (both two-sided) ( $p \leq 0.05$  for statistical significance). Comparison of lung weights among test groups were performed by nonparametric one-way analysis using the two-sided Kruskal–Wallis test, followed by a two-sided Wilcoxon test for the hypothesis of equal medians in case of  $p \leq 0.05$ . The cell proliferation data was analyzed by a pairwise comparison of each dose group with the control group using the Wilcoxon test (one-sided,  $*p \leq 0.05$ ,  $**p \leq 0.01$ ).

## 8.2 Thirteen and 52 weeks of exposure within the long-term inhalation study

A part of the results obtained after 13 weeks of exposure to 50 mg/m<sup>3</sup> BaSO<sub>4</sub> was already presented in paper 2: Konduru, N., Keller, J. et al. "Biokinetics and effects of barium sulfate nanoparticles". All other results obtained after inhalation exposure of 13 and 52 weeks to CeO<sub>2</sub> and BaSO<sub>4</sub> are described in this chapter.

### 8.2.1. Aerosol characterization

The aerosols were generated by brush dust generators (Ma-Hock *et al.* 2007). The aerosols were analysed as described in the *Material and Methods* of paper 1 and 2. The particle concentrations and particle size distributions are summarized in table 8. The target concentrations were met and maintained well throughout the studies. Particle size distribution demonstrated that all particles were in the respirable range for rats. The particles were largely agglomerated.

**Table 8 Aerosol concentrations and particle size distributions after 52 weeks of exposure**

Test material	Targeted concentrations [mg/m <sup>3</sup> ]	Measured concentrations [mg/m <sup>3</sup> ] ± SD	MMAD [µm] / GSD
CeO <sub>2</sub> NM-212	0.1	0.1 ± 0.1	2.3 / 2.4
CeO <sub>2</sub> NM-212	0.3	0.3 ± 0.1	1.7 / 2.3
CeO <sub>2</sub> NM-212	1	1.0 ± 0.1	1.5 / 2.3
CeO <sub>2</sub> NM-212	3	3.0 ± 0.4	1.4 / 2.1
BaSO <sub>4</sub>	50	49.9 ± 5.6	2.0 / 2.0

Presented mean values of >14 measurements (MMAD, GSD); MMAD: mass median aerodynamic diameter, GSD: geometric standard deviation

### 8.2.2. Results: Lung and lymph node burdens

Directly after 13 and 52 weeks of exposure, the lavaged lungs, aliquots of lavage fluids and tracheobronchial and mediastinal lymph nodes of five animals per group were used to determine lung burden (as described in the *Material and Methods* of paper 2). The amounts of BaSO<sub>4</sub> in lungs and lymph nodes were estimated by measuring Ba with Inductively coupled plasma optical emission spectrometry (ICP-MS) and extrapolating to BaSO<sub>4</sub> (assuming that it was still particulate). The same method was applied to lung burdens of CeO<sub>2</sub>. During the exposure period, lung burdens increased with longer exposure duration (table 9). Only a slight translocation of the nanoparticles to the tracheobronchial and mediastinal lymph nodes was observed (0.5 and 1.9 % of the BaSO<sub>4</sub> and CeO<sub>2</sub> lung burden, respectively) (table 9).

**Table 9 Overview of organ burden analysis after 13 and 52 weeks of exposure to CeO<sub>2</sub> (NM-212) and BaSO<sub>4</sub>**

	13 weeks		52 weeks	
<b>Study days</b>	94		367	
<b>Time point</b>	One day after last exposure			
<b>Number of animals</b>	5		5	
<b>Examined organs</b>	Lung, tracheobronchial and mediastinal lymph nodes		Lung	
<b>Test material</b>	CeO <sub>2</sub> NM-212		BaSO <sub>4</sub> NM-212	
<b>Test Concentrations [mg/m<sup>3</sup>]</b>	0.1	3	50	3
<b>Lung burden [µg] ±SD</b>	11.96 ±2.82		42.07 ±11.05	
<b>Lung burden [mg] ±SD</b>	1.39 ±0.16		1.73 ±0.85	2.61 ±0.52
<b>Tracheobronchial lymph node burden [µg] ±SD</b>	ND	11.93 ±14.21	5.92 ±6.52	ND
<b>Mediastinal lymph node burden [µg] ±SD</b>	ND	13.78 ±15.85	2.27 ±3.38	ND

ND: not determined, SD: standard deviation, n=5; burden is mg or µg per lung; lavaged lungs and corresponding aliquots were used for determination of lung burden by ICP-MS.

### 8.2.3. Results: Bronchoalveolar lavage

Bronchoalveolar lavage fluids were assessed for 5 animals per group after 13 (paper 2: nano-BaSO<sub>4</sub> BALF results) and 52 weeks of exposure (table 10). The procedure and analysis of BALF is described in paper 1 and 2.

#### Exposure to nano-CeO<sub>2</sub>

After 13 weeks, exposure to 0.1, 0.3, 1 and 3 mg/m<sup>3</sup> CeO<sub>2</sub> induced a dose-dependent increase in neutrophil cell counts with a statistically significant increase in total cells (table 10). Lymphocytes and monocytes were significantly increased only at 3 mg/m<sup>3</sup>. Macrophage numbers and total cell counts were statistically significantly increased also at lower concentrations (0.1 and 0.3 mg/m<sup>3</sup>). The enzymes GGT, LDH and ALP were statistically significantly increased by aerosol concentrations of 1 mg/m<sup>3</sup> and above. Total protein and NAG were increased only at 3 mg/m<sup>3</sup>. Cell mediators (MCP-1, CINC-1 and Osteopontin) were statistically significant increased at 1 mg/m<sup>3</sup> and above.

After 52 weeks of exposure to aerosol concentrations of 0.3 mg/m<sup>3</sup> CeO<sub>2</sub> and above, neutrophils and lymphocytes were more elevated than after 13 weeks, but total cell counts were only increased at 3 mg/m<sup>3</sup>. Exposure of 0.1 mg/m<sup>3</sup> CeO<sub>2</sub> caused no changes in BALF cell numbers. Total protein and the enzyme LDH were significantly increased at 1 and 3 mg/m<sup>3</sup>. ALP and NAG levels were not affected at any aerosol concentration whereas GGT were significantly increased at all concentrations. MCP-1 and CINC-1 levels were still elevated but to a lower extent compared with 13 weeks of exposure.

#### Exposure to nano-BaSO<sub>4</sub>

After 13 weeks of 50 mg/m<sup>3</sup> nano-BaSO<sub>4</sub> exposure, neutrophil and total cell numbers were significantly increased (table 10). The enzyme ALP and the cell mediators MCP-1 and CINC-1 were elevated as well.

After 52 weeks of exposure, neutrophil and total cells were even more increased than after 13 weeks. Additionally, monocyte and lymphocytes levels were elevated. The levels of ALP were elevated after 13 weeks of exposure but declined to near control levels after 52 weeks whereas all other enzymes were significantly increased. With the exception of MCS-F, all other cell mediators were more elevated after 52 weeks of exposure than after 13 weeks.

#### Comparison of exposure to nano-CeO<sub>2</sub> and -BaSO<sub>4</sub>

After 13 weeks of exposure, 3 mg/m<sup>3</sup> nano-CeO<sub>2</sub> elicited higher increases in (pro-)inflammatory parameters (neutrophils, lymphocytes, total cells, MCP-1, NAG) than 50 mg/m<sup>3</sup> BaSO<sub>4</sub>. However, this reversed after 52 weeks of exposure where nearly all other parameters (neutrophil, lymphocytes, total protein and enzymes) were more increased at 50 mg/m<sup>3</sup> BaSO<sub>4</sub> compared to 3 mg/m<sup>3</sup> CeO<sub>2</sub>.

A comparison of neutrophil numbers in BAL fluid (x-fold of concurrent control) after 1, 4, 13 and 52 weeks of exposure to nano- CeO<sub>2</sub> and - BaSO<sub>4</sub> is presented in figure 8-8.

**Figure 8-8 Neutrophil numbers in BAL fluid (x-fold of concurrent control)** after **A** 1 and 4 weeks of exposure, **B** 13 and 52 weeks of exposure to CeO<sub>2</sub> (NM-212) and BaSO<sub>4</sub>. Mean absolute values with standard deviation of BALF neutrophils are presented in table 10.

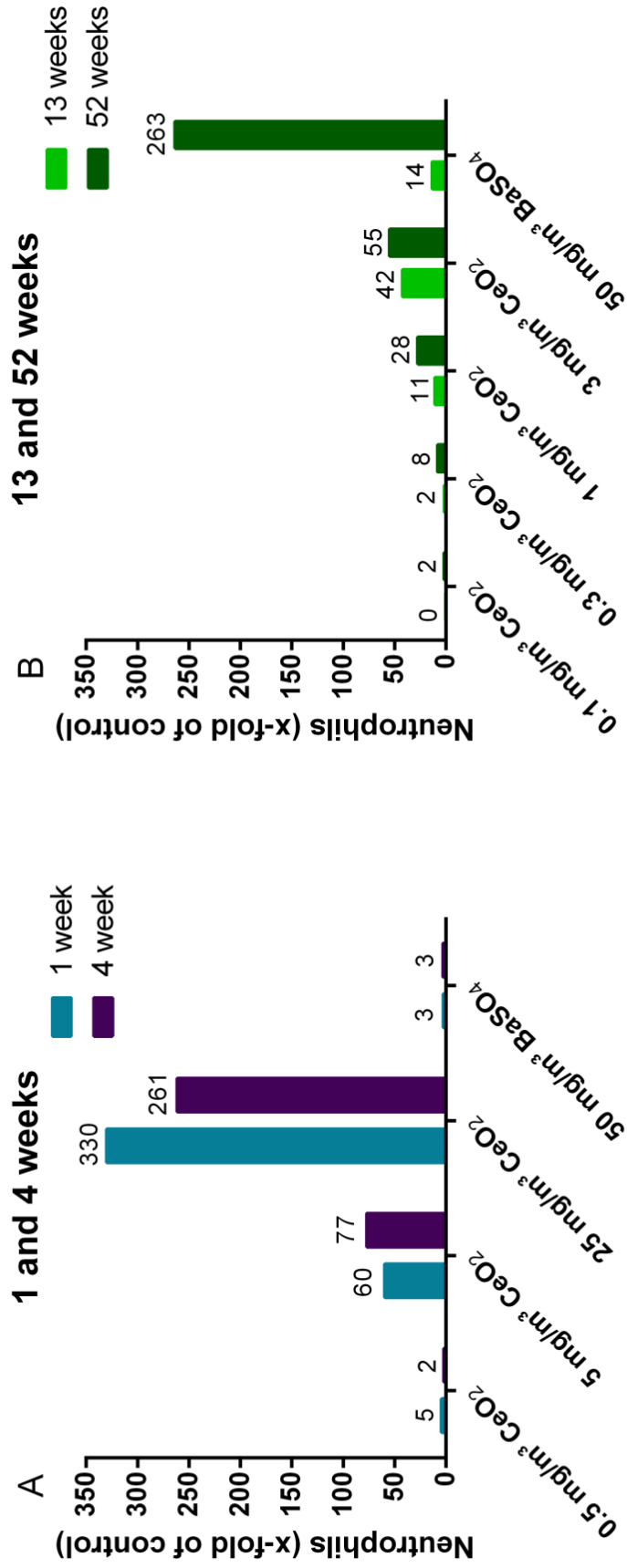


**Table 10 Bronchoalveolar lavage fluid analysis after 13 and 52 weeks of exposure to CeO<sub>2</sub> and BaSO<sub>4</sub>**

Test material		CeO <sub>2</sub> NM-212					BaSO <sub>4</sub>	
		Control	0.1	0.3	1	3	50	
Mean values ± SD								
Total cells (counts/μL)								
13 weeks	66.3±22.04	115.22**±23.72	98.70*±30.49	117.51*±43.99	163.33**±57.29	96.08*±16.89		
52 weeks	54.27±20.27	59.95±26.52	60.97±20.18	68.56±28.69	96.06*±29.29	222.73*±95.18		
Neutrophils (counts/μL)								
13 weeks	1.71±0.66	0.53±0.58	2.85±3.45	18.56**±11.68	72.59**±54.65	23.46*±20.06		
52 weeks	0.58±0.69	1.05±0.99	4.82**±3.94	16.07**±5.17	31.97**±14.23	152.75**±74.45		
Lymphocytes (counts/μL)								
13 weeks	0.55±0.42	0.27±0.26	0.38±0.63	2.21±2.23	5.43**±3.52	1.84±1.89		
52 weeks	0.56±0.36	1.30±1.12	9.79*±18.06	6.69**±2.16	9.72**±5.97	14.35**±4.25		
Macrophages (counts/μL)								
13 weeks	63.99±22.36	114.37**±24.06	95.43*±27.12	96.30±46.85	83.52±15.72	70.37±23.68		
52 weeks	53.01±19.77	57.49±25.85	46.10±12.59	45.33±26.17	53.57±12.31	53.54±37.05		
Monocytes (counts/μL)								
13 weeks	0.00±0.00	0.00±0.00	0.00±0.00	0.13±0.30	0.94**±0.67	0.10±0.13		
52 weeks	0.04±0.06	0.04±0.06	0.16±0.18	0.29*±0.24	0.43*±0.40	1.14*±1.73		
Eosinophils (counts/μL)								
13 weeks	0.04±0.08	0.00±0.00	0.04±0.08	0.13±0.20	0.25±0.39	0.06±0.13		
52 weeks	0.00±0.00	0.00±0.00	0.00±0.00	0.00±0.00	0.05±0.10	0.06±0.13		

\* statistically significant, p < 0.05; \*\* statistically significant, p < 0.01; n=5; mean values and standard deviation (SD); lungs were lavaged one day after last exposure.

**Continuation of Table 10 Bronchoalveolar lavage fluid analysis after 13 and 52 weeks of exposure to CeO<sub>2</sub> and BaSO<sub>4</sub>**

Test material		CeO <sub>2</sub> NM-212					BaSO <sub>4</sub>
		Control	0.1	0.3	1	3	
Total protein (mg/L)							
13 weeks	52 ±10	57±9	60±23	60±18	84*±26	64 ±13	
52 weeks	31±8	33±12	67±73	61**±11	73**±28	135**±72	
GGT (nkat/L)							
13 weeks	41±7	40±5	53±13	80**±18	106**±26	41 ±7	
52 weeks	26±4	37**±6	38*±9	70**±23	65**±14	126**±66	
LDH (µkat/L)							
13 weeks	0.38±0.06	0.43±0.03	0.52±0.16	0.61**±0.18	0.95**±0.33	0.53±0.17	
52 weeks	0.35±0.04	0.37±0.08	0.44±0.13	0.66**±0.14	0.80**±0.19	1.67**±0.69	
ALP (µkat/L)							
13 weeks	0.51±0.10	0.45±0.06	0.58±0.09	0.73*±0.17	0.84**±0.19	0.87**±0.21	
52 weeks	0.44±0.12	0.54±0.10	0.48±0.13	0.58±0.19	0.50±0.06	0.60±0.21	
NAG (nkat/L)							
13 weeks	35±7	35±5	37±13	43±9	51**±8	41±14	
52 weeks	37±7	42±14	38±8	47±9	47±12	73**±30	
MCP-1 (pg/mL)							
13 weeks	24.2±8.4	19.1±7.5	30.8±26.4	111.4**±100.1	620**±613.5	176.7** ±126.1	
52 weeks	15.3±8.2	17.9±7.1	49.3*±37.6	169.4**±113.9	378.2**±245.5	2300.7**±1463.1	
CINC-1/IL-8 (pg/mL)							
13 weeks	93.7±18.7	60.6±38.9	77.7±38.9	172.3*±100.7	280.6*±190.8	223.8*±125.7	
52 weeks	82.4±25.4	68.8±37.1	69.7±26.5	132.9*±49.1	180.6*±114.8	514.2*±333.6	
M-CSF (pg/mL)							
13 weeks	14±0	14±0	14±0	14±0	14±0	14±0	
52 weeks	21±12	18±3	18±4	27±12	25±15	31±16	
Osteopontin (pg/mL)							
13 weeks	49.02±40.86	37.40±32.69	118.49±133.12	136.87*±72.89	300.41*±253.01	234.02±240.06	
52 weeks	162.79±98.61	166.71±187.14	135.32±61.53	175.72±88.75	228.80±217.96	1092.70**±607.68	

\* statistically significant, p < 0.05; \*\* statistically significant, p < 0.01; n=5; mean values and standard deviation (SD); lungs were lavaged one day after last exposure.

#### 8.2.4. Results: Hematology and acute phase proteins in blood

Hematology, clinical chemistry and acute phase proteins were measured in the blood of 5 animals per group (see detailed procedure in paper 1).

In blood, a slight increase of neutrophil counts was observed for CeO<sub>2</sub> NM-212 after 1 week (5 days) of exposure to 25 mg/m<sup>3</sup> (see paper 1). Exposure of 4 weeks to CeO<sub>2</sub> NM-212 and BaSO<sub>4</sub> elicited no increase of neutrophil counts (table 11 and 12).

Thirteen and 52 weeks of inhalation exposure to nano-CeO<sub>2</sub> did not affect hematology and clinical chemistry parameters in blood at any tested concentration apart from increased haptoglobin (HAPT) and  $\alpha$ 2-macroglobulin (A2M) levels in serum after 52 weeks of exposure to 3 mg/m<sup>3</sup> CeO<sub>2</sub> (table 11). A dose-dependent increase was observed for A2M after 52 weeks of exposure using the median values rather than the means (median values of 10.94 and 11.64 for 1 and 3 mg/m<sup>3</sup>, respectively). After 13 weeks, the acute phase protein A2M was only significantly increased at 1 mg/m<sup>3</sup>, but had returned to near control values by 52 weeks. The change was not dose-dependent and regarded as incidental.

Nano-BaSO<sub>4</sub> inhalation exposure showed no changes in hematology and clinical chemistry parameters in blood apart from a slight increase in (absolute and relative) neutrophil numbers and a not statistically significant elevation in HAPT and A2M levels after 52 weeks of exposure (table 11).

A summary of neutrophil levels in BALF (x-fold of control) and of neutrophil levels and acute phase proteins in blood (x-fold of control) after 4, 13 and 52 weeks of exposure to CeO<sub>2</sub> and BaSO<sub>4</sub> is presented in table 12.

**Table 11 Mean neutrophil levels and acute phase proteins in blood after 13 and 52 weeks of exposure to CeO<sub>2</sub> and BaSO<sub>4</sub>**

Test material	CeO <sub>2</sub>					BaSO <sub>4</sub>
	Control	0.1	0.3	1	3	
<b>Test Concentrations [mg/m<sup>3</sup>]</b>						<b>50</b>
Mean values ± SD						
Neutrophils (giga/L)						
13 weeks	0.63±0.25	0.95±0.16	0.78±0.10	0.93±0.30	1.09±0.35	0.76±0.06
52 weeks	0.67±0.17	0.79±0.19	0.70±0.17	1.02±0.20	0.97±0.29	1.23*±0.61
Neutrophils (%)						
13 weeks	15.2±4.60	23.4±4.3	19.8±5.0	22.4±7.6	25.4±9.8	20.7±1.8
52 weeks	26.7±5.80	33.8±5.8	28.1±4.5	32.6±7.1	32.3±4.8	38.5*±9.6
Acute phase proteins (µg/mL)						
HAPT						
13 weeks	204.00±47.01	223.60±67.11	228.60±55.86	192.20±51.45	229.20±58.14	239.00±56.14
52 weeks	139.60±74.26	215.40±54.45	184.20±73.96	173.60±37.35	251.40*±63.06	295.8*±113.17
A2M						
13 weeks	14.55±5.90	18.18±4.22	20.69±4.55	22.66*±7.06	19.65±4.45	21.63±8.33
52 weeks	8.86±2.14	9.52±2.17	9.88±4.48	12.39±3.98	12.19*±1.61	14.44±9.63

\* statistically significant, p < 0.05; \*\* statistically significant, p < 0.01; n=5; SD: standard deviation, HAPT: haptoglobin, A2M: α2-macroglobulin; blood were collected directly after 13 weeks of exposure and one day after 52 weeks of exposure.

**Table 12 Neutrophil levels in BAL and neutrophil levels and acute phase proteins in blood after 4, 13 and 52 weeks of exposure to CeO<sub>2</sub> and BaSO<sub>4</sub>**

<b>CeO<sub>2</sub> (NM-212)</b>			
<b>Study</b>	<b>4 weeks</b>	<b>13 weeks</b>	<b>52 weeks</b>
<b>Aerosol concentration [mg/m<sup>3</sup>]</b>	25	3	3
<b>Lung burden [mg]</b>	2.6	1.4	2.6
<b>Neutrophil BAL [x-fold of control]</b>	<b>262**</b>	<b>43**</b>	<b>55**</b>
<b>Neutrophil blood [x-fold of control]</b>	1.0	2.0	1.0
<b>Haptoglobin [x-fold of control]</b>	1.0	1.0	<b>2.0*</b>
<b>A2M [x-fold of control]</b>	1.0	1.0	<b>1.0*</b>
<b>50 mg/m<sup>3</sup> BaSO<sub>4</sub></b>			
<b>Study</b>	<b>4 weeks</b>	<b>13 weeks</b>	<b>52 weeks</b>
<b>Lung burden [mg]</b>	0.8	1.7	10.2
<b>Neutrophil BAL [x-fold of control]</b>	3.0	<b>14.0*</b>	<b>263.0**</b>
<b>Neutrophil blood [x-fold of control]</b>	1.0	1.0	<b>2.0*</b>
<b>Haptoglobin [x-fold of control]</b>	1.0	1.0	<b>2.0*</b>
<b>A2M [x-fold of control]</b>	1.0** (0.6)	1.0	2.0

Values of neutrophils and acute phase proteins are rounded to the first decimal place.

### 8.3. Summary of relevant results after 1, 4, 13 and 52 weeks of exposure to nano-CeO<sub>2</sub> (NM-212)

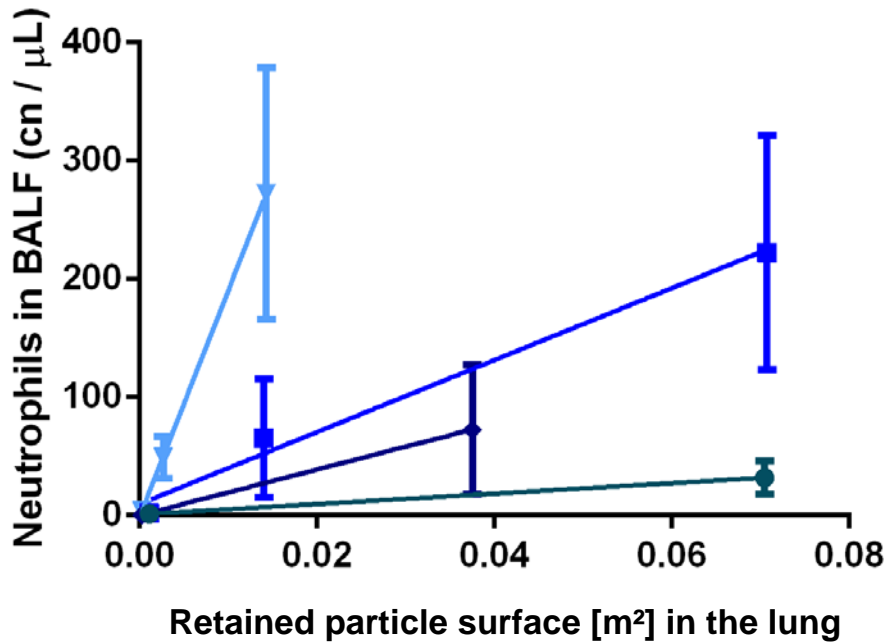
To compare total lung burden (based on mass or particle surface area) and dose rate, neutrophils in BALF and absolute lung weights after 1, 4, 13 and 52 weeks of exposure to CeO<sub>2</sub> NM-212 were put into relation to the lung burden or lung burden per exposure time (table 13 and figure 8-9). Retained particle surface area was calculated based on the surface area derived from Brunauer-Emmet-Teller (BET) measurements (see paper 1 and 2, physico-chemical characterization).

**Table 13: Inhalation exposure to nano-CeO<sub>2</sub> (NM-212): Correlation between dose-rate and associated response using mass lung burden and retained particle surface area in the lung as dose metrics**

Study/ Exposure days	Aerosol concentration [mg/m <sup>3</sup> ]	Lung burden [µg] ±SD	Retained particle surface area [m <sup>2</sup> ]	Dose rate [µg/day]	Neutrophil BAL [cn/µL] ±SD	Neutrophil		Absolute lung weight [g] ±SD	Absolute lung weight [%]*
						BAL	[x-fold of control]		
1 week/ 5	0.5	11±1.0	0.00027	2.2	3.70±2.53	5		0.89±0.2	96
	5	100±9.0	0.0027	20	49.19±17.68	60		0.91±0.05	98
4 weeks/ 20	25	530±120	0.01431	106	272.30±106.62	330		1.048±0.1	113
	0.5	41±7	0.00108	2.05	1.75±1.13	2		1.01±0.13	102
13 weeks/ 67	5	520±60	0.01404	26	65.66±50.23	77		1.11**±0.07	113
	25	2620±290	0.07074	131	222.29±99.25	262		1.28**±0.15	130
52 weeks/ 253	0.1	11.96±2.82	0.000297	0.18	0.53±0.58	0.3		1.53±0.13	103
	3	1390±0.16	0.03753	20.75	72.59±54.65	43		1.57±0.18	106
	0.1	42.07±11.05	0.001134	0.17	1.05±0.99	2		1.88±0.12	108
	3	2610±0.52	0.0702	10.32	31.97±14.23	55		1.96±0.15	113

\*compared to the control group (set to 100%); Wilcoxon (two-sided): \*p ≤ 0.05, \*\*p ≤ 0.01; absolute lung weights: n=5 (1 week) and n=10 (4 weeks)

**Figure 8-9 Neutrophil counts in BALF correlated with retained particle surface in the lung** after 1, 4, 13 and 52 weeks of exposure to CeO<sub>2</sub> NM-212 using the aerosol concentrations of 0.5, 5, and 25 mg/m<sup>3</sup> (1 and 4 weeks) and 0.1 and 3 mg/m<sup>3</sup> (13 and 52 weeks) CeO<sub>2</sub> NM-212 for each point



- ▲— 1 week CeO<sub>2</sub> NM-212
- 4 weeks CeO<sub>2</sub> NM-212
- ◆— 13 weeks CeO<sub>2</sub> NM-212
- 52 weeks CeO<sub>2</sub> NM-212

## 9. Discussion

In this body of work, biokinetics and toxicity of inhaled cerium dioxide and barium sulfate nanoparticles were examined after 1, 4, 13 and 52 weeks of exposure. The following sections discuss the results on biokinetics and effects of nano-CeO<sub>2</sub> (9.1) and -BaSO<sub>4</sub> (9.2) in the lung and systemic effects of both nanoparticles (9.3).

### 9.1 Biokinetics and effects of CeO<sub>2</sub> in the lung

Before starting the inhalation exposure, the tested nano-CeO<sub>2</sub> was studied in cell-free *in vitro* solubility assays as reported previously (Molina *et al.* 2014). In these assays, CeO<sub>2</sub> (NM-212) demonstrated a very low solubility in fluids simulating different compartments of the body (e.g. below 0.001 wt% in phagolysosomal simulant fluid (PSF), 0.02 wt% in 0.1 N HCl) and recrystallized in PSF, a model of macrophage dissolution and clearance of particles. However, nano-CeO<sub>2</sub> is not completely insoluble and is able to release cerium ions (Schwabe *et al.* 2014; Yokel *et al.* 2014a; Yokel *et al.* 2014b). This process is highly dependent on the particle size and composition of the surrounding medium. This was valid at a pH below 4.6 and even at a pH of 8 in the presence of chelating agents. In the environment, the following four steps seem to be involved in chemical transformation of nano-CeO<sub>2</sub>: dissolution of Ce in the (3+) oxidation state, reduction of Ce<sup>4+</sup> to Ce<sup>3+</sup> in acidic media and release of Ce<sup>3+</sup>, complexation with chelating agents and precipitation on the surface (Kakuwa & Matsumoto 2006, Schwabe *et al.* 2014). These pathways may also play a role *in vivo*.

Consistently to the *in vitro* dissolution assays, inhaled CeO<sub>2</sub> showed high biopersistence in the lungs and a low bioavailability in the presented inhalation studies. Intratracheal instillation of the same, but neutron activated <sup>141</sup>CeO<sub>2</sub> (dose of around 250 µg per lung) showed prolonged lung retention and a slow clearance with an estimated half-time of 140 days (Molina *et al.* 2014). In our short-term study with 1 week (5 days) of exposure, lung burdens were about one-fourth of those after 4 weeks of exposure. In the short-term study with 4 weeks of exposure, inhaled CeO<sub>2</sub> was deposited in the lungs and cleared with a retention half-time of 40 days at aerosol concentrations of 0.5 mg/m<sup>3</sup> (lung burden of 0.041±0.007 mg/lung decreased to 0.009±0.004 mg 129 days post-exposure). At higher aerosol concentrations of 25 mg/m<sup>3</sup>, the clearance was retarded with a retention half-life above 200 days (lung burden of 2.62±0.20 mg/lung decreased to 1.8±0.26 mg 129 days post-exposure). Retardation of clearance was already observed at aerosol concentrations of 5 mg/m<sup>3</sup> since the lung burdens stayed nearly constant during 4 weeks of post-exposure (lung burden of around 0.5 mg/lung). In the long-term study, the lung burden of CeO<sub>2</sub> after 13 weeks was nearly doubled after 52 weeks of exposure at aerosol concentrations of 0.1 and 3 mg/m<sup>3</sup>. However, no information on time course of lung retention and clearance kinetics has been available during post-exposure in the long-term study so far.

Lymph node burdens after short-term exposure were higher than after long-term exposure. In general, lymph node burdens were low (below 14 and 2 % of the initial lung burden after 4 and 13 weeks, respectively) indicating that, at least at this lung burden range, it plays no major role for particle clearance.

In the lung, inflammation was associated with retardation of pulmonary clearance in the short-term studies. In the long-term study, local inflammation in the lung was observed by increases in BAL neutrophils, lymphocytes and monocytes after 13 weeks of exposure. BAL changes (cell counts, enzyme activities, total protein and cell mediator levels) after 52 weeks of exposure to 3 mg/m<sup>3</sup> CeO<sub>2</sub> were comparable to those after 13 weeks. Minor changes in BAL were observed at lower aerosol concentrations of 1 mg/m<sup>3</sup>. Exposure to 0.3 mg/m<sup>3</sup> elicited no BAL changes after 13 weeks and only minor changes after 52 weeks (neutrophils, GGT, MCP-1). In animals exposed to lower aerosol concentrations rather than in those exposed to higher, BAL lymphocytes were higher increased than neutrophils after 52 weeks of exposure indicating a later phase of inflammation.

The strongest increase in BAL neutrophils indicating pulmonary inflammation was observed after 1 week of exposure. The increase in BAL neutrophils appeared to be attenuated after 4 and 13 weeks of exposure. One week of exposure to 25 mg/m<sup>3</sup> CeO<sub>2</sub> caused a lung burden of 0.5 mg and elicited a 330-fold increase of BAL neutrophils whereas a lung burden of 2.6 mg was observed after 4 and 52 weeks of exposure to 25 and 3 mg/m<sup>3</sup> CeO<sub>2</sub>, respectively. This burden caused 262-fold and 55-fold increases in BALF neutrophils, respectively (figure 8-8 and table 13). The dose-rate at 3 mg/m<sup>3</sup> for 52 weeks (10.3 µg/day) is 13 times lower than that of 4 weeks exposure to 25 mg/m<sup>3</sup> (131 µg/day). The initial pulmonary inflammation after 1 week of exposure correlates with the dose rate rather than with the lung burden (see paper 1, conclusion).

For CeO<sub>2</sub>, the particle surface area was the dose metrics correlating best with pulmonary inflammation based on BAL neutrophils. This was shown by dose-response curves using different dose-metrics (surface area, mass, volume) for the two tested CeO<sub>2</sub> (NM-211 and NM-212) in the 1 week study (see paper 1, figure 7). To compare total lung burden and dose rate, neutrophils in BALF after 1, 4, 13 and 52 weeks of exposure to CeO<sub>2</sub> NM-212 were put into relation to the lung burden or lung burden per exposure time (table 13 and figure 8-9). The dose rate was linearly correlated with the observed lung effects at all exposure times and aerosol concentrations. The neutrophil response observed in BALF was obviously driven by the dose rate of particle surface entering the lung. Dose rate did not obviously correlate with other lung response parameters (absolute lung weight) (table 13). The increase of absolute lung weights after 1 and 4 weeks of exposure was rather affected by the exposure duration than by dose rate.

After exposure to 5 and 25 mg/m<sup>3</sup> CeO<sub>2</sub>, the initial pulmonary inflammation based on BAL neutrophils was supplemented and dominated by mononuclear cells, especially macrophages. In the 4 week study, alveolar histiocytosis progressed towards a granulomatous inflammation after 4 weeks plus 4 weeks post-exposure at aerosol concentrations of 5 and 25 mg/m<sup>3</sup>. The later inflammatory phase was only detectable by histopathology. The progression of the later reaction towards a granulomatous type

was clearly driven by the continuous presence of the particles in the lung. Histopathology after 13 and 52 weeks of exposure was not part of this body of work.

Despite the differences in the early and later phase of the reaction (neutrophil vs. macrophage; dose-rate vs dose), the observations made in the short-term studies have relevance for the longer exposure. At lung burdens of 2.6 mg after 4 and 52 weeks of exposure and an increasing duration of particle presence in the lung, biological responses in the lung (e.g. granulomatous inflammation) may show a further progression after 52 weeks. However, the further development of the granulomatous inflammation and the occurrence of possible morphological changes will be studied in another project within the long-term study.

Besides pulmonary inflammation, increased epithelial cell proliferation in the lung may be an indicator for potential lung tumor formation (ECETOC 2013; ILSI Risk Science Institute Workshop Participants 2000). For assessment of cell proliferation in paraffin-embedded tissue sections, 5-bromodeoxyuridine (BrdU) immunohistochemistry is the method of choice (Muskhelishvili *et al.* 2003). In our short-term studies, statistically significant increased proliferation rates of epithelial cells, especially in the terminal bronchioli and alveoli, were shown after 1 and 4 weeks of exposure (table 7). At lung burdens of around 0.5 mg after 1 week of exposure, cell proliferation rates of inhaled CeO<sub>2</sub> (aerosol concentration of 25 mg/m<sup>3</sup>) were comparable or slightly higher than those of nano-TiO<sub>2</sub> (10 mg/m<sup>3</sup>) although the deposited particle surface per lung was 2 times lower for CeO<sub>2</sub> (0.014 m<sup>2</sup>) than for TiO<sub>2</sub> (0.028 m<sup>2</sup>) (Ma-Hock *et al.* 2009). At lung burdens of around 0.5 mg after 4 week of exposure, inhaled CeO<sub>2</sub> (5 mg/m<sup>3</sup>) elicited a slightly lower proliferation rate than after 1 week of exposure (25 mg/m<sup>3</sup>). The increased response after shorter exposure may be explained by the higher dose-rate after 1 week than after 4 weeks of exposure. The age of the animals may have a further impact since younger animals may show higher cell turnover rates than older due to ongoing organ development and growth. In our short-term studies, epithelial cells of the alveoli and terminal bronchioli proliferated stronger than those of the large/medium bronchi, especially in the test groups exposed to CeO<sub>2</sub>. This may be explained by higher particle deposition and particle-cell interaction in these areas since most of the particles were found within the alveoli. No other particle induced changes of epithelial cells were observed by histopathology.

Cell proliferation rates can also be influenced by increased cell turnover rates due to tissue growth. Further investigations such as evaluation of epithelial cell apoptosis would be necessary to clarify this question. Furthermore, comparative data on cell proliferation in the lung after inhalation of nanoparticles is limited to a few studies. Statistically significant cell proliferation rates of the 1 and 4 week study were measured. The biological relevance of this increase remains questionable as cell proliferation rates in young, growing animals are rather variable. In this case, the endpoint tumor formation after inhalation of nanoparticles can only be revealed by histopathology after 2 years of inhalation exposure. Cell proliferation data may be used in the future to establish a test system for predicting possible tumour development already after shorter exposure.

For neoplastic responses in rats after inhalation of PSLT, the mode of action may require particle accumulation in the lungs, persistent (neutrophilic) inflammation and epithelial cell proliferation

(ECETOC 2013; ILSI Risk Science Institute Workshop Participants 2000). In our inhalation studies, all three processes were observed. Whether the extent and interaction of these processes will lead to lung tumour formation or not can only be revealed by histopathology after 2 years of exposure in the current long-term inhalation study.

## 9.2. Biokinetics and effects of BaSO<sub>4</sub> in the lung

Barium sulfate nanoparticles were also characterized and tested in cell-free *in vitro* solubility studies (see paper 2). The cell-free *in vitro* studies showed very low dissolution (0.1 wt%) of nano-BaSO<sub>4</sub> in PSF. A consistent negligible dissolution in simulated physiological saline fluid was previously observed for micron-BaSO<sub>4</sub> (Cullen *et al.* 2000; Cullen *et al.* 1999). But in the short-term *in vivo* studies inhaled nano-BaSO<sub>4</sub> showed an unusual fast short-term clearance which may be explained by higher *in vivo* biosolubility compared to our *in vitro* cell-free static system since the observed fast lung clearance and high systemic bioavailability of inhaled BaSO<sub>4</sub> cannot be explained by any known physiological process. The available cell-free biological simulation fluids may lack critical constituents of the lung which facilitate a more rapid dissolution. Moreover, the cell-free system determined the dissolution in a static mode which may not adequately reflect the dynamics of an *in vivo* system and kinetics of the dissolution process (e.g. removal of barium ions from the dissolution compartment resulting in a steady state condition). Such limitations of abiotic, static solubility assays to estimate *in vivo* biosolubility have been previously described (ECETOC 2013).

Differences in biosolubility of particles can affect particle clearance kinetics and overload conditions. In our 4 week study, 95 % of BaSO<sub>4</sub> initial lung burden was cleared within 35 days post-exposure (a lung burden of 0.84 mg/lung 1 day post-exposure decreased to a lung burden of 0.04 mg/lung after 35 days post-exposure). The retention half-time of inhaled BaSO<sub>4</sub> was calculated with around 7 days (see equation used for calculations of CeO<sub>2</sub> retention half-times in paper 1). The retention half-time of instilled <sup>131</sup>BaSO<sub>4</sub> (0.28 ± 0.004 mg/lung) was 9.6 days (see paper 2). Pulmonary micron-BaSO<sub>4</sub> clearance was reported to consist of 52 % mucociliary clearance and 48 % transport from the lung via blood to extrapulmonary tissues and organs, assuming macrophage involvement and disposal of sulfate particles (Spritzer & Watson 1964; IPCS 1990). Dissolution *in vivo* is a known mechanism for particle clearance (ECETOC 2013). Dissolution of BaSO<sub>4</sub> in the lungs (e.g. in the phagolysosome of macrophages) may contribute to their rapid clearance and translocation to extrapulmonary organs and tissues. After instillation, <sup>131</sup>BaSO<sub>4</sub> was found in faeces (30 % of instilled dose) and bone (29 %). Whether the instilled <sup>131</sup>Ba measured in the bones was particulate <sup>131</sup>BaSO<sub>4</sub> or ionic <sup>131</sup>Ba could not be determined in this study.

In our inhalation study, lung burdens increased strongly with a longer exposure period (from 1.73 ± 0.85 mg after 13 weeks to 10.21 ± 2.69 mg after 52 weeks, see table 9). This may indicate a change in clearance from short-term to long-term exposure. This could be due to overwhelmed macrophage-

dependent particle clearance, it may indicate a saturation of the process facilitating the dissolution of BaSO<sub>4</sub> in the lung or could be a combination of both.

After inhalation, deposited micron-BaSO<sub>4</sub> has been reported to be cleared from the lung and elevated barium levels were detected in the bone (Einbrodt *et al.* 1972; Cuddihy *et al.* 1974). This clearance may also be transferable to BaSO<sub>4</sub> nanoparticles. After 10 days (50 hours) of inhalation exposure to micron-BaSO<sub>4</sub>, the barium burden in the lung was 83 µg/g dried tissue whereas the barium burden in the femur was 1300 µg/g dried tissue, around 16-fold higher than in the lung (Einbrodt *et al.* 1972). Whether the translocated barium was in an ionic or particulate form was not assessed in this study. The majority of inhaled BaSO<sub>4</sub> may be retained in the skeleton and to a much lesser extent in the soft tissues. Barium translocation to the bone had already been observed to be similar to other heavy earth alkaline metals like calcium and strontium (Moore 1964).

In the periodic table, barium neighbors calcium in the group of alkaline earth metals. The ratio of calcium to barium atoms in the body is 1000 to 1 (Straube & Donate 2013). In the bone, calcium is embedded in hydroxyapatite crystals. But as barium may mimic calcium in the body, barium ions may also be incorporated in the bone matrix, mainly in areas of active bone growth in the distal regions (Bligh & Taylor 1963; IPCS 1990; Moore 1964). In an *in vitro* model for bone metabolism, the replacement of calcium by barium seems to be limited to the surface of the hydroxyapatite crystal whereas strontium is able to replace calcium also in the interior of the crystal (Stark 1968). Barium uptake into the bone seems to be rapid and, 1.5 till 5 times faster than calcium or strontium (Reeves 1986). Barium incorporation into the bone was reported to be increased in young growing animals and reduced in mature animals (Bligh & Taylor 1963). This may help to explain the results of our studies since the rats were around 6 weeks old, still developing, at the start of inhalation exposure and will be around 2 years old after long-term exposure ends. At this time, it is not known why BaSO<sub>4</sub> has such a fast clearance after short-term exposure and if there is a (specific, active) process for barium transport from the lung to the bone. The half-time of barium in the bone is around 50 days (Machata 1988). Saturation of a specific process may also partly explain the decrease of barium clearance out of the lung and the corresponding high barium burden in the lung after 52 weeks of exposure.

Variations in pulmonary barium burden and clearance mechanisms were already observed after 40 inhalation exposures to 40 mg/m<sup>3</sup> micron-BaSO<sub>4</sub> (Einbrodt *et al.* 1972). After the first 14 exposures, barium content in the lungs increased but decreased rapidly during the next 4 weeks. It increased again during the post-exposure period of 4 weeks. The author stated that barium redistribution from extrapulmonary organs via blood to the lung might play a role. Barium translocation to rat femora and jaw was also reported. Barium content in the femora peaked after 10 exposures and decreased thereafter during further exposures and the post-exposure period.

To follow up the distribution and clearance mechanism of inhaled BaSO<sub>4</sub> in our studies, further investigations have to include the analysis of barium content in blood, bone and bone marrow. The mechanism of barium deposition in the bone is also unclear. Proposed mechanisms include ionic exchange with calcium at actively calcifying surfaces and rapid process of adsorption of colloidal particles on to the bone surfaces (Bligh & Taylor 1963). It is necessary to determine in which form -

ionic or particle - BaSO<sub>4</sub> was rapidly cleared from the lung and translocated to the bone as well as how and where it was integrated in the bone. Since barium is mainly excreted in the faeces and to a lesser extent in the urine (see paper 2: by 28 days post-dosing, 30% of the <sup>131</sup>Ba instilled dose was excreted in the faeces and only 4.4% in the urine) (Cember *et al.* 1961), analysis of faeces and urine of exposed animals may also contribute to excretion and clearance mechanisms of inhaled BaSO<sub>4</sub> and has to be investigated in the ongoing long-term study.

BaSO<sub>4</sub> (nano)particles are used as filler in poly methyl methacrylate (PMMA) bone cements for orthopedic reasons (Gillani *et al.* 2010). BaSO<sub>4</sub> particles which are used as radiopaque agent within the bone cement seems to promote osteolysis at the bone-implant interface (Wimhurst *et al.* 2001). Increased inflammatory response and pathological bone resorption by enhancing macrophage-osteoclast differentiation were also reported with BaSO<sub>4</sub> containing cement (concentrations of 5 µg/ml added to murine monocytes culture with osteoblast-like UMR106 cells) (Lazarus *et al.* 1994; Sabokbar *et al.* 2000). Therefore, biological effects in bone by translocated BaSO<sub>4</sub> after inhalation have to be further evaluated in the long-term inhalation study.

After inhalation and deposition in the lung, nano-PSLT can be taken up by macrophages which then can translocate to the lymph nodes (as mentioned in chapter 4.2.1.-4.2.3.). This mechanism has generally only a minor contribution to the total lung clearance of particles (Ma-Hock *et al.* 2009; IARC 2010; Ravenzwaay *et al.* 2009). In the present work, after 13 weeks of exposure, barium burden in the tracheobronchial and mediastinal lymph nodes was generally low (around 0.5 % of the initial lung burden). This is consistent with other inhalation studies with micron-BaSO<sub>4</sub> (Einbrodt *et al.* 1972).

Other inhaled PSLT nanoparticles, such as nano-TiO<sub>2</sub> and -CeO<sub>2</sub>, were found within macrophages and also free in pulmonary blood vessels (figure 8-6 and 8-7) (Eydner *et al.* 2012). There are two possible mechanisms which may underlay this observation: nanoparticles may be phagocytized by pulmonary macrophages and translocated within macrophages from the lung tissue into the blood. Or free nanoparticles translocated from the lung to the blood vessels and were phagocytized by pulmonary intravascular macrophages; these macrophages were, however, reported to be rare in rats (Brain *et al.* 1999; Geiser 2010; Lehnert 1992). It is of interest whether nano-BaSO<sub>4</sub> may translocate freely or cell-associated (within macrophages) from the lungs to the blood and further into extrapulmonary tissues. The mechanistic basis of the observed nanoparticles which were found within macrophages and also free in pulmonary blood vessels warrants further investigations.

In the lung, inhaled BaSO<sub>4</sub> elicited vanishing low effects after 4 weeks of exposure to high aerosol concentrations. These observations were consistent with the previous short-term inhalation study after 1 week of exposure (Landsiedel *et al.* 2014). This may be explained by the low inherent toxicity and the remarkable fast clearance of BaSO<sub>4</sub> from the lungs.

With a burden of 0.84 mg/lung, nano-BaSO<sub>4</sub> elicited no inflammation and no morphological changes in the lung (and extra-pulmonary organs) (see figure 8-5) after short-term exposure of 4 weeks and a subsequent post-exposure period of 4 weeks, besides a negligible elevation of some BAL parameters (neutrophils, MCP-1, total protein). A moderate neutrophilic response in BAL (13-fold of control) was

observed at a burden of 1.73 mg/lung after 13 weeks of exposure. This change led to corresponding increases of enzyme levels (GGT, ALP) indicating slight pulmonary inflammation. Increased numbers of neutrophils (263-fold of concurrent control), lymphocytes and monocytes showed a stronger pulmonary inflammation after 52 weeks of exposure (burden of 10 mg/lung). Additional elevation of total protein and all enzyme levels and MCP-1 may indicate a strong response to recruit and activate monocytes and macrophages into the lung.

In another study, prolonged exposure to high aerosol concentrations led to high lung burdens and, eventually, pulmonary inflammation occurred. In a 118 day-inhalation study, pulmonary response and lung retention and clearance were compared for two micron-TiO<sub>2</sub> and -BaSO<sub>4</sub> tested at 50 mg/m<sup>3</sup> and 75 mg/m<sup>3</sup>, respectively (Cullen *et al.* 1999). After 90 days with 64 exposures, micron-BaSO<sub>4</sub> elicited a burden of around 7.5 mg in the lung and 0.5 mg in the lymph nodes. Neutrophil response in BAL was generally low (at background levels), besides a slight peak after 90 days (around 600 000 neutrophils, 12 % of total cells). These findings are in contrast to our effect data. In the same study, at equal mass burdens of the two dusts, micron-TiO<sub>2</sub> elicited a pulmonary inflammation based on increased neutrophil numbers in BALF (around 28 % of total cells). Differences of the two particles were explained by the smaller surface area of micron-BaSO<sub>4</sub> (3.13 m<sup>2</sup>/g) compared to micron-TiO<sub>2</sub> (6.68 m<sup>2</sup>/g) (Tran *et al.* 2000).

The change in inflammatory potential and toxicity after 52 weeks of exposure parallels the increase of the test material in the lungs. In the phagolysosomal simulation fluid of our cell free studies, BaSO<sub>4</sub> nanoparticles changed their physico-chemical properties and showed difference in charge at different pH and recrystallized later over 28 days of incubation. These altered properties may lead to differences in clearance and pulmonary toxicity.

Overall, BaSO<sub>4</sub> nanoparticles are clearly deposited in the lung in our inhalation studies, especially after 52 weeks of exposure. On the other hand, the clearance rate is faster after short-term exposure than the clearance of other PSLT nanoparticles indicating a yet unknown clearance mechanism of BaSO<sub>4</sub> particles from the lung or dissolution of BaSO<sub>4</sub> particles *in vivo* (albeit there was no indication of this *in vitro*). The question on which of the two mechanisms are involved is of utmost interest and needs to be addressed in future investigations.

The first case (clearance of undissolved BaSO<sub>4</sub> nanoparticles) implies a hitherto unknown particle clearance mechanism. Additionally, this would point out the need to re-frame the concept of PSLT effects in the lung, since, in the case of the presented results, biopersistence would not correlate with high lung retention or lung burdens.

The latter case (bio-dissolution of BaSO<sub>4</sub> nanoparticles) implies that the *in vivo* biopersistence (or rather the non-biopersistence) of a (nano-)particle cannot always be predicted from *in vitro* dissolution (or rather insolubility) in biological simulation fluids. With the presented results, BaSO<sub>4</sub> (nano)particles may not be considered to be a classical PSLT (albeit indicated to be one by chemical properties and initial *in vitro* dissolution tests). On the other hand, there are certain indications of

particle effects in the lung (especially after 52 weeks of exposure) but no indication of barium intoxication as described in the literature (Bhoelan *et al.* 2014).

The actual lung burden is always a function of both: the deposition and the clearance rate. The aerosol concentration was quite high for BaSO<sub>4</sub> in our studies. Low aerosol concentrations of biopersistent particles may result in the same lung burden as high aerosol concentrations of rapidly-cleared particles: aerosol concentrations of 3 mg/m<sup>3</sup> CeO<sub>2</sub> and 50 mg/m<sup>3</sup> BaSO<sub>4</sub> resulted in similar lung burdens after 13 weeks of exposure (table 9). The effects of the (nano-)particles in the lung, however, depend on the properties of the deposited material, the dose-rate and the toxicity of the released ions: aerosol concentrations of 3 mg/m<sup>3</sup> CeO<sub>2</sub> and 50 mg/m<sup>3</sup> BaSO<sub>4</sub> resulted in similar lung burdens after 13 weeks of exposure, but the effects (based on BALF parameters) differed. Different (nano-)particles will span a continuous range of solubilities in the lung without a distinct threshold dividing poorly soluble from soluble (nano-)particles. Likewise, most (nano-)particle may not exhibit mere particle effects or mere released-ion effects. Hence, BaSO<sub>4</sub> (nano-)particles could be regarded as not being a classical PSLT or representing the lower toxicity and biopersistence end of PSLT.

### 9.3. Systemic effects

Systemic toxicity for inhaled PSLT seems to be less relevant since translocation rates to extra-pulmonary organs are low and very rarely associated with toxic effects (Landsiedel *et al.* 2012a; Moreno-Horn & Gebel 2014). This was also observed in our studies with 1, 4, 13 and 52 weeks of exposure to nano-CeO<sub>2</sub> and -BaSO<sub>4</sub>. There were, however, small amounts of particles translocating from the lung and slight effects secondary to local pulmonary inflammation.

In blood, a slight neutrophilia was observed for CeO<sub>2</sub> NM-212 after 1 week (5 days) of exposure to 25 mg/m<sup>3</sup> (see paper 1). The neutrophilia in blood was considered to be secondary since a pronounced inflammation was found in the lung at these aerosol concentrations. Exposure of 4 and 13 weeks to CeO<sub>2</sub> NM-212 and BaSO<sub>4</sub> elicited no neutrophilia. After 52 weeks of exposure, a slight neutrophilia in blood was apparent for 50 mg/m<sup>3</sup> BaSO<sub>4</sub> (table 11 and 12). Consistent to the 1 week study, the neutrophilia in blood after 52 weeks of BaSO<sub>4</sub> exposure seems to be rather a concomitant effect of the corresponding local inflammation in the lung.

There is a concern that occupational exposure to nanoparticles can lead to an increased risk in cardiovascular diseases (Donaldson *et al.* 2001). Various inhaled nanoparticles (e.g. carbon black, TiO<sub>2</sub>) seem to be capable to induce an acute phase response in the blood (Halappanavar *et al.* 2011; Saber *et al.* 2009; Saber *et al.* 2013). The major acute phase protein of the rat is alpha-2-macroglobulin which is a proteinase inhibitor in serum. It is able to bind foreign substances or particles as humoral defense (Borth 1992). Alpha-2-macroglobulin is further a carrier of growth factors with regulatory functions of growth factor activity and is increased in inflammation (Bhattacharjee *et al.* 2005). Its expression is furthermore enhanced by Interleukin-6. The second acute phase protein haptoglobin is able to scavenge hemoglobin which is released into blood by hemolysis or red blood

cell turnover (Quaye 2008). Its increase is linked to diseases which exhibit inflammatory causes. Haptoglobin is also a novel specific granule protein of neutrophils and its synthesis takes place during differentiation of granulocytes (Theilgaard-Monch *et al.* 2006). After storage, it is released by activated neutrophils. Furthermore, haptoglobin is involved in free radical quenching, tissue repair and regeneration (Quaye 2008). Increase of haptoglobin levels in plasma were already observed after intravenous exposure to 0.8 mg silica nanoparticles (particle diameter of 70 nm) in mice (Higashisaka *et al.* 2011). The alteration of acute phase protein levels in blood may reflect the level of inflammation (Donaldson *et al.* 2001; Halappanavar *et al.* 2011; Saber *et al.* 2009; Saber *et al.* 2013). Activated leukocytes migrate to the site of inflammation in the lung. They pass the blood stream and release cytokines which are able to trigger acute phase response (Gabay 1999). This acute phase response is generated during inflammation over time leading to altered serum levels of acute phase proteins.

In our inhalation studies, the acute phase proteins haptoglobin and alpha-2-macroglobulin (A2M) (3 mg/m<sup>3</sup> CeO<sub>2</sub>, 50 mg/m<sup>3</sup> BaSO<sub>4</sub>) were slightly increased in blood after 52 weeks but not after 4 or 13 weeks of exposure (table 11 and 12). For 50 mg/m<sup>3</sup> BaSO<sub>4</sub>, a late onset of pulmonary inflammation occurred after 52 weeks accompanied by a slight increase of neutrophils.

Four weeks exposure of 25 mg/m<sup>3</sup> CeO<sub>2</sub> showed a pronounced lung inflammation, but no increase in neutrophils and acute phase proteins in blood (table 12). After 52 weeks of exposure to 3 mg/m<sup>3</sup>, lung burdens (of 2.6 mg) were comparable to those after 4 weeks of exposure to 25 mg/m<sup>3</sup>. Although pulmonary inflammation based on increased BALF neutrophils was around 5-times lower after 52 weeks than after 4 weeks and no neutrophilia in blood was apparent, both acute phase proteins were slightly increased even after 52 weeks. Since altered levels of acute-phase proteins reflect the presence and intensity of inflammation (Gabay 1999; Davidson 2013), the duration of pulmonary inflammation may be also a decisive parameter. The increase in acute phase proteins may be explained by the longer lasting pulmonary inflammation after 52 weeks compared to 4 weeks of exposure. A good correlation was shown for dose-rate and initial inflammation in the lung (based on BALF neutrophils) after short-term exposure. Here, the dose rate seems not to be the driver for the increase of the acute phase proteins after 52 weeks. This may indicate a different mechanism.

Overall, the increase in acute phase proteins in blood seems to be no nanoparticle-specific effect, but rather, together with the slight neutrophilia in blood, a concomitant effect of recruitment of neutrophils into the lung and of pulmonary inflammation and released mediators.

After 4 weeks of exposure to 25 mg/m<sup>3</sup> CeO<sub>2</sub>, translocation of CeO<sub>2</sub> from the lung to the liver was low since liver burdens were below 2 µg at two time points and during 8 weeks of post-exposure (see paper 1) unless there was a rapid hepato-biliary excretion of CeO<sub>2</sub> from the liver. Cerium in bile was, however, not measured. Low translocation of CeO<sub>2</sub> deposited in the lung was also confirmed by an intratracheal instillation study where less than 1 % of the total instilled <sup>141</sup>Ce concentration was found in extrapulmonary tissues after 28 days (Molina *et al.* 2014). Furthermore, no morphological changes of extra-pulmonary organs could be detected in histopathology after short-term exposure of both nanoparticles.

## 10. Conclusion

Differences in toxic potency of various PSLT (nano-)particles were reported earlier (ECETOC 2013; ILSI Risk Science Institute Workshop Participants 2000). In this body of work, two different nanoparticles were tested in our inhalation studies.

In the short-term studies, inhaled nano-BaSO<sub>4</sub> showed an unusually fast short-term clearance. This may be explained by higher *in vivo* dissolution compared to our cell-free *in vitro* solubility studies since the observed fast lung clearance and high systemic bioavailability of inhaled BaSO<sub>4</sub> cannot be achieved by any known physiological process unless there may be a specific rapid translocation of nano-BaSO<sub>4</sub>. It is of utmost interest which mechanisms are involved; this needs to be addressed in future investigations. In the long-term study, lung burdens increased strongly with longer exposure period indicating a change in clearance from short-term to long-term exposure. Long-term exposure to high aerosol concentrations of nano-BaSO<sub>4</sub> led to high lung burdens and, eventually, pulmonary inflammation based on increased BALF parameters. There were no indications of barium-ion toxicity and the effects are regarded as being particle effects in the lung. Nano-BaSO<sub>4</sub> seems to exhibit peculiar characteristics concerning kinetics and effects compared to nano-PSLT. Nano-BaSO<sub>4</sub> could be regarded as not being a classical PSLT, but rather soluble *in vivo* albeit indicated to be insoluble by its chemical properties. The remarkably low toxicity of inhaled nano-BaSO<sub>4</sub> could only partly be assigned to its fast lung clearance, but may also be the result of its low inherent toxicity.

Nano-CeO<sub>2</sub>, on the other hand, was biopersistent. Low lung burdens were cleared at physiological rates whereas higher burdens induced retarded clearance and toxicity already after short-term exposure. Comparing the observed effects in our studies with the literature data, CeO<sub>2</sub> seems to possess a higher toxicity than TiO<sub>2</sub> (Ma-Hock *et al.* 2009; Eydner *et al.* 2012). It may represent the higher toxicity and high biopersistence end of the group of PSLT.

Comparing the two tested nanoparticles, aerosol concentrations of 3 mg/m<sup>3</sup> CeO<sub>2</sub> and 50 mg/m<sup>3</sup> BaSO<sub>4</sub> resulted in similar lung burdens after 13 weeks of exposure, but the effects (based on BALF parameters) were different; this probably depends on the properties of the deposited material, the dose-rate and the toxicity of the released ions. Different (nano-)particles will span a continuous range of solubilities in the lung without a distinct threshold dividing poorly soluble from soluble (nano-)particles. Likewise, most particle may not exhibit mere particle effects or mere released-ion effects.

The local no observed adverse effect concentrations in the lung (NOAEC) of CeO<sub>2</sub> - based on BALF in female rats after 13 and 52 weeks of exposure - are 0.3 and 0.1 mg/m<sup>3</sup>, respectively. The local NOAEC of BaSO<sub>4</sub> in the lung - based on BALF in female rats after 13 and 52 weeks of exposure - is below 50 mg/m<sup>3</sup>.

Inhalation exposure to CeO<sub>2</sub> and BaSO<sub>4</sub> elicited no or only minimal systemic effects after short-term and long-term exposure.

## Conclusion

The two nanoparticles examined in this body of work differed in their particle kinetics and effects in the lung already after one week and up to 52 weeks of exposure. Whether the lung burdens and effects observed within the first 52 weeks of exposure will lead to lung tumour formation will be revealed by histopathology after 2 years of exposure in the current long-term inhalation study.

## 11. References

- Aalapati, S., Ganapathy, S., Manapuram, S., Anumolu, G. & Prakya, B. M. (2014). Toxicity and bio-accumulation of inhaled cerium oxide nanoparticles in CD1 mice. *Nanotoxicology*, 8, 786-798.
- Adamson, I. Y. R., Letourneau, H. L. & Bowden, D. H. (1989). Enhanced Macrophage Fibroblast Interactions in the Pulmonary Interstitium Increases Fibrosis After Silica Injection to Monocyte-Depleted Mice. *American Journal of Pathology*, 134, 411-418.
- Alber, A., Howie, S. E. M., Wallace, W. A. H. & Hirani, N. (2012). The role of macrophages in healing the wounded lung. *International Journal of Experimental Pathology*, 93, 243-251.
- Anderson, A. H. (2010). Carbon Black Industry, Handbook of Texas Online. Texas State Historical Association, <http://www.tshaonline.org/handbook/online/articles/doc01>
- Aninwene, G. E., Stout, D., Yang, Z. F. & Webster, T. J. (2013). Nano-BaSO<sub>4</sub>: a novel antimicrobial additive to pellethane. *International Journal of Nanomedicine*, 8, 1197-1205.
- Antaria . Antaria: Ceria. 2014. 18-8-2014. Ref Type: Online Source, <http://www.antaria.com/IRM/Company/ShowPage.aspx/PDFs/1096-68184674/AntariaStrengthensEuropeanDistribution>
- Arora, S., Rajwade, J. M. & Paknikar, K. M. (2012). Nanotoxicology and in vitro studies: The need of the hour. *Toxicol Appl Pharmacol*, 258, 151-165.
- Arts, J. H., Hadi, M., Keene, A. M., Kreiling, R., Lyon, D., Maier, M., Michel, K., Petry, T., Sauer, U. G., Warheit, D., Wiench, K. & Landsiedel, R. (2014). A critical appraisal of existing concepts for the grouping of nanomaterials. *Regul. Toxicol. Pharmacol.*, 70, 492-506.
- Babin, K., Antoine, F., Goncalves, D. M. & Girard, D. (2013). TiO<sub>2</sub>, CeO<sub>2</sub> and ZnO nanoparticles and modulation of the degranulation process in human neutrophils. *Toxicology Letters*, 221, 57-63.
- Baggs, R. B., Ferin, J. & Oberdörster, G. (1997). Regression of pulmonary lesions produced by inhaled titanium dioxide in rats. *Veterinary Pathology*, 34, 592-597.
- Bailey, M. R., Kreyling, W. G., Andre, S., Batchelor, A., Collier, C. G., Drosselmeyer, E., Ferron, G. A., Foster, P., Haider, B., Hodgson, A., Masse, R., Metivier, H., Morgan, A., Muller, H. L., Patrick, G., Pearman, I., Pickering, S., Ramsden, D., Stirling, C. & Talbot, R. J. (1989). An Interspecies Comparison of the Lung Clearance of Inhaled Monodisperse Cobalt Oxide Particles .1. Objectives and Summary of Results. *Journal of Aerosol Science*, 20, 169-188.
- Barlow, P. G., Clouter-Baker, A., Donaldson, K., Maccallum, J. & Stone, V. (2005). Carbon black nanoparticles induce type II epithelial cells to release chemotaxins for alveolar macrophages. *Part Fibre Toxicol.*, 2, 11.
- Becker, H., Herzberg, F., Schulte, A. & Kolossa-Gehring, M. (2011). The carcinogenic potential of nanomaterials, their release from products and options for regulating them. *International Journal of Hygiene and Environmental Health*, 214, 231-238.
- Bedoret, D., Wallemacq, H., Marichal, T., Desmet, C., Calvo, F. Q., Henry, E., Closset, R., Dewals, B., Thielen, C., Gustin, P., de Leval, L., Van Rooijen, N., Le Moine, A., Vanderplasschen, A., Cataldo, D., Drion, P. V., Moser, M., Lekeux, P. & Bureau, F. (2009). Lung interstitial macrophages alter dendritic cell functions to prevent airway allergy in mice. *Journal of Clinical Investigation*, 119, 3723-3738.
- Bellmann, B., MUHLE, H., Creutzenberg, O., Dasenbrock, C., Kilpper, R., MacKenzie, J. C., Morrow, P. & Mermelstein, R. (1991). Lung clearance and retention of toner, utilizing a tracer technique, during chronic inhalation exposure in rats. *Fundam Appl Toxicol*, 17, 300-313.
- Bermudez, E., Mangum, J. B., Wong, B. A., Asgharian, B., Hext, P. M., Warheit, D. B. & Everitt, J. I. (2004). Pulmonary responses of mice, rats, and hamsters to subchronic inhalation of ultrafine titanium dioxide particles. *Toxicological Sciences*, 77, 347-357.
- Bhattacharjee, G., Arandjelovic, S., Mackman, N., Gonias, S. L. & Edgington, T. S. (2005). Enhancement of tissue factor dependent procoagulant activity and factor xa generation by alpha(2)-macroglobulin. *Blood*, 106, 550A.
- Bhoelan, B. S., Stevering, C. H., van der Boog, A. T. J., & van der Heyden, M. A. G. (2014). Barium toxicity and the role of the potassium inward rectifier current. *Clinical Toxicology*, 52(6), 584-593.
- Blasco, C. & Pico, Y. (2011). Determining nanomaterials in food. *Trac-Trends in Analytical Chemistry*, 30, 84-99.

## References

- Bleeker, E. A. J., De Jong, W. H., Geertsma, R. E., Groenewold, M., Heugens, E. H. W., Koers-Jacquemijns, M., Van De Meent, D., Popma, J. R., Rietveld, A. G., Wijnhoven, S. W. P., Cassee, F. R. & Oomen, A. G. (2013). Considerations on the EU definition of a nanomaterial: Science to support policy making. *Regulatory Toxicology and Pharmacology*, 65, 119-125.
- Bligh, P. H. & Taylor, D. M. (1963). Comparative Studies of Metabolism of Strontium and Barium in Rat. *Biochemical Journal*, 87, 612
- Borm, P. J. A., Tran, L. & Donaldson, K. (2011). The carcinogenic action of crystalline silica: A review of the evidence supporting secondary inflammation-driven genotoxicity as a principal mechanism. *Critical Reviews in Toxicology*, 41, 756-770.
- Borth, W. (1992). Alpha(2)-Macroglobulin, A Multifunctional Binding-Protein with Targeting Characteristics. *Faseb Journal*, 6, 3345-3353.
- Bowden D.H., Hedgecock C. & Adamson I.Y. (1989). Silica-induced pulmonary fibrosis involves the reaction of particles with interstitial rather than alveolar macrophages. *Journal of Pathology*, 73-80.
- Brain, J. D., Knudson, D. E., Sorokin, S. P. & Davis, M. A. (1976). Pulmonary Distribution of Particles Given by Intratracheal Instillation Or by Aerosol Inhalation. *Environmental Research*, 11, 13-33.
- Brain, J. D., Molina, R. M., DeCamp, M. M., & Warner, A. E. (1999). Pulmonary intravascular macrophages: their contribution to the mononuclear phagocyte system in 13 species. *American Journal of Physiology-Lung Cellular and Molecular Physiology*, 276(1), L146-L154.
- Brody, A. R. & Roe, M. W. (1983). Deposition Pattern of Inorganic Particles at the Alveolar Level in the Lungs of Rats and Mice. *American Review of Respiratory Disease*, 128, 724-729.
- Brown, S. C., Boyko, V., Meyers, G., Voetz, M. & Wohlleben, W. (2013). Towards Advancing Nano-object Count Metrology – A Best Practice Framework. *Environ Health Perspect*, doi:10.1289/ehp.1306957.
- Burello, E. & Worth, A. (2011a). Computational Nanotoxicology Predicting Toxicity of Nanoparticles. *Nature Nanotechnology*, 6, 138-139.
- Burello, E. & Worth, A. P. (2011b). QSAR modeling of nanomaterials. *Wiley Interdisciplinary Reviews-Nanomedicine and Nanobiotechnology*, 3, 298-306.
- Cassee, F. R., van Balen, E. C., Singh, C., Green, D., Muijser, H., Weinstein, J. & Dreher, K. (2011). Exposure, health and ecological effects review of engineered nanoscale cerium and cerium oxide associated with its use as a fuel additive. *Crit Rev.Toxicol.*, 41, 213-229.
- Cember, H., Watson, J. A. & Novak, M. E. (1961). The influence of radioactivity and lung burden on the pulmonary clearance rate of barium sulfate. *American Industrial Hygiene Association Journal*, 22(1), 27-32.
- Chakravarthi VP & Balaji SN (2010). Application of Nanotechnology in Veterinary Medicine. *Veterinary World*, 3, 477-480.
- Cherrie, J. W., Brosseau, L. M., Hay, A. & Donaldson, K. (2013). Low-toxicity dusts: current exposure guidelines are not sufficiently protective. *Ann.Occup.Hyg.*, 57, 685-691.
- Corma, A., Atienzar, P., Garcia, H. & Chane-Ching, J. Y. (2004). Hierarchically mesostructured doped CeO<sub>2</sub> with potential for solar-cell use. *Nature Materials*, 3, 394-397.
- Crowell, R. E., Heaphy, E., Valdez, Y. E., Mold, C. & Lehnert, B. E. (1992). Alveolar and Interstitial Macrophage Populations in the Murine Lung. *Experimental Lung Research*, 18, 435-446.
- Cuddihy, R. G., Hall, R. P. & Griffith, W. C. (1974). Inhalation Exposures to Barium Aerosols: Physical, Chemical and Mathematical-Analysis. *Health Physics*, 26(5), 405-416.
- Cullen, R. T., Tran, C. L., Buchanan, D., Davis, J. M., Donaldson, K., Jones, A. D. & Searl, A. Health and Safety Executive Contract Research Report: Investigations into the pulmonary effects of low toxicity dusts. Part I: Relative toxicological potency of dusts. Health and Safety Executive Contract Research Report 216/1999. 1999. Sudbury, UK, HSE Books. Ref Type: Report
- Cullen, R. T., Tran, C. L., Buchanan, D., Davis, J. M., Searl, A., Jones, A. D. & Donaldson, K. (2000). Inhalation of poorly soluble particles. I. Differences in inflammatory response and clearance during exposure. *Inhal Toxicol*, 12, 1089-1111.
- Dankovic, D., Kuempel, E. & Wheeler, M. (2007). An approach to risk assessment for TiO<sub>2</sub>. *Inhalation Toxicology*, 19, 205-212.
- Davidson, S. J. (2013). Inflammation and Acute Phase Proteins in Haemostasis, chapter 2, Acute Phase Proteins. In Sabina Janciauskiene (Ed) *Acute Phase Proteins* (book), DOI: 10.5772/55998.

## References

- De Capitani, E. M., Algranti, E., Handar, A. M. Z., Altemani, A. M. A., Ferreira, R. G., Balthazar, A. B., Cerqueira, E. M. F. P. & Ota, J. S. (2007). Wood charcoal and activated carbon dust pneumoconiosis in three workers. *American Journal of Industrial Medicine*, 50, 191-196.
- Deutsche Forschungsgesellschaft (DFG) . General threshold limit value for dust (R fraction) (Biopersistent granular dusts) [MAK Value Documentation, 2012]. 2014. Wiley-VCH Verlag GmbH & Co. KGaA.  
Ref Type: Report
- DFG Deutsche Forschungsgemeinschaft (2013a). List of MAK and BAT Values 2013: *Maximum Concentrations and Biological Tolerance Values at the Workplace*. Wiley-VCH Verlag GmbH & Co. KGaA.
- DFG Deutsche Forschungsgemeinschaft (2013b). Nanomaterials; report of the Commission for the Investigation of Health Hazards of Chemical Compounds in the Work Area . Wiley-VCH Verlag.
- Doig A.T. (1976). Baritosis: a benign pneumoconiosis. *Thorax*, 31, 30-39.
- Donaldson, K. (2000). Nonneoplastic lung responses induced in experimental animals by exposure to poorly soluble nonfibrous particles. *Inhalation Toxicology*, 12, 121-139.
- Donaldson, K., Borm, P. J., Oberdörster, G., Pinkerton, K. E., Stone, V. & Tran, C. L. (2008). Concordance between in vitro and in vivo dosimetry in the proinflammatory effects of low-toxicity, low-solubility particles: the key role of the proximal alveolar region. *Inhal Toxicol*, 20, 53-62.
- Donaldson, K. & Poland, C. A. (2013). Nanotoxicity: challenging the myth of nano-specific toxicity. *Current Opinion in Biotechnology*, 24, 724-734.
- Donaldson, K., Stone, V., Seaton, A. & MacNee, W. (2001). Ambient particle inhalation and the cardiovascular system:potential mechanisms. *Environ Health Perspect* [109], 523-527.
- Donaldson, K. & Tran, C. L. (2002). Inflammation caused by particles and fibers. *Inhal Toxicol*, 14, 5-27.
- Donaldson, K., Brown, D., Clouter, A., Duffin, R., MacNee, W., Renwick, L., Tran, L. & Stone, V. (2002). The pulmonary toxicology of ultrafine particles. *Journal of Aerosol Medicine*, 15, 213-220.
- Donaldson, K. & Poland, C. A. (2012). Inhaled nanoparticles and lung cancer - what we can learn from conventional particle toxicology. *Swiss medical weekly*, 142, 13547.
- Driscoll, K. E. (2000). TNF alpha and MIP-2: role in particle-induced inflammation and regulation by oxidative stress. *Toxicology Letters*, 112, 177-183.
- Driscoll, K. E., Carter, J. M., Hassenbein, D. G. & Howard, B. (1997). Cytokines and particle-induced inflammatory cell recruitment. *Environ.Health Perspect.*, 105 Suppl 5, 1159-1164.
- Driscoll, K. E., Carter, J. M., Howard, B. W., Hassenbein, D. G., Pepelko, W., Baggs, R. B. & Oberdörster, G. (1996). Pulmonary inflammatory, chemokine, and mutagenic responses in rats after subchronic inhalation of carbon black. *Toxicol Appl Pharmacol*, 136, 372-380.
- Driscoll, K. E., Hassenbein, D. G., Carter, J. M., Kunkel, S. L., Quinlan, T. R. & Mossman, B. T. (1995a). TNF alpha and increased chemokine expression in rat lung after particle exposure. *Toxicology Letters*, 82-3, 483-489.
- Driscoll, K. E., Hassenbein, D. G., Howard, B. W., Isfort, R. J., Cody, D., Tindal, M. H., Suchanek, M. & Carter, J. M. (1995b). Cloning, Expression, and Functional-Characterization of Rat Mip-2 - A Neutrophil Chemoattractant and Epithelial-Cell Mitogen. *Journal of Leukocyte Biology*, 58, 359-364.
- Driscoll, K. E., Maurer, J. K., Higgins, J. & Poynter, J. (1995c). Alveolar Macrophage Cytokine and Growth-Factor Production in A Rat Model of Crocidolite-Induced Pulmonary Inflammation and Fibrosis. *Journal of Toxicology and Environmental Health*, 46, 155-169.
- Driscoll,K.E.,Deyo,I.C.,Howard,B.W.,Hassenbein,D.G.,Bertram,T. (1997). Effects of particle exposure and particle-elicited inflammatory cells on mutation in rat alveolar type II cells. *Carcinogenesis*, 18, 423-430.
- ECETOC . ECETOC: Poorly Soluble Particles / Lung Overload, Technical Report No. 122. European Centre for Ecotoxicology and Toxicology of Chemicals. 122. 2013. Brussels, European Centre for Ecotoxicology and Toxicology of Chemicals. Ref Type: Report
- Einbrodt, H. J., Wobker, F. & Klippel, H. G. (1972). Experimental Studies on Accumulation and Distribution of Barium Sulfate in Rat Following Inhalation. *Internationales Archiv fur Arbeitsmedizin*, 30, 237-&.

## References

- Elder, A., Gelein, R., Silva, V., Feikert, T., Opanashuk, L., Carter, J., Potter, R., Maynard, A., Ito, Y., Finkelstein, J. & Oberdörster, G. (2006). Translocation of inhaled ultrafine manganese oxide particles to the central nervous system. *Environ Health Perspect*, 114, 1172-1178.
- Elder, A. & Oberdörster, G. (2006). Translocation and effects of ultrafine particles outside of the lung. *Clin. Occup. Environ Med*, 5, 785-796.
- Environmental Protection Agency (EPA). (2009) Report: Toxicological review of Cerium Oxide and Cerium Compounds. Environmental Protection Agency EPA/635/R-08/002F . 15-4-2014.
- Etheridge, M. L., Campbell, S. A., Erdman, A. G., Haynes, C. L., Wolf, S. M., & McCullough, J. (2013). The big picture on nanomedicine: the state of investigational and approved nanomedicine products. *Nanomedicine: Nanotechnology, Biology and Medicine*, 9(1), 1-14.
- European Commission . (2004) Report: Community Health and Consumer Protection: Nanotechnologies: A preliminary risk analysis on the basis of a workshop organized in Brussels by the Health and Consumer Protection Directorate General of the European Commission.
- European Commission . (2011a) Report: COMMISSION RECOMMENDATION of 18 October 2011 on the definition of nanomaterial 2011/696/EU .
- European Commission . (2011b) Report: List of materials in the JRC Nanomaterials (NM) Repository, Institute of Health and Consumer Protection. European Commission. 26-9-2014b.
- European Commission . (2011c) Regulation (EU) No 1169/2011 of the European Parliament and of the Council of 25 October 2011 on the provision of food information to consumers, amending Regulations (EC) No 1924/2006 and (EC) No 1925/2006 of the European Parliament and of the Council, and repealing Commission Directive 87/250/EEC, Council Directive 90/496/EEC, Commission Directive 1999/10/EC, Directive 2000/13/EC of the European Parliament and of the Council, Commission Directives 2002/67/EC and 2008/5/EC and Commission Regulation (EC) No 608/2004. L 304/18. Off J Eur Union.
- European Commission . (2013a) Report: Classification, Labeling and packaging of nanomaterials in REACH and CLP. [Doc. CA/90/2009 Rev2].
- European Commission . (2013b) Report: Introduction to nanotechnologies. 2013b. 7-4-2014b.
- European Commission . (2014) JRC Science and Policy Reports: JRC Repository: NM-Series of Representative Manufactured Nanomaterials: Cerium Dioxide, NM-211, NM-212, NM-213. Characterisation and Test Item Preparation. JRC89825. Publications Office of the European Union.
- Eydner, M., Schaudien, D., Creutzenberg, O., Ernst, H., Hansen, T., Baumgartner, W. & Rittinghausen, S. (2012). Impacts after inhalation of nano- and fine-sized titanium dioxide particles: morphological changes, translocation within the rat lung, and evaluation of particle deposition using the relative deposition index. *Inhal. Toxicol.*, 24, 557-569.
- Fabian, E., Landsiedel, R., Ma-Hock, L., Wiench, K., Wohlleben, W. & van Ravenzwaay, B. (2008). Tissue distribution and toxicity of intravenously administered titanium dioxide nanoparticles in rats. *Archives of Toxicology*, 82, 151-157.
- Ferin, J., Oberdörster, G. & Penney, D. P. (1992). Pulmonary retention of ultrafine and fine particles in rats. *Am J Respir. Cell Mol. Biol*, 6, 535-542.
- Gabay, C. (1999). Mechanisms of disease - Acute-phase proteins and other systemic responses to inflammation (vol 340, pg 448, 1999). *New England Journal of Medicine*, 340, 1376.
- Gallagher, J., Sams, R., Inmon, J., Gelein, R., Elder, A., Oberdörster, G. & Prahalad, A. K. (2003). Formation of 8-oxo-7,8-dihydro-2'-deoxyguanosine in rat lung DNA following subchronic inhalation of carbon black. *Toxicol Appl Pharmacol*, 190, 224-231.
- Gebel, T. (2012). Small difference in carcinogenic potency between GBP nanomaterials and GBP micromaterials. *Archives of Toxicology*, 86, 995-1007.
- Gebel, T., Marchan, R. & Hengstler, J. (2013). The nanotoxicology revolution. *Archives of Toxicology*, 87, 2057-2062.
- Gebel, T., Foth, H., Damm, G., Freyberger, A., Kramer, P. J., Lilienblum, W., Röhl, C., Schupp, T., Weiss, C., Wollin, K. M. & Hengstler, J. G. (2014). Manufactured nanomaterials: categorisation and approaches to hazard assessment. *Critical Reviews in Toxicology*, 88(12):2191-211.
- Geiser, M. (2002). Morphological aspects of particle uptake by lung phagocytes. *Microscopy Research and Technique*, 57, 512-522.
- Geiser, M. (2010). Update on Macrophage Clearance of Inhaled Micro- and Nanoparticles. *Journal of Aerosol Medicine and Pulmonary Drug Delivery*, 23, 207-217.
- Gentek, R., Molawi, K. & Sieweke, M. H. (2014). Tissue macrophage identity and self-renewal. *Immunol.Rev.*, 262, 56-73.

## References

- Geraets, L., Oomen, A. G., Schroeter, J. D., Coleman, V. A. & Cassee, F. R. (2012). Tissue distribution of inhaled micro- and nano-sized cerium oxide particles in rats: results from a 28-day exposure study. *Toxicol.Sci.*, 127, 463-473.
- Gill, K. K., Nazzal, S. & Kaddourni, A. (2014). Paclitaxel loaded PEG<sub>5000</sub>-DSPE micelles as pulmonary delivery platform: Formulation characterization, tissue distribution, plasma pharmacokinetics, and toxicological evaluation. *European Journal of Pharmaceutics and Biopharmaceutics*, 79, 276-284.
- Gillani, R., Ercan, B., Qiao, A. & Webster, T. J. (2010). Nanofunctionalized zirconia and barium sulfate particles as bone cement additives. *International Journal of Nanomedicine*, 5, 1-11.
- Givvimani S., Leevy, M. & Tyagi S.C. (2011) Report: Barium Angiography in Small Animals. Application Note # AP0108. Bruker.
- Gojova, A., Lee, J. T., Jung, H. S., Guo, B., Barakat, A. I. & Kennedy, I. M. (2009). Effect of cerium oxide nanoparticles on inflammation in vascular endothelial cells. *Inhal.Toxicol.*, 21 Suppl 1, 123-130.
- Gordon, S. (2003). Alternative activation of macrophages. *Nature Reviews Immunology*, 3, 23-35.
- Gosens, I., Mathijssen, L., Bokkers, B., Muijser, H. & Cassee, F. R. (2013). Comparative hazard identification of nano- and micro-sized cerium oxide particles based on 28-day inhalation studies in rats. *Nanotoxicology*, 8:6, 643-653.
- Green, F. H. Y. (2000). Pulmonary responses to inhaled poorly soluble particulate in the human. *Inhalation Toxicology*, 12, 59-95.
- Gregoratto, D., Bailey, M. R. & Marsh, J. W. (2011). Particle Clearance in the Alveolar-Interstitial Region of the Human Lungs: Model Validation. *Radiation Protection Dosimetry*, 144, 353-356.
- Greim, H., Borm, P., Schins, R., Donaldson, K., Driscoll, K., Hartwig, A., Kuempel, E., Oberdörster, G. & Speit, G. (2001). Toxicity of fibers and particles. Report of the workshop held in Munich, Germany, 26-27 October 2000. *Inhal Toxicol*, 13, 737-754.
- Greim, H. & Ziegler-Skylakakis, K. (2007). Risk assessment for biopersistent granular particles. *Inhal.Toxicol.*, 19 Suppl 1, 199-204.
- Grommes, J. & Soehnlein, O. (2011). Contribution of neutrophils to acute lung injury. *Mol.Med.*, 17, 293-307.
- Halappanavar, S., Jackson, P., Williams, A., Jensen, K. A., Hougaard, K. S., Vogel, U., Yauk, C. L. & Wallin, H. (2011). Pulmonary Response to Surface-Coated Nanotitanium Dioxide Particles Includes Induction of Acute Phase Response Genes, Inflammatory Cascades, and Changes in MicroRNAs: A Toxicogenomic Study. *Environmental and Molecular Mutagenesis*, 52, 425-439.
- Heinrich, U., Fuhst, R., Rittinghausen, S., Creutzenberg, O., Bellmann, B., Koch, M. & Levsen, K. (1995). Chronic inhalation exposure of Wistar rats and two different strains of mice to diesel engine exhaust, carbon black, and titanium dioxide. *Inhal Toxicol*, 7, 533-556.
- Henderson, R., Mauderly, J.L., Pickrell, J.A., Hahn, F., Muhle, H. & Rebar, A.H. (1987). Comparative study of bronchoalveolar lavage fluid-effect of species, age and method of lavage. *Experimental Lung Research*, 13, 329-342.
- Higashisaka, K., Yoshioka, Y., Yamashita, K., Morishita, Y., Fujimura, M., Nabeshi, H., Nagano, K., Abe, Y., Kamada, H., Tsunoda, S., Yoshikawa, T., Itoh, N. & Tsutsumi, Y. (2011). Acute phase proteins as biomarkers for predicting the exposure and toxicity of nanomaterials. *Biomaterials*, 32, 3-9.
- Hirst, S. M., Karakoti, A., Singh, S., Self, W., Tyler, R., Seal, S. & Reilly, C. M. (2013). Bio-distribution and in vivo antioxidant effects of cerium oxide nanoparticles in mice. *Environ.Toxicol.*, 28, 107-118.
- Holma, B. (1969). Scanning Electron Microscopic Observation of Particles Deposited in Lung. *Archives of Environmental Health*, 18, 330-339.
- Hussell, T. & Bell, T. J. (2014). Alveolar macrophages: plasticity in a tissue-specific context. *Nature Reviews Immunology*, 14, 81-93.
- IARC (1996). Report: IARC monographs on the evaluation of carcinogenic risks to humans. Volume 65. Printing processes and printing inks, carbon black and some nitro compounds. *Monogr Eval Carcinog Risks Hum*, 65, 1-578.
- IARC (1997). Report: IARC monographs on the evaluation of carcinogenic risks to humans. Volume 68. Silica, some silicates, coal dust and para-amid fibrils. Volume 68.
- IARC (2010). Report: IARC Monographs on the Evaluation of Carcinogenic Risks to Humans: Volume 93, Carbon black, Titanium Dioxide and Talc. WHO Press.

## References

- ILSI Risk Science Institute Workshop Participants (2000). The relevance of the rat lung response to particle overload for human risk assessment: a workshop consensus report. ILSI Risk Science Institute Workshop Participants. *Inhal.Toxicol.*, 12, 1-17.
- IPCS (1990). Report: Barium, International Programme on Chemical Safety (Environmental Health Criteria 107). Geneva, World Health Organization.
- ISO (2008). Report: ISO 7780:1995 Air quality - Particle size fraction definitions for health-related sampling.
- Janssen, W. J., Barthel, L., Muldrow, A., Oberley-Deegan, R. E., Kearns, M. T., Jakubzick, C. & Henson, P. M. (2011). Fas Determines Differential Fates of Resident and Recruited Macrophages during Resolution of Acute Lung Injury. *American Journal of Respiratory and Critical Care Medicine*, 184, 547-560.
- Johnston, C. J., Driscoll, K. E., Finkelstein, J. N., Baggs, R., O'Reilly, M. A., Carter, J., Gelein, R. & Oberdörster, G. (2000). Pulmonary chemokine and mutagenic responses in rats after subchronic inhalation of amorphous and crystalline silica. *Toxicological Sciences*, 56, 405-413.
- Joint Research Centre of the European Commission (2010). Report: Considerations on a definition of nanomaterial for regulatory purposes (JRC Reference Reports).
- Kakuwa, Y., & Matsumoto, R. (2006). Cerium negative anomaly just before the Permian and Triassic boundary event—the upward expansion of anoxia in the water column. *Palaeogeography, Palaeoclimatology, Palaeoecology*, 229(4), 335-344.
- Kilbourn, B. (2003). Kirk-Othmer encyclopedia of chemical technology: Cerium and Cerium compounds. New York: John Wiley and Sons, Inc.
- Kittel, B., Ruehl-Fehlert, C., Morawietz, G., Klapwijk, J., Elwell, M. R., Lenz, B., O'Sullivan, M. G., Roth, D. R. & Wadsworth, P. F. (2004). Revised guides for organ sampling and trimming in rats and mice - Part 2 - A joint publication of the RITA and NACAD groups. *Experimental and Toxicologic Pathology*, 55, 413-431.
- Klein, C. L., Wiench, K., Wiemann, M., Ma-Hock, L., van, Ravenzwaay, B. & Landsiedel, R. (2012). Hazard identification of inhaled nanomaterials: making use of short-term inhalation studies. *Arch.Toxicol.*, 86, 1137-1151.
- Kolling, A., Ernst, H., Rittinghausen, S. & Heinrich, U. (2011). Relationship of pulmonary toxicity and carcinogenicity of fine and ultrafine granular dusts in a rat bioassay. *Inhalation Toxicology*, 23, 544-554.
- Kreyling, W. G., Semmler, M., Erbe, F., Mayer, P., Takenaka, S., Schulz, H., Oberdörster, G. & Ziesenis, A. (2002). Translocation of ultrafine insoluble iridium particles from lung epithelium to extrapulmonary organs is size dependent but very low. *Journal of Toxicology and Environmental Health-Part A*, 65, 1513-1530.
- Kreyling, W. G., Semmler-Behnke, M., Seitz, J., Scymczak, W., Wenk, A., Mayer, P., Takenaka, S. & Oberdörster, G. (2009). Size dependence of the translocation of inhaled iridium and carbon nanoparticle aggregates from the lung of rats to the blood and secondary target organs. *Inhalation Toxicology*, 21 Suppl 1, 55-60.
- Kroll, A., Pillukat, M. H., Hahn, D. & Schneckeburger, J. (2012). Interference of engineered nanoparticles with in vitro toxicity assays. *Archives of Toxicology*, 86, 1123-1136.
- Kuempel, E. D., Atfield, M. D., Stayner, L. T. & Castranova, V. (2014). Human and Animal Evidence Supports Lower Occupational Exposure Limits for Poorly-Soluble Respirable Particles: Letter to the Editor re: 'Low-Toxicity Dusts: Current Exposure Guidelines Are Not Sufficiently Protective' by Cherrie, Brosseau, Hay and Donaldson. *Ann.Occup.Hyg.*
- Kuempel, E. D., O'Flaherty, E. J. & Stayner, L. T. (2001). A biomathematical model of particle clearance and retention in the lungs of coal miners. *Regul.Toxicol Pharmacol*, 34, 67-87.
- Kumari, M., Singh, S. P., Chinde, S., Rahman, M. F., Mahboob, M. & Grover, P. (2014). Toxicity Study of Cerium Oxide Nanoparticles in Human Neuroblastoma Cells. *Int J Toxicol*, 33, 86-97.
- Landsiedel, R., Fabian, E., Ma-Hock, L., Wohlleben, W., Wiench, K., Oesch, F. & van Ravenzwaay, B. (2012a). Toxicokinetics of nanomaterials. *Archives of Toxicology*, 86, 1021-1060.
- Landsiedel, R., Ma-Hock, L., Haussmann, H. J., van Ravenzwaay, B., Kayser, M. & Wiench, K. (2012b). Inhalation studies for the safety assessment of nanomaterials: status quo and the way forward. *Wiley Interdisciplinary Reviews-Nanomedicine and Nanobiotechnology*, 4, 399-413.
- Landsiedel, R., Ma-Hock, L., Hofmann, T., Wiemann, M., Strauss, V., Treumann, S., Wohlleben, W., Groeters, S., Wiench, K. & Ravenzwaay, B. v. (2014). Application of short-term inhalation studies to assess the inhalation toxicity of nanomaterials. *Particle and Fibre Toxicology*, 11:16.
- Laskin, D. L., Weinberger, B. & Laskin, J. D. (2001). Functional heterogeneity in liver and lung macrophages. *Journal of Leukocyte Biology*, 70, 163-170.

## References

- Lazarus, M. D., Cuckler, J. M., Schumacher, H. R., Ducheyne, P. & Baker, D. G. (1994). Comparison of the Inflammatory Response to Particulate Polymethylmethacrylate Debris with and Without Barium-Sulfate. *Journal of Orthopaedic Research*, 12, 532-541.
- Lee, K. P., Henry, N. W., III, Trochimowicz, H. J. & Reinhardt, C. F. (1986). Pulmonary response to impaired lung clearance in rats following excessive TiO<sub>2</sub> dust deposition. *Environ Res*, 41, 144-167.
- Lehnert, B. E. (1992). Pulmonary and thoracic macrophage subpopulations and clearance of particles from the lung. *Environmental health perspectives*, 97, 17.
- Lewicka, Z. A., Benedetto, A. F., Benoit, D. N., Yu, W. W., Fortner, J. D. & Colvin, V. L. (2011). The structure, composition, and dimensions of TiO<sub>2</sub> and ZnO nanomaterials in commercial sunscreens. *Journal of Nanoparticle Research*, 13, 3607-3617.
- Li, J. J., Muralikrishnan, S., Ng, C. T., Yung, L. Y. L. & Bay, B. H. (2010). Nanoparticle-induced pulmonary toxicity. *Experimental Biology and Medicine*, 235, 1025-1033.
- Liden, G. (2011). The European Commission Tries to Define Nanomaterials. *Annals of Occupational Hygiene*, 55, 1-5.
- Lobatto, M. E., Fuster, V., Fayad, Z. A., & Mulder, W. J. (2011). Perspectives and opportunities for nanomedicine in the management of atherosclerosis. *Nature Reviews Drug Discovery*, 10(11), 835-852.
- Liu, R., Yin, L. H., Pu, Y. P., Li, Y. H., Zhang, X. Q., Liang, G. Y., Li, X. B., Zhang, J. A., Li, Y. F. & Zhang, X. Y. (2010a). The Immune Toxicity of Titanium Dioxide on Primary Pulmonary Alveolar Macrophages Relies on their Surface Area and Crystal Structure. *Journal of Nanoscience and Nanotechnology*, 10, 8491-8499.
- Liu, R., Zhang, X. Y., Pu, Y. P., Yin, L. H., Li, Y. H., Zhang, X. Q., Liang, G. Y., Li, X. B. & Zhang, J. (2010b). Small-Sized Titanium Dioxide Nanoparticles Mediate Immune Toxicity in Rat Pulmonary Alveolar Macrophages In Vivo. *Journal of Nanoscience and Nanotechnology*, 10, 5161-5169.
- Lohmannmatthes, M. L., Steinmuller, C. & Frankeullmann, G. (1994). Pulmonary Immune Cells - Pulmonary Macrophages. *European Respiratory Journal*, 7, 1678-1689.
- Lucarelli, M., Gatti, A. M., Savarino, G., Quattroni, P., Martinelli, L., Monari, E. & Boraschi, D. (2004). Innate defence functions of macrophages can be biased by nano-sized ceramic and metallic particles. *European Cytokine Network*, 15, 339-346.
- Lynch, I., Feitshans, I. L., & Kendall, M. (2015). 'Bio-nano interactions: new tools, insights and impacts': summary of the Royal Society discussion meeting. *Philosophical Transactions of the Royal Society B: Biological Sciences*, 370(1661), 20140162.
- Ma, J., Young, S., Mercer, R., Barger, M., Schwegler-Berry, D., Ma, J. K. & Castranova, V. (2014). Interactive effects of cerium oxide and diesel exhaust nanoparticles in inducing pulmonary fibrosis. *Toxicol Appl Pharmacol*.
- Ma, J. Y., Mercer, R. R., Barger, M., Schwegler-Berry, D., Scabilloni, J., Ma, J. K. & Castranova, V. (2012). Induction of pulmonary fibrosis by cerium oxide nanoparticles. *Toxicol Appl Pharmacol*, 262, 255-264.
- Ma, J. Y., Zhao, H. W., Mercer, R. R., Barger, M., Rao, M., Meighan, T., Schwegler-Berry, D., Castranova, V. & Ma, J. K. (2011). Cerium oxide nanoparticle-induced pulmonary inflammation and alveolar macrophage functional change in rats. *Nanotoxicology*, 5, 312-325.
- Ma-Hock, L., Burkhard, S., Strauss, V., Gamer, A. O., Wiench, K., van Ravenzwaay, B. & Landsiedel, R. (2009). Development of a short-term inhalation test in the rat using nano-titanium dioxide as a model substance. *Inhalation Toxicology*, 21, 102-118.
- Ma-Hock, L., Gamer, A. O., Landsiedel, R., Leibold, E., Frechen, T., Sens, B., Linsenbuehler, M. & van Ravenzwaay, B. (2007). Generation and characterization of test atmospheres with nanomaterials. *Inhalation Toxicology*, 19, 833-848.
- Machata, G. (1988). Handbook on Toxicity of Inorganic Compounds: Barium. New York: Marcel Dekker, Incop.
- Madl, A. K., Plummer, L. E., Carosino, C. & Pinkerton, K. E. (2014). Nanoparticles, Lung Injury, and the Role of Oxidant Stress. *Annual Review of Physiology*, Vol 76, 76, 447-465.
- Maier, M., Hannebauer, B., Holldorff, H. & Albers, P. (2006). Does lung surfactant promote disaggregation of nanostructured titanium dioxide? *Journal of Occupational and Environmental Medicine*, 48, 1314-1320.
- Matrix Insign Ltd (2014). Report: A Study to support the Impact Assessment of relevant regulatory options for nanomaterials in the framework of REACH.
- Mauderly, J. L., Snipes, M. B., Barr, E. B., Belinsky, S. A., Bond, J. A., Brooks, A. L., ... & Griffith, W. C. (1994). Pulmonary toxicity of inhaled diesel exhaust and carbon black in chronically exposed rats. Part I: Neoplastic and nonneoplastic lung lesions. *Research Report (Health Effects Institute)*, (68 Pt 1), 1.

## References

- Maus, U. A., Janzen, S., Wall, G., Srivastava, M., Blackwell, T. S., Christman, J. W., Seeger, W., Welte, T. & Lohnmeyer, J. (2006). Resident alveolar macrophages are replaced by recruited monocytes in response to endotoxin-induced lung inflammation. *Am J Respir Cell Mol Biol*, 35, 227-235.
- Maynard, A. D. & Kuempel, E. D. (2005). Airborne nanostructured particles and occupational health. *Journal of Nanoparticle Research*, 7, 587-614.
- McDonald, J. W., Ghio, A. J., Sheehan, C. E., Bernhardt, P. F. & Roggli, V. L. (1995). Rare-Earth (Cerium Oxide) Pneumoconiosis - Analytical Scanning Electron-Microscopy and Literature-Review. *Modern Pathology*, 8, 859-865.
- Mercer, R. R., Scabilloni, J. F., Hubbs, A. F., Battelli, L. A., McKinney, W., Friend, S., ... & Porter, D. W. (2013a). Distribution and fibrotic response following inhalation exposure to multi-walled carbon nanotubes. *Particle and fibre toxicology*, 10(1), 33.
- Mercer, R. R., Scabilloni, J. F., Hubbs, A. F., Wang, L., Battelli, L. A., McKinney, W., ... & Porter, D. W. (2013b). Extrapulmonary transport of MWCNT following inhalation exposure. *Particle and fibre toxicology*, 10(1), 38.
- Molina, R. M., Konduru, N., Jimenez, R., Wohlleben, W. & Brain, J. D. (2014). Bioavailability, distribution and clearance of tracheally instilled, gavaged or injected cerium dioxide nanoparticles and ionic cerium. *Environmental Science: Nano*.
- Monteiller, C., Tran, L., MacNee, W., Faux, S., Jones, A., Miller, B. & Donaldson, K. (2007). The pro-inflammatory effects of low-toxicity low-solubility particles, nanoparticles and fine particles, on epithelial cells in vitro: the role of surface area. *Occupational and Environmental Medicine*, 64, 609-615.
- Moore, W. (1964). Comparative Metabolism of Barium-133 + Calcium-45 by Embryonic Bone Grown in Vitro. *Radiation Research*, 21, 376-382.
- Moreno-Horn, M. & Gebel, T. Granular biodurable nanomaterials: No convincing evidence for systemic toxicity. *Critical Reviews in Toxicology* [26], 1-27. 2014.
- Morfeld, P., Treumann, S., Ma-Hock, L., Bruch, J. & Landsiedel, R. (2012). Deposition behavior of inhaled nanostructured TiO<sub>2</sub> in rats: fractions of particle diameter below 100 nm (nanoscale) and the slicing bias of transmission electron microscopy. *Inhalation Toxicology*, 24, 939-951.
- Morrow, P. E. (1988). Possible Mechanisms to Explain Dust Overloading of the Lungs. *Fundamental and Applied Toxicology*, 10, 369-384.
- Morrow, P. E., Haseman, J. K., Hobbs, C. H., Driscoll, K. E., Vu, V. & Oberdörster, G. (1996). The maximum tolerated dose for inhalation bioassays: Toxicity vs overload. *Fundamental and Applied Toxicology*, 29, 155-167.
- Muhle, H., Bellmann, B., Creutzenberg, O., Dasenbrock, C., Ernst, H., Kilpper, R., MacKenzie, J. C., Morrow, P., Mohr, U., Takenaka, S. & . (1991). Pulmonary response to toner upon chronic inhalation exposure in rats. *Fundam Appl Toxicol*, 17, 280-299.
- Murray, E. P., Tsai, T. & Barnett, S. A. (1999). A direct-methane fuel cell with a ceria-based anode. *Nature*, 400, 649-651.
- Muskhelishvili, L., Latendresse, J. R., Kodell, R. L. & Henderson, E. B. (2003). Evaluation of cell proliferation in rat tissues with BrdU, PCNA, Ki-67(MIB-5) immunohistochemistry and in situ hybridization for histone mRNA. *Journal of Histochemistry & Cytochemistry*, 51, 1681-1688.
- Nalabotu, S. K., Kollu, M. B., Triest, W. E., Ma, J. Y., Manne, N. D. P. K., Katta, A., Addagarla, H. S., Rice, K. M. & Blough, E. R. (2011). Intratracheal instillation of cerium oxide nanoparticles induces hepatic toxicity in male Sprague-Dawley rats. *International Journal of Nanomedicine*, 6, 2327-2335.
- National Institute for Occupational Safety and Health (NIOSH) (2011). Current Intelligence Bulletin: Evaluation of Health Hazards and Recommendations for Occupational Exposure to Titanium Dioxide. 2011.160.
- Nel, A., Xia, T., Madler, L. & Li, N. (2006). Toxic potential of materials at the nanolevel. *Science*, 311, 622-627.
- Nikula, K. J., Snipes, M. B., Barr, E. B., Griffith, W. C., HENDERSON, R. F. & MAUDERLY, J. L. (1995). Comparative pulmonary toxicities and carcinogenicities of chronically inhaled diesel exhaust and carbon black in F344 rats. *Fundam. Appl. Toxicol.*, 25, 80-94.
- Noel, A., Maghni, K., Cloutier, Y., Dion, C., Wilkinson, K. J., Halle, S., Tardif, R. & Truchon, G. (2012). Effects of inhaled nano-TiO<sub>2</sub> aerosols showing two distinct agglomeration states on rat lungs. *Toxicology Letters*, 214, 109-119.
- Nurkiewicz, T. R., Porter, D. W., Barger, M., Millicchia, L., Rao, K. M. K., Marvar, P. J., Boegehold, M. A. (2006). Systemic microvascular dysfunction and inflammation after pulmonary particulate matter exposure. *Environmental health perspectives*, 412-419.
- Oberdörster, G. (1988). Lung clearance of inhaled insoluble and soluble particles. *J Aerosol Med*, 1, 289-330.
- Oberdörster, G. (1995). Lung particle overload: implications for occupational exposures to particles. *Regul. Toxicol Pharmacol*, 21, 123-135.

## References

- Oberdörster, G. (2002a). Toxicokinetics and effects of fibrous and nonfibrous particles. *Inhalation Toxicology*, 14, 29-56.
- Oberdörster, G., Sharp, Z., Atudorei, V., Elder, A., Gelein, R., Lunts, A., Kreyling, W. & Cox, C. (2002b). Extrapulmonary translocation of ultrafine carbon particles following whole-body inhalation exposure of rats. *Journal of Toxicology and Environmental Health-Part A*, 65, 1531-1543.
- Oberdörster, G. (2010). Safety assessment for nanotechnology and nanomedicine: concepts of nanotoxicology. *Journal of Internal Medicine*, 267, 89-105.
- Oberdörster, G., Ferin, J., Gelein, R., Soderholm, S. C. & Finkelstein, J. (1992). Role of the Alveolar Macrophage in Lung Injury - Studies with Ultrafine Particles. *Environmental Health Perspectives*, 97, 193-199.
- Oberdörster, G., Ferin, J. & Lehnert, B. E. (1994). Correlation between particle size, in vivo particle persistence, and lung injury. *Environ. Health Perspect.*, 102 Suppl 5, 173-179.
- Oberdörster, G., Ferin, J., Soderholm, S. C., Gelein, R., Cox, C., Baggs, R. & Morrow, P. E. (1994). Increased pulmonary toxicity of inhaled ultrafine particles: Due to lung overload alone? *The Annals of Occupational Hygiene*, 38, 295-302.
- Oberdörster, G., Oberdörster, E. & Oberdörster, J. (2005). Nanotoxicology: An Emerging Discipline Evolving from Studies of Ultrafine Particles. *Environ. Health Perspect.*, 113, 823-839.
- Oberdörster, G., Sharp, Z., Atudorei, V., Elder, A., Gelein, R., Kreyling, W. & Cox, C. (2004). Translocation of inhaled ultrafine particles to the brain. *Inhalation Toxicology*, 16, 437-445.
- OECD (2009). Test No. 453: Combined Chronic Toxicity/Carcinogenicity Studies, OECD Guidelines for the Testing of Chemicals, Section 4. *OECD Publishing*.
- OECD (2010). List of manufactured nanomaterials and list of endpoints for phase one of the OECD testing programme. Series on the Safety of Manufactured Nanomaterials No. 6. *OECD publishing*.
- OECD (2012). List of representative manufactured nanomaterials for testing. 26-9-2014.
- Oomen, A. G., Bos, P. M., Fernandes, T. F., Hund-Rinke, K., Boraschi, D., Byrne, H. J., Aschberger, K., Gottardo, S., von der K. F., Kuhnle, D., Hristozov, D., Marcomini, A., Migliore, L., Scott-Fordsmand, J., Wick, P. & Landsiedel, R. (2014). Concern-driven integrated approaches to nanomaterial testing and assessment - report of the NanoSafety Cluster Working Group 10. *Nanotoxicology*.
- Organisation for Economic Cooperation and Development (OECD) (1998). OECD Principles on Good Laboratory Practice (as revised in 1997). ENV/MC/CHEM(98)17. Organisation for Economic Cooperation and Development, Paris. 26-1-1998.
- Organization for Economic Cooperation and Development (OECD) (2009). OECD Guidelines for Testing of Chemicals, Section 4: Health Effects, No.412, "Repeated Dose Inhalation Toxicity: 28day or 14day Study".
- Packroff, R. & Baron, M. (2013). Nanomaterials at the Workplace: Occupational Safety and Health. In W. Luther & A. Zweck (Eds) *Safety Aspects of Engineered Nanomaterials* (pp. 235-257). Pan Stanford Publishing Pte. Ltd.
- Paranjpe, M. & Muller-Goymann, C. C. (2014). Nanoparticle-Mediated Pulmonary Drug Delivery: A Review. *International Journal of Molecular Sciences*, 15, 5852-5873.
- Pauluhn, J. (2011a) Common mechanism-based study design for inhalation toxicity testing of poorly soluble (nano-/ultrafine-) particles: Are new testing strategies and interpretation guidelines needed? *Nanocon 2011*.
- Pauluhn, J. (2011b). Poorly soluble particulates: Searching for a unifying denominator of nanoparticles and fine particles for DNEL estimation. *Toxicology*, 279, 176-188.
- PROSPECT (2010). Report: Ecotoxicology Test Protocols for Representative Nanomaterials in Support of the OECD Sponsorship Programme: Toxicological Review of Nano Cerium Oxide.
- Quaye, I. K. (2008). Haptoglobin, inflammation and disease. *Transactions of the Royal Society of Tropical Medicine and Hygiene*, 102, 735-742.
- Randolph, G. J. (2001). Dendritic cell migration to lymph nodes: cytokines, chemokines, and lipid mediators. *Seminars in Immunology*, 13, 267-274.
- Ravenzwaay, B. v., Landsiedel, R., Fabian, E., Burkhard, S., Strauss, V. & Ma-Hock, L. (2009). Comparing fate and effects of three particles of different surface properties: Nano-TiO<sub>2</sub>, pigmentary TiO<sub>2</sub> and quartz. *Toxicology Letters*, 186, 152-159.
- Reeves, A. L. (1986). Book: Handbook on the toxicology of metals. Vol II. Specific metals. Barium. Amsterdam: Elsevier Science Publishers.

## References

- Rittinghausen, S., Bellmann, B., Creutzenberg, O., Ernst, H., Kolling, A., Mangelsdorf, I., Kellner, R., Beneke, S. & Ziemann, C. (2013). Evaluation of immunohistochemical markers to detect the genotoxic mode of action of fine and ultrafine dusts in rat lungs. *Toxicology*, 303, 177-186.
- Roller, M. & Pott, F. (2006). Lung tumor risk estimates from rat studies with not specifically toxic granular dusts. *Living in A Chemical World: Framing the Future in Light of the Past*, 1076, 266-280.
- Rollins, B. J., Walz, A. & Baggiolini, M. (1991). Recombinant Human Mcp-1/Je Induces Chemotaxis, Calcium Flux, and the Respiratory Burst in Human Monocytes. *Blood*, 78, 1112-1116.
- Romero-Ibarra, I. C., Rodriguez-Gattorno, G., Garcia-Sanchez, M. F., Sanchez-Solis, A. & Manero, O. (2010). Hierarchically Nanostructured Barium Sulfate Fibers. *Langmuir*, 26, 6954-6959.
- Rushton, E. K., Jiang, J., Leonard, S. S., Eberly, S., Castranova, V., Biswas, P., Oberdörster, G. (2010). Concept of assessing nanoparticle hazards considering nanoparticle dose-metric and chemical/biological response metrics. *Journal of Toxicology and Environmental Health, Part A*, 73(5-6), 445-461.
- Russel, W. M. S. & Burch, R. L. (1959). Book: The Principles of Human Experimental Technique. London.
- Saber, A. T., Halappanavar, S., Folkmann, J. K., Bornholdt, J., Boisen, A. M., Moller, P., Williams, A., Yauk, C., Vogel, U., Loft, S. & Wallin, H. (2009). Lack of acute phase response in the livers of mice exposed to diesel exhaust particles or carbon black by inhalation. *Part Fibre Toxicol*, 6, 12.
- Saber, A. T., Lamson, J. S., Jacobsen, N. R., Ravn-Haren, G., Hougaard, K. S., Nyendi, A. N., Wahlberg, P., Madsen, A. M., Jackson, P., Wallin, H. & Vogel, U. (2013). Particle-Induced Pulmonary Acute Phase Response Correlates with Neutrophil Influx Linking Inhaled Particles and Cardiovascular Risk. *PLOS ONE*, 8(7), e69020.
- Sabokbar, A., Hirayama, T., Diaz, J., Itonaga, I., Murray, D. W., Lidgren, L. & Athanasou, N. A. Effect on osteoclast differentiation and bone resorption of bone cement containing two new radio-opaque contrast media. 46th Annual Meeting, Orthopaedic Research Society, March 12-15, 2000. 2000. Conference Proceeding.
- Sager, T. M., Kommineni, C. & Castranova, V. (2008). Pulmonary response to intratracheal instillation of ultrafine versus fine titanium dioxide: role of particle surface area. *Particle and Fibre Toxicology*, 5.
- Schins, R. P. F. & Knaapen, A. M. (2007). Genotoxicity of poorly soluble particles. *Inhalation Toxicology*, 19, 189-198.
- Schulte, P. A., Murashov, V., Zumwalde, R., Kuempel, E. D. & Geraci, C. L. (2010). Occupational exposure limits for nanomaterials: state of the art. *Journal of Nanoparticle Research*, 12, 1971-1987.
- Schwabe, F., Schulin, R., Rupper, P., Rotzetter, A., Stark, W. & Nowack, B. (2014). Dissolution and transformation of cerium oxide in plant growth media. *Journal of Nanoparticle Research*, 16[2668].
- Scott, C. L., Henri, S. & Guilliams, M. (2014). Mononuclear phagocytes of the intestine, the skin, and the lung. *Immunol.Rev.*, 262, 9-24.
- Semmler, M., Seitz, J., Erbe, F., Mayer, P., Heyder, J., Oberdörster, G., & Kreyling, W. G. (2004). Long-term clearance kinetics of inhaled ultrafine insoluble iridium particles from the rat lung, including transient translocation into secondary organs. *Inhalation toxicology*, 16(6-7), 453-459.
- Singh, C., Friedrichs, S., Gibson, N., Jensen, K. A., Levin, M., Birkedal, R., Pojana, G., Wohlleben, W., Schulte, S., Wiench, K., Marshall, D., Hund-Rinke, K., Kördel, W. & Klein, C. L. NM-Series of Representative Manufactured Nanomaterials: Zinc Oxide NM-110, NM-111, NM-112, NM-113. Characterisation and test item preparation. EUR Report 25066. 2011.
- Snipes, M. B. (1989). Long-Term Retention and Clearance of Particles Inhaled by Mammalian-Species. *Critical Reviews in Toxicology*, 20, 175-211.
- Spritzer, A. A. & Watson, J. A. (1964). The Measurement of Ciliary Clearance in the Lungs of Rats. *Health Physics*, 10, 1093-1097.
- Srinivas, A., Rao, P. J., Selvam, G., Murthy, P. B. & Reddy, P. N. (2011). Acute inhalation toxicity of cerium oxide nanoparticles in rats. *Toxicol.Lett.*, 205, 105-115.
- Standiford, T. J., Kunkel, S. L., Basha, M. A., Chensue, S. W., Lynch, J. P., Toews, G. B., Westwick, J. & Strieter, R. M. (1990). Interleukin-8 Gene-Expression by A Pulmonary Epithelial-Cell Line - A Model for Cytokine Networks in the Lung. *Journal of Clinical Investigation*, 86, 1945-1953.
- Stark, W. J., Stoessel, P.R., Wohlleben, W., Hafner, A. (2015). Industrial Applications of Nanomaterials. *Chemical Society Reviews*.
- Stark, G. (1968). Thesis/Dissertation: Untersuchungen an synthetischem Hydroxylapatit im Hinblick auf den Knochenstoffwechsel von Calcium, Strontium, Barium und Radium. *Biophysik* 5[1], 55-65. Springer.

## References

- Steinmuller, C., Franke-Ullmann, G., Lohmann-Matthes, M. L. & Emmendorffer, A. (2000). Local activation of nonspecific defense against a respiratory model infection by application of interferon-gamma - Comparison between rat alveolar and interstitial lung macrophages. *Am J Respir Cell Mol Biol*, 22, 481-490.
- Stöber, W., Einbrodt, H. J., & Klosterkötter, W. (1965). Quantitative studies of dust retention in animal and human lungs after chronic inhalation. *Inhaled Particles and Vapours, II (Davies CN, ed)*. Oxford, UK: Pergamon Press, 409-418.
- Stone, V., Johnston, H. & Schins, R. P. F. (2009). Development of in vitro systems for nanotoxicology: methodological considerations. *Critical Reviews in Toxicology*, 39, 613-626.
- Straube, R. & Donate, H. P. (2013). Magazine Article: Bariumintoxication in clinical environmental medicine: clinical picture, diagnostic procedure and therapy. *Umwelt, Medizin, Gesellschaft* 2013 26[3], 194-197.
- Szozda, R. (1996). Pneumoconiosis in carbon black workers. *Journal of UOEH*, 18, 223-228.
- Tamm, I. & Kortsik, C. (1999). Severe barium sulfate aspiration into the lung: Clinical presentation, prognosis and therapy. *Respiration*, 66, 81-84.
- Teunenbroek, T., Dijkzeul, A. & Hoehener, K. NANoREG-A common European approach to the regulatory testing of nanomaterials, press release. 2013. 9-4-2014.
- Kuhlbusch, T. A., Krug, H. F., & Nau, K. (2009). NanoCare-Health Related Aspects of Nanomaterials: Final Scientific Report. DECHEMA, ISBN: 978-3-89746-108-6.
- Theilgaard-Monch, K., Jacobsen, L. C., Nielsen, M. J., Rasmussen, T., Udby, L., Gharib, M., Arkwright, P. D., Gombart, A. F., Calafat, J., Moestrup, S. K., Porse, B. T. & Borregaard, N. (2006). Haptoglobin is synthesized during granulocyte differentiation, stored in specific granules, and released by neutrophils in response to activation. *Blood*, 108, 353-361.
- Tran, C. L., Buchanan, D., Cullen, R. T., Searl, A., Jones, A. D. & Donaldson, K. (2000). Inhalation of poorly soluble particles. II. Influence Of particle surface area on inflammation and clearance. *Inhal Toxicol*, 12, 1113-1126.
- Valberg, P. A., Bruch, J. & McCunney, R. J. (2009). Are rat results from intratracheal instillation of 19 granular dusts a reliable basis for predicting cancer risk? *Regulatory Toxicology and Pharmacology*, 54, 72-83.
- Voloudaki, A., Ergazakis, N. & Gourtsoyannis, N. (2003). Late changes in barium sulfate aspiration: HRCT features. *European Radiology*, 13, 2226-2229.
- Wakefield, G., Wu, X. P., Gardener, M., Park, B. & Anderson, S. (2008). Envirox fuel-borne catalyst: Developing and launching a nano-fuel additive. *Technology Analysis & Strategic Management*, 20, 127-136.
- Wang, X. R. & Christiani, D. C. (2000). Respiratory symptoms and functional status in workers exposed to silica, asbestos, and coal mine dusts. *Journal of Occupational and Environmental Medicine*, 42, 1076-1084.
- Wimhurst, J. A., Brooks, R. A. & Rushton, N. (2001). The effects of particulate bone cements at the bone-implant interface. *Journal of Bone and Joint Surgery-British Volume*, 83B, 588-592.
- Wohlleben, W., Ma-Hock, L., Boyko, V., Cox, G., Egenolf, H., Freiburger, H., Hinrichsen, B., Hirth, S. & Landsiedel, R. (2013). Nanospecific Guidance in REACH: A Comparative Physical-Chemical Characterization of 15 Materials with Methodical Correlations. *Journal of ceramic science and technology*, 4, 93-104.
- Xia, T., Kovochich, M., Liong, M., Madler, L., Gilbert, B., Shi, H. B., Yeh, J. I., Zink, J. I. & Nel, A. E. (2008). Comparison of the Mechanism of Toxicity of Zinc Oxide and Cerium Oxide Nanoparticles Based on Dissolution and Oxidative Stress Properties. *Acs Nano*, 2, 2121-2134.
- Yokel, R. A., Au, T. C., MacPhail, R., Hardas, S. S., Butterfield, D. A., Sultana, R., Goodman, M., Tseng, M. T., Dan, M., Haghazari, H., Unrine, J. M., Graham, U. M., Wu, P. & Grulke, E. A. (2012). Distribution, Elimination, and Biopersistence to 90 Days of a Systemically Introduced 30 nm Ceria-Engineered Nanomaterial in Rats. *Toxicological Sciences*, 127, 256-268.
- Yokel, R. A., Florence, R., Tseng, M., Graham, U., Sultana, R., Butterfield, D. A., Wu, P. & Grulke, E. (2008). Conference Proceeding: Biodistribution and toxicity of systemically-introduced nanoscale ceria. *Nanotox 2008 Zürich*, 87.
- Yokel, R. A., Hussain, S., Garantziotis, S., Demokritou, P., Castranova, V. & Cassee, F. R. (2014a). The Yin: An adverse health perspective of nanoceria: uptake, distribution, accumulation, and mechanisms of its toxicity. *Environmental Science: Nano*, 1, 406-428.
- Yokel, R. A., Unrine, J. M., Wu, P., Wang, B. & Grulke, E. A. (2014b). Nanoceria biodistribution and retention in the rat after its intravenous administration are not greatly influenced by dosing schedule, dose, or particle shape. *Environmental Science: Nano*, 1, 549-560.
- Zhang, M., Zhang, B., Li, X. H., Yin, Z. L. & Guo, X. Y. (2011). Synthesis and surface properties of submicron barium sulfate particles. *Applied Surface Science*, 258, 24-29.

## 12. Annex

### 12.1. Abbreviations

AAALAC, Association for Assessment and Accreditation of Laboratory Animal Care International

AAN, Average Agglomeration Numbers

ALP, Alkaline phosphatase

AUC, Area under the curve

BALF, Bronchoalveolar lavage fluid

BALT, Bronchus-associated lymphoid tissue

BET, Brunauer-Emmet-Teller

Ceria, Cerium dioxide

CINC, Cytokine-induced neutrophil chemoattractant

FaSSIF, Fasted State Simulated Intestinal Fluid

GGT,  $\gamma$ -Glutamyl-transferase

GSD, Geometric standard deviation

ICP-AES, Inductively coupled plasma atomic emission spectrometry

ICP-MS, Inductively coupled plasma optical emission spectrometry

IL, interleukin

LDH, lactate dehydrogenase

M-CSF, macrophage colony stimulating factor

MCP, monocyte chemoattractant protein

MMAD, mass median aerodynamic diameter

MPPD, multiple-path particle dosimetry model

NAG, N-acetyl- $\beta$ -glucosaminidase

NOAEC, no observed adverse effect concentration

OPN, osteopontin

PMN, polymorphnuclear neutrophil

PSF, phagolysosomal simulant fluid

PSP, poorly soluble particles with low toxicity

SAD, selected area electron diffraction

SEM, scanning electron microscopy

SIMS, secondary ion mass spectrometry

SMPS, scanning mobility particle sizer

STIS, short term inhalation study protocol

TEM, transmission electron microscopy

TGA, thermogravimetric analysis

TiO<sub>2</sub>, titanium dioxide

XPS, X-ray photoelectron spectroscopy

## 12.2. Erklärung/Declaration

"Ich erkläre: Ich habe die vorgelegte Dissertation selbständig und ohne unerlaubte fremde Hilfe und nur mit den Hilfen angefertigt, die ich in der Dissertation angegeben habe. Alle Textstellen, die wörtlich oder sinngemäß aus veröffentlichten oder nicht veröffentlichten Schriften entnommen sind, und alle Angaben, die auf mündlichen Auskünften beruhen, sind als solche kenntlich gemacht. Bei den von mir durchgeführten und in der Dissertation erwähnten Untersuchungen habe ich die Grundsätze guter wissenschaftlicher Praxis, wie sie in Promotionsordnung des Fachbereichs Veterinärmedizin 06.11.2012 7.40.10 Nr. 1 S. 8 der "Satzung der Justus-Liebig-Universität Gießen zur Sicherung guter wissenschaftlicher Praxis" niedergelegt sind, eingehalten."

"I declare that I have completed this dissertation single-handedly without the unauthorized help of a second party and only with the assistance acknowledged therein. I have appropriately acknowledged and referenced all text passages that are derived literally from or are based on the content of published or unpublished work of others, and all information that relates to verbal communications. I have abided by the principles of good scientific conduct laid down in the charter of the Justus-Liebig-University of Giessen in carrying out the investigations described in the dissertation."

Jana Keller

### 12.3. Acknowledgment

I would like to thank all those people, who have been involved into this period of life with my doctoral thesis in every possible way.

Grateful thanks to Christiane Herden and Günter Oberdörster for their supervision, guidance and helpful suggestions and corrections.

I would like to thank the NanoMILE and NanoREG (EU-projects) and project partners allowing me to do the research within their framework.

Thanks to the colleagues at University of Harvard, Joe Brain and Ramon Molina, for inspiring ideas and the collaboration.

Deep thanks to my colleagues and team at BASF:

Robert Landsiedel, my supervisor, for his support, patience and guidance, for fruitful (and heated) discussions and his willingness to let me grow and leave.

Sibylle Gröters for her veterinary friendship and guidance, always encouraging me and supporting me.

Lan Ma-Hock, Wendel Wohlleben and Karin Wiench for their support in (nano)toxicology questions, I had a great time with you.

Thomas Hoffmann for his advice in difficult questions.

Karin Küttler and Volker Strauß for their help in (histo)- and clinical pathological questions

The inhalation lab team, the (histo-)pathology team, the cell proliferation guys (:-)), for their professional technical assistance, for the great atmosphere, wonderful moments and (too) many cookies, cakes and sweets. 😊

Thanks to my current lab team and group, to all the vets, colleagues and other students at BASF and all my supporters during my PhD. I had a wonderful time and will take on new challenges.

Thanks to my friends and colleagues at home.

Finally, I would like to thank my family for their love and unending support over the course of my PhD, my time at BASF and throughout my entire life.